ORNL/TM-2017/736

The DD Neutron Generator as an Alternative to Am(Li) Isotopic Neutron Source in the Uranium Neutron Coincidence Collar

Robert D. McElroy, Jr.
Steven L. Cleveland

December 2017

OAK RIDGE NATIONAL LABORATORY
MANAGED BY UT-BATTELLE FOR THE US DEPARTMENT OF ENERGY

ORNL/TM-2017/736

Nuclear Security and Isotope Technology Division

THE DD NEUTRON GENERATOR AS AN ALTERNATIVE TO AM(LI) ISOTOPIC NEUTRON SOURCE IN THE URANIUM NEUTRON COINCIDENCE COLLAR

Robert D. McElroy Jr.
Steven L. Cleveland

Date Published: December 2017

Prepared by
OAK RIDGE NATIONAL LABORATORY
Oak Ridge, TN 37831-6283
managed by
UT-BATTELLE, LLC
for the
US DEPARTMENT OF ENERGY
under contract DE-AC05-00OR22725

CONTENTS

LIST OF FIGURES

LIST OF TABLES

ABBREVIATED TERMS

AWCC	Active Well Coincidence Counter
BWR	boiling water reactor
COTS	commercial off-the-shelf
DD/AWCC	deuterium-deuterium neutron generator/Active Well Coincidence Counter
DD/UNCL	deuterium-deuterium neutron generator/Uranium Neutron Coincidence Collar
DU	depleted uranium
HDPE	high-density polyethylene
HEU	highly enriched uranium
HM	heavy metal [correction]
JSR	Jomar Shift Register
LEU	low-enriched uranium
LD	linear density
MCNP	Monte Carlo N-Particle [software package]
MCS	multichannel scaling
NBL	New Brunswick Laboratory
NBS	National Bureau of Standards
NDA	nondestructive assay
OD	outer diameter
ORNL	Oak Ridge National Laboratory
PWR	pressurized water reactor
UNCL	Uranium Neutron Coincidence Collar
VISED	MCNP Visualization Editor

ACKNOWLEDGMENTS

This material is based upon work supported by the NA-241's Next Generation Safeguards Initiative within the Office of Nonproliferation and Arms Control, National Nuclear Security Administration, US Department of Energy.

EXECUTIVE SUMMARY

The ^{235}U mass assay of bulk uranium items, such as oxide canisters, fuel pellets, and fuel assemblies, is not achievable by traditional gamma-ray assay techniques because of the limited penetration of the item by the characteristic ^{235}U gamma rays. Instead, fast neutron interrogation methods such as active neutron coincidence counting must be used. For international safeguards applications, the most commonly used active neutron systems, the Active Well Coincidence Counter (AWCC), Uranium Neutron Coincidence Collar (UNCL), and ^{252}Cf Shuffler, rely on fast neutron interrogation using an isotopic neutron source [i.e., ^{252}Cf or Am(Li)] to achieve better measurement accuracies than are possible using gamma-ray techniques for high-mass, high-density items. However, the Am(Li) sources required for the AWCC and UNCL systems are no longer manufactured, and newly produced systems rely on limited supplies of sources salvaged from disused instruments. The ^{252}Cf shuffler systems rely on the use of high-output ^{252}Cf sources, which while still available have become extremely costly for use in routine operations and require replacement every 5–7 years. Lack of a suitable alternative neutron interrogation source would leave a potentially significant gap in the safeguarding of uranium processing facilities.

Previously we examined the performance of Oak Ridge National Laboratory's Large Volume Active Well Coincidence Counter modified to accept a commercially available deuterium-deuterium (DD) neutron generator to examine the potential of the DD neutron generator as an alternative to the isotopic sources [1]. That work indicated that the DD generator was a viable replacement for the AWCC applications, but because of the large dimensions of that generator, the DD/AWCC would have to be run as a delayed neutron counting system to provide equivalent measurement precision. In this work we examine the performance of a standard UNCL modified to accept the DD neutron generator for the assay of ^{235}U based on the results of Monte Carlo N-Particle (MCNP) simulations and measurements of depleted uranium and highly enriched uranium items. The projected performance of the modified UNCL for fresh pressurized water reactor fuel assemblies operated in both traditional coincidence counting and delayed neutron counting modes is presented.

Project Summary

- The UNCL was modified to accept the Thermo-Fisher MP320 Pulsed Neutron Generator.
- MCNP models of the as-built integrated DD neutron generator and UNCL (DD/UNCL) system were created.
- Simulations of UNCL measurement with various LEU fuel assemblies, enrichments, and densities were performed to provide a broad understanding of the system response and performance capabilities. (The descriptions of the simulated fuel assemblies are the same as those in the recent neutron rodeo project to examine the performance of alternative neutron detection techniques for the assay of fresh fuel assemblies [2]).
- The results of the simulations have been compared with the simulated and measured performance of the UNCL operated with an Am(Li) source.
- Measurements of depleted uranium and highly enriched uranium items were performed to validate the MCNP simulations and provide measured performance values for the DD/UNCL.
- The performance of the DD/UNCL has been evaluated for two different operating modes.
  - Active coincidence counting
  - Pulsed neutron generator–delayed neutron counting

- The performance of the DD/UNCL was evaluated for additional neutron generator types via MCNP simulations.
  - Am(Li) isotopic source
  - MP320 Pulsed Neutron Generator
  - nGen310 Neutron Generator
  - nGen-300c Pulsed Neutron Generator
  - Hypothetical very compact neutron generator
  - Variations with the nGen-300c and nGen-310 to improve performance through neutron spectrum tailoring (These attempts were unsuccessful.)

- Bias estimates using the DD/UNCL for both active coincidence counting and delayed neutron counting were evaluated. Both methods yield similar measurement biases to those achieved from the Am(Li)-based measurements.

- Measurement precision for the DD/UNCL for both active coincidence counting and delayed neutron counting was evaluated.
  - The measurement precision obtainable using the DD generators for active coincidence counting was approximately 50% larger (poorer) in the thermal mode and two to three times larger (poorer) in fast mode than those achievable with the Am(Li) source.
  - Measurement precision using the delayed neutron counting method was found to improve the performance achieved by the Am(Li)-based UNCL assay for the same measurement times.

Performance of the DD/UNCL Operated in Coincidence Counting Mode

To operate the DD/UNCL counter in as near a manner as possible to the Am(Li)-based UNCL measurement, the neutron generator is operated in steady state or continuous mode. The measurement proceeds identically to the Am(Li)-based UNCL system with two differences. The inherent variability of the neutron yield from the generator must be accounted for and requires the addition of a flux monitor (a small, low efficiency ^{3}He tube) to the system. The neutron generator will be operated at a somewhat higher yield than is available from the Am(Li) source (200,000 versus 50,000 n/s) to provide optimal measurement precision.

The measurement biases associated with the UNCL are dominated by the measurement geometry (e.g., relative source, detector, and fuel assembly locations) with secondary effects due to interrogating neutron energy distribution. The single point interrogation and asymmetric detector arrangement result in a measurement that is impacted by the dimensions and arrangement of the fuel assembly resulting in the need for the heavy metal correction (refer to reference [3] for a description of the heavy metal correction). So we do not expect to see significant differences in the measurement biases with the choice of neutron generator.

The DD generator average neutron energy is sufficient to induce fission in ^{238}U. However, when operated in thermal interrogation mode, the ^{235}U signal dominates, and there is little difference in the response profiles as a function of ^{235}U linear density. When operated in fast mode (with cadmium liners in place), the ^{238}U contribution to the signal acts as a vertical offset in the response profile. The biases caused by the increased sensitivity to ^{238}U are correctable using the existing heavy metal correction currently applied to the Am(Li)-based measurements.

The simulations of the various neutron generator types indicate that the measurement biases, following application of historically applied correction factors, are equivalent to those obtained using the Am(Li) interrogation source. That is the DD/UNCL will provide equivalent accuracy to that obtained from the Am(Li)-based system.

The simulated measurement precision from the DD/UNCL systems was poorer than the simulated or observed precision of the Am(Li)-based system for each neutron generator examined (when configured for active coincidence counting).

Operation of the DD/UNCL in fast mode for coincidence counting will require an increase in total measurement time to provide the same total measurement uncertainty currently achieved with the UNCL system. However, operated in thermal mode the difference in precision between Am(Li) and generator measurements is sufficiently small relative to the measurement biases that the interrogating sources can be considered equivalent.

Performance of the DD/UNCL Operated in Delayed Neutron Counting Mode

From the DD/AWCC study [1] previously completed we saw that delayed neutron counting with operation of the neutron generators in pulsed mode provided improved measurement precision relative to the active coincidence counting approach. Because the simulated results of the DD/UNCL system indicated that the active coincidence counting method would result in degradation of the measurement precision, the potential for delayed neutron counting was investigated for the assay of the fresh fuel assemblies.

The neutron generator was operated in pulsed mode, with a repetition rate of 250 Hz or slower and neutron pulse width of 5% or narrower. In keeping with the parameters of the neutron rodeo [2], the performance was examined for measurement times of 600 and 1,800 seconds. As with the rodeo and actual UNCL measurements, it is assumed that a passive neutron measurement is completed prior to start of the active neutron interrogation. The delayed neutron measurement offers significant improvement in measurement precision compared to the Am(Li)-based measurement. Unlike the coincidence measurement, the accidentals coincidence rates do not limit the interrogating neutron strength that can be applied. We arbitrarily chose a neutron yield equivalent to that from a 1 μg ^{252}Cf source (2E6 n/s) for these simulations that produces an exposure of approximately 5 mR/h at 60 cm from the UNCL.

Biases originating from the physical arrangement of the measurement were expected to be similar for the delayed neutron and active coincidence measurements because the induced fission distribution is the same for each measurement. Slight differences are expected because of the differences in detection efficiencies for the coincidence and the delayed (single) neutron events and because of the differences in the multiplication effect. This behavior is seen in the simulated results; however, application of the existing bias correction techniques (e.g., heavy metal and poison rod) provides nearly identical results for the delayed neutron and Am(Li)-based coincidence measurements.

For each generator configuration considered, the measurement precision for the delayed neutron measurements was equal or superior to that obtained for the Am(Li)-based coincidence measurement. However, the timing characteristics of the nGen-300 pulsing neutron generator (i.e., slow repetition rate) allow a greater fraction of the delayed neutrons to be counted, resulting in significantly improved measurement precision relative to both the Am(Li)-based UNCL measurement and the MP320-based delayed neutron measurement.

- Using the MP320 neutron generator, modest improvements in precision are predicted depending upon the fuel assembly type, typically 30% smaller (better) than that those achievable with the Am(Li) source.

- Using the nGen-300c generator, modest improvements in precision are predicted, typically 50%–70% smaller (2–3 times better) in both thermal and fast modes than that those achievable with the Am(Li) source.

Conclusion

The DD neutron generator using the thermal mode coincidence counting methodology is a viable replacement for Am(Li). It is a near drop in replacement for the existing Am(Li) measurement and provides similar accuracy and measurement precision. However, in the fast mode, degradation in measurement precision would require a significant increase in measurement time to obtain similar performance. Based upon these simulations, the DD neutron generator using the delayed neutron counting methodology is a viable replacement for Am(Li). With the nGen-300 DD neutron generator, the method is expected to provide equivalent accuracy with significant improvement in measurement precision or a corresponding reduction in measurement time in both fast and thermal interrogation modes.

ABSTRACT

The ^{235}U mass assay of bulk uranium items, such as oxide canisters, fuel pellets, and fuel assemblies, is not achievable by traditional gamma-ray assay techniques due to the limited penetration of the item by the characteristic ^{235}U gamma rays. Instead, fast neutron interrogation methods such as active neutron coincidence counting must be used. For international safeguards applications, the most commonly used active neutron systems, the Active Well Coincidence Counter (AWCC), Uranium Neutron Coincidence Collar (UNCL) and ^{252}Cf Shuffler, rely on fast neutron interrogation using an isotopic neutron source [i.e., ^{252}Cf or Am(Li)] to achieve better measurement accuracies than are possible using gamma-ray techniques for high-mass, high-density items. However, the Am(Li) sources required for the AWCC and UNCL systems are no longer manufactured, and newly produced systems rely on limited supplies of sources salvaged from disused instruments. The ^{252}Cf shuffler systems rely on the use of high-output ^{252}Cf sources, which while still available have become extremely costly for use in routine operations and require replacement every 5–7 years. Lack of a suitable alternative neutron interrogation source would leave a potentially significant gap in the safeguarding of uranium processing facilities.

Previously we examined the performance of Oak Ridge National Laboratory's (ORNL's) Large Volume Active Well Coincidence Counter (LV-AWCC) modified to accept a commercially available deuterium-deuterium (DD) neutron generator to examine the potential of the DD neutron generator as an alternative to the isotopic sources [1]. That work indicated that the DD generator was a viable replacement for the AWCC applications, but because of the large dimensions of that generator, the DD/AWCC would have to be run as delayed neutron counting system to provide equivalent measurement precision. In this work, we examine the performance of a standard UNCL modified to accept the DD neutron generator for the assay of ^{235}U based on the results of Monte Carlo N-Particle (MCNP) simulations and measurements of depleted uranium (DU) and highly enriched uranium items. The projected performance of the modified UNCL for fresh pressurized water reactor (PWR) fuel assemblies operated in both traditional coincidence counting and delayed neutron counting modes is presented.

1. INTRODUCTION

1.1 URANIUM NEUTRON COLLAR

The UNCL [4] is an active neutron interrogation system used to provide the ^{235}U linear density (LD) of fresh fuel assemblies during routine inspection activities by the International Atomic Energy Agency and European Atomic Energy Community in support of international safeguards. The UNCL, shown in Figures 1 and 2, is rectangular in configuration, three sides of which are arrays of ^{3}He proportional counters embedded in high-density polyethylene (HDPE). The fourth (active) side contains the Am(Li) neutron source, which is also embedded in HDPE. During use, the collar is placed around the fuel assembly bringing the Am(Li) neutron source into close proximity with the fuel assembly while encompassing three of the four sides with the neutron detector array. Neutrons emitted from the Am(Li) source induce fission within the fuel assembly resulting in the emission of additional neutrons. Neutrons from both interrogation source and induced fission events are detected in the ^{3}He proportional detectors. Neutron coincidence counting is employed to distinguish the induced fission from the interrogating source events. The ^{235}U linear density (i.e., mass ^{235}U per unit length of fuel assembly) is inferred from the observed neutron coincidence rate, and the result is compared with declared value for the fuel assembly.

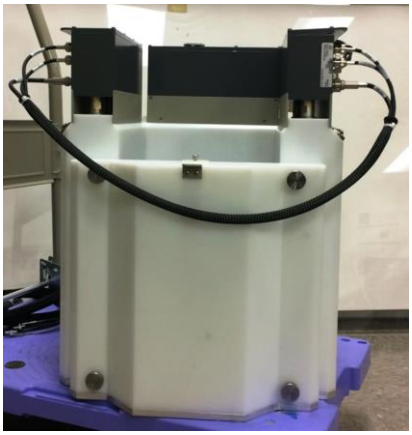

Figure 1. Photograph of the JCC-71 UNCL configured in active mode for PWR fuel assemblies.

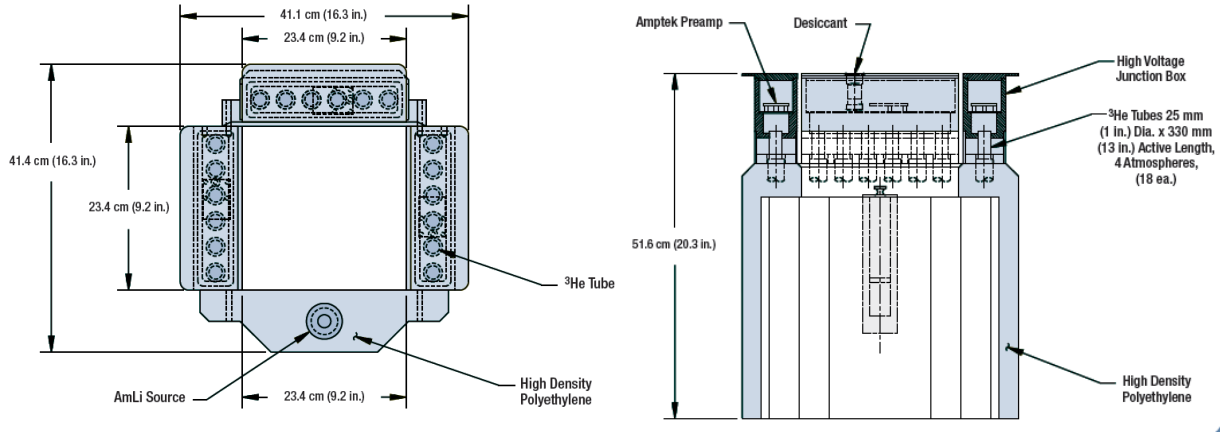

Figure 2. Cross-sectional drawings of the UNCL shown configured in the active mode for PWR fuel assemblies [5].

1.2 OPERATION OF THE UNCL

Neutrons released from the Am(Li) source induce fission within the fuel assembly, which results in the release of coincident neutrons. The neutron coincidence rate is related to the ^{235}U linear density by an empirically defined relation (typically the rational function is used). The coincidence, or doubles, rate is measured using a coincidence shift register such as the Jomar Shift Register (JSR)-12 or JSR-15 with duration of 10–30 minutes.

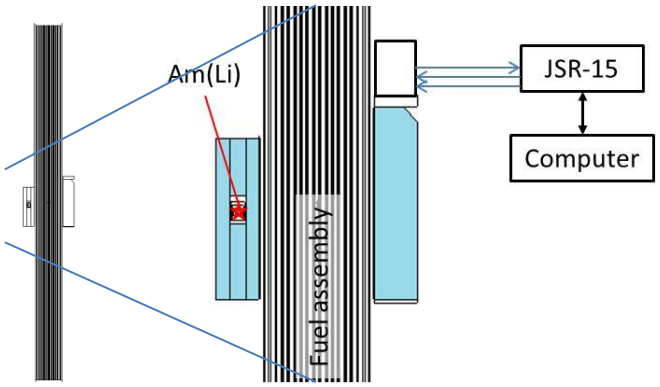

Figure 3. Cartoon showing the arrangement of the UNCL about the fuel assembly during measurement.

The UNCL is operated in either fast or thermal modes. The thermal mode provides greater sensitivity by allowing slow neutrons moderated in the HDPE detector modules to return to the fuel assembly. These slow neutrons have a greater likelihood of inducing fission increasing the measured doubles rate. However, while operation in thermal mode offers good measurement precision (1%–2% in 10 minutes), the assay result is significantly impacted by the presence of poison rods (10s of percent).

In the fast mode configuration a cadmium curtain is inserted inside the UNCL to prevent reentry of the thermalized neutrons into the fuel assembly. This degrades the measurement precision (3%–4% in 10 minutes) but lowers the sensitivity to the poison rods by about a factor of 3. For comparison, the calibration curves for a typical UNCL in thermal and fast modes are shown in Figure 4. The doubles rates are approximately 10 times greater in thermal mode than in fast.

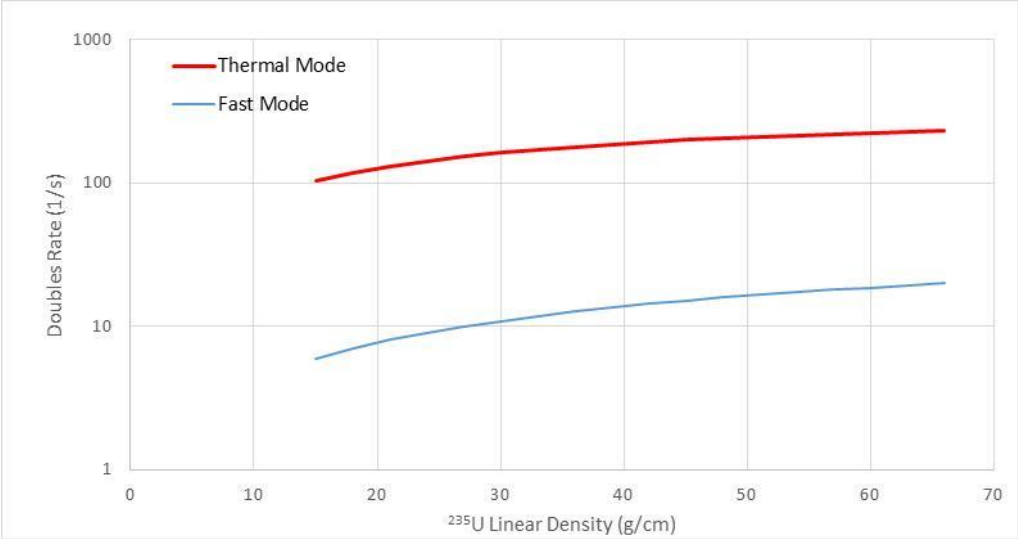

Figure 4. Comparison of the calibration curves for the UNCL in thermal and fast modes.

1.3 CORRECTIONS TO THE OBSERVED DOUBLES RATE

A number of correction factors may be applied to the observed doubles rates [6]. These correction factors allow the use of a common linear density calibration to be applied to all UNCL systems (assuming they have been cross calibrated at Los Alamos National Laboratory).

$$D_{corr} = k \cdot D_0 = (k_0 \cdot k_1 \cdot k_2 \cdot k_3 \cdot k_4 \cdot k_5) \cdot D_0 ,$$

Where the traditional correction factors to the observed doubles rate are

k_0: Am(Li) source strength, which accounts for ^{241}Am decay or use of a different Am(Li) source.
k_1: Electronics drift, which corrects for changes in the UNCL with time based on QC trending.
k_2: Detector efficiency, which is a cross calibration parameter to adjust the response of UNCL to that of a reference UNCL system.
k_3: Burnable poison, Gd_2O_3, is an empirical calibration factor to correct for the presence of poison rods.
k_4: Heavy metal loading, g U/cm, which is essentially an enrichment correction factor.
k_5: Other.

Due to the difference in interrogating neutron energies, we would expect the heavy metal and burnable poison corrections (k_3 and k_4) to have more impact on the observed rates for the DD generator assays. To provide a reasonable comparison of the expected performance of the DD/Collar versus the UNCL, it will be necessary to apply these corrections to both the simulated and measured doubles rates.

1.3.1 Heavy Metal Correction (k_4)

This factor has been called both the heavy metal and uranium mass correction. It is better described as an enrichment correction factor; however, it is implemented as a function the uranium linear density. For PWR assemblies the correction factor is given as [6]

$$k_4 = 1 + \lambda_1 \cdot (\lambda_0 - \lambda) ,$$

where λ is the uranium linear density (g/cm),
λ_1 is an empirically determined calibration factor, = 3.89E-4,
λ_0 is the reference density value (historically = 1,215 g/cm).

These values, from reference [6], are the same for both fast and thermal modes of the UNCL.

1.3.2 Poison Rod Correction (k_3)

The poison rod correction is also discussed in reference [6] is shown here. This correction requires different parameters for fast and thermal modes as well as boiling water reactor (BWR) and PWR assemblies. The thermal mode correction factor for PWR assemblies is given as

$$k_3 = 1 + \frac{9.86 \cdot n}{N} \cdot \left(1 - e^{-0.647 \cdot Gd}\right) \cdot (1 - 0.176 \cdot E_N) ,$$

and the fast mode correction factor for PWR assemblies is

$$k_3 = 1 + \frac{n}{N} \cdot 0.602 \cdot \left(1 - e^{-0.647 \cdot Gd}\right) ,$$

where n is the number of poison rods,
N is the number of fuel rods (fuel + poison),
Gd is the weight percent of the gadolinium in the poison rods,
E_N is the declared enrichment.

1.4 UNCL VERSUS UNCL-II

There are two primary variants of the neutron collar, the UNCL and UNCL-II. The UNCL is a general purpose counter comprised of three individual neutron slabs and an active slab to house the Am(Li) neutron source. The configuration of the UNCL is adjustable to accommodate either PWR or BWR fuel assemblies, which are somewhat smaller. The UNCL is normally provided with a fourth detector bank to replace the active slab to allow for passive neutron coincidence measurement of MOX fuel assemblies. The UNCL-II is optimized for use as an active neutron collar and is fabricated as two pieces: a U-shaped neutron detector assembly and an active slab for the Am(Li) source. The UNCL-II itself has two variants: one sized for PWR assemblies and the other for BWR assemblies as shown in Figure 5. The UNCL-II provides somewhat improved performance for the PWR and BWR fuel assemblies compared to the UNCL.

NOTE: This work only examines the performance of the UNCL configured for PWR assemblies.

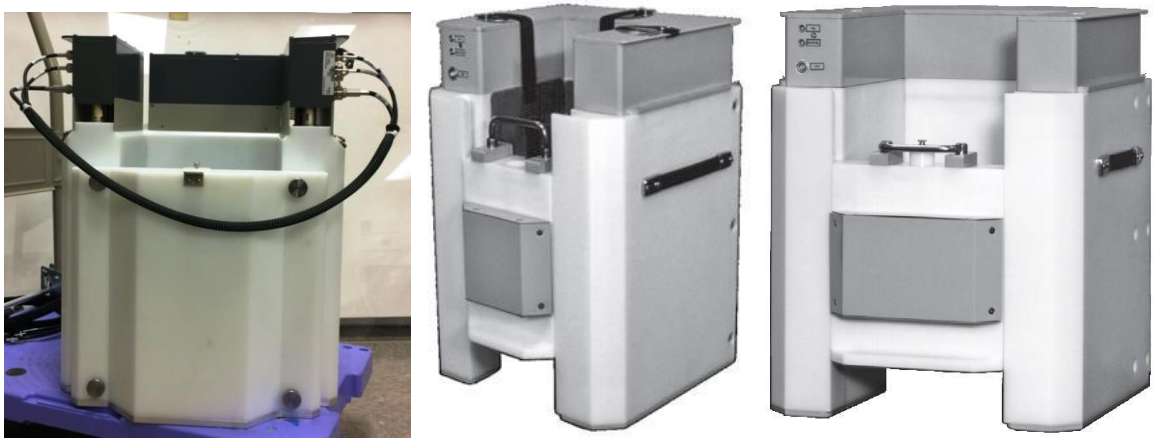

Figure 5. Photographs of the Canberra JCC-71 UNCL (*left*), JCC-72 UNCL-II-BWR (*center*), and the JCC-73 UNCL-II-PWR (*right*) neutron collars [5].

2. INTERROGATING NEUTRON SOURCES

Am(Li) is an isotopic neutron interrogation source producing neutrons by means of the $^{7}Li(\alpha,n)^{10}B$ reaction where the α particles are provided by the decay of ^{241}Am. Am(Li) has been the preferred source for active neutron interrogation in international safeguards because of its long isotopic half-life (433 years), long working life (~30 years), predictable neutron emission rate, and the energy spectrum of the emitted neutrons is better matched to the ^{235}U fission cross-sections than those of ^{238}U, providing a measure of selectivity in the measurement process. The Am(Li) sources are also relatively compact, allowing close geometric coupling with the item of interest and facilitating mechanical integration with the assay system. Recently there has been a drive to minimize the use of isotopic sources in international safeguards, and it is no longer possible to obtain these sources commercially in the western world.

Replacement of the Am(Li) source by a neutron generator in existing or new safeguards assay systems requires some level of modification. This can be a simple mechanical modification that is just enough to shoehorn the much larger neutron generator tube into an existing system design or a redesign of the assay system to fully optimize the response to the neutron interrogation source. The scope of this study is to evaluate the feasibility of using a commercial off-the-shelf (COTS) neutron generator with a minimally modified existing neutron collar, the UNCL.

The neutron generator does have some advantages over the isotopic source:

- Off switch: The generator only produces neutrons when required, simplifying background measurements and minimizing personnel exposure.
- Safety: The generator is made safe by removing power.
- Pulsed mode: This mode allows additional interrogation and analysis techniques.
- Transportation: No radioactive materials simplifies transportation of the source.
- Export: Not dual-use export restricted.

2.1 AM(LI) NEUTRON SOURCE

The Am(Li) neutron interrogation source is assumed to have been produced by Gammatron and packaged within an AN-HP stainless steel source capsule. The source capsule is placed within a tungsten source bottle to shield against the 60 keV photons from the decay of ^{241}Am. The chemical form of the Am(Li) source material is assumed to be AmO_2 mixed with Li_2O and LiOH. However, to facilitate comparison with other studies [7], [8], the Obninsk neutron energy distribution [9] is used to describe the Am(Li) neutron source term in the MCNP modeling efforts.

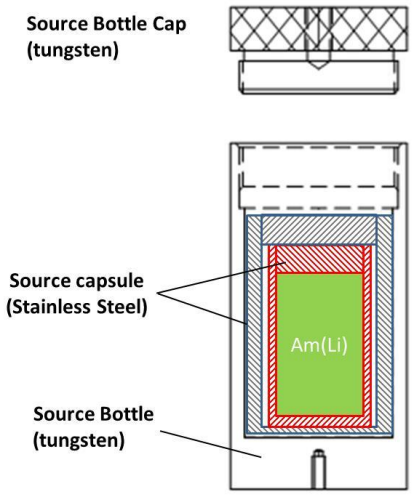

Figure 6. Sketch showing the relative arrangement of the Am(Li) source capsule used with the UNCL.

Table 1. Typical $^{241}AmO_2$ Li neutron source characteristics

Mass of ^{241}Am:	0.35 g
^{241}Am activity:	1.2 Ci
Emission rate:	5×10^4 n/s
Chemical form:	AmO_2
Isotope:	^{241}Am
Capsule type:	AN-HP
Capsule dimensions:	20 mm outer diameter (OD) × 50 mm tall
Capsule material:	Stainless steel
Capsule construction:	Double encapsulation, welded

2.2 DD NEUTRON GENERATOR

The DD neutron generator was selected over the more common deuterium-tritium (DT) generator to minimize induced fissions in ^{238}U. Although the 2.5 MeV neutrons from the DD reaction and 14 MeV neutrons from the DT reaction both exceed the fission threshold in ^{238}U, it is a much simpler task to minimize sensitivity to ^{238}U by the interrogation source if the lower energy DD neutron generator is used. Additionally, the lack of tritium simplifies shipping, and the lower neutron energy requires less additional shielding.

The DD neutron generator selected for this evaluation is a ThermoFisher Scientific model MP320 (**Error! eference source not found.**). The generator may be operated in steady state (non-pulsed) mode with a maximum yield of ~2.E6 n/s and an average neutron energy of 2.48 MeV. Although not a small neutron generator tube by today's standard, the 12.1 cm diameter tube can be fit within the LV-AWCC or standard AWCC end-plugs. The principal drawbacks of the tube are its overall length (~56 cm) and location of the target line (i.e., point of neutron generation) ~14.4 cm from the end of the tube. This results in a greater source-to-sample separation, additional shielding, and an increase in system footprint.

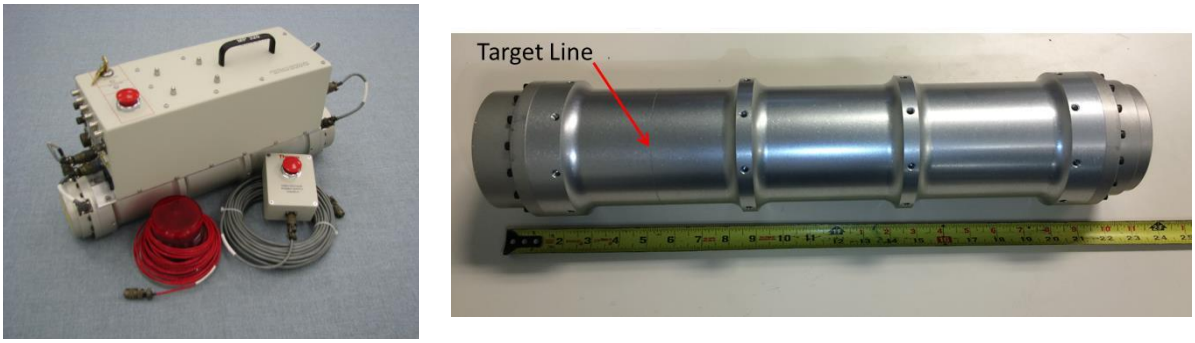

Figure 7. Photograph of the complete MP320 system (*left*) and the MP320 DD neutron generator tube detached from the controller (*right*).

Table 2. MP320 characteristics

Type of generator:	DD
Maximum emission rate:	2×10^6 n/s
Neutron energy:	2.48 MeV
Steady state/pulsed:	Both
Pulsed mode	
Frequency range:	250 Hz to 20 kHz
Duty cycle:	5%–100%, 5 µs minimum pulse width
Generator tube dimensions	
Diameter:	12.06 cm
Length:	55.88 cm
Target line:	13.97 cm

2.3 OTHER DD NEUTRON GENERATORS CONSIDERED

2.3.1 Starfire nGen Series

Since the inception of this project, a somewhat more compact DD neutron generator, the Starfire nGen™ Neutron Generator, has been released [10, 11]. This generator places the source generation at the end of the generator tube and is somewhat smaller in diameter. Although the generator tube itself is only 3 in. in diameter, a cooling shroud would be required for most safeguards applications, increasing the outer diameter to 3.5 in. (8.9 mm). This mechanical arrangement is better suited to safeguards applications than the MP320 generators. At the time of this writing, the MP320 and the nGen series were cost competitive (i.e., the costs were within 20% of each other). The primary downside compared to the MP320 generator is that the nGen series cannot be switched back and forth between pulsed and steady-state operation—two separate generators would be required.

Table 3. Starfire nGen characteristics

	nGen-300c	nGen-310
Type of generator:	DD	DD
Neutron yield:	1×10^7 n/s time avg	1×10^7 n/s
Neutron energy:	2.48 MeV	2.48 MeV
Steady state/pulsed:	Pulsed	Steady state
Pulsed mode		
Frequency range:	1 shot to 200 kHz	N/A
Duty cycle:	4%	100%
Generator tube dimensions		
Diameter (with shroud):	8.9 cm	8.9 cm
Length:	46 cm	46 cm
Target line:	<3 mm	<3 mm

2.3.2 The Very Compact DD Neutron Generator

For this study we have also considered a fictitious neutron generator with the same dimensions as the Am(Li) source outer tungsten bottle. This "ideal" neutron generator was assumed to produce an output of 10^7 n/s in either steady-state or pulsed modes. The small size would allow it to fit into the existing AWCC and UNCL systems without modification (except to accommodate the wires).

Table 4. Very compact neutron generator characteristics

Type of generator:	DD
Maximum emission rate:	1×10^7 n/s
Neutron energy:	2.48 MeV
Steady state/pulsed:	Both
Pulsed mode	
Frequency range:	One shot to 200 kHz
Duty cycle:	10 μs pulse width
Generator tube dimensions	
Diameter:	3.2 cm
Length:	5.7 cm
Target line:	2.8 cm

2.4 MEASUREMENT PRECISION FOR THE ACTIVE COINCIDENCE MEASUREMENT

The measurement precision of the active coincidence measurement is limited by the accidentals coincidence rate, which is related to the total neutron detection rate as

$$A = S^2 \cdot G \, ,$$

where A is the accidentals coincidence rate,
G is the coincidence gate width,
S is the total neutron counting rate.

The relative doubles rate measurement precision for active neutron coincidence counting can be approximated as

$$\frac{\sigma_D}{D} \cong \frac{\sqrt{2 \cdot \left(\varepsilon \cdot S_0 + S_{active} + S_{bkg} + S_{passive}\right)^2 \cdot G + D_{bkg} + D_{passive} + D_{active}}}{D \cdot \sqrt{t}},$$

where D is the observed doubles rates,
σ_D is the measurement uncertainty in the observed doubles rate,
S_0 is the neutron interrogation source strength,
ε is the detection efficiency for the interrogation neutron with the assembly in place,
S_{active} is the singles rate due to the induced fission within the fuel assembly,
$S_{passive}$ is the passive singles rate from spontaneous fission and (α, n) reactions in the fuel,
S_{bkg} is the background singles rate,
D_{active} is the doubles rate resulting from induced fission within the assembly,
$D_{passive}$ is the doubles rate due to spontaneous fission and (α, n) reactions in the fuel,
D_{bkg} is the background doubles rate,
t is the active measurement time.

As the interrogating source strength increases, the background and passive signal can be ignored so that the approximate relative error is given by

$$\frac{\sigma_D}{D} \cong \frac{\sqrt{2 \cdot (\varepsilon \cdot S_0)^2 \cdot G + D_{active}}}{D_{active} \cdot \sqrt{t}}.$$

For a given assembly, the doubles rates is proportional to the interrogating neutron source rate:

$$D_{active} = f(m) \cdot S_0$$

where $f(m)$ is the doubles rate response function per source neutron.

For active coincidence counting, the singles and doubles rates are proportional to the interrogating source strength, and the totals rate is roughly independent of the presence of the sample.

$$\frac{\sigma_D}{D} \cong \frac{\sqrt{2 \cdot (\varepsilon \cdot S_0)^2 \cdot G + D}}{D \cdot \sqrt{t}} = \frac{\sqrt{2 \cdot \varepsilon^2 \cdot G + f(m)/S_0}}{f(m) \cdot \sqrt{t}}$$

For a given ^{235}U linear density, as the interrogating source strength continues to increase the measurement precision reaches a lower limit,

$$\lim_{S_0 \to \infty} \frac{\sigma_D}{D} = \frac{\sqrt{2\varepsilon^2 \cdot G}}{f(m) \cdot \sqrt{t}} = \frac{const.}{f(m) \cdot \sqrt{t}}.$$

This tells us that the measurement precision achievable by active neutron coincidence counting is ultimately limited by the properties of the coincidence counting system, not the intensity of the interrogating source. As seen in Figure 8, the measurement precision for the Am(Li)-based UNCL approaches its minimum for interrogating source strengths greater than 50,000 n/s. To avoid this limitation in the measurement precision, a different measurement approach must be employed.

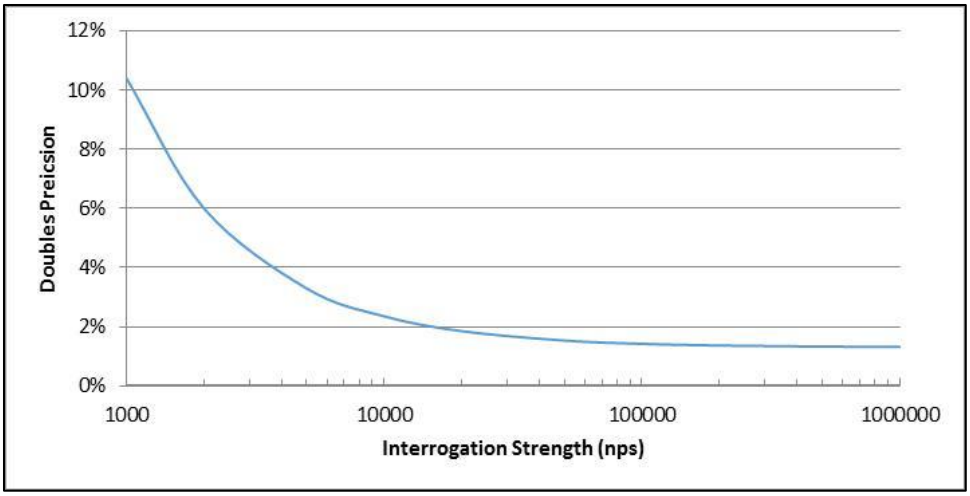

Figure 8. Doubles rate precision as a function of Am(Li) source strength for a representative fuel assembly.

Delayed neutron counting is an obvious alternative to active neutron coincidence counting. The delayed neutron measurement uses the same neutron generator, the same detector assembly, and the same counting arrangement as the active coincidence measurement. So we can expect the measurement response functions to exhibit similar behaviors and allow the existing correction factor forms to be applied in both methods. However, unlike the active coincidence measurement, the measurement precision continues to improve with increasing interrogation strength, allowing improvement in measurement performance beyond what is presently achievable with the Am(Li)-based UNCL measurements.

3. SIMULATED FUEL ASSEMBLIES FOR THE MCNP PERFORMANCE STUDY

To provide a performance comparison between the standard UNCL and the UNCL with DD generator, both configurations were modeled using MCNP6 Version 1.0 [12]. The performance of these systems was examined using the same series of simulated fuel assemblies as detailed for use in a recent comparison of alternative neutron detector techniques [2]. These assembly definitions are somewhat crude (lacking structural elements, and some material densities differ from true assemblies) but are sufficient to demonstrate relative performance of the DD/UNCL in comparison to the standard unit. The fuel assembly test cases include:

- Eight calibration assemblies, each a17 × 17 array with 264 fuel pins and 25 cooling channels. The ^{235}U enrichment was varied to provide linear mass densities 15–65 g ^{235}U/cm.
- Twelve assorted fuel configurations consisting of 14 × 14, 15 ×15, 16 × 16, and 17 × 17 intact arrays.
- Three sets of six assemblies, each a 17 × 17 array, containing differing numbers of burnable poison rods of varying composition.
- Six "partial defect" assemblies, each a 17 ×17 array, substituting DU rods for an increasing number of fuel pins.

The simulated fuel assemblies used in this study are described in the following sections.

3.1 DESCRIPTION OF THE SIMULATED CALIBRATION ASSEMBLIES

The comparison between the Am(Li) and DD generator performance included simulations of eight fuel 17 × 17 assemblies consisting of 264 fuel pins and 25 empty fuel guide tubes (Figure 9). For each assembly, the ^{235}U enrichment varied while all other parameters remained unchanged (

Table 5). Each assembly was 300 cm in length.

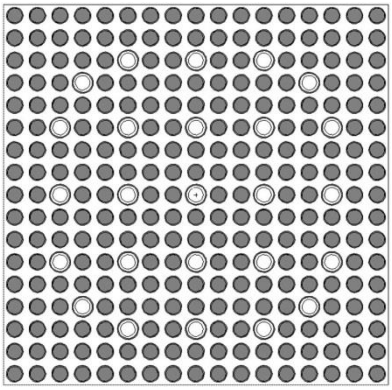

Figure 9. Cross-sectional images of the mock calibration fuel assemblies generated from the MCNP input files. The 17 × 17 assemblies consist of 264 fuel pins and 25 empty guide tubes.

Table 5. Input parameters for the 17 × 17 calibration assemblies

Assembly	Cal 1	Cal 2	Cal 3	Cal 4	Cal 5	Cal 6	Cal 7	Cal 8
Grid	17 × 17	17 × 17	17 × 17	17 × 17	17 × 17	17 × 17	17 × 17	17 × 17
Fuel pins	264	264	264	264	264	264	264	264
Array size (cm)	21.4	21.4	21.4	21.4	21.4	21.4	21.4	21.4
Pellet density (g/cm^3)	10.41	10.41	10.41	10.41	10.41	10.41	10.41	10.41
Pellet OD (cm)	0.8255	0.8255	0.8255	0.8255	0.8255	0.8255	0.8255	0.8255
Cladding OD (cm)	0.95	0.95	0.95	0.95	0.95	0.95	0.95	0.95
Cladding thickness (cm)	0.057	0.057	0.057	0.057	0.057	0.057	0.057	0.057
Enrichment (%)	1.16	1.54	1.93	2.70	3.47	4.24	4.63	5.01
Linear density (g ^{235}U/cm)	15.05	19.97	25.02	35.01	44.99	54.98	60.02	64.95

3.2 DESCRIPTION OF THE ASSORTED INTACT ASSEMBLIES

The UNCL is generally calibrated using a single set of assemblies, and this calibration is applied to other assemblies by application of appropriate correction factors (Section 1.3). This collection of 12 assemblies consists of various configurations, which serve to evaluate the effectiveness of the heavy metal correction factor (Figure 10). The 12 assemblies include 14 × 14, 15 × 15, 16 × 16, and 17 × 17 arrays with various arrangements of empty channels. The parameters for these assemblies are provided in

Table 6.

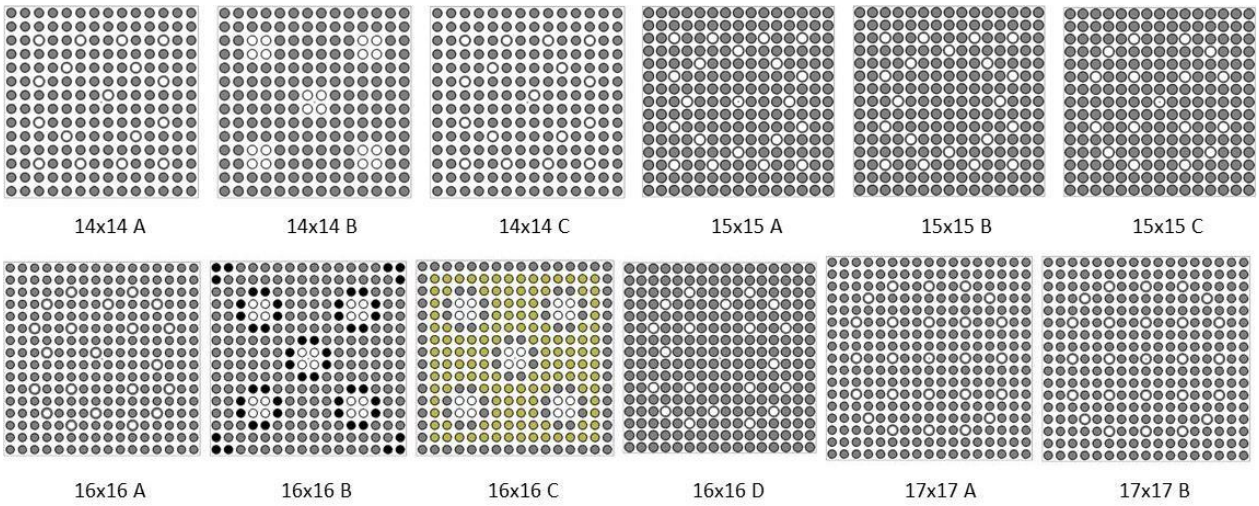

Figure 10. Cross-sectional images of the mock intact fuel assemblies generated from the MCNP input files.

Table 6. Input parameters for the various intact fuel assemblies

Assembly	14×14 A	14×14 B	14×14 C	15×15 A	15×15 B	15×15 C	16×16 A	16×16 B	16×16 C	16×16 D	17×17 A	17×17 B
Grid:	14 × 14	14 × 14	14 × 14	15 × 15	15 × 15	15 × 15	16 × 16	16 × 16	16 × 16	16 × 16	17 × 17	17 × 17
Array size (cm)	19.7	20.6	19.7	21.4	21.5	21.7	19.7	20.7	20.7	22.96	21.4	21.4
Pellet density (g/cm^3)	10.42	10.44	10.42	10.64	10.45	10.52	10.42	10.42	10.42	10.5	10.52	10.52
Pellet OD (cm)	0.875	0.968	0.875	0.929	0.911	0.940	0.784	0.819	0.819	0.911	0.819	0.819
Cladding OD (cm)	1.016	1.118	1.016	1.072	1.075	1.09	0.914	0.95	0.95	1.075	0.95	0.95
Cladding (cm)	0.062	0.066	0.062	0.062	0.073	0.064	0.057	0.057	0.057	0.073	0.057	0.057
Fuel pins 1	179	176	179	204	205	208	235	184	136	236	264	264
Enrichment type	3.80	3.13	2.00	4.50	5.00	4.55	4.50	4.50	2.92	4.50	3.22	4.20
Fuel pins 2								52	100			
Enrichment								4.00	2.42			
Linear density (g U/cm)	989	1,192	989	1,297	1,231	1,339	1,042	1,115	1,060	1,424	1,282	1,305
Linear density (g ^{235}U/cm)	37.57	37.31	19.77	58.37	61.54	60.91	46.89	50.13	30.93	64.08	41.54	54.19

3.3 DESCRIPTION OF THE SIMULATED ASSEMBLIES CONTAINING BURNABLE POISON RODS

To examine the impact of burnable poison rods on the performance of the UNCL, 18 different loadings of gadolinium were simulated. The 18 configurations included six different configurations of increasing numbers of poison rods, each at three different gadolinium loadings. The details of the assemblies are listed in

Table 7. The different configurations are designated by the number of poison rods and the gadolinium weight percentage. For example, BF6_4 indicates an assembly containing four burnable poison rods, each containing 6 w% gadolinium. The ^{235}U linear density for each of the burnable poison cases is shown in Table 8.

Table 7. Input parameters for the burnable poison fuel assemblies. The designation designator, n, in each assembly name represents the gadolinium content in wt% for each of the three gadolinium loadings (e.g., BP6-4 indicates 6 Gd wt% with four poison rods).

Assembly	BPn_4	BPn_8	BPn_12	BPn_16	BPn_20	BPn_24
Grid	17 × 17	17 × 17	17 × 17	17 × 17	17 × 17	17 × 17
Array size (cm)	21.4	21.4	21.4	21.4	21.4	21.4
Pellet density (g/cm3)	10.41	10.41	10.41	10.41	10.41	10.41
Poison density (g/cm^3)	10.21	10.21	10.21	10.21	10.21	10.21
Pellet OD (cm)	0.8255	0.8255	0.8255	0.8255	0.8255	0.8255
Cladding OD (cm)	0.95	0.95	0.95	0.95	0.95	0.95
Cladding thickness (cm)	0.057	0.057	0.057	0.057	0.057	0.057
Fuel pin enrichment (%)	4.00	4.00	4.00	4.00	4.00	4.00
Poison rod enrichment (%)	2.60	2.60	2.60	2.60	2.60	2.60
Fuel pins	260	256	252	248	244	240

Poison rods	4	8	12	16	20	24
Linear density (g ^{235}U/cm)	51.54	51.22	50.90	50.58	50.26	49.94

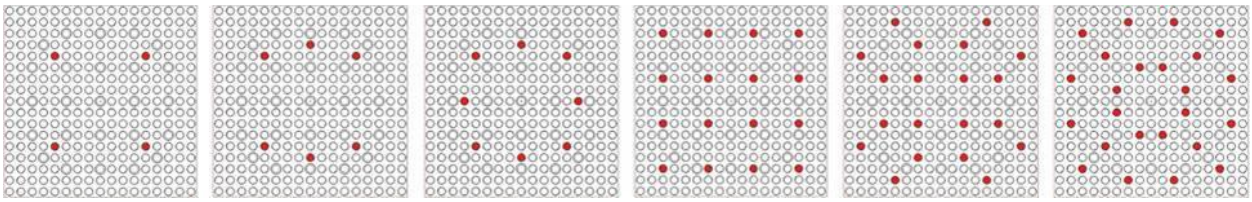

Figure 11. Distribution of the poison rods (red circles) within the simulated 17 ×17 fuel assemblies. The assemblies contain 4, 8, 12, 16, 20, and 24 burnable poison rods, respectively.

Table 8. ^{235}U linear density for the poison rod configurations

Gd content (wt%)	BPn-4	BPn-8	BPn-12	BPn-16	BPn-20	BPn-24
6	51.54	51.22	50.90	50.58	50.26	49.94
8	51.53	51.20	50.87	50.54	50.20	49.87
10	51.52	51.17	50.83	50.49	50.15	49.80

3.4 DESCRIPTION OF THE SIMULATED ASSEMBLIES FOR PARTIAL DEFECT ANALYSIS

To examine the response of the collar for partial defect analysis, a series of six fuel simulated assemblies were configured with an increasing number of DU rods substituted for fuel rods (Figure 12). The reference assembly has the same configuration as the calibration simulation CAL-6. The simulations will determine whether the DD/UNCL is more or less sensitive to substitution than the traditional collar. The assembly parameters are summarized in Table 9.

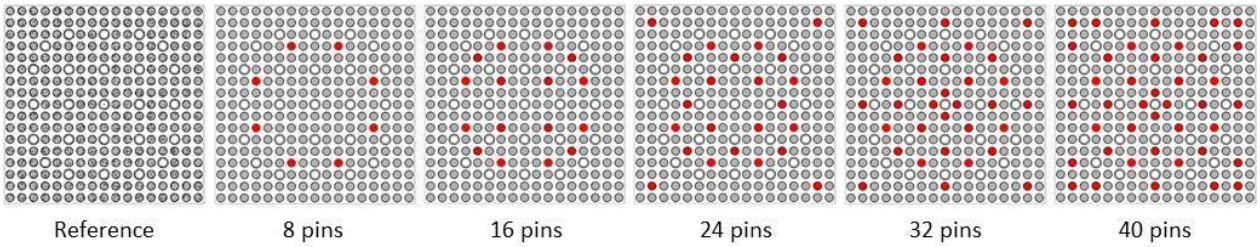

Figure 12. Distribution of the DU pins (red) within the simulated 17 × 17 assembly.

Table 9. Input parameters for the fuel assemblies for partial defect analysis

Assembly	PD-0	PD-8	PD-16	PD-24	PD-32	PD-40
Grid:	17 × 17	17 × 17	17 × 17	17 × 17	17 × 17	17 × 17
Array size (cm)	21.4	21.4	21.4	21.4	21.4	21.4
Pellet density (g/cm^3)	10.41	10.41	10.41	10.41	10.41	10.41
Pellet OD (cm)	0.8255	0.8255	0.8255	0.8255	0.8255	0.8255
Cladding OD (cm)	0.95	0.95	0.95	0.95	0.95	0.95
Cladding thickness (cm)	0.057	0.057	0.057	0.057	0.057	0.057
Fuel pin enrichment (%)	4.24	4.24	4.24	4.24	4.24	4.24
DU rod enrichment (%)	0.20	0.20	0.20	0.20	0.20	0.20
Fuel pins	264	256	248	240	232	224
DU rods	0	8	16	24	32	40
Linear density (g ^{235}U/cm)	54.97	53.38	51.80	50.21	48.62	47.03

4. AM(LI)/UNCL SIMULATED PERFORMANCE

To provide a performance baseline, the standard UNCL was modeled using MCNP6 Version 1.0 [12]. Figure 13 provides a screenshot of the MCNP input file describing the UNCL. The fuel assembly definitions used in the comparison were the same as provided for use in the neutron rodeo [2] and discussed in Section 3 above. The fuel assemblies include various array sizes (14 × 14 to 17 × 17) and include poison and partial defect configurations. Figure 14 illustrates the measurement arrangement with a fuel assembly in place inside the collar.

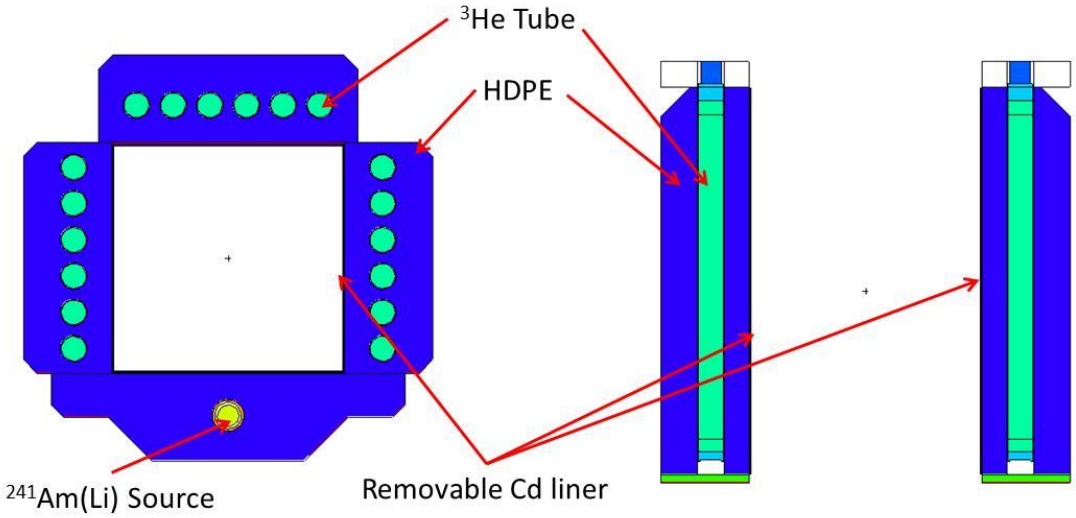

Figure 13. Screenshots from the MCNP input file using the MCNP Vsualization Editor VISED viewer showing cross-sectional views of the standard UNCL configured for PWR fuel assemblies in active mode.

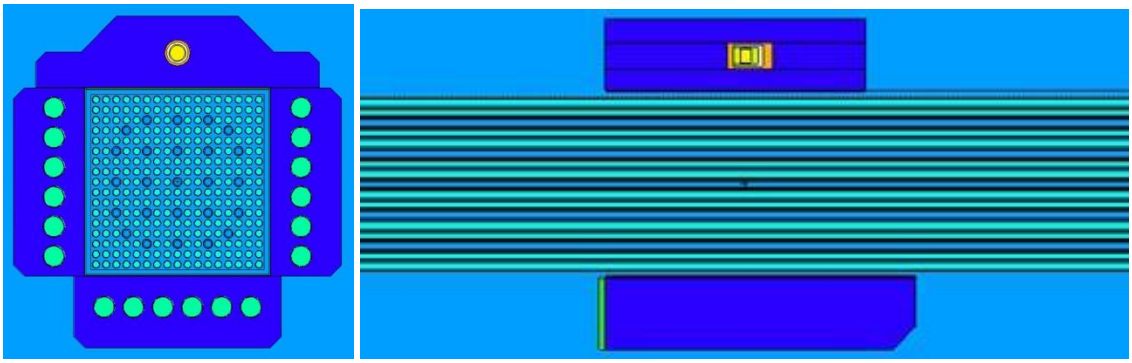

Figure 14. Screenshots from the VISED visualization tool of the MCNP input file for the 17 × 17 pin array used for the simulated calibrations.

NOTE: The MCNP simulations were of sufficient duration to provide <0.3% precision in the calculated doubles rates. Measurement precisions provided in the tables below represent the expected measurement precision from measurements on the simulated materials for assay times noted in the tables (e.g., 600 or 1,800 seconds).

4.1 AM(LI)/UNCL SIMULATED CALIBRATION

The simulated calibration rates based on the assemblies described in Section 3.1 are presented in Tables 10 and 11. The Am(Li) source term was adjusted to best fit the measured doubles rates reported by Menlove et al. [6, 3]. The results are plotted in Figure 15 for the thermal mode and in Figure 16 for the fast interrogation mode. As can be seen in figures, the MCNP simulations closely match the reported rates. We do note that it was necessary to apply different source terms to the thermal and fast mode simulations. These differences are attributable to the greater uranium linear density relative to the book calibration, uncertainty in the neutron energy distribution from Am(Li), and manufacturing differences between the unit modeled in this study and that used at Los Alamos National Laboratory for the collar calibrations. However, this approach allows us to easily use the measured calibration parameters reported in [6] for the performance comparison. We also note that the count rates measured at ORNL for a JCC-71 UNCL (Am(Li) source N458) agree with the predicted values based on these simulations.

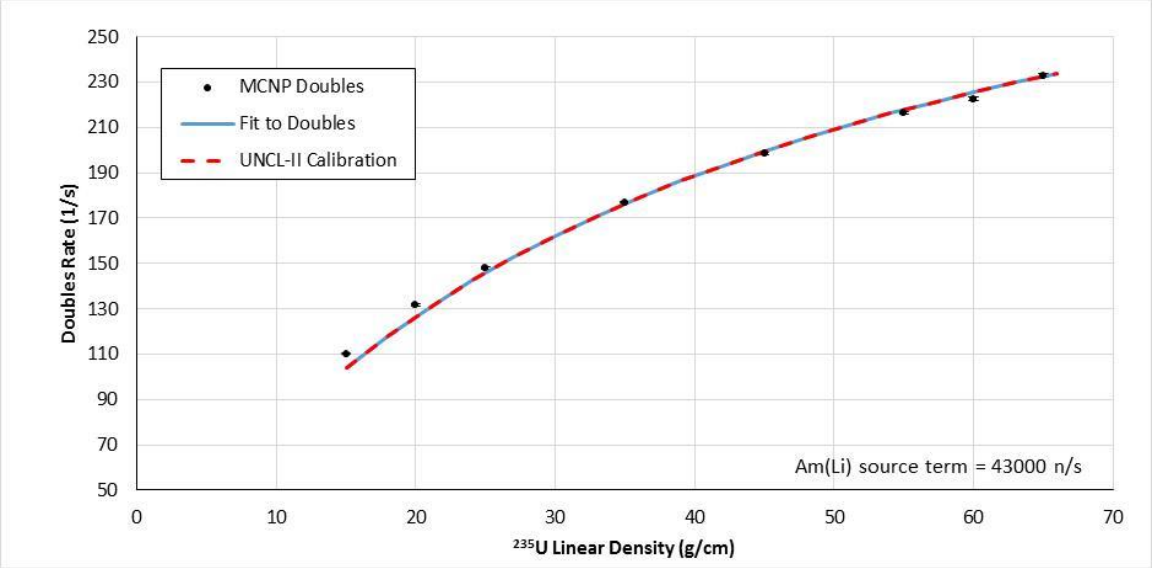

Figure 15. Am(Li) thermal mode calibration results (43,000 n/s source term) overlain with the measured UNCL-II calibration results [6].

Table 10. Simulated thermal mode, Am(Li)-based UNCL measurement results for the calibration assemblies‡

Fuel assembly ID	Declared LD ^{235}U (g/cm)	Singles rate (1/s)	Doubles rate (1/s)	600 sec σ_D (1/s)	1800 sec σ_D (1/s)	Analyzed LD ^{235}U (g/cm)*	600 sec LD uncert (g/cm)	1800 sec LD uncert (g/cm)	600 sec Total uncert (%)†	1800 sec Total uncert (%)†
17x17_cal_15	15.0	2,214.4	110.2	± 1.15	± 0.67	16.27	± 0.24	± 0.14	2.5	2.2
17x17_cal_20	20.0	2,330.7	131.6	± 1.22	± 0.70	21.20	± 0.30	± 0.18	2.5	2.2
17x17_cal_25	25.0	2,421.3	147.9	± 1.27	± 0.73	25.57	± 0.37	± 0.21	2.5	2.2
17x17_cal_35	35.0	2,554.2	177.0	± 1.34	± 0.77	35.21	± 0.51	± 0.30	2.5	2.2
17x17_cal_45	45.0	2,638.0	198.5	± 1.39	± 0.80	44.47	± 0.67	± 0.39	2.5	2.2
17x17_cal_55	55.0	2,701.8	216.4	± 1.43	± 0.82	54.15	± 0.86	± 0.50	2.6	2.2
17x17_cal_60	60.0	2,732.0	222.6	± 1.44	± 0.83	58.05	± 0.95	± 0.55	2.6	2.2
17x17_cal_65	65.0	2,762.0	232.8	± 1.46	± 0.84	65.25	± 1.11	± 0.64	2.6	2.2

‡ Uncertainties are the expected measurement performance values.
† Includes a 2% systematic contribution to the uncertainty.
* Heavy metal correction has been applied.

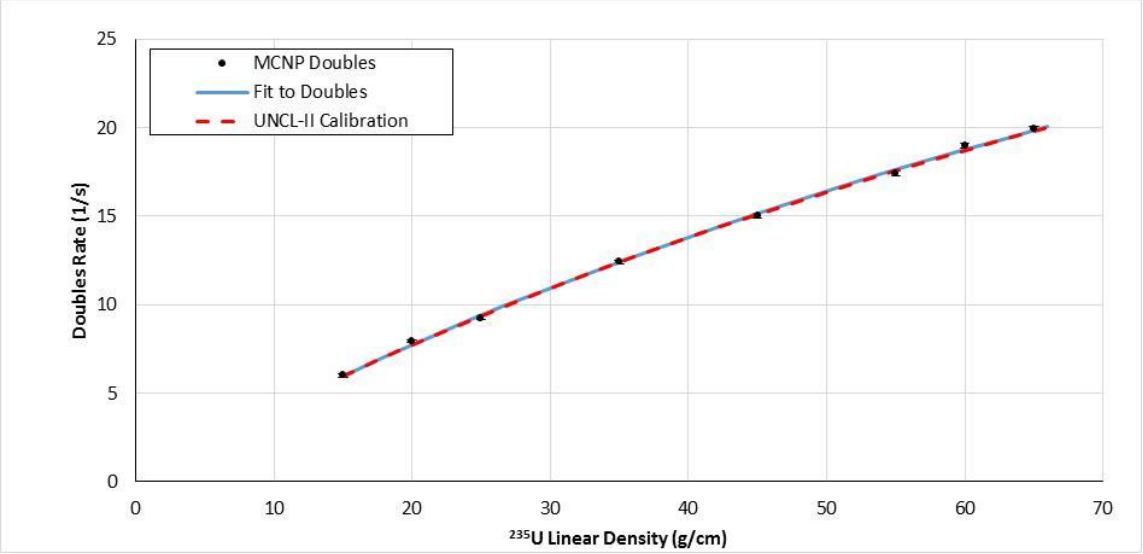

Figure 16. Am(Li) fast mode calibration results (50,940 n/s source term) overlain with the measured UNCL-II calibration results [6]. Note that the expected and measured curves are nearly identical for the assumed source strength.

Table 11. Simulated fast mode, Am(Li)-based UNCL measurement results for the calibration assemblies‡

Fuel assembly ID	Declared LD ^{235}U (g/cm)	Singles rate (1/s)	Doubles rate (1/s)	600 sec σ_D (1/s)	1,800 sec σ_D (1/s)	Analyzed LD ^{235}U (g/cm)*	600 sec LD uncert (g/cm)	1,800 sec LD uncert (g/cm)	600 sec total uncert (%)†	1,800 sec total uncert (%)†
17x17_cal_15	15.0	999.9	6.1	± 0.52	± 0.30	15.01	± 1.45	± 0.84	9.8	5.9
17x17_cal_20	20.0	1,010.5	8.1	± 0.53	± 0.30	20.52	± 1.57	± 0.91	7.9	4.9
17x17_cal_25	25.0	1,020.7	9.4	± 0.53	± 0.31	24.48	± 1.67	± 0.96	7.1	4.4
17x17_cal_35	35.0	1,039.9	12.7	± 0.55	± 0.32	34.82	± 1.93	± 1.11	5.9	3.8
17x17_cal_45	45.0	1,053.2	15.3	± 0.56	± 0.32	44.29	± 2.18	± 1.26	5.3	3.5
17x17_cal_55	55.0	1,069.3	17.7	± 0.57	± 0.33	53.84	± 2.45	± 1.41	5.0	3.3
17x17_cal_60	60.0	1,074.4	19.4	± 0.57	± 0.33	60.79	± 2.65	± 1.53	4.8	3.2
17x17_cal_65	65.0	1,081.8	20.3	± 0.58	± 0.33	65.03	± 2.78	± 1.61	4.7	3.2

‡ Uncertainties are the expected measurement performance values.
† Includes a 2% systematic contribution to the uncertainty.
* Heavy metal correction has been applied.

4.2 AM(LI)/UNCL SIMULATED PERFORMANCE FOR VARIOUS INTACT ASSEMBLIES

A series of simulations were performed using the descriptions for the assorted intact fuel assemblies described in Section 3.2. The simulated assay results are provided in Tables 12–15 and shown in Figures 17–18 for operation in the thermal and fast assay modes. For consistency with the evaluations in Ref. [2] measurement biases are discussed in terms of a somewhat ill-defined "mass defect" (i.e., the difference between the measured and declared linear ^{235}U density). The results are shown before and after application of the heavy metal correction, illustrating the need to apply the correction factors when considering the relative performance of the measurement for a given assembly. As can be seen in the Figure 18, the heavy metal correction is quite effective in improving the fast mode measurement performance using the parameters provided by Menlove et al. [3] and reproduced in Section 1.3.1 above.

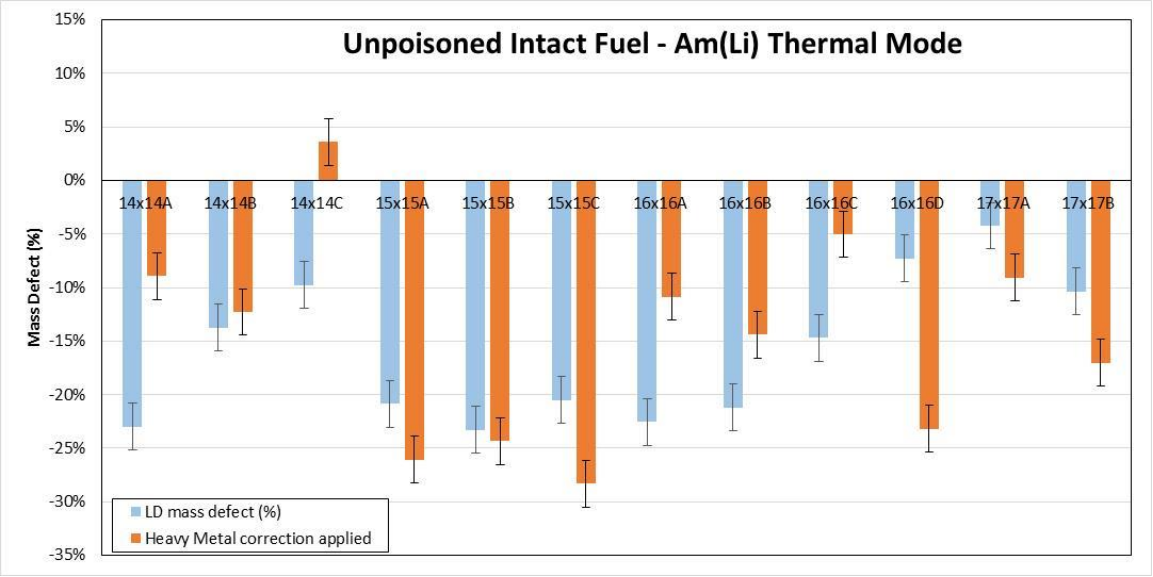

Figure 17. Results of the MCNP simulations for the UNCL with Am(Li) sources for the assorted intact fuel assemblies in the thermal mode. Error bars represent the project 1 sigma uncertainties for an 1,800 second measurement time.

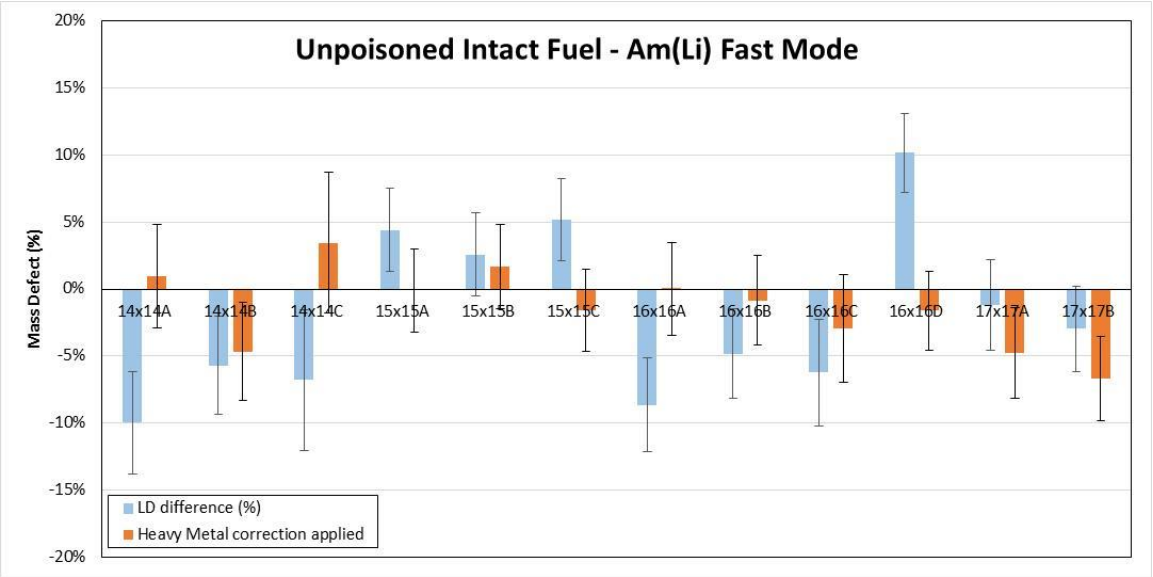

Figure 18. Results of the MCNP simulations for the UNCL with Am(Li) sources for the assorted intact fuel assemblies in the fast mode. Error bars represent the project 1 sigma uncertainties for an 1,800 second measurement time.

Table 12. Simulated thermal mode, Am(Li)-based UNCL measurement results for the unpoisoned, intact fuel assemblies‡

Fuel assembly ID	Declared LD ^{235}U (g/cm)	Singles rate (1/s)	Doubles rate (1/s)	600 sec σ_D (1/s)	1,800 sec σ_D (1/s)	Analyzed LD ^{235}U (g/cm)	600 sec LD uncert (g/cm)	1,800 sec LD uncert (g/cm)	600 sec Total uncert (%)†	1,800 sec Total uncert (%)†
14x14A	**37.57**	2,653.9	159.0	± 1.33	± 0.77	**28.93**	**± 0.42**	± 0.25	2.5	2.2
14x14B	**37.31**	2,609.4	168.7	± 1.32	± 0.76	**32.18**	**± 0.46**	± 0.27	2.5	2.2
14x14C	**19.78**	2,446.0	117.5	± 1.21	± 0.70	**17.85**	**± 0.27**	± 0.16	2.5	2.2
15x15A	**58.37**	2,727.7	202.0	± 1.39	± 0.80	**46.20**	**± 0.70**	± 0.40	2.5	2.2
15x15B	**61.54**	2,754.5	204.0	± 1.40	± 0.81	**47.20**	**± 0.72**	± 0.42	2.5	2.2
15x15C	**60.91**	2,726.5	206.3	± 1.39	± 0.80	**48.41**	**± 0.74**	± 0.43	2.5	2.2
16x16A	**46.90**	2,705.4	179.9	± 1.36	± 0.79	**36.33**	**± 0.54**	± 0.31	2.5	2.2
16x16B	**50.16**	2,705.7	187.7	± 1.37	± 0.79	**39.53**	**± 0.59**	± 0.34	2.5	2.2
16x16C	**30.95**	2,548.2	150.8	± 1.28	± 0.74	**26.40**	**± 0.38**	± 0.22	2.5	2.2
16x16D	**64.07**	2,731.3	224.7	± 1.40	± 0.81	**59.41**	**± 0.95**	± 0.55	2.6	2.2
17x17A	**41.29**	2,623.1	187.7	± 1.34	± 0.77	**39.54**	**± 0.57**	± 0.33	2.5	2.2
17x17B	**54.82**	2,702.3	207.7	± 1.38	± 0.80	**49.14**	**± 0.75**	± 0.43	2.5	2.2

‡ Uncertainties are the expected measurement performance values.
† Includes a 2% systematic contribution to the uncertainty.

Table 13. Simulated thermal mode, defect analysis results for the unpoisoned, intact fuel assemblies

Fuel Assembly ID	Defect without correction			Defect with HM correction applied		
	LD mass defect (%)	#σ 600 sec	#σ 1,800 sec	LD mass defect (%)	#σ 600 sec	#σ 1,800 sec
14x14A	−23.0	12.0	13.8	−8.9	3.8	4.5
14x14B	−13.7	6.5	7.4	−12.3	5.7	6.5
14x14C	−9.8	4.3	5.0	3.6	1.4	1.6
15x15A	−20.9	10.5	12.1	−26.1	14.2	16.2
15x15B	−23.3	12.1	13.9	−24.3	12.8	14.7
15x15C	−20.5	10.3	11.8	−28.3	16.0	18.2
16x16A	−22.5	11.7	13.4	−10.9	4.8	5.5
16x16B	−21.2	10.8	12.4	−14.4	6.6	7.7
16x16C	−14.7	7.0	8.0	−5.0	2.1	2.4
16x16D	−7.3	3.1	3.6	−23.2	12.3	13.9
17x17A	−4.2	1.8	2.0	−9.1	4.1	4.6
17x17B	−10.4	4.6	5.3	−17.0	8.3	9.5
Average bias	**−16.0%**			**14.7%**		
Std. deviation	**6.8%**			**9.5%**		

Table 14. Simulated fast mode, Am(Li)-based UNCL measurement results for the unpoisoned, intact fuel assemblies‡

Fuel assembly ID	Declared LD ^{235}U (g/cm)	Singles rate (1/s)	Doubles rate (1/s)	600 sec σ_D (1/s)	1800 sec σ_D (1/s)	Analyzed LD ^{235}U (g/cm)	600 sec LD uncert (g/cm)	1800 sec LD uncert (g/cm)	600 sec Total uncert (%)†	1800 sec Total uncert (%)†
14x14A	37.57	1,164.9	12.1	± 0.56	± 0.32	33.82	± 1.92	± 1.11	6.0	3.8
14x14B	37.31	1,111.2	12.4	± 0.53	± 0.31	35.18	± 1.87	± 1.08	5.7	3.7
14x14C	19.78	1,137.0	7.2	± 0.54	± 0.31	18.44	± 1.55	± 0.90	8.7	5.3
15x15A	58.37	1,132.4	18.9	± 0.55	± 0.32	60.94	± 2.51	± 1.45	4.6	3.1
15x15B	61.54	1,148.3	19.4	± 0.56	± 0.32	63.12	± 2.60	± 1.50	4.6	3.1
15x15C	60.91	1,129.0	19.6	± 0.55	± 0.32	64.05	± 2.58	± 1.49	4.5	3.1
16x16A	46.90	1,156.8	14.6	± 0.56	± 0.32	42.84	± 2.11	± 1.22	5.3	3.5
16x16B	49.92	1,142.0	15.8	± 0.55	± 0.32	47.51	± 2.20	± 1.27	5.0	3.3
16x16C	30.95	1,112.5	10.6	± 0.53	± 0.31	29.02	± 1.74	± 1.00	6.3	4.0
16x16D	64.07	1,088.4	21.0	± 0.54	± 0.31	70.57	± 2.67	± 1.54	4.3	3.0
17x17A	41.54	1,074.7	14.1	± 0.52	± 0.30	41.05	± 1.94	± 1.12	5.1	3.4
17x17B	54.19	1,093.2	17.0	± 0.53	± 0.31	52.59	± 2.23	± 1.29	4.7	3.2

‡ Uncertainties are the expected measurement performance values.
† Includes a 2% systematic contribution to the uncertainty.

Table 15. Simulated fast mode, defect analysis results for the unpoisoned, intact fuel assemblies

Fuel assembly ID	Defect without correction			Defect with HM correction applied		
	LD mass defect (%)	#σ 600 sec	#σ 1,800 sec	LD mass defect (%)	#σ 600 sec	#σ 1,800 sec
14x14A	−10.0	1.8	2.9	0.9	0.2	0.2
14x14B	−5.7	1.1	1.7	−4.7	0.9	1.3
14x14C	−6.8	0.8	1.4	3.4	0.4	0.6
15x15A	4.4	0.9	1.4	−0.1	0.0	0.0
15x15B	2.6	0.5	0.8	1.7	0.4	0.5
15x15C	5.1	1.1	1.6	−1.6	0.4	0.5
16x16A	−8.6	1.8	2.7	0.0	0.0	0.0
16x16B	−4.8	1.0	1.5	−0.9	0.2	0.3
16x16C	−6.2	1.1	1.7	−2.9	0.5	0.8
16x16D	10.1	2.2	3.1	−1.6	0.4	0.6
17x17A	−1.2	0.2	0.4	−4.8	1.0	1.5
17x17B	−3.0	0.7	1.0	−6.7	1.5	2.3
Average bias	**−2.0%**			**−1.4%**		
Std. deviation	**6.3%**			**2.9%**		

4.3 AM(LI)/UNCL SIMULATED PERFORMANCE FOR BURNABLE POISONS

The performance of the UNCL for assemblies containing burnable poisons is an important question when considering an alternative neutron interrogation source. The difference in neutron energy distribution from the sources and the change in moderating assembly to accommodate the larger, relative to Am(Li), source

will change the relative thermal neutron population in the interrogating neutron distribution. The simulated assemblies containing poison rods allow examination of the potential impact. Figure 19 illustrates the impact of the poison rods on the thermal mode mass results for the UNCL using an Am(Li) neutron source, and the fast mode results are shown in Figure 20. As can be seen, the number of poison rods is more important than rod's poison loading. The effectiveness of the poison rod correction can also be seen in the plots as the average bias is reduced to <1%, and the typical deviation from the expected value is reduced to less than 2% in both thermal and fast modes. The simulated rates and defect levels are presented in Tables 16–19.

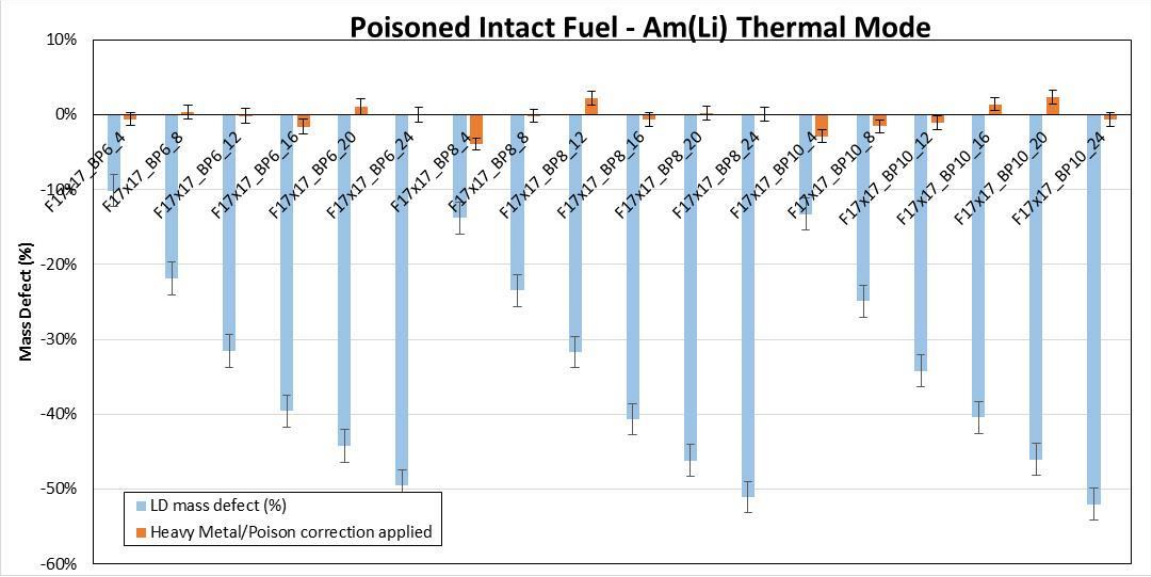

Figure 19. Thermal mode simulated assay results for the various burnable poison loadings with and without the heavy metal and poison rod correction.

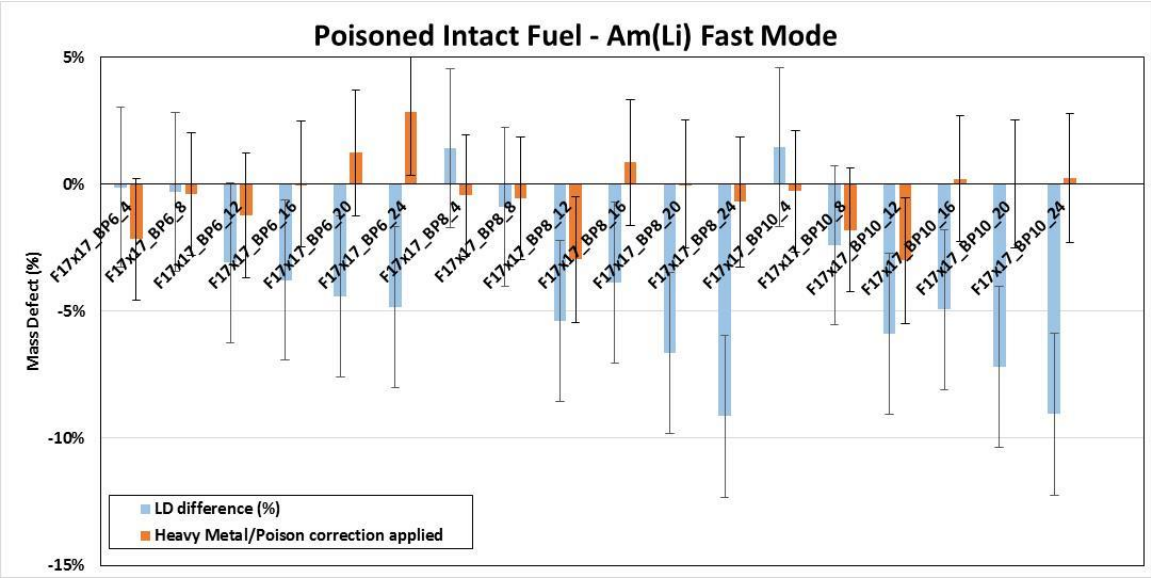

Figure 20. Fast mode assay results for the various burnable poison loadings with and without the heavy metal and poison rod correction.

Table 16. Simulated thermal mode, Am(Li)-based UNCL measurement results for the poisoned, intact fuel assemblies‡

Fuel assembly ID	Declared LD ^{235}U (g/cm)	Singles rate (1/s)	Doubles rate (1/s)	600 sec σ_D (1/s)	1800 sec σ_D (1/s)	Analyzed LD ^{235}U (g/cm)	600 sec LD uncert (g/cm)	1800 sec LD uncert (g/cm)	600 sec Total uncert (%)†	1800 sec Total uncert (%)†
BP6_4	51.50	2,603.9	202.2	± 1.34	± 0.77	46.27	± 0.68	± 0.39	2.5	2.2
BP6_8	51.20	2,522.5	188.8	± 1.31	± 0.76	40.01	± 0.57	± 0.33	2.5	2.2
BP6_12	50.90	2,438.6	176.0	± 1.28	± 0.74	34.83	± 0.48	± 0.28	2.4	2.2
BP6_16	50.60	2,350.4	164.1	± 1.24	± 0.71	30.59	± 0.41	± 0.24	2.4	2.1
BP6_20	50.30	2,282.3	156.2	± 1.21	± 0.70	28.05	± 0.38	± 0.22	2.4	2.1
BP6_24	49.90	2,199.3	146.6	± 1.17	± 0.68	25.18	± 0.33	± 0.19	2.4	2.1
BP8_4	51.50	2,603.8	198.4	± 1.20	± 0.69	44.40	± 0.58	± 0.34	2.4	2.1
BP8_8	51.20	2,509.8	186.9	± 1.16	± 0.67	39.19	± 0.49	± 0.28	2.4	2.1
BP8_12	50.90	2,430.7	175.8	± 1.12	± 0.65	34.76	± 0.42	± 0.24	2.3	2.1
BP8_16	50.50	2,337.6	162.2	± 1.08	± 0.62	29.95	± 0.36	± 0.21	2.3	2.1
BP8_20	50.20	2,263.9	152.8	± 1.05	± 0.60	27.01	± 0.32	± 0.18	2.3	2.1
BP8_24	49.90	2,187.7	143.9	± 1.01	± 0.58	24.42	± 0.28	± 0.16	2.3	2.1
BP10_4	51.50	2,599.2	198.9	± 1.20	± 0.69	44.65	± 0.58	± 0.34	2.4	2.1
BP10_8	51.20	2,504.1	185.1	± 1.16	± 0.67	38.44	± 0.48	± 0.28	2.4	2.1
BP10_12	50.80	2,415.9	172.2	± 1.12	± 0.64	33.41	± 0.41	± 0.23	2.3	2.1
BP10_16	50.50	2,328.9	162.5	± 1.08	± 0.62	30.08	± 0.36	± 0.21	2.3	2.1
BP10_20	50.20	2,255.4	153.1	± 1.04	± 0.60	27.09	± 0.31	± 0.18	2.3	2.1
BP10_24	49.80	2,175.9	141.9	± 1.01	± 0.58	23.89	± 0.27	± 0.16	2.3	2.1

‡ Uncertainties are the expected measurement performance values.
† Includes a 2% systematic contribution to the uncertainty.

Table 17. Simulated thermal mode, defect analysis results for the poisoned, intact fuel assemblies.

Fuel assembly ID	Defect without correction			HM and poison corrections applied		
	LD mass defect (%)	#σ 600 sec	#σ 1,800 sec	LD mass defect (%)	#σ 600 sec	#σ 1,800 sec
BP6_4	−10.2	4.6	5.2	−0.6	0.2	0.3
BP6_8	−21.9	11.4	12.9	0.4	0.1	0.2
BP6_12	−31.6	19.0	21.4	−0.2	0.1	0.1
BP6_16	−39.5	27.1	30.5	−1.6	0.6	0.7
BP6_20	−44.2	32.9	37.0	1.1	0.4	0.5
BP6_24	−49.5	40.9	45.9	0.0	0.0	0.0
BP8_4	−13.8	6.7	7.5	−3.9	1.7	1.9
BP8_8	−23.5	13.0	14.4	−0.2	0.1	0.1
BP8_12	−31.7	19.8	21.9	2.2	0.9	1.0
BP8_16	−40.7	29.5	32.4	−0.6	0.3	0.3
BP8_20	−46.2	37.1	40.7	0.2	0.1	0.1
BP8_24	−51.1	45.2	49.5	0.0	0.0	0.0
BP10_4	−13.3	6.4	7.2	−2.9	1.2	1.4
BP10_8	−24.9	14.1	15.6	−1.5	0.6	0.7
BP10_12	−34.2	22.2	24.6	−1.1	0.4	0.5
BP10_16	−40.4	29.2	32.1	1.4	0.5	0.6
BP10_20	−46.0	36.9	40.4	2.4	0.9	1.0
BP10_24	−52.0	47.0	51.5	−0.7	0.3	0.3
Average bias	**−34.2%**			**−0.3%**		
Std. deviation	**13.6%**			**1.6%**		

Table 18. Simulated fast mode, Am(Li)-based UNCL measurement results for the poisoned, intact fuel assemblies‡

Fuel assembly ID	Declared LD ^{235}U (g/cm)	Singles rate (1/s)	Doubles rate (1/s)	600 sec σ_D (1/s)	1,800 sec σ_D (1/s)	Analyzed LD ^{235}U (g/cm)	600 sec LD uncert (g/cm)	1,800 sec LD uncert (g/cm)	600 sec Total uncert (%)†	1,800 sec Total uncert (%)†
BP6_4	51.50	1,059.2	16.7	± 0.52	± 0.30	51.44	± 2.14	± 1.24	4.6	3.1
BP6_8	51.20	1,054.4	16.6	± 0.52	± 0.30	51.03	± 2.13	± 1.23	4.6	3.1
BP6_12	50.90	1,051.0	16.2	± 0.51	± 0.30	49.33	± 2.08	± 1.20	4.7	3.2
BP6_16	50.60	1,048.0	16.1	± 0.51	± 0.30	48.69	± 2.06	± 1.19	4.7	3.2
BP6_20	50.30	1,044.3	15.9	± 0.51	± 0.29	48.07	± 2.04	± 1.18	4.7	3.2
BP6_24	49.90	1,039.7	15.8	± 0.51	± 0.29	47.48	± 2.02	± 1.17	4.7	3.2
BP8_4	51.50	1,060.7	16.9	± 0.52	± 0.30	52.23	± 2.16	± 1.25	4.6	3.1
BP8_8	51.20	1,053.5	16.6	± 0.52	± 0.30	50.74	± 2.12	± 1.22	4.6	3.1
BP8_12	50.90	1,047.4	15.9	± 0.51	± 0.30	48.16	± 2.05	± 1.18	4.7	3.2
BP8_16	50.50	1,043.8	16.0	± 0.51	± 0.29	48.55	± 2.05	± 1.18	4.7	3.2
BP8_20	50.20	1,038.1	15.6	± 0.51	± 0.29	46.87	± 2.00	± 1.16	4.7	3.2
BP8_24	49.90	1,032.4	15.2	± 0.50	± 0.29	45.34	± 1.96	± 1.13	4.8	3.2
BP10_4	51.50	1,056.8	16.9	± 0.52	± 0.30	52.25	± 2.16	± 1.25	4.6	3.1
BP10_8	51.20	1,052.5	16.4	± 0.52	± 0.30	49.97	± 2.10	± 1.21	4.7	3.1
BP10_12	50.80	1,044.1	15.8	± 0.51	± 0.29	47.81	± 2.04	± 1.18	4.7	3.2
BP10_16	50.50	1,039.3	15.9	± 0.51	± 0.29	48.01	± 2.03	± 1.17	4.7	3.2
BP10_20	50.20	1,035.3	15.5	± 0.51	± 0.29	46.59	± 1.99	± 1.15	4.7	3.2
BP10_24	49.80	1,028.9	15.2	± 0.50	± 0.29	45.29	± 1.95	± 1.13	4.8	3.2

‡ Uncertainties are the expected measurement performance values.
† Includes a 2% systematic contribution to the uncertainty.

Table 19. Simulated fast mode, defect analysis results for the poisoned, intact fuel assemblies

Fuel assembly ID	Defect without correction			HM and poison corrections applied		
	LD mass defect (%)	#σ 600 sec	#σ 1,800 sec	LD mass defect (%)	#σ 600 sec	#σ 1,800 sec
BP6_4	−0.1	0.0	0.0	−2.2	0.5	0.7
BP6_8	−0.3	0.1	0.1	-0.4	0.1	0.1
BP6_12	−3.1	0.7	1.0	−1.2	0.3	0.4
BP6_16	−3.8	0.8	1.2	0.0	0.0	0.0
BP6_20	−4.4	1.0	1.5	1.2	0.3	0.4
BP6_24	−4.8	1.1	1.6	2.8	0.6	0.9
BP8_4	1.4	0.3	0.5	−0.4	0.1	0.1
BP8_8	−0.9	0.2	0.3	−0.5	0.1	0.2
BP8_12	−5.4	1.2	1.8	−3.0	0.6	1.0
BP8_16	−3.9	0.9	1.3	0.9	0.2	0.3
BP8_20	−6.6	1.5	2.2	0.0	0.0	0.0
BP8_24	−9.1	2.1	3.1	−0.7	0.1	0.2
BP10_4	1.5	0.3	0.5	−0.3	0.1	0.1
BP10_8	−2.4	0.5	0.8	−1.8	0.4	0.6
BP10_12	−5.9	1.3	2.0	−3.0	0.7	1.0
BP10_16	−4.9	1.1	1.6	0.2	0.0	0.1
BP10_20	−7.2	1.6	2.4	0.0	0.0	0.0
BP10_24	−9.0	2.1	3.1	0.2	0.0	0.1
Average bias	**−3.8%**			**−0.4%**		
Std. deviation	**3.2%**			**1.4%**		

4.4 AM(LI)/UNCL SIMULATED PARTIAL DEFECT ANALYSIS

One of the primary uses of the UNCL is to identify substitutions of fuel pins with empty channels or pins loaded with DU. This series of simulations examines the performance of the UNCL using an Am(Li) source for increasing numbers of rods substituted with DU. The mass defect relative to the "declared" value is shown in Figure 21 for the thermal mode and in Figure 22 for the fast mode. Rates and performance values are provided in Tables 20–23. Although the assembly configuration 17x17-PD_0 is the same as the 17x17_Cal_55, the simulations result in noticeable defects where normally none would be expected. This is the result of the MCNP random seed used in these simulations to prevent the injection of unintended biases into the analysis results. Keeping in mind that the effective measurement precision of the simulations is much better than that obtained even in an 1,800 second measurement, it is easy to understand the challenges of identifying substitutions with the UNCL.

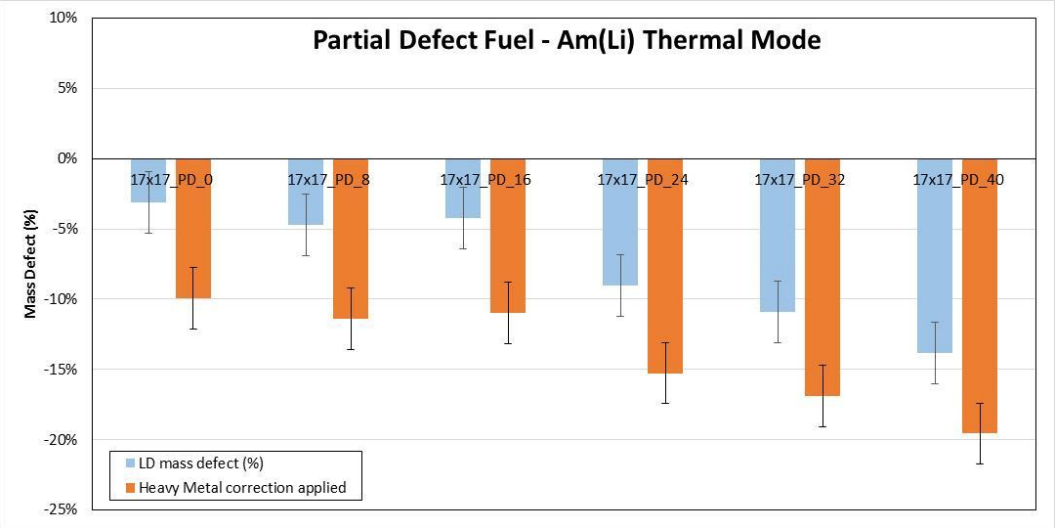

Figure 21. Thermal mode simulated assay results for the partial defect loadings with and without the heavy metal correction.

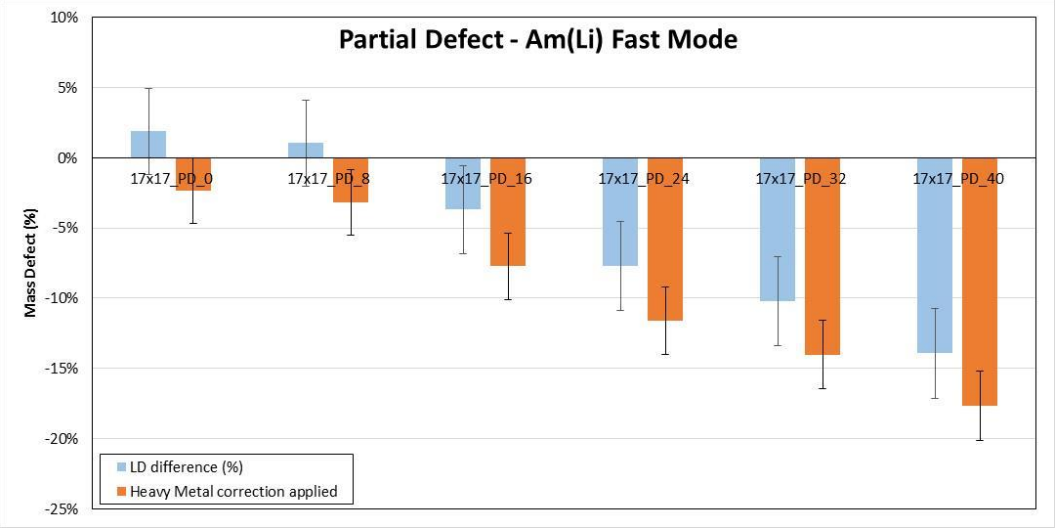

Figure 22. Fast mode simulated assay results for the partial defect loadings with and without the heavy metal correction.

Table 20. Simulated thermal mode, Am(Li)-based UNCL measurement results for the partial defect assembly configurations‡

Fuel assembly ID	Declared LD ^{235}U (g/cm)	Singles rate (1/s)	Doubles rate (1/s)	600 sec σ_D (1/s)	1,800 sec σ_D (1/s)	Analyzed LD ^{235}U (g/cm)	600 sec LD uncert (g/cm)	1,800 sec LD uncert (g/cm)	600 sec Total uncert (%)†	1,800 sec Total uncert (%)†
PD_0	54.98	2,703.9	215.0	± 1.39	± 0.80	53.29	± 0.82	± 0.47	2.5	2.2
PD_8	54.98	2,691.4	213.4	± 1.38	± 0.80	52.38	± 0.80	± 0.46	2.5	2.2
PD_16	54.98	2,691.0	213.9	± 1.38	± 0.80	52.65	± 0.81	± 0.47	2.5	2.2
PD_24	54.98	2,677.2	209.2	± 1.37	± 0.79	50.01	± 0.76	± 0.44	2.5	2.2
PD_32	54.98	2,663.9	207.4	± 1.36	± 0.79	48.99	± 0.73	± 0.42	2.5	2.2
PD_40	54.98	2,655.3	204.3	± 1.36	± 0.78	47.37	± 0.70	± 0.41	2.5	2.2

‡ Uncertainties are the expected measurement performance values.
† Includes a 2% systematic contribution to the uncertainty.

Table 21. Simulated thermal mode, defect analysis results for the partial defect assembly configurations†

Fuel assembly ID	Defect without correction			HM and poison corrections applied		
	LD mass defect (%)	#σ 600 sec	#σ 1,800 sec	LD mass defect (%)	#σ 600 sec	#σ 1,800 sec
PD_0	−3.1	1.3	1.5	−9.9	4.4	5.1
PD_8	−4.7	2.0	2.3	−11.4	5.2	5.9
PD_16	−4.2	1.8	2.0	−11.0	5.0	5.7
PD_24	−9.1	4.0	4.6	−15.3	7.3	8.3
PD_32	−10.9	4.9	5.6	−16.9	8.3	9.4
PD_40	−13.8	6.4	7.4	−19.6	9.9	11.2

† Cells highlighted in green indicate a reasonable probability of detection of the substitution.

Table 22. Simulated fast mode, Am(Li)-based UNCL measurement results for the partial defect assembly configurations‡

Fuel assembly ID	Declared LD ^{235}U (g/cm)	Singles rate (1/s)	Doubles rate (1/s)	600 sec σ_D (1/s)	1,800 sec σ_D (1/s)	Analyzed LD ^{235}U (g/cm)	600 sec LD uncert (g/cm)	1,800 sec LD uncert (g/cm)	600 sec Total uncert (%)†	1,800 sec Total uncert (%)†
PD_0	54.98	1,068.3	17.8	± 0.52	± 0.30	56.03	± 2.26	± 1.31	4.5	3.1
PD_8	54.98	1,068.5	17.7	± 0.52	± 0.30	55.56	± 2.25	± 1.30	4.5	3.1
PD_16	54.98	1,062.8	17.1	± 0.52	± 0.30	52.91	± 2.18	± 1.26	4.6	3.1
PD_24	54.98	1,061.1	16.5	± 0.52	± 0.30	50.67	± 2.12	± 1.23	4.6	3.1
PD_32	54.98	1,060.3	16.2	± 0.52	± 0.30	49.27	± 2.09	± 1.21	4.7	3.2
PD_40	54.98	1,057.9	15.7	± 0.51	± 0.30	47.18	± 2.04	± 1.18	4.8	3.2

‡ Uncertainties are the expected measurement performance values.
† Includes a 2% systematic contribution to the uncertainty.

Table 23. Simulated fast mode, defect analysis results for the partial defect assembly configurations

Fuel assembly ID	Defect without correction			HM and poison corrections applied		
	LD mass defect (%)	#σ 600 sec	#σ 1,800 sec	LD mass defect (%)	#σ 600 sec	#σ 1,800 sec
PD_0	1.9	0.4	0.6	−2.4	0.5	0.8
PD_8	1.1	0.2	0.3	−3.2	0.7	1.1
PD_16	−3.8	0.9	1.3	−7.7	1.9	2.7
PD_24	−7.9	1.8	2.7	−11.6	2.9	4.2
PD_32	−10.4	2.5	3.7	−14.0	3.5	5.2
PD_40	−14.2	3.5	5.2	−17.6	4.5	6.7

† Cells highlighted in green indicate a reasonable probability of detection of the substitution.

5. MP320 DD GENRATOR/UNCL SIMULATED PERFORMANCE

This section examines the performance of the integrated DD neutron generator and UNCL system operated as an active neutron coincidence counter (in the same fashion as the standard Am(Li)-based UNCL). In this operating mode, the neutron generator is operated in a steady-state (continuous) mode. The active slab containing the Am(Li) source is replaced with a similar slab enlarged to accept the neutron generator as illustrated by the MCNP screenshots in Figure 23 and in the photographs of the modified system in Figure 24.

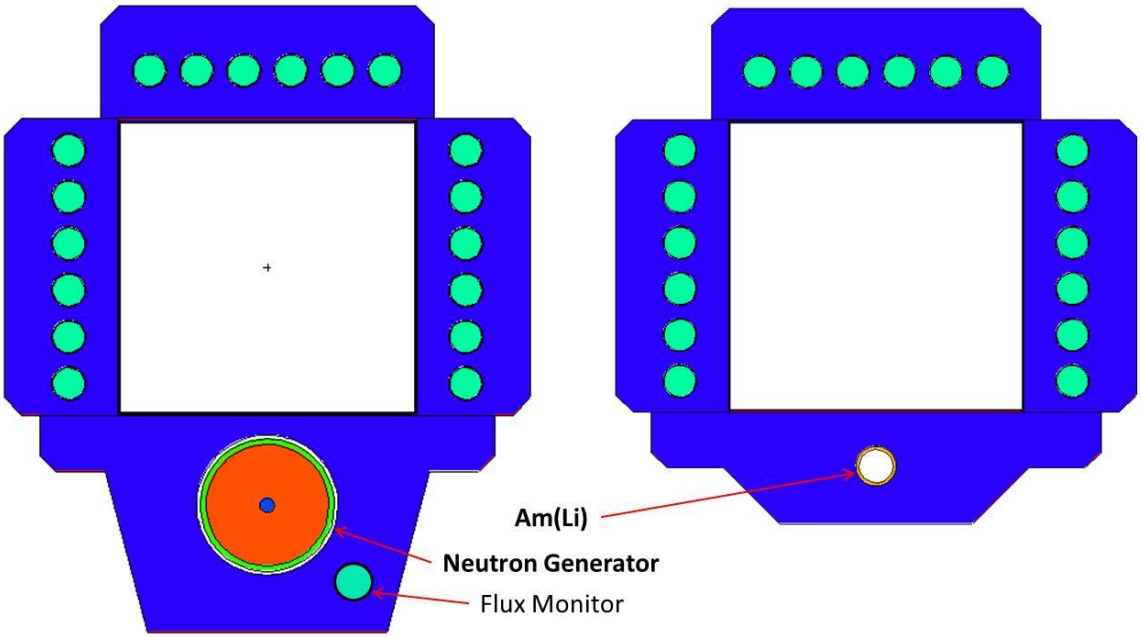

Figure 23. Screenshots of the MCNP VISED displays showing the modified UNCL (*left*) and the standard UNCL (*right*).

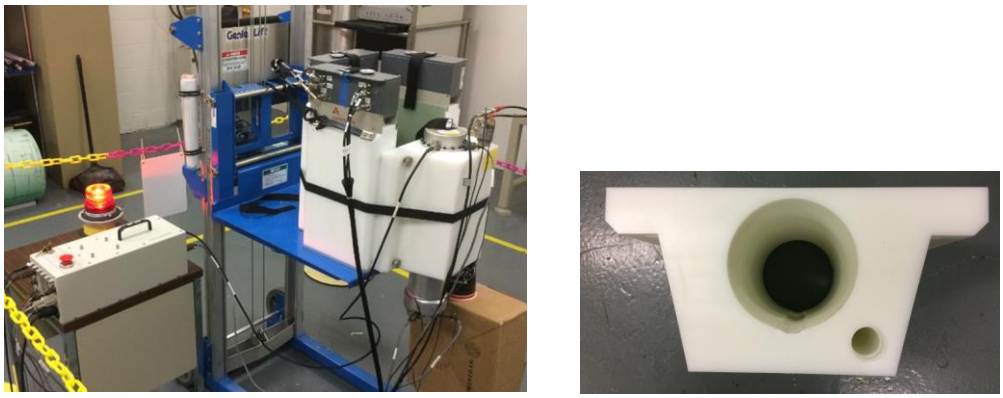

Figure 24. Photograph of the modified UNCL during testing (*left*) and the modified active slab for use with the MP320 generator (*right*).

The MP320 generator used in this study has been described previously in Section 2.2 and is installed in the UNCL as shown in Figure 24. Data is acquired using the same shift register electronics (a Canberra JSR-15) as used with the Am(Li)-based measurements. To track the fluctuations in the neutron output from the generator, a single ^{3}He proportional flux monitor tube has been added, and its output signal fed to one of the JSR-15's auxiliary scalar inputs (Figure 25).

The series of MCNP simulations for evaluation of active neutron coincidence performance of the Am(Li)/UNCL system discussed in Section 4 have been repeated for this arrangement, and the results are presented in the following sections.

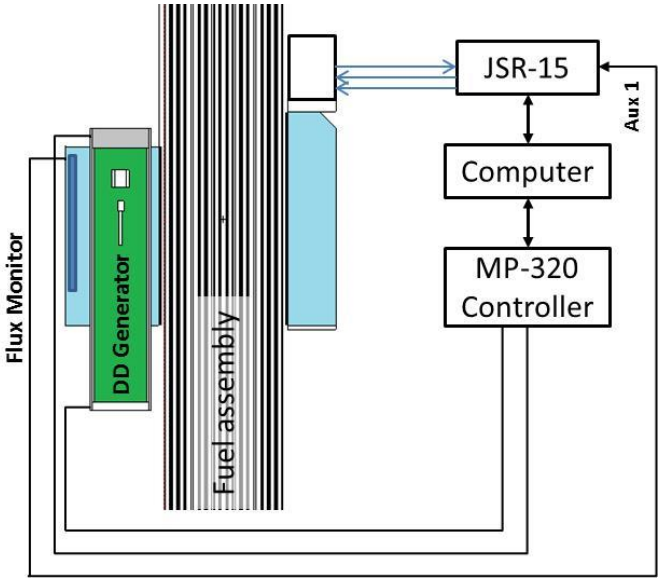

Figure 25. Schematic of the arrangement of the DD/UNCL measurement configuration for active coincidence counting.

5.1 DD/UNCL SIMULATED CALIBRATION

As was done for the Am(Li) source simulations discussed in Section 4, simulated thermal and fast calibration curves for the DD/UNCL were generated using the same assemblies described in Section 3.1. The neutron generator source term was adjusted to best reproduce the measured doubles rates reported by Menlove et al. [6, 3] for the thermal interrogation mode. The simulated thermal mode rates are provided in Table 24, and a comparison of the resulting calibration curve with the Am(Li)-based curve is shown in Figure 26. As Figure 26 shows, the thermal coincidence response as a function of linear density is very similar for all but the lowest ^{235}U loadings. This is not unexpected because the thermal mode induced fission rates are dominated by neutrons that have thermalized within the UNCL's active slab prior to reaching the fuel assembly.

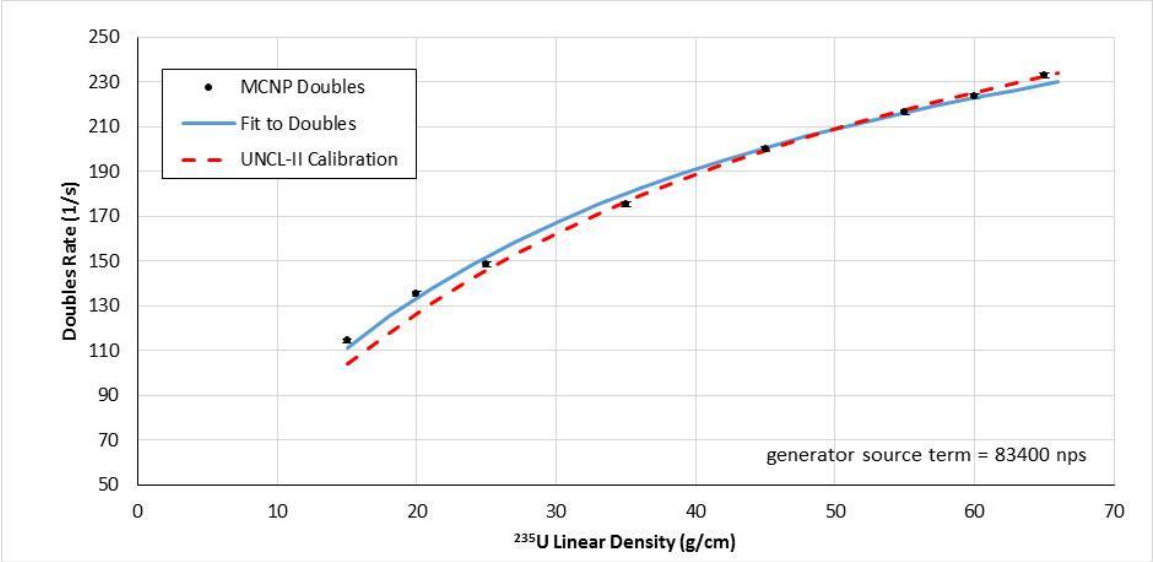

Figure 26. DD/UNCL thermal mode calibration results (83,200 n/s source term) overlain with the measured UNCL-II calibration results [6].

Table 24. Simulated thermal mode, DD/UNCL measurement results for the calibration assemblies‡ (83,200 n/s source term)

Fuel assembly ID	Declared LD ^{235}U (g/cm)	Singles rate (1/s)	Doubles rate (1/s)	600 sec σ_D (1/s)	1,800 sec σ_D (1/s)	Analyzed LD ^{235}U (g/cm)	600 sec LD uncert (g/cm)	1,800 sec LD uncert (g/cm)	600 sec Total uncert (%)†	1,800 sec Total uncert (%)†
17x17_cal_15	15.0	4,055.8	114.5	± 1.97	± 1.14	15.64	± 0.41	± 0.24	3.3	2.5
17x17_cal_20	20.0	4,169.4	135.5	± 2.03	± 1.17	20.45	± 0.51	± 0.30	3.2	2.5
17x17_cal_25	25.0	4,250.5	148.7	± 2.07	± 1.20	24.03	± 0.60	± 0.35	3.2	2.5
17x17_cal_35	35.0	4,366.0	175.4	± 2.13	± 1.23	33.08	± 0.84	± 0.49	3.2	2.5
17x17_cal_45	45.0	4,460.0	199.9	± 2.18	± 1.26	44.54	± 1.21	± 0.70	3.4	2.5
17x17_cal_55	55.0	4,533.2	216.4	± 2.22	± 1.28	54.97	± 1.60	± 0.92	3.5	2.6
17x17_cal_60	60.0	4,565.8	223.5	± 2.24	± 1.29	60.33	± 1.82	± 1.05	3.6	2.7
17x17_cal_65	65.0	4,589.7	232.9	± 2.25	± 1.30	68.65	± 2.18	± 1.26	3.8	2.7

‡ Uncertainties are the expected measurement performance values.
† Includes a 2% systematic contribution to the uncertainty.

The moderating effect of the HDPE in the active slab is illustrated in Figure 27. The plots on the right side show the induced fission rates in the fast mode configuration (i.e., cadmium curtains have been installed) for both the Am(Li) and neutron generator models. The plots on the left show the induced fission rate for the same assembly when operated in thermal mode. The fission rates induced by the thermalized neutrons far exceed the fast neutron induced fission rates, so we would not expect that the difference in average neutron energy between the Am(Li) and DD generator to have any significant effect in the thermal mode.

As seen in Figure 26 the neutron generator thermal response profile closely tracks that from the Am(Li) source. This is because in thermal mode, the induced fission rate is dominated by interrogating neutrons that have been thermalized in the moderator of the active bank prior to reaching the fuel assembly (Figure 27). The difference in interrogation energy (2.5 versus 0.5 keV) is washed out by the thermalization, so we expect a similar dependence with ^{235}U linear density for the DD generator and the Am(Li) sources.

However, when operated in fast mode (cadmium liners in place), the probability for inducing fission of the ^{238}U relative to inducing fission in ^{235}U increases significantly for the DD generator. Since the ^{238}U mass within each of the calibration assemblies does not vary significantly with enrichment, the coincidence signal from the ^{238}U events is nearly constant for the calibration assemblies. The ^{235}U signal essentially sits atop this ^{238}U active background signal and results in a reduction in the sensitivity of the DD generator measurement relative to the traditional Am(Li) based system.

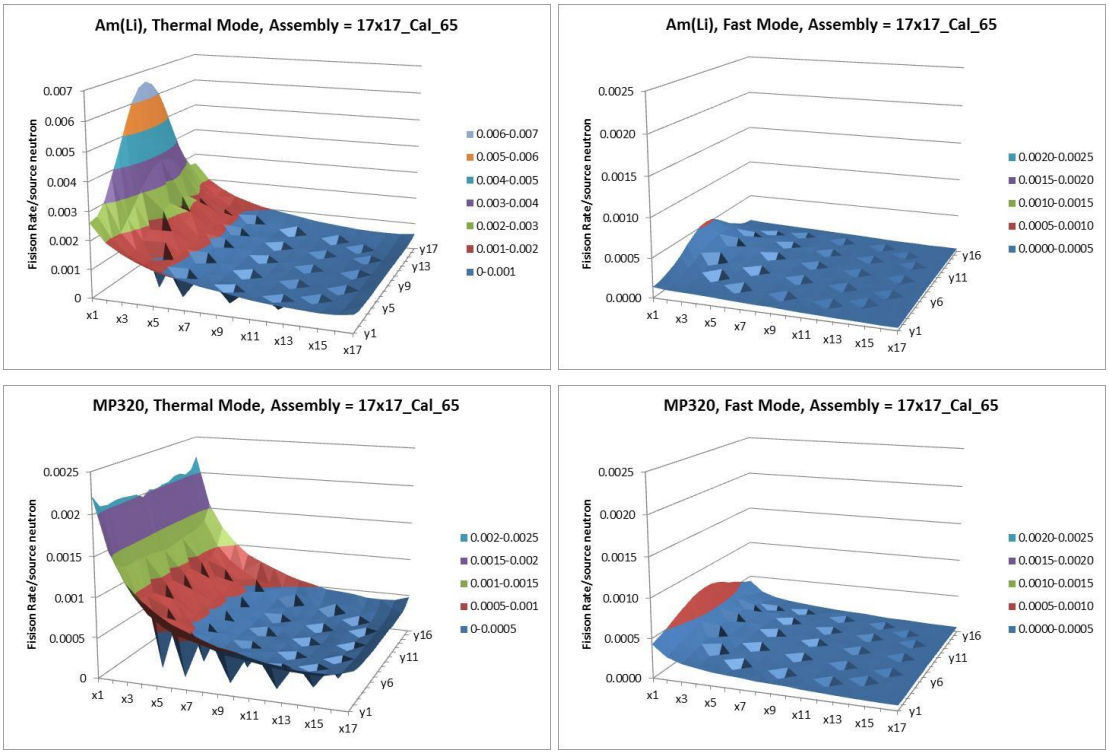

Figure 27. Comparison of the induced fission rates from the Am(Li)- and DD generator–based UNCL systems in both thermal and fast modes as a function of pin location within the assembly. Note the difference in vertical scale for the Am(Li) thermal mode plot.

Figure 28 replots the fast interrogation mode data shown in Figure 27 on a more readable scale. In both cases the fission events are concentrated near the interrogation source; however, because the neutron generation is further from the assembly using the MP320, the interrogation of the assembly is slightly more uniform using the generator than with the Am(Li) source.

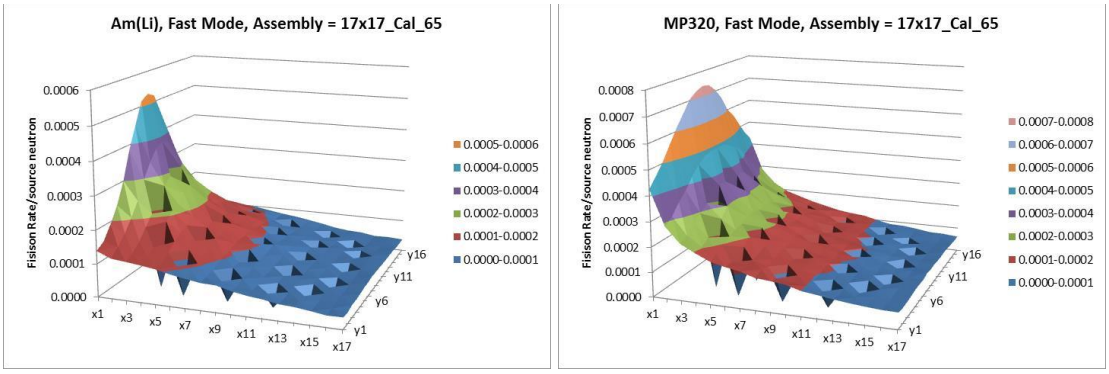

Figure 28. Comparison of the induced fission rates from the Am(Li)- and DD generator–based UNCL systems in fast modes as a function of pin location within the assembly.

The simulated calibration curve for the DD/UNCL operated in fast mode is shown in Figure 29, and the expected count rates and performance is summarized in Table 25. To illustrate the differences in slope, the neutron generator source term was adjusted to provide equivalent doubles rates for the 17x17_Cal_65 assembly. The shallow slope of the DD/UNCL response curve adversely effects the measurement precision of the reported ^{235}U linear density as the measurement is less sensitive to changes in the ^{235}U loading. For example, comparing the results in Table 11 with those in Table 25, we see that even though the fast mode singles and doubles rates for the assemblies 17x17_Cal_60 and 17x17_Cal_65 are equivalent for the Am(Li) and DD neutron interrogations, the expected measurement precision using the DD generator is a factor of 2 poorer than for the equivalent Am(Li)-based measurement.

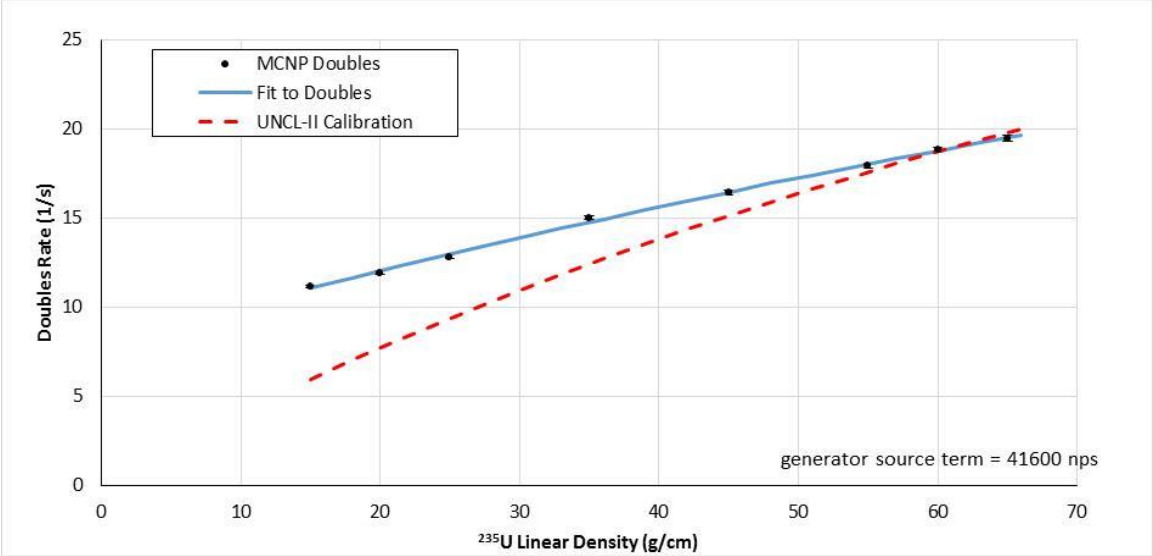

Figure 29. DD/UNCL fast mode calibration results 41,600 n/s source term) overlain with the measured UNCL-II calibration results [6].

Table 25. Simulated fast mode, DD/UNCL measurement results for the calibration assemblies‡ (41,600 n/s source term)

Fuel assembly ID	Declared LD ^{235}U (g/cm)	Singles rate (1/s)	Doubles rate (1/s)	600 sec σ_D (1/s)	1,800 sec σ_D (1/s)	Analyzed LD ^{235}U (g/cm)	600 sec LD uncert (g/cm)	1,800 sec LD uncert (g/cm)	600 sec Total uncert (%)†	1,800 sec Total uncert (%)†
17x17_cal_15	15.0	1,412.6	11.2	± 0.71	± 0.41	15.55	± 3.62	± 2.09	23.4	13.6
17x17_cal_20	20.0	1,421.1	11.9	± 0.72	± 0.41	19.48	± 3.73	± 2.15	19.3	11.2
17x17_cal_25	25.0	1,426.7	12.8	± 0.72	± 0.42	24.14	± 3.86	± 2.23	16.1	9.4
17x17_cal_35	35.0	1,438.7	15.0	± 0.73	± 0.42	36.30	± 4.22	± 2.44	11.8	7.0
17x17_cal_45	45.0	1,448.8	16.4	± 0.74	± 0.42	44.90	± 4.52	± 2.61	10.3	6.1
17x17_cal_55	55.0	1,458.8	17.9	± 0.74	± 0.43	54.31	± 4.88	± 2.82	9.2	5.6
17x17_cal_60	60.0	1,463.5	18.8	± 0.74	± 0.43	60.45	± 5.14	± 2.97	8.7	5.3
17x17_cal_65	65.0	1,466.0	19.5	± 0.75	± 0.43	64.92	± 5.35	± 3.09	8.5	5.2

‡ Uncertainties are the expected measurement performance values.
† Includes a 2% systematic contribution to the uncertainty.

The neutron generator source term used to create Figure 29 and populate Table 25 was selected for easy comparison with the doubles rates obtained using the Am(Li) source and does not provide optimum performance. Increasing the neutron generator yield can improve the measurement precision somewhat. Table 26 provides the expected measurement performance for the DD/UNCL system if the source term is increased to 2E5 n/s.

Table 26. Simulated fast mode, DD/UNCL measurement results for the calibration assemblies‡ (200,000 n/s source term)

Fuel assembly ID	Declared LD ^{235}U (g/cm)	Singles rate (1/s)	Doubles rate (1/s)	600 sec σ_D (1/s)	1,800 sec σ_D (1/s)	Analyzed LD ^{235}U (g/cm)	600 sec LD uncert (g/cm)	1,800 sec LD uncert (g/cm)	600 sec Total uncert (%)†	1,800 sec Total uncert (%)†
17x17_cal_15	15.0	6,791.3	53.6	± 3.20	± 1.85	15.55	± 3.38	± 1.95	21.8	12.7
17x17_cal_20	20.0	6,832.1	57.3	± 3.22	± 1.86	19.48	± 3.48	± 2.01	18.0	10.5
17x17_cal_25	25.0	6,859.2	61.5	± 3.23	± 1.87	24.14	± 3.59	± 2.07	15.0	8.8
17x17_cal_35	35.0	6,917.0	72.1	± 3.26	± 1.88	36.30	± 3.92	± 2.26	11.0	6.6
17x17_cal_45	45.0	6,965.4	79.0	± 3.28	± 1.90	44.90	± 4.19	± 2.42	9.6	5.8
17x17_cal_55	55.0	7,013.6	86.1	± 3.31	± 1.91	54.31	± 4.53	± 2.61	8.6	5.2
17x17_cal_60	60.0	7,035.9	90.5	± 3.32	± 1.92	60.45	± 4.77	± 2.75	8.1	5.0
17x17_cal_65	65.0	7,048.1	93.6	± 3.33	± 1.92	64.92	± 4.95	± 2.86	7.9	4.8

‡ Uncertainties are the expected measurement performance values.
† Includes a 2% systematic contribution to the uncertainty.

5.2 DD/UNCL SIMULATED PERFORMANCE FOR VARIOUS INTACT ASSEMBLIES

A series of simulations were performed using the descriptions for the assorted intact fuel assemblies described in Section 3.2. The simulated assay results are provided in Table 27 through Table 30 and shown in Figures 30 and 31 for operation in the thermal and fast assay modes. The results are shown before and after application of the heavy metal correction, illustrating the need to apply the correction factors when considering the relative performance of the measurement for a given assembly. For the DD generator–based measurement, the heavy metal (enrichment) correction becomes more important, relative to the Am(Li) interrogation, due to the increased fission rates in ^{238}U. The functional form is used for the correction

$$k_4 = 1 + \lambda_1 \cdot (\lambda_0 - \lambda) .$$

However, in this case the parameters λ_0 and $\lambda_1$are determined by a fit to the MCNP simulated rates. For these simulations, using the calibration assembly description linear density as the reference (taken as a whole, including the poisoned and partial defect assemblies) the data is best represented when

Thermal mode	Fast mode
λ_0 = 1,297 g/cm	λ_0 = 1,297 g/cm
λ_1 = 5.75E-4 cm/g	λ_1 = 6.60E-4 cm/g

The results suggest that the heavy metal correction for thermal mode interrogation may require assembly-specific calibrations.

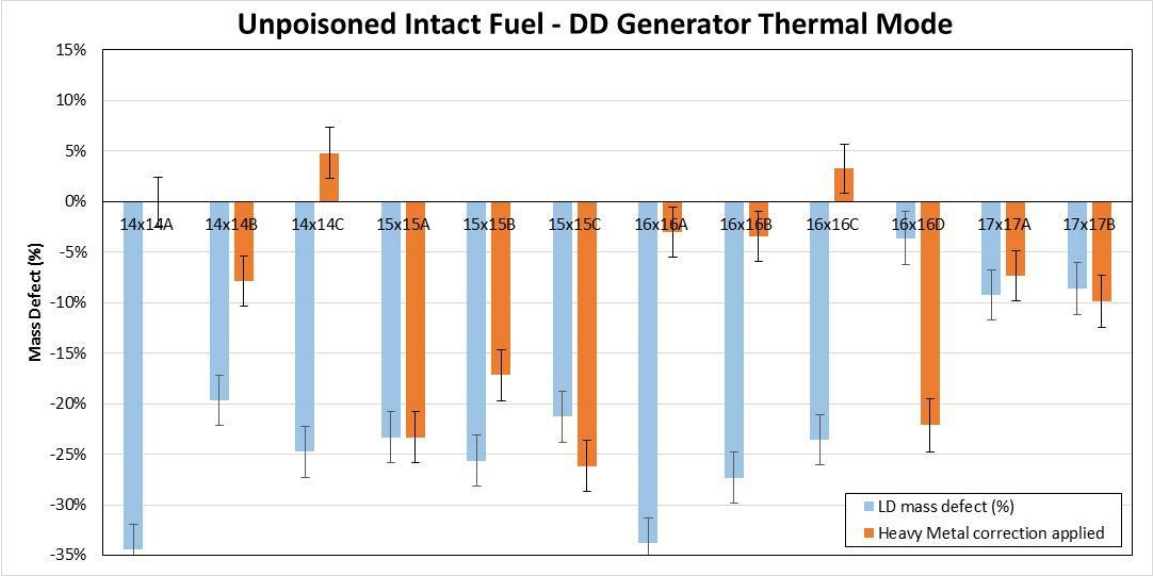

Figure 30. DD/UNCL (MP320 generator) thermal mode simulated assay results for the assorted intact fuel assemblies. Error bars represent the projected 1 sigma uncertainties for 1,800 second measurement time.

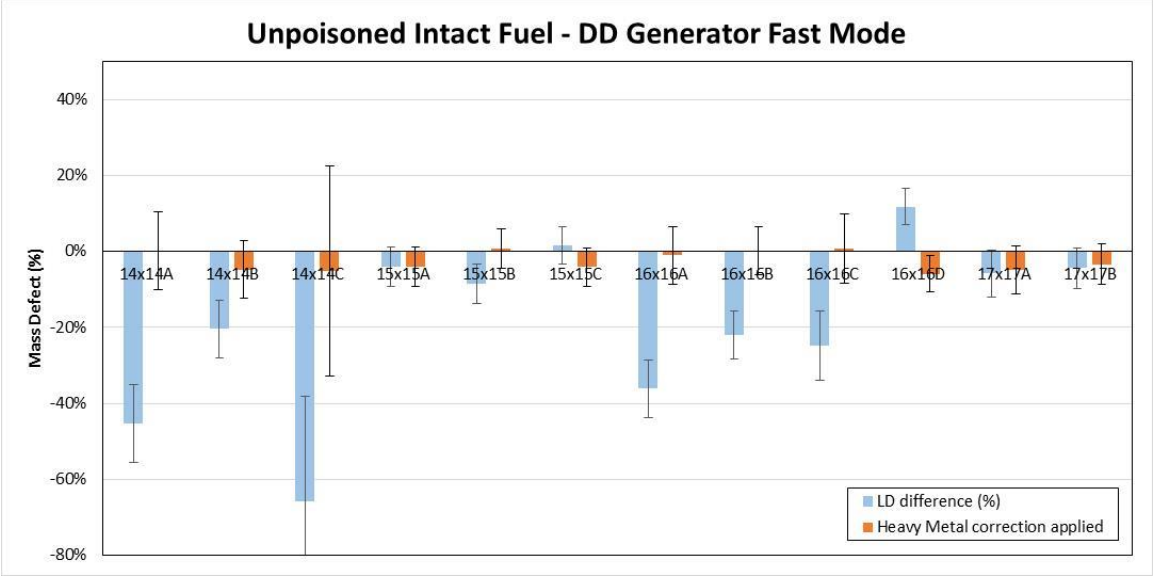

Figure 31. DD/UNCL (MP320 generator) fast mode simulated assay results for the assorted intact fuel assemblies. Error bars represent the projected 1 sigma uncertainties for 1,800 second measurement time.

Table 27. Simulated thermal mode, DD generator–based UNCL measurement results for the unpoisoned, intact fuel assemblies‡

Fuel assembly ID	Declared LD ^{235}U (g/cm)	Singles rate (1/s)	Doubles rate (1/s)	600 sec σ_D (1/s)	1,800 sec σ_D (1/s)	Analyzed LD ^{235}U (g/cm)	600 sec LD uncert (g/cm)	1,800 sec LD uncert (g/cm)	600 sec Total uncert (%)†	1,800 sec Total uncert (%)†
14x14A	**37.57**	4348.2	150.8	± 2.07	± 1.20	24.64	± 0.62	± 0.36	3.2	2.5
14x14B	**37.31**	4365.8	167.1	± 2.08	± 1.20	29.97	± 0.75	± 0.43	3.2	2.5
14x14C	**19.78**	4145.6	110.8	± 1.96	± 1.13	14.88	± 0.39	± 0.23	3.3	2.5
15x15A	**58.37**	4526.9	200.3	± 2.17	± 1.25	44.74	± 1.21	± 0.70	3.4	2.5
15x15B	**61.54**	4536.2	202.1	± 2.17	± 1.26	45.75	± 1.24	± 0.72	3.4	2.5
15x15C	**60.91**	4550.6	205.8	± 2.18	± 1.26	47.95	± 1.32	± 0.76	3.4	2.6
16x16A	**46.90**	4405.1	170.1	± 2.10	± 1.21	31.05	± 0.78	± 0.45	3.2	2.5
16x16B	**50.16**	4449.1	183.5	± 2.13	± 1.23	36.46	± 0.94	± 0.54	3.3	2.5
16x16C	**30.95**	4285.2	147.4	± 2.04	± 1.18	23.66	± 0.58	± 0.34	3.2	2.5
16x16D	**64.07**	4584.0	225.2	± 2.20	± 1.27	61.73	± 1.84	± 1.06	3.6	2.6
17x17A	**41.29**	4420.6	185.8	± 2.12	± 1.22	37.48	± 0.96	± 0.55	3.2	2.5
17x17B	**54.82**	4501.0	209.2	± 2.16	± 1.25	50.09	± 1.38	± 0.80	3.4	2.6

‡ Uncertainties are the expected measurement performance values.
† Includes a 2% systematic contribution to the uncertainty.

Table 28. Simulated DD generator–based UNCL thermal mode, defect analysis results for the unpoisoned, intact fuel assemblies.

Fuel Assembly ID	Defect without correction			Defect with HM correction applied		
	LD mass defect (%)	#σ 600 sec	#σ 1,800 sec	LD mass defect (%)	#σ 600 sec	#σ 1,800 sec
14x14A	−34.4	16.4	21.3	0.0	0.0	0.0
14x14B	−19.7	7.7	9.9	−12.3	4.1	5.4
14x14C	−24.8	9.9	13.1	3.6	1.0	1.3
15x15A	−23.3	9.1	12.0	−26.1	10.3	13.7
15x15B	−25.7	10.2	13.6	−24.3	8.6	11.9
15x15C	−21.3	8.0	10.6	−28.3	11.7	15.5
16x16A	−33.8	15.9	20.7	−10.9	3.1	4.4
16x16B	−27.3	11.6	15.1	−14.4	4.2	6.0
16x16C	−23.6	9.7	12.5	−5.0	1.4	2.0
16x16D	−3.6	1.1	1.4	−23.2	9.1	12.0
17x17A	−9.2	3.1	4.1	−9.1	3.0	4.0
17x17B	−8.6	2.8	3.7	−17.0	5.7	7.8
Average bias	**−21.3%**			**−13.9%**		
Std. deviation	**9.7%**			**10.3%**		

Table 29. Simulated fast mode, DD generator–based UNCL, based UNCL measurement results for the unpoisoned, intact fuel assemblies‡.

Fuel assembly ID	Declared LD ^{235}U (g/cm)	Singles rate (1/s)	Doubles rate (1/s)	600 sec σ_D (1/s)	1,800 sec σ_D (1/s)	Analyzed LD ^{235}U (g/cm)	600 sec LD uncert (g/cm)	1,800 sec LD uncert (g/cm)	600 sec Total uncert (%)†	1,800 sec Total uncert (%)†
14x14A	37.57	7,003.6	58.3	± 3.25	± 1.88	20.55	± 3.54	± 2.04	17.2	9.9
14x14B	37.31	6,981.6	66.5	± 3.24	± 1.87	29.72	± 3.74	± 2.16	12.7	7.3
14x14C	19.78	6,923.7	45.1	± 3.21	± 1.85	6.78	± 3.22	± 1.86	47.6	27.5
15x15A	58.37	7,159.5	87.4	± 3.33	± 1.92	56.06	± 4.62	± 2.67	8.5	4.8
15x15B	61.54	7,164.6	87.6	± 3.33	± 1.92	56.34	± 4.63	± 2.67	8.5	4.7
15x15C	60.91	7,171.2	91.5	± 3.34	± 1.93	61.87	± 4.85	± 2.80	8.1	4.5
16x16A	46.90	7,035.0	66.7	± 3.27	± 1.89	29.97	± 3.77	± 2.18	12.7	7.3
16x16B	49.92	7,052.7	74.2	± 3.28	± 1.89	38.89	± 4.01	± 2.32	10.5	6.0
16x16C	30.95	6,971.9	60.8	± 3.24	± 1.87	23.29	± 3.58	± 2.07	15.5	8.9
16x16D	64.07	7,117.0	97.9	± 3.31	± 1.91	71.63	± 5.23	± 3.02	7.6	4.2
17x17A	41.54	6,968.5	74.4	± 3.24	± 1.87	39.11	± 3.97	± 2.29	10.4	5.9
17x17B	54.19	7,027.5	84.3	± 3.27	± 1.89	51.80	± 4.39	± 2.53	8.7	4.9

‡ Uncertainties are the expected measurement performance values.
† Includes a 2% systematic contribution to the uncertainty.

Table 30. Simulated DD generator–based UNCL fast mode, defect analysis results for the unpoisoned, intact fuel assemblies

Fuel assembly ID	Defect without correction			Defect with HM correction applied		
	LD mass defect (%)	#σ 600 sec	#σ 1,800 sec	LD mass defect (%)	#σ 600 sec	#σ 1,800 sec
14x14A	−45.3	4.8	8.2	0.2	0.0	0.0
14x14B	−20.3	2.0	3.4	−4.8	0.4	0.7
14x14C	−65.7	4.0	7.0	−5.3	0.2	0.4
15x15A	−4.0	0.5	0.8	−4.0	0.5	0.8
15x15B	−8.4	1.1	1.8	0.8	0.1	0.2
15x15C	1.6	0.2	0.3	−4.2	0.5	0.9
16x16A	−36.1	4.4	7.5	−1.0	0.1	0.2
16x16B	−22.1	2.7	4.5	0.2	0.0	0.0
16x16C	−24.8	2.1	3.6	0.6	0.0	0.1
16x16D	11.8	1.4	2.3	−5.9	0.8	1.4
17x17A	−5.9	0.6	1.0	−4.9	0.5	0.8
17x17B	−4.4	0.5	0.9	−3.5	0.4	0.7
Average bias	**−18.6%**			**−2.6%**		
Std. deviation	**22.0%**			**2.6%**		

5.3 DD/UNCL SIMULATED PERFORMANCE FOR BURNABLE POISONS

The performance of the UNCL for assemblies containing burnable poisons is an important question when considering an alternative neutron interrogation source. The difference in neutron energy distribution from the sources and the change in moderating assembly to accommodate the larger, relative to Am(Li), source will change the relative thermal neutron population in the interrogating neutron distribution. The simulated assemblies containing poison rods allow examination of the potential impact. Figure 32 illustrates the impact of the poison rods on the thermal mode mass results for the UNCL using an Am(Li) neutron source, and the fast mode results are shown in Figure 33. As can be seen, the number of poison rods is more important than rod's poison loading. The effectiveness of the poison rod correction can also be seen in the plots. The average bias is reduced to <1%, and the typical deviation from the expected value is reduced to less than 2% in both thermal and fast modes. The simulated rates and defect levels are presented in Tables 32–35.

The parameters in the expression for the poison rod correction factor, k_3, were adjusted by a fit to the MCNP simulations. The expression for k_3 from discussed above in Section 1.3.2 [6] is shown here with the potentially adjustable parameters *a*, *b*, and *c*.

$$k_3 = 1 + \frac{a \cdot n}{N} \cdot \left(1 - e^{-b \cdot Gd}\right) \cdot (1 - c \cdot E_N)$$

where n is the number of poison rods,
N is the number of fuel rods (fuel + poison),
Gd is the weight percent of the gadolinium in the poison rods,
E_N is the declared enrichment.

It was found that it was only necessary to adjust the parameter, b, to obtain results similar to those obtained for the Am(Li)-based UNCL system. The parameters for the MP320/UNCL system are provided in Table 31.

Table 31. Poison Rod Correction Parameters for the MP320/UNCL system.

Parameter	Thermal mode		Fast mode	
	Am(Li)	MP320	Am(Li)	MP320
a	9.86	3.11	0.602	0.555
b	0.647	0.647	0.647	0.647
c	0.176	0.176	—	—

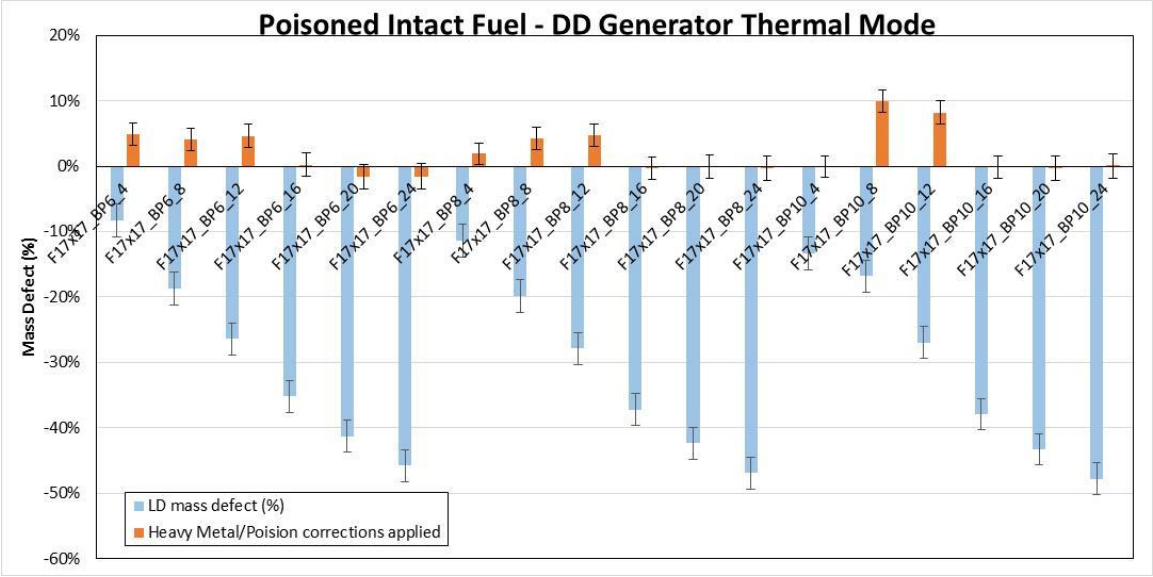

Figure 32. DD/UNCL (MP320) thermal mode simulated assay results for the various burnable poison loadings with and without the heavy metal and poison rod correction.

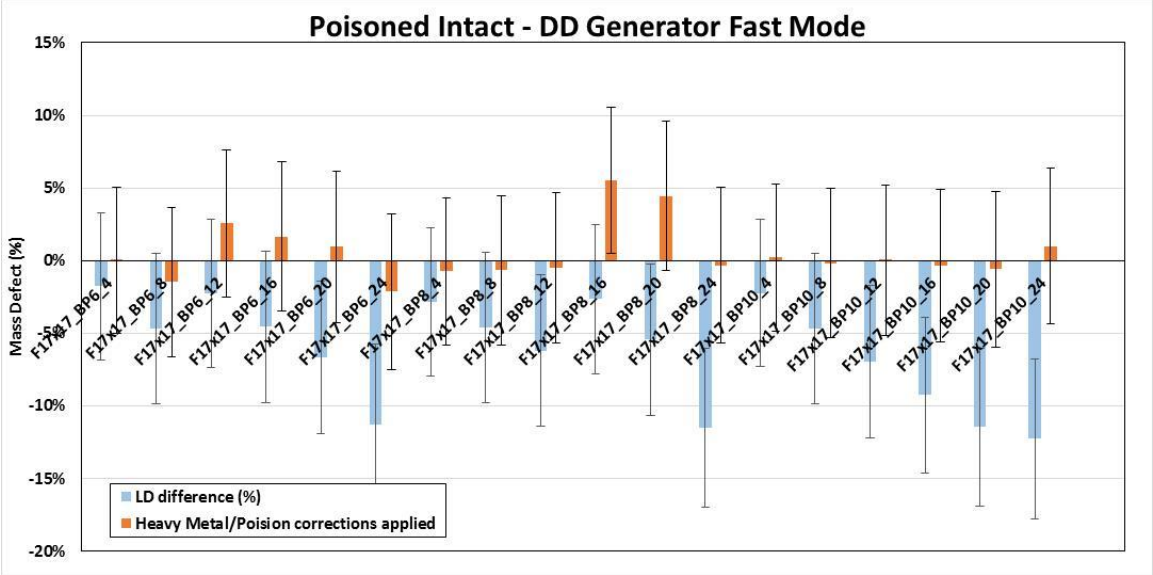

Figure 33. DD/UNCL (MP320) fast mode assay results for the various burnable poison loadings with and without the heavy metal and poison rod correction.

Table 32. Simulated thermal mode, DD/ UNCL measurement results for the poisoned, intact fuel assemblies‡.

Fuel assembly ID	Declared LD ^{235}U (g/cm)	Singles rate (1/s)	Doubles rate (1/s)	600 sec σ_D (1/s)	1,800 sec σ_D (1/s)	Analyzed LD ^{235}U (g/cm)	600 sec LD uncert (g/cm)	1,800 sec LD uncert (g/cm)	600 sec Total uncert (%)†	1,800 sec Total uncert (%)†
BP6_4	51.50	4,442.3	204.6	± 2.13	± 1.23	47.26	± 1.27	± 0.73	3.3	2.5
BP6_8	51.20	4,392.3	194.3	± 2.12	± 1.22	41.60	± 1.08	± 0.62	3.3	2.5
BP6_12	50.90	4,322.5	185.7	± 2.08	± 1.20	37.45	± 0.94	± 0.54	3.2	2.5
BP6_16	50.60	4,230.4	174.6	± 2.04	± 1.18	32.78	± 0.80	± 0.46	3.2	2.4
BP6_20	50.30	4,180.1	165.9	± 2.02	± 1.17	29.53	± 0.71	± 0.41	3.1	2.4
BP6_24	49.90	4,121.4	158.6	± 1.99	± 1.15	27.05	± 0.65	± 0.37	3.1	2.4
BP8_4	51.50	4,445.4	201.9	± 2.05	± 1.19	45.65	± 1.17	± 0.67	3.2	2.5
BP8_8	51.20	4,385.6	193.2	± 2.03	± 1.17	41.03	± 1.02	± 0.59	3.2	2.5
BP8_12	50.90	4,320.0	184.1	± 2.00	± 1.15	36.71	± 0.88	± 0.51	3.1	2.4
BP8_16	50.50	4,220.3	171.9	± 1.95	± 1.13	31.72	± 0.74	± 0.43	3.1	2.4
BP8_20	50.20	4,164.1	164.2	± 1.92	± 1.11	28.94	± 0.67	± 0.38	3.0	2.4
BP8_24	49.90	4,108.6	156.8	± 1.90	± 1.10	26.48	± 0.60	± 0.35	3.0	2.4
BP10_4	51.50	4,440.8	200.1	± 2.05	± 1.18	44.64	± 1.14	± 0.66	3.2	2.5
BP10_8	51.20	4,375.7	196.3	± 2.02	± 1.17	42.59	± 1.06	± 0.61	3.2	2.5
BP10_12	50.80	4,307.9	185.0	± 1.99	± 1.15	37.11	± 0.89	± 0.51	3.1	2.4
BP10_16	50.50	4,214.0	170.9	± 1.95	± 1.12	31.36	± 0.73	± 0.42	3.1	2.4
BP10_20	50.20	4,152.1	162.8	± 1.92	± 1.11	28.47	± 0.65	± 0.38	3.0	2.4
BP10_24	49.80	4,101.8	155.3	± 1.89	± 1.09	26.01	± 0.59	± 0.34	3.0	2.4

‡ Uncertainties are the expected measurement performance values.
† Includes a 2% systematic contribution to the uncertainty.

Table 33. Simulated thermal mode, defect analysis results for the poisoned, intact fuel assemblies

Fuel assembly ID	Defect without correction			HM and poison corrections applied		
	LD mass defect (%)	#σ 600 sec	#σ 1,800 sec	LD mass defect (%)	#σ 600 sec	#σ 1,800 sec
BP6_4	−8.2	2.7	3.5	5.3	1.4	1.9
BP6_8	−18.8	7.0	9.2	4.9	1.3	1.8
BP6_12	−26.4	11.2	14.5	5.8	1.5	2.0
BP6_16	−35.2	17.2	22.2	1.6	0.4	0.6
BP6_20	−41.3	22.5	28.9	0.0	0.0	0.0
BP6_24	−45.8	27.1	34.8	0.3	0.1	0.1
BP8_4	−11.4	3.9	5.2	1.6	0.5	0.6
BP8_8	−19.9	7.8	10.1	3.6	1.0	1.3
BP8_12	−27.9	12.4	15.9	3.7	1.0	1.4
BP8_16	−37.2	19.3	24.6	−1.4	0.4	0.5
BP8_20	−42.4	24.1	30.6	−1.3	0.4	0.5
BP8_24	−46.9	29.2	37.0	−1.8	0.5	0.7
BP10_4	−13.3	4.7	6.2	−0.8	0.2	0.3
BP10_8	−16.8	6.3	8.2	8.3	2.2	2.9
BP10_12	−27.0	11.8	15.2	6.0	1.6	2.1
BP10_16	−37.9	19.9	25.3	−2.7	0.8	1.0
BP10_20	−43.3	25.1	31.8	−3.3	0.9	1.3
BP10_24	−47.8	30.2	38.2	−3.4	0.9	1.3
Average Bias	**−30.4%**			**1.5%**		
Std. Deviation	**13.2%**			**3.6%**		

Table 34. Simulated fast mode, DD/UNCL measurement results for the poisoned, intact fuel assemblies‡

Fuel assembly ID	Declared LD ^{235}U (g/cm)	Singles rate (1/s)	Doubles rate (1/s)	600 sec σ_D (1/s)	1,800 sec σ_D (1/s)	Analyzed LD ^{235}U (g/cm)	600 sec LD uncert (g/cm)	1,800 sec LD uncert (g/cm)	600 sec Total uncert (%)†	1,800 sec Total uncert (%)†
BP6_4	51.50	6,983.6	83.4	± 3.25	± 1.87	50.59	± 4.32	± 2.50	8.5	4.9
BP6_8	51.20	6,973.7	82.0	± 3.24	± 1.87	48.79	± 4.26	± 2.46	9.0	5.0
BP6_12	50.90	6,958.1	82.7	± 3.24	± 1.87	49.76	± 4.28	± 2.47	8.8	5.0
BP6_16	50.60	6,947.7	81.6	± 3.23	± 1.87	48.29	± 4.23	± 2.44	9.0	5.1
BP6_20	50.30	6,940.8	80.6	± 3.23	± 1.86	46.94	± 4.18	± 2.41	9.1	5.1
BP6_24	49.90	6,923.8	78.5	± 3.22	± 1.86	44.28	± 4.09	± 2.36	9.5	5.3
BP8_4	51.50	6,990.1	82.9	± 3.25	± 1.88	50.02	± 4.31	± 2.49	8.8	5.0
BP8_8	51.20	6,974.6	82.1	± 3.24	± 1.87	48.84	± 4.26	± 2.46	9.0	5.0
BP8_12	50.90	6,960.8	81.2	± 3.24	± 1.87	47.75	± 4.22	± 2.44	9.1	5.1
BP8_16	50.50	6,940.1	82.3	± 3.23	± 1.86	49.16	± 4.25	± 2.45	8.9	5.0
BP8_20	50.20	6,928.2	81.0	± 3.22	± 1.86	47.46	± 4.19	± 2.42	9.1	5.1
BP8_24	49.90	6,909.6	78.4	± 3.21	± 1.85	44.16	± 4.08	± 2.36	9.5	5.3
BP10_4	51.50	6,982.5	83.2	± 3.25	± 1.87	50.35	± 4.31	± 2.49	8.8	4.9
BP10_8	51.20	6,973.5	82.0	± 3.24	± 1.87	48.79	± 4.26	± 2.46	9.0	5.0
BP10_12	50.80	6,953.6	80.8	± 3.23	± 1.87	47.27	± 4.20	± 2.42	9.1	5.1
BP10_16	50.50	6,933.1	79.7	± 3.22	± 1.86	45.82	± 4.14	± 2.39	9.3	5.2
BP10_20	50.20	6,922.5	78.6	± 3.22	± 1.86	44.44	± 4.10	± 2.37	9.4	5.3
BP10_24	49.80	6,893.2	78.1	± 3.20	± 1.85	43.69	± 4.06	± 2.34	9.5	5.4

‡ Uncertainties are the expected measurement performance values.
† Includes a 2% systematic contribution to the uncertainty.

Table 35. Simulated fast mode, defect analysis results for the poisoned, intact fuel assemblies

Fuel Assembly ID	Defect without correction			HM and Poison corrections applied		
	LD mass defect (%)	#σ 600 sec	#σ 1,800 sec	LD mass defect (%)	#σ 600 sec	#σ 1,800 sec
BP6_4	−1.8	0.2	0.3	0.4	0.0	0.1
BP6_8	−4.7	0.6	0.9	−0.7	0.1	0.1
BP6_12	−2.2	0.3	0.4	3.7	0.4	0.7
BP6_16	−4.6	0.5	0.9	3.2	0.4	0.6
BP6_20	−6.7	0.8	1.3	2.8	0.3	0.5
BP6_24	−11.3	1.3	2.2	0.1	0.0	0.0
BP8_4	−2.9	0.3	0.6	−0.7	0.1	0.1
BP8_8	−4.6	0.5	0.9	−0.6	0.1	0.1
BP8_12	−6.2	0.7	1.2	−0.3	0.0	0.1
BP8_16	−2.7	0.3	0.5	5.8	0.6	1.0
BP8_20	−5.5	0.6	1.1	4.7	0.5	0.8
BP8_24	−11.5	1.4	2.3	0.0	0.0	0.0
BP10_4	−2.2	0.3	0.4	0.0	0.0	0.0
BP10_8	−4.7	0.6	0.9	−0.7	0.1	0.1
BP10_12	−7.0	0.8	1.4	−0.7	0.1	0.1
BP10_16	−9.3	1.1	1.8	−1.3	0.1	0.2
BP10_20	−11.5	1.4	2.3	−1.8	0.2	0.3
BP10_24	−12.3	1.5	2.4	−0.4	0.0	0.1
Average bias	**−6.2%**			**0.8%**		
Std. deviation	**3.5%**			**2.2%**		

5.4 DD/UNCL SIMULATED PARTIAL DEFECT ANALYSIS

This series of simulations examines the performance of the UNCL using an MP320 DD neutron generator for increasing numbers of rods substituted with DU. The mass defect relative to the declared value is shown in Figure 34 for the thermal mode and in Figure 35 for the fast mode. Rates and performance values are provided in Tables 36–39. Because heavy metal content for the simulated assembly is the same as the simulated calibration assemblies, the heavy metal correction will be equal to 1, so application of the correction will have no impact on the results.

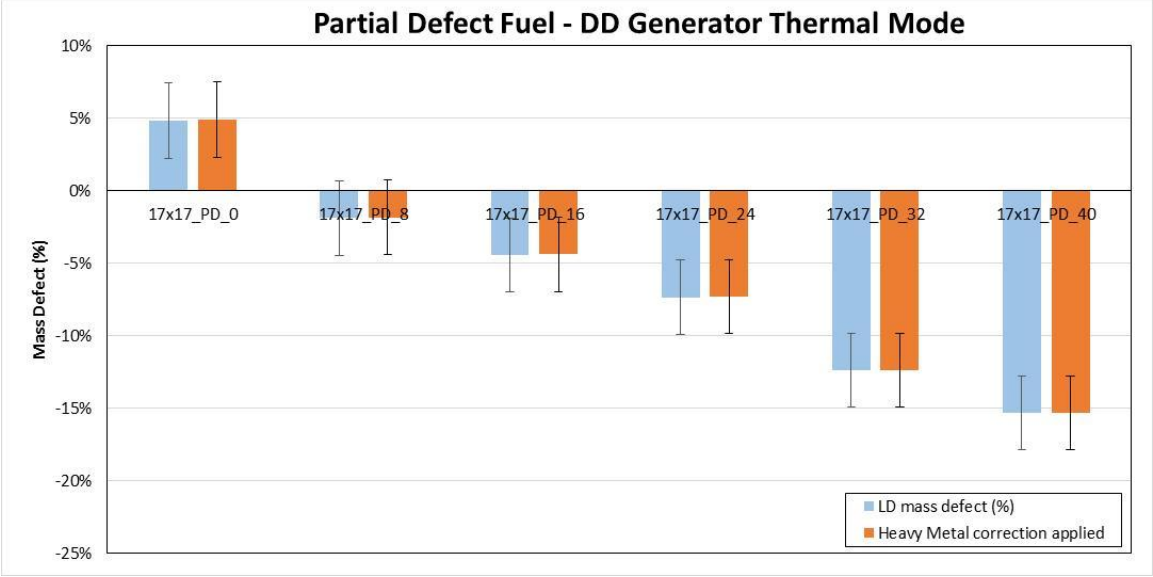

Figure 34. DD/UNCL (MP320) thermal mode simulated assay results for the partial defect loadings with and without the heavy metal correction.

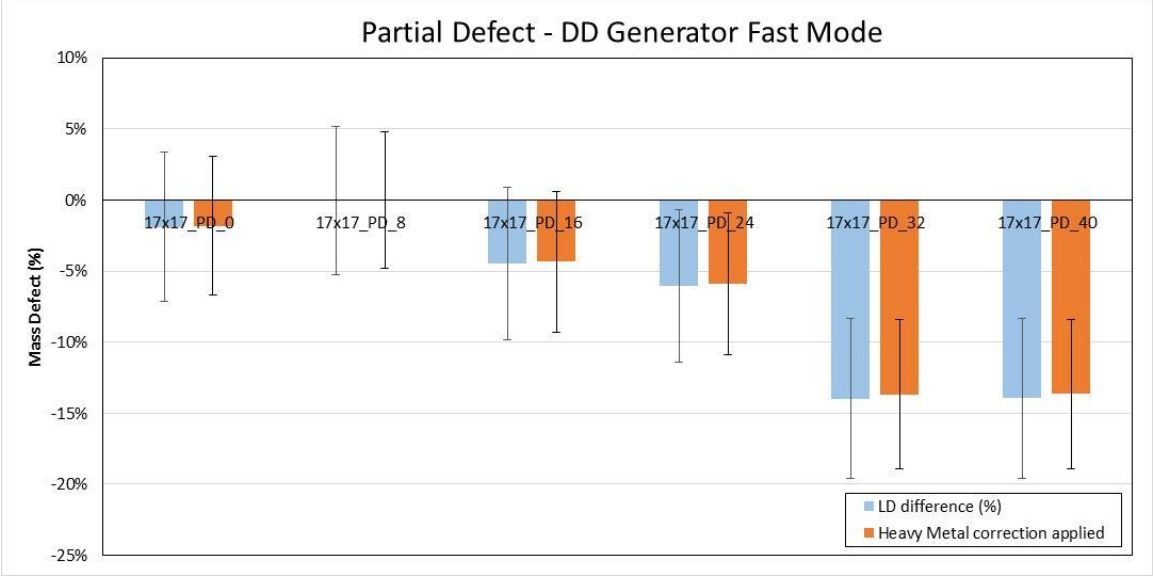

Figure 35. DD/UNCL (MP320) fast mode simulated assay results for the partial defect loadings with and without the heavy metal correction.

Table 36. Simulated thermal mode, DD/UNCL measurement results for the partial defect assembly configurations‡

Fuel assembly ID	Declared LD ^{235}U (g/cm)	Singles rate (1/s)	Doubles rate (1/s)	600 sec σ_D (1/s)	1,800 sec σ_D (1/s)	Analyzed LD ^{235}U (g/cm)	600 sec LD uncert (g/cm)	1,800 sec LD uncert (g/cm)	600 sec Total uncert (%)†	1,800 sec Total uncert (%)†
PD_0	54.98	4,533.4	220.1	± 2.18	± 1.26	57.66	± 1.67	± 0.96	3.5	2.6
PD_8	54.98	4,530.4	215.0	± 2.18	± 1.26	53.95	± 1.53	± 0.88	3.5	2.6
PD_16	54.98	4,508.6	213.0	± 2.17	± 1.25	52.55	± 1.47	± 0.85	3.4	2.6
PD_24	54.98	4,504.5	210.6	± 2.16	± 1.25	50.95	± 1.41	± 0.81	3.4	2.6
PD_32	54.98	4,496.4	206.2	± 2.16	± 1.25	48.17	± 1.31	± 0.76	3.4	2.5
PD_40	54.98	4,480.4	203.4	± 2.15	± 1.24	46.55	± 1.25	± 0.72	3.4	2.5

‡ Uncertainties are the expected measurement performance values.
† Includes a 2% systematic contribution to the uncertainty.

Table 37. Simulated DD/UNCL thermal mode, defect analysis results for the partial defect assembly configurations.

Fuel assembly ID	Defect without correction			HM and poison corrections applied		
	LD mass defect (%)	#σ 600 sec	#σ 1,800 sec	LD mass defect (%)	#σ 600 sec	#σ 1,800 sec
PD_0	4.9	1.3	1.8	4.9	1.3	1.8
PD_8	−1.9	0.6	0.7	−1.8	0.5	0.7
PD_16	−4.4	1.3	1.8	−4.4	1.3	1.8
PD_24	−7.3	2.3	3.1	−7.3	2.3	3.1
PD_32	−12.4	4.2	5.6	−12.4	4.2	5.5
PD_40	−15.3	5.4	7.1	−15.3	5.4	7.1

Table 38. Simulated fast mode, Am(Li)-based UNCL measurement results for the partial defect assembly configurations‡

Fuel assembly ID	Declared LD ^{235}U (g/cm)	Singles rate (1/s)	Doubles rate (1/s)	600 sec σ_D (1/s)	1,800 sec σ_D (1/s)	Analyzed LD ^{235}U (g/cm)	600 sec LD uncert (g/cm)	1,800 sec LD uncert (g/cm)	600 sec Total uncert (%)†	1,800 sec Total uncert (%)†
PD_0	54.98	7,008.6	85.9	± 3.26	± 1.88	53.96	± 4.45	± 2.57	8.5	5.2
PD_8	54.98	7,001.4	86.6	± 3.26	± 1.88	54.96	± 4.48	± 2.59	8.4	5.1
PD_16	54.98	7,006.7	84.8	± 3.26	± 1.88	52.57	± 4.40	± 2.54	8.6	5.2
PD_24	54.98	6,989.6	84.2	± 3.25	± 1.88	51.71	± 4.36	± 2.52	8.7	5.3
PD_32	54.98	6,979.4	81.0	± 3.24	± 1.87	47.44	± 4.22	± 2.44	9.1	5.5
PD_40	54.98	6,979.6	81.0	± 3.24	± 1.87	47.45	± 4.22	± 2.44	9.1	5.5

‡ Uncertainties are the expected measurement performance values.
† Includes a 2% systematic contribution to the uncertainty.

Table 39. Simulated fast mode, defect analysis results for the partial defect assembly configurations

Fuel assembly ID	Defect without correction			HM and poison corrections applied		
	LD mass defect (%)	#σ 600 sec	#σ 1,800 sec	LD mass defect (%)	#σ 600 sec	#σ 1,800 sec
PD_0	−1.9	0.2	0.4	−1.8	0.2	0.4
PD_8	0.0	0.0	0.0	0.0	0.0	0.0
PD_16	−4.4	0.5	0.9	−4.4	0.5	0.9
PD_24	−6.0	0.7	1.2	−5.9	0.7	1.2
PD_32	−13.7	1.7	2.9	−13.7	1.7	2.9
PD_40	−13.7	1.7	2.9	−13.7	1.7	2.9

6. SIMULATED PERFORMANCE USING THE NGEN-310 DD GENERATOR

Shortly after start of this evaluation the Starfire nGen DD neutron generators were made commercially available. These generators are somewhat smaller in diameter than the MP320 generator discussed above, but they also provide a more convenient neutron emission position. The neutron emission site is located within a 3 mm of the end of the generator tube, allowing the source to be positioned closer to the fuel assemblies and potentially affording improved measurement precision. To take advantage of the target location, the generator is now mounted horizontally in the simulations rather than vertically as shown in Figure 36. Unfortunately, no details of the interior of the generator tube were available for this study, so the tube was represented as a simple cylinder containing copper and SF_6 gas. The same series of MCNP simulations for evaluation of active coincidence performance discussed in Sections 4 and 5 have been repeated for this arrangement, and the results are presented in the following sections.

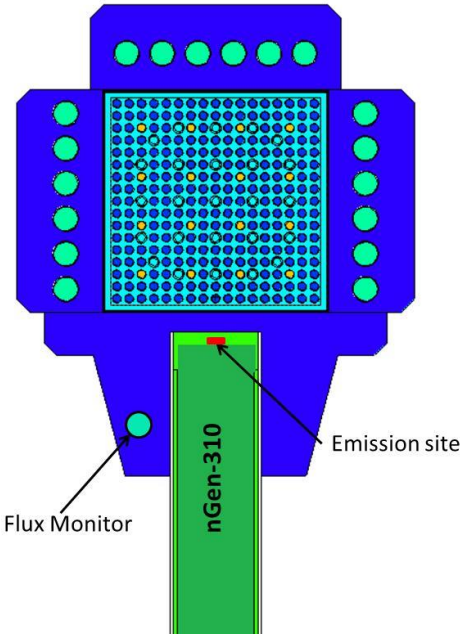

Figure 36. Screenshot of the MCNP VISED displays showing the modified UNCL with the horizontally mounted nGen-310 neutron generator.

6.1 NGEN DD/UNCL SIMULATED CALIBRATION

As was done for the Am(Li) source simulations discussed in Section 4, simulated thermal and fast calibration curves for the DD/UNCL were generated using the same assemblies described in Section 3.1. The neutron generator source term was adjusted to best reproduce the measured doubles rates reported by Menlove et al. [6, 3] for the thermal interrogation mode. The simulated thermal mode rates are provided in Table 40, and a comparison of the resulting calibration curve with the Am(Li)-based curve is shown in Figure 37. As can be seen in Figure 37, and as was seen for the MP320 generator results, the thermal coincidence response as a function of linear density is very similar to the Am(Li) response for all but the lowest ^{235}U loadings. Note, the plots were created using unrealistically low neutron generator source terms that were selected to allow simple comparison of the response profiles.

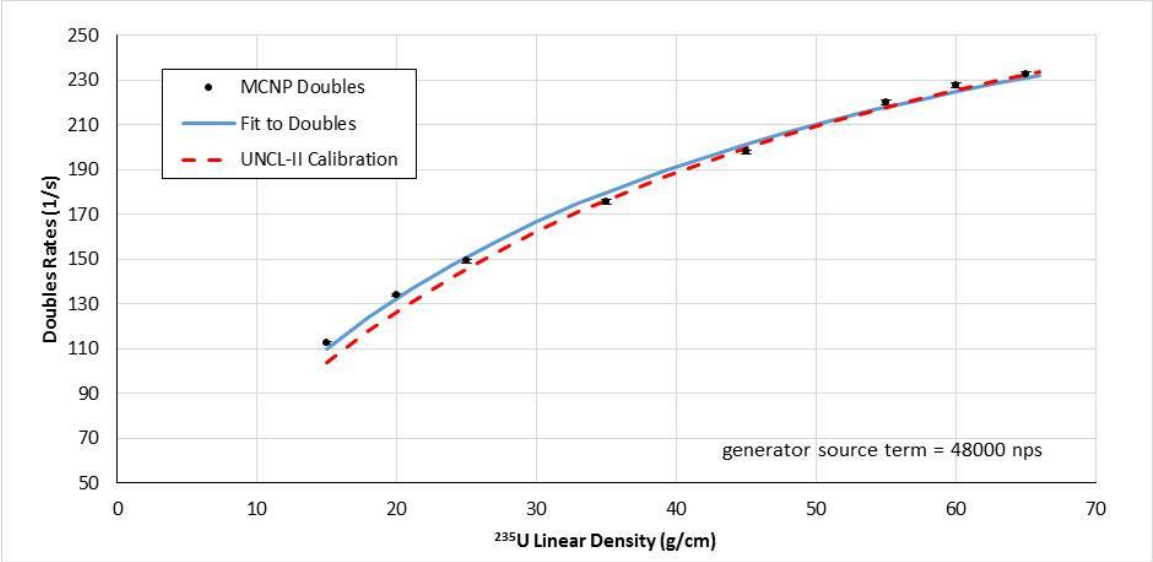

Figure 37. DD/UNCL (nGen-310) thermal mode calibration results (48,000 n/s source term) overlain with the measured UNCL-II thermal calibration curve [6].

The neutron generator source term was adjusted to best reproduce the measured doubles rates reported by Menlove et al. [6, 3] for the fast interrogation mode. The simulated fast mode rates are provided in Table 41 and a comparison of the resulting calibration curve with the Am(Li)-based curve is shown in Figure 38. The fast mode results for the nGen-310 interrogation are similar to those obtained for the MP320 generator. To provide optimal counting precision, the neutron generator would be operated at a much higher rate than used to produce the data in Table 41. The generator would normally be operated to produce an interrogating source strength of 200,00 n/s. The rates and precision values at this higher setting are provided in Table 42.

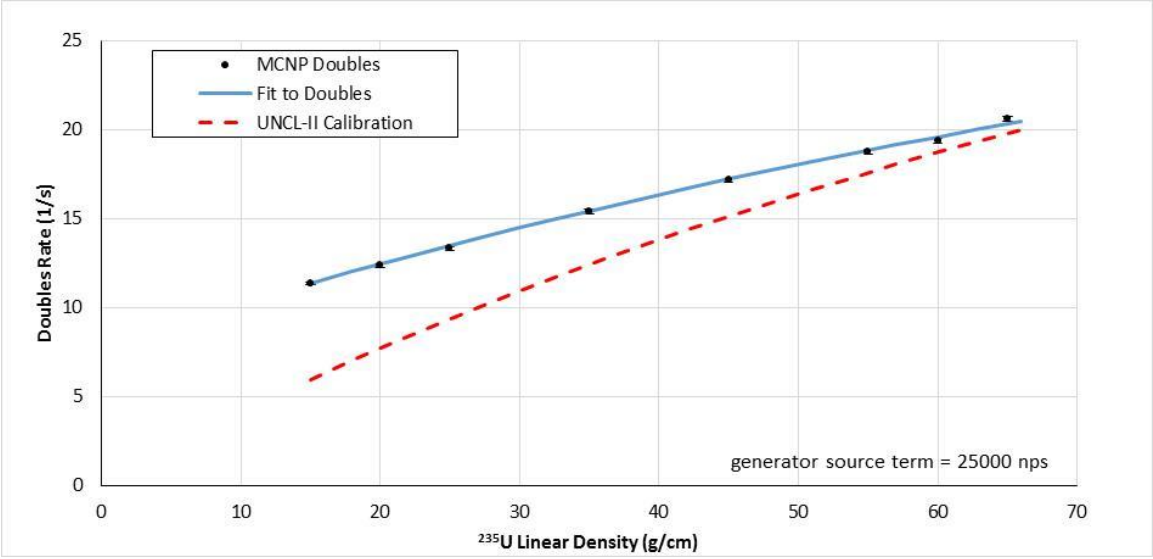

Figure 38. DD/UNCL (nGen-310) fast mode calibration results (25,000 n/s source term) overlain with the measured UNCL-II fast calibration curve [6].

Table 40. Simulated thermal mode, nGen-310 DD/UNCL measurement results for the calibration assemblies‡ (200,000 n/s source term)

Fuel assembly ID	Declared LD ^{235}U (g/cm)	Singles rate (1/s)	Doubles rate (1/s)	600 sec σ_D (1/s)	1,800 sec σ_D (1/s)	Analyzed LD ^{235}U (g/cm)	600 sec LD uncert (g/cm)	1,800 sec LD uncert (g/cm)	600 sec Total uncert (%)†	1,800 sec Total uncert (%)†
17x17_cal_15	15.0	3844.5	112.6	± 1.87	± 1.08	15.54	± 0.38	± 0.22	3.2	2.5
17x17_cal_20	20.0	3958.1	134.0	± 1.93	± 1.12	20.38	± 0.48	± 0.28	3.1	2.4
17x17_cal_25	25.0	4035.3	149.1	± 1.97	± 1.14	24.43	± 0.57	± 0.33	3.1	2.4
17x17_cal_35	35.0	4156.7	175.7	± 2.04	± 1.18	33.29	± 0.79	± 0.45	3.1	2.4
17x17_cal_45	45.0	4240.9	197.9	± 2.09	± 1.20	43.14	± 1.07	± 0.62	3.2	2.5
17x17_cal_55	55.0	4315.7	219.8	± 2.13	± 1.23	56.31	± 1.50	± 0.87	3.3	2.5
17x17_cal_60	60.0	4330.0	227.5	± 2.14	± 1.23	62.09	± 1.71	± 0.99	3.4	2.6
17x17_cal_65	65.0	4363.9	232.5	± 2.15	± 1.24	66.25	± 1.88	± 1.09	3.5	2.6

‡ Uncertainties are the expected measurement performance values.
† Includes a 2% systematic contribution to the uncertainty.

Table 41. Simulated fast mode, nGen-310 DD/UNCL measurement results for the calibration assemblies‡ (25,000 n/s source term)

Fuel assembly ID	Declared LD ^{235}U (g/cm)	Singles rate (1/s)	Doubles rate (1/s)	600 sec σ_D (1/s)	1,800 sec σ_D (1/s)	Analyzed LD ^{235}U (g/cm)	600 sec LD uncert (g/cm)	1,800 sec LD uncert (g/cm)	600 sec Total uncert (%)†	1,800 sec Total uncert (%)†
17x17_cal_15	15.0	1384.6	11.4	± 0.70	± 0.40	14.86	± 3.22	± 1.86	21.8	12.7
17x17_cal_20	20.0	1393.4	12.3	± 0.71	± 0.41	19.49	± 3.36	± 1.94	17.3	10.1
17x17_cal_25	25.0	1399.7	13.3	± 0.71	± 0.41	24.22	± 3.50	± 2.02	14.6	8.6
17x17_cal_35	35.0	1409.8	15.4	± 0.72	± 0.41	34.82	± 3.84	± 2.22	11.2	6.7
17x17_cal_45	45.0	1417.2	17.1	± 0.72	± 0.42	44.59	± 4.20	± 2.43	9.6	5.8
17x17_cal_55	55.0	1427.9	18.7	± 0.73	± 0.42	54.34	± 4.65	± 2.68	8.8	5.3
17x17_cal_60	60.0	1432.3	19.4	± 0.73	± 0.42	58.43	± 4.86	± 2.80	8.5	5.2
17x17_cal_65	65.0	1438.2	20.6	± 0.74	± 0.42	67.04	± 5.35	± 3.09	8.2	5.0

‡ Uncertainties are the expected measurement performance values.
† Includes a 2% systematic contribution to the uncertainty.

Table 42. Simulated fast mode, nGen-310 DD/UNCL measurement results for the calibration assemblies‡ (200,000 n/s source term)

Fuel assembly ID	Declared LD ^{235}U (g/cm)	Singles rate (1/s)	Doubles rate (1/s)	600 sec σ_D (1/s)	1,800 sec σ_D (1/s)	Analyzed LD ^{235}U (g/cm)	600 sec LD uncert (g/cm)	1,800 sec LD uncert (g/cm)	600 sec Total uncert (%)†	1,800 sec Total uncert (%)†
17x17_cal_15	15.0	11,076.5	90.8	± 5.18	± 2.99	14.86	± 2.98	± 1.72	20.1	11.7
17x17_cal_20	20.0	11,147.2	98.7	± 5.21	± 3.01	19.49	± 3.10	± 1.79	16.0	9.4
17x17_cal_25	25.0	11,197.7	106.5	± 5.24	± 3.02	24.22	± 3.22	± 1.86	13.5	7.9
17x17_cal_35	35.0	11,278.3	123.1	± 5.28	± 3.05	34.82	± 3.53	± 2.04	10.3	6.2
17x17_cal_45	45.0	11,337.6	137.1	± 5.30	± 3.06	44.59	± 3.86	± 2.23	8.9	5.4
17x17_cal_55	55.0	11,423.0	149.9	± 5.35	± 3.09	54.34	± 4.26	± 2.46	8.1	4.9
17x17_cal_60	60.0	11,458.3	154.9	± 5.36	± 3.10	58.43	± 4.45	± 2.57	7.9	4.8
17x17_cal_65	65.0	11,505.2	164.8	± 5.39	± 3.11	67.04	± 4.90	± 2.83	7.6	4.7

‡ Uncertainties are the expected measurement performance values.
† Includes a 2% systematic contribution to the uncertainty.

6.2 NGEN DD/UNCL SIMULATED PERFORMANCE FOR VARIOUS INTACT ASSEMBLIES

A series of simulations were performed using the descriptions for the assorted intact fuel assemblies described in Section 3.2. The simulated assay results are provided in Tables 43–46 and shown in Figures 39 and 40 for operation in the thermal and fast assay modes. The results are shown before and after application of the heavy metal correction illustrating the need to apply the correction factors when considering the relative performance of the measurement for a given assembly. For the DD generator–based measurement the heavy metal (enrichment) correction becomes more important because, relative to the Am(Li) interrogation, due to the increased fission rates in ^{238}U. The functional form is used for the correction

$$k_4 = 1 + \lambda_1 \cdot (\lambda_0 - \lambda)$$

However, in this case, the parameters λ_0 and $\lambda_1$are determined by a fit to the MCNP simulated rates. For these simulations using the calibration assembly description linear density as the reference (taken as a whole, including the poisoned and partial defect assemblies) the data is best represented when

Thermal mode	Fast mode
λ_0 = 1,297 g/cm	λ_0 = 1,297 g/cm
λ_1 = 6.50E-4 cm/g	λ_1 = 6.53E-4 cm/g

The results suggest that the heavy metal correction for thermal mode interrogation may require assembly-specific calibrations.

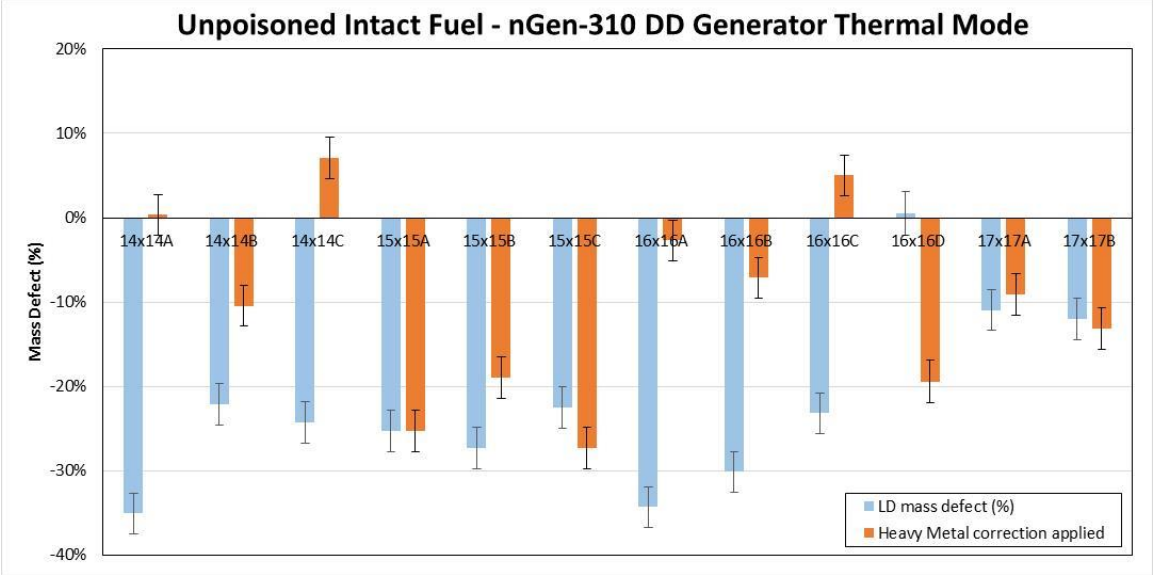

Figure 39. DD/UNCL (nGen-310) thermal mode simulated assay results for the assorted intact fuel assemblies. Error bars represent the projected 1 sigma uncertainties for an 1,800 second measurement time.

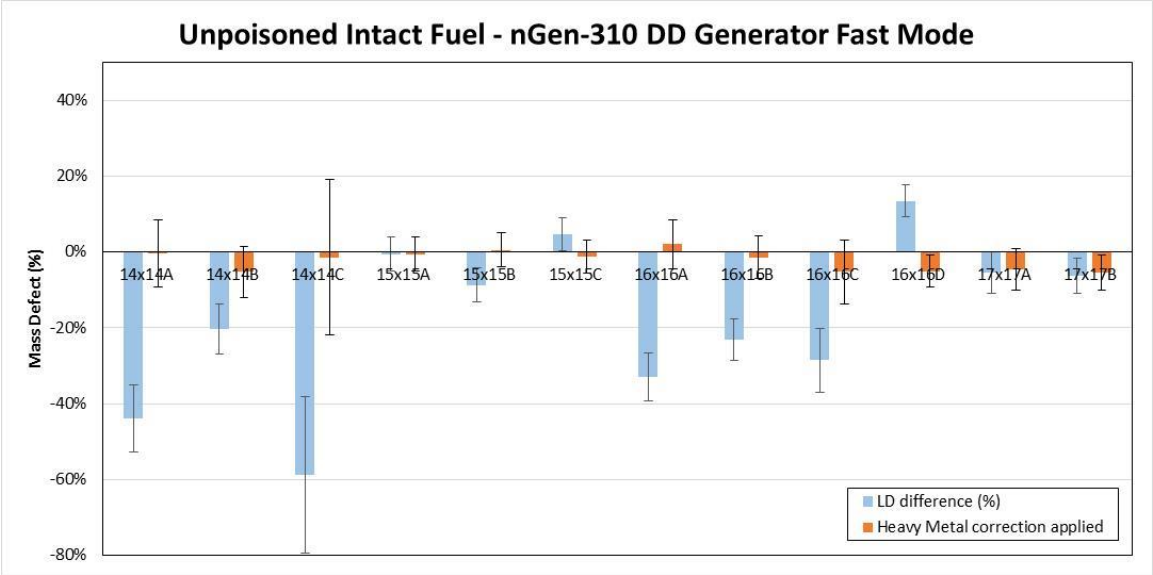

Figure 40. DD/UNCL (nGen-310) fast mode simulated assay results for the assorted intact fuel assemblies. Error bars represent the projected 1 sigma uncertainties for an 1,800 second measurement time.

Table 43. Simulated thermal mode, nGen-310 DD generator (48,000 n/s) based UNCL measurement results for the unpoisoned, intact fuel assemblies‡

Fuel assembly ID	Declared LD ^{235}U (g/cm)	Singles rate (1/s)	Doubles rate (1/s)	600 sec σ_D (1/s)	1,800 sec σ_D (1/s)	Analyzed LD ^{235}U (g/cm)	600 sec LD uncert (g/cm)	1,800 sec LD uncert (g/cm)	600 sec Total uncert (%)†	1,800 sec Total uncert (%)†
14x14A	**37.57**	4142.0	149.1	± 1.98	± 1.14	24.40	± 0.57	± 0.33	3.1	2.4
14x14B	**37.31**	4156.5	164.0	± 1.99	± 1.15	29.06	± 0.67	± 0.39	3.1	2.4
14x14C	**19.78**	3952.1	109.8	± 1.88	± 1.08	14.97	± 0.38	± 0.22	3.2	2.5
15x15A	**58.37**	4322.1	198.9	± 2.08	± 1.20	43.64	± 1.08	± 0.62	3.2	2.5
15x15B	**61.54**	4331.7	201.0	± 2.08	± 1.20	44.75	± 1.11	± 0.64	3.2	2.5
15x15C	**60.91**	4331.2	205.5	± 2.08	± 1.20	47.22	± 1.18	± 0.68	3.2	2.5
16x16A	**46.90**	4209.5	169.1	± 2.02	± 1.16	30.82	± 0.72	± 0.42	3.1	2.4
16x16B	**50.16**	4231.7	180.1	± 2.03	± 1.17	35.05	± 0.83	± 0.48	3.1	2.4
16x16C	**30.95**	4088.9	146.9	± 1.95	± 1.13	23.79	± 0.55	± 0.32	3.1	2.4
16x16D	**64.07**	4369.4	230.3	± 2.11	± 1.22	64.39	± 1.77	± 1.02	3.4	2.6
17x17A	**41.29**	4216.4	184.3	± 2.03	± 1.17	36.77	± 0.87	± 0.50	3.1	2.4
17x17B	**54.82**	4289.9	207.2	± 2.07	± 1.19	48.23	± 1.20	± 0.70	3.2	2.5

‡ Uncertainties are the expected measurement performance values.
† Includes a 2% systematic contribution to the uncertainty.

Table 44. Simulated DD generator–based UNCL thermal mode using the nGen-310 neutron generator, defect analysis results for the unpoisoned, intact fuel assemblies

Fuel assembly ID	Defect without correction			Defect with HM correction applied		
	LD mass defect (%)	#σ 600 sec	#σ 1,800 sec	LD mass defect (%)	#σ 600 sec	#σ 1,800 sec
14x14A	−35.0	17.5	22.4	0.4	0.1	0.1
14x14B	−22.1	9.3	11.8	−10.5	3.7	4.8
14x14C	−24.3	10.0	13.0	7.1	1.9	2.6
15x15A	−25.2	10.6	13.7	−25.2	10.6	13.7
15x15B	−27.3	11.8	15.2	−18.9	7.0	9.3
15x15C	−22.5	9.0	11.7	−27.3	12.0	15.4
16x16A	−34.3	17.0	21.6	−2.7	0.8	1.1
16x16B	−30.1	13.9	17.8	−7.1	2.2	3.0
16x16C	−23.1	9.8	12.5	5.0	1.4	1.9
16x16D	0.5	0.1	0.2	−19.4	7.7	9.9
17x17A	−11.0	4.0	5.1	−9.1	3.2	4.1
17x17B	−12.0	4.3	5.5	−13.2	4.8	6.2
Average bias	**−22.2%**			**−10.1%**		
Std. deviation	**10.3%**			**11.3%**		

Table 45. Simulated fast mode, nGen-310 DD generator (200,000 n/s) based UNCL measurement results for the unpoisoned, intact fuel assemblies‡

Fuel assembly ID	Declared LD ^{235}U (g/cm)	Singles rate (1/s)	Doubles rate (1/s)	600 sec σ_D (1/s)	1,800 sec σ_D (1/s)	Analyzed LD ^{235}U (g/cm)	600 sec LD uncert (g/cm)	1,800 sec LD uncert (g/cm)	600 sec Total uncert (%)†	1,800 sec Total uncert (%)†
14x14A	**37.57**	11,562.7	101.4	± 5.36	± 3.09	21.08	± 3.22	± 1.86	15.3	8.8
14x14B	**37.31**	11,479.6	115.3	± 5.32	± 3.07	29.75	± 3.42	± 1.97	11.7	6.6
14x14C	**19.78**	11,428.2	78.9	± 5.29	± 3.05	8.16	± 2.91	± 1.68	35.7	20.6
15x15A	**58.37**	11,761.8	154.4	± 5.46	± 3.15	58.00	± 4.51	± 2.60	8.0	4.5
15x15B	**61.54**	11,787.5	152.2	± 5.47	± 3.16	56.17	± 4.44	± 2.56	8.1	4.6
15x15C	**60.91**	11,771.9	161.2	± 5.46	± 3.15	63.80	± 4.80	± 2.77	7.8	4.3
16x16A	**46.90**	11,586.8	118.0	± 5.37	± 3.10	31.44	± 3.50	± 2.02	11.3	6.4
16x16B	**50.16**	11,596.0	128.3	± 5.38	± 3.10	38.38	± 3.71	± 2.14	9.9	5.6
16x16C	**30.95**	11,454.3	103.1	± 5.31	± 3.06	22.10	± 3.22	± 1.86	14.7	8.4
16x16D	**64.07**	11,621.6	170.9	± 5.39	± 3.11	72.68	± 5.24	± 3.02	7.5	4.2
17x17A	**41.29**	11,393.0	129.6	± 5.28	± 3.05	39.25	± 3.67	± 2.12	9.6	5.4
17x17B	**54.82**	11,481.1	145.3	± 5.33	± 3.07	50.77	± 4.10	± 2.37	8.3	4.7

‡ Uncertainties are the expected measurement performance values.
† Includes a 2% systematic contribution to the uncertainty.

Table 46. Simulated DD generator–based UNCL fast mode using the nGen-310 neutron generator operating at 200,000 n/s, defect analysis results for the unpoisoned, intact fuel assemblies

Fuel Assembly ID	Defect without correction			Defect with HM correction applied		
	LD mass defect (%)	#σ 600 sec	#σ 1,800 sec	LD mass defect (%)	#σ 600 sec	#σ 1,800 sec
14x14A	−43.9	5.0	8.5	−0.3	0.0	0.0
14x14B	−20.3	2.1	3.6	−5.3	0.5	0.8
14x14C	−58.8	3.9	6.8	−1.5	0.1	0.1
15x15A	−0.6	0.1	0.1	−0.6	0.1	0.1
15x15B	−8.7	1.1	1.9	0.6	0.1	0.1
15x15C	4.7	0.6	0.9	−1.3	0.2	0.3
16x16A	−33.0	4.2	7.1	2.0	0.2	0.3
16x16B	−23.1	3.0	5.0	−1.5	0.2	0.3
16x16C	−28.6	2.7	4.5	−5.2	0.4	0.7
16x16D	13.4	1.5	2.5	−5.0	0.7	1.1
17x17A	−5.5	0.6	1.0	−4.6	0.5	0.8
17x17B	−6.3	0.8	1.3	−5.4	0.7	1.1
Average Bias	**−17.5%**			**−2.3%**		
Std. Deviation	**21.1%**			**2.6%**		

6.3 NGEN DD/UNCL SIMULATED PERFORMANCE FOR BURNABLE POISONS

The performance of the UNCL for assemblies containing burnable poisons is an important question when considering an alternative neutron interrogation source. The difference in neutron energy distributions from the sources and the change in moderating assembly to accommodate the larger, compared to Am(Li), source will change the relative thermal neutron population in the interrogating neutron distribution. The simulated assemblies containing poison rods allow examination of the potential impact. Figure 41 illustrates the impact of the poison rods on the thermal mode mass results for the UNCL using an Am(Li) neutron source, and the fast mode results are shown in Figure 42. As can be seen the number of poison rods is more important than rod's poison loading. The effectiveness of the poison rod correction can also be seen in the plots because the average bias is reduced to <1% and the typical deviation from the expected value is reduced to less than 2% in both thermal and fast modes. The simulated rates and defect levels are presented in Tables 48–49.

The parameters in the expression for the poison rod correction factor, k_3, were adjusted by a fit to the MCNP simulations. The expression for k_3 from Section 1.3.2 [6] is shown here with the potentially adjustable parameters *a*, *b*, and *c*.

$$k_3 = 1 + \frac{a \cdot n}{N} \cdot \left(1 - e^{-b \cdot Gd}\right) \cdot (1 - c \cdot E_N)$$

where n is the number of poison rods,
N is the number of fuel rods (fuel + poison),
Gd is the weight percent of the gadolinium in the poison rods,
E_N is the declared enrichment.

The parameters for the nGen-310/UNCL system are provided in Table 47.

Table 47. Poison rod correction parameters for the nGen-310/UNCL system

Parameter	Thermal mode		Fast mode	
	Am(Li)	nGen-310	Am(Li)	nGen-310
a	9.86	3.23	0.602	0.504
b	0.647	0.647	0.647	0.647
c	0.176	0.176	—	—

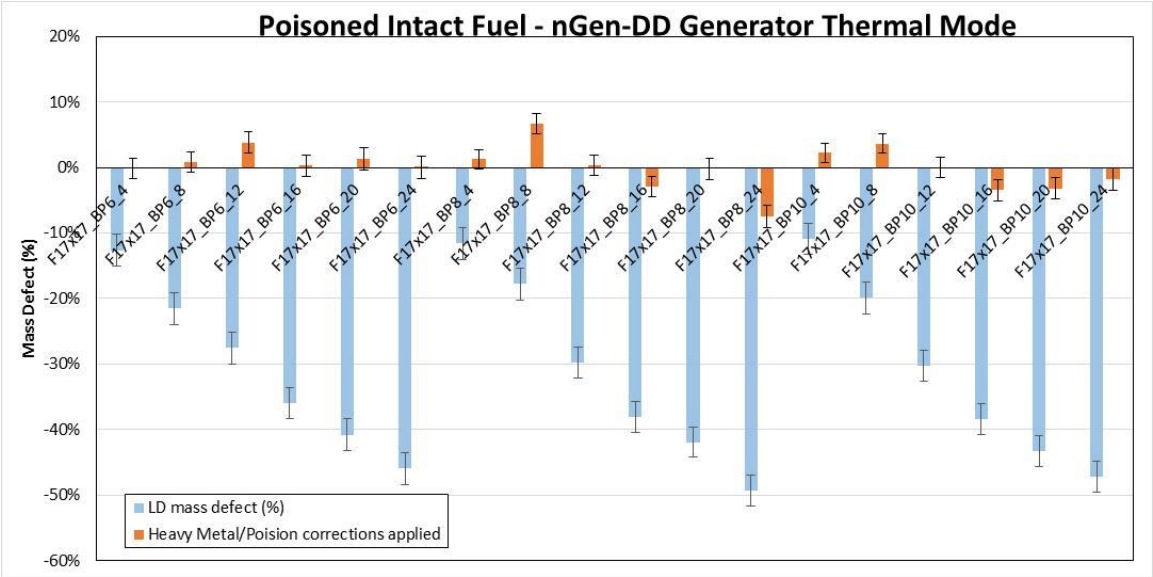

Figure 41. DD/UNCL (nGen-310) thermal mode simulated assay results for the various burnable poison loadings with and without the heavy metal and poison rod correction.

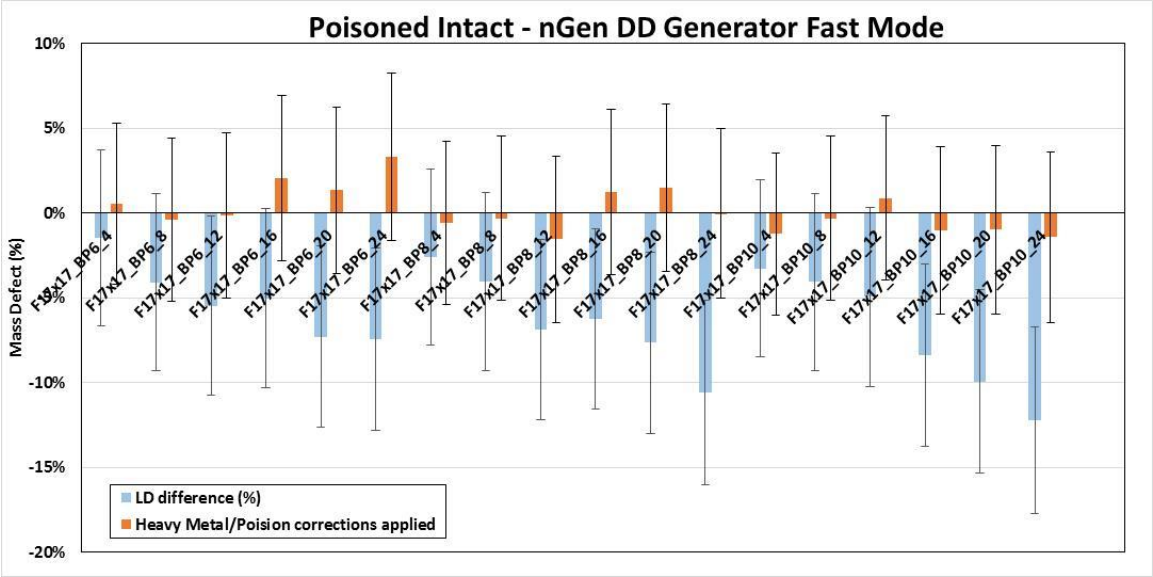

Figure 42. DD/UNCL (nGen-310) fast mode simulated assay results for the various burnable poison loadings with and without the heavy metal and poison rod correction.

Table 48. Simulated thermal mode, nGen-310 DD/UNCL measurement results for the poisoned, intact fuel assemblies‡

Fuel assembly ID	Declared LD ^{235}U (g/cm)	Singles rate (1/s)	Doubles rate (1/s)	600 sec σ_D (1/s)	1,800 sec σ_D (1/s)	Analyzed LD ^{235}U (g/cm)	600 sec LD uncert (g/cm)	1,800 sec LD uncert (g/cm)	600 sec Total uncert (%)†	1,800 sec Total uncert (%)†
BP6_4	**51.50**	4,229.4	201.4	± 2.04	± 1.18	44.99	± 1.09	± 0.63	3.1	2.4
BP6_8	**51.20**	4,166.7	191.9	± 2.02	± 1.16	40.19	± 0.95	± 0.55	3.1	2.4
BP6_12	**50.90**	4,099.2	184.5	± 1.98	± 1.15	36.86	± 0.85	± 0.49	3.1	2.4
BP6_16	**50.60**	4,014.9	173.4	± 1.95	± 1.12	32.43	± 0.73	± 0.42	3.0	2.4
BP6_20	**50.30**	3,961.1	166.1	± 1.92	± 1.11	29.80	± 0.66	± 0.38	3.0	2.4
BP6_24	**49.90**	3,907.4	157.6	± 1.90	± 1.10	26.97	± 0.60	± 0.34	3.0	2.4
BP8_4	**51.50**	4,227.2	202.4	± 1.95	± 1.13	45.53	± 1.06	± 0.61	3.1	2.4
BP8_8	**51.20**	4,163.1	195.8	± 1.92	± 1.11	42.08	± 0.96	± 0.55	3.0	2.4
BP8_12	**50.90**	4,085.8	181.7	± 1.89	± 1.09	35.71	± 0.78	± 0.45	3.0	2.4
BP8_16	**50.50**	4,007.5	170.4	± 1.85	± 1.07	31.31	± 0.67	± 0.39	2.9	2.4
BP8_20	**50.20**	3,951.7	164.3	± 1.83	± 1.05	29.16	± 0.62	± 0.36	2.9	2.3
BP8_24	**49.90**	3,883.5	152.2	± 1.79	± 1.04	25.33	± 0.53	± 0.31	2.9	2.3
BP10_4	**51.50**	4,220.3	203.1	± 1.95	± 1.13	45.89	± 1.07	± 0.62	3.1	2.4
BP10_8	**51.20**	4,166.7	193.6	± 1.92	± 1.11	41.01	± 0.93	± 0.54	3.0	2.4
BP10_12	**50.80**	4,075.9	181.0	± 1.88	± 1.09	35.40	± 0.77	± 0.45	3.0	2.4
BP10_16	**50.50**	3,994.2	169.9	± 1.85	± 1.07	31.13	± 0.67	± 0.38	2.9	2.4
BP10_20	**50.20**	3,941.1	162.2	± 1.82	± 1.05	28.45	± 0.60	± 0.35	2.9	2.3
BP10_24	**49.80**	3,881.2	155.4	± 1.79	± 1.04	26.28	± 0.55	± 0.32	2.9	2.3

‡ Uncertainties are the expected measurement performance values.
† Includes a 2% systematic contribution to the uncertainty.

Table 49. Simulated thermal mode, defect analysis results for the poisoned, intact fuel assemblies using the nGen-310 neutron generator

Fuel assembly ID	Defect without correction			HM and poison corrections applied		
	LD mass defect (%)	#σ 600 sec	#σ 1,800 sec	LD mass defect (%)	#σ 600 sec	#σ 1,800 sec
BP6_4	−12.6	4.6	5.9	−0.2	0.1	0.1
BP6_8	−21.5	8.8	11.3	0.8	0.2	0.3
BP6_12	−27.6	12.5	15.8	3.8	1.0	1.4
BP6_16	−35.9	18.6	23.5	0.3	0.1	0.1
BP6_20	−40.8	23.0	28.9	1.3	0.4	0.5
BP6_24	−46.0	28.5	35.8	0.0	0.0	0.0
BP8_4	−11.6	4.3	5.4	1.3	0.4	0.5
BP8_8	−17.8	7.2	9.1	6.7	1.9	2.5
BP8_12	−29.8	14.3	18.0	0.3	0.1	0.1
BP8_16	−38.0	20.9	26.1	−2.9	0.9	1.2
BP8_20	−41.9	24.7	30.8	−0.2	0.1	0.1
BP8_24	−49.2	33.4	41.4	−7.4	2.3	3.1
BP10_4	−10.9	4.0	5.1	2.2	0.7	0.9
BP10_8	−19.9	8.2	10.4	3.7	1.1	1.4
BP10_12	−30.3	14.7	18.4	0.0	0.0	0.0
BP10_16	−38.4	21.2	26.5	−3.5	1.1	1.4
BP10_20	−43.3	26.2	32.6	−3.2	1.0	1.3
BP10_24	−47.2	30.9	38.3	−1.8	0.5	0.7
Average bias	**−31.3%**			**0.1%**		
Std. deviation	**12.9%**			**3.2%**		

Table 50. Simulated fast mode, nGen-310 DD generator (200,000 n/s) measurement results for the poisoned, intact fuel assemblies‡

Fuel assembly ID	Declared LD ^{235}U (g/cm)	Singles rate (1/s)	Doubles rate (1/s)	600 sec σ_D (1/s)	1,800 sec σ_D (1/s)	Analyzed LD ^{235}U (g/cm)	600 sec LD uncert (g/cm)	1,800 sec LD uncert (g/cm)	600 sec Total uncert (%)†	1,800 sec Total uncert (%)†
BP6_4	**51.50**	1,424	18.2	± 0.68	± 0.39	50.75	± 4.20	± 2.42	8.5	5.2
BP6_8	**51.20**	1,421	17.9	± 0.68	± 0.39	49.11	± 4.13	± 2.38	8.6	5.2
BP6_12	**50.90**	1,418	17.7	± 0.68	± 0.39	48.11	± 4.08	± 2.35	8.7	5.3
BP6_16	**50.60**	1,417	17.7	± 0.68	± 0.39	48.06	± 4.07	± 2.35	8.7	5.3
BP6_20	**50.30**	1,415	17.5	± 0.68	± 0.39	46.63	± 4.01	± 2.32	8.8	5.4
BP6_24	**49.90**	1,413	17.4	± 0.68	± 0.39	46.18	± 3.99	± 2.30	8.9	5.4
BP8_4	**51.50**	1,423	18.1	± 0.68	± 0.39	50.16	± 4.17	± 2.41	8.6	5.2
BP8_8	**51.20**	1,420	17.9	± 0.68	± 0.39	49.13	± 4.12	± 2.38	8.6	5.2
BP8_12	**50.90**	1,417	17.6	± 0.68	± 0.39	47.39	± 4.05	± 2.34	8.8	5.3
BP8_16	**50.50**	1,415	17.6	± 0.68	± 0.39	47.35	± 4.04	± 2.33	8.8	5.3
BP8_20	**50.20**	1,412	17.4	± 0.68	± 0.39	46.36	± 4.00	± 2.31	8.8	5.4
BP8_24	**49.90**	1,410	17.1	± 0.67	± 0.39	44.62	± 3.93	± 2.27	9.0	5.5
BP10_4	**51.50**	1,423	18.0	± 0.68	± 0.39	49.82	± 4.16	± 2.40	8.6	5.2
BP10_8	**51.20**	1,420	17.9	± 0.68	± 0.39	49.12	± 4.12	± 2.38	8.6	5.2
BP10_12	**50.80**	1,416	17.8	± 0.68	± 0.39	48.29	± 4.08	± 2.36	8.7	5.3
BP10_16	**50.50**	1,413	17.4	± 0.68	± 0.39	46.26	± 3.99	± 2.31	8.9	5.4
BP10_20	**50.20**	1,410	17.2	± 0.67	± 0.39	45.21	± 3.95	± 2.28	9.0	5.4
BP10_24	**49.80**	1,408	17.0	± 0.67	± 0.39	43.70	± 3.89	± 2.24	9.1	5.5

‡ Uncertainties are the expected measurement performance values.
† Includes a 2% systematic contribution to the uncertainty.

Table 51. Simulated fast mode, defect analysis results for the poisoned, intact fuel assemblies using the nGen-310 neutron generator operating at 200,000 n/s

Fuel assembly ID	Defect without correction			HM and poison corrections applied		
	LD mass defect (%)	#σ 600 sec	#σ 1,800 sec	LD mass defect (%)	#σ 600 sec	#σ 1,800 sec
BP6_4	−1.5	0.2	0.3	0.6	0.1	0.1
BP6_8	−4.1	0.5	0.8	−0.4	0.0	0.1
BP6_12	−5.5	0.7	1.1	−0.1	0.0	0.0
BP6_16	−5.0	0.6	1.0	2.1	0.2	0.4
BP6_20	−7.3	0.9	1.5	1.4	0.2	0.3
BP6_24	−7.4	0.9	1.5	3.3	0.4	0.6
BP8_4	−2.6	0.3	0.5	−0.6	0.1	0.1
BP8_8	−4.0	0.5	0.8	−0.3	0.0	0.1
BP8_12	−6.9	0.8	1.4	−1.5	0.2	0.3
BP8_16	−6.2	0.8	1.3	1.3	0.1	0.2
BP8_20	−7.6	0.9	1.5	1.5	0.2	0.3
BP8_24	−10.6	1.3	2.2	0.0	0.0	0.0
BP10_4	−3.3	0.4	0.6	−1.2	0.1	0.2
BP10_8	−4.1	0.5	0.8	−0.3	0.0	0.1
BP10_12	−4.9	0.6	1.0	0.9	0.1	0.2
BP10_16	−8.4	1.0	1.7	−1.0	0.1	0.2
BP10_20	−9.9	1.2	2.0	−1.0	0.1	0.2
BP10_24	−12.2	1.5	2.5	−1.4	0.2	0.3
Average bias	**−6.2%**			**0.2%**		
Std. deviation	**2.9%**			**1.3%**		

6.4 NGEN-310 DD/UNCL SIMULATED PARTIAL DEFECT ANALYSIS

This series of simulations examines the performance of the UNCL using an nGen-310 DD neutron generator for the substitution configurations. The series examines the expected response with an increasing number of DU rods substituted for LEU fuel rods. The mass defect relative to the declared value is shown in Figure 43 for the thermal mode and in Figure 44 for the fast mode. Rates and performance values are provided in Tables 52–55. Because heavy metal content for the simulated assembly is the same as the simulated calibration assemblies, the heavy metal correction will be equal to 1, so application of the correction will have no impact on the results.

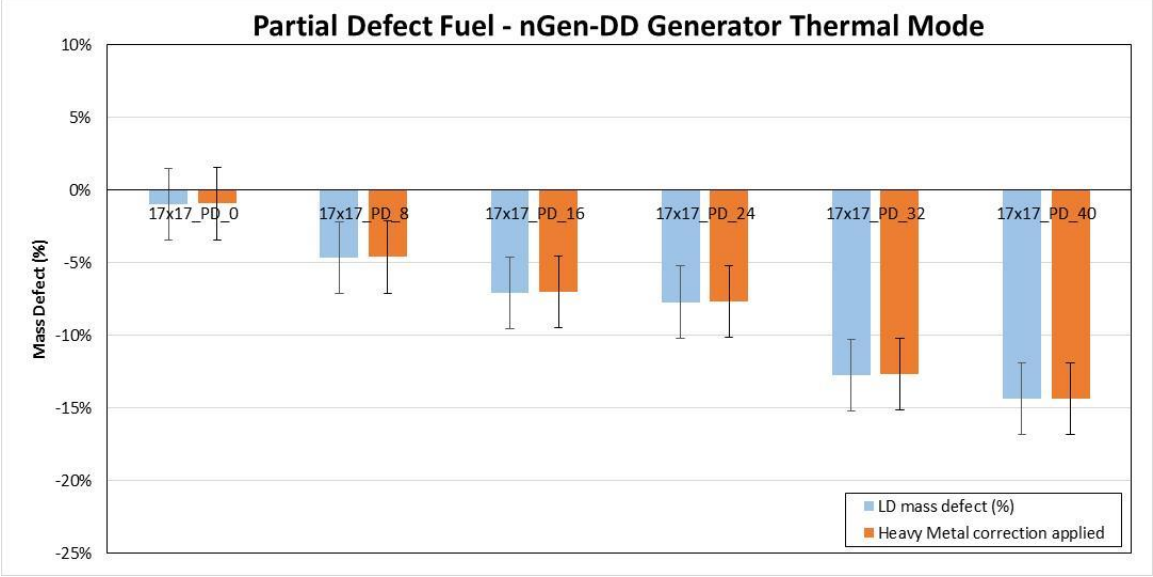

Figure 43. DD/UNCL (nGen-310) thermal mode simulated assay results for the partial defect loadings with and without the heavy metal correction.

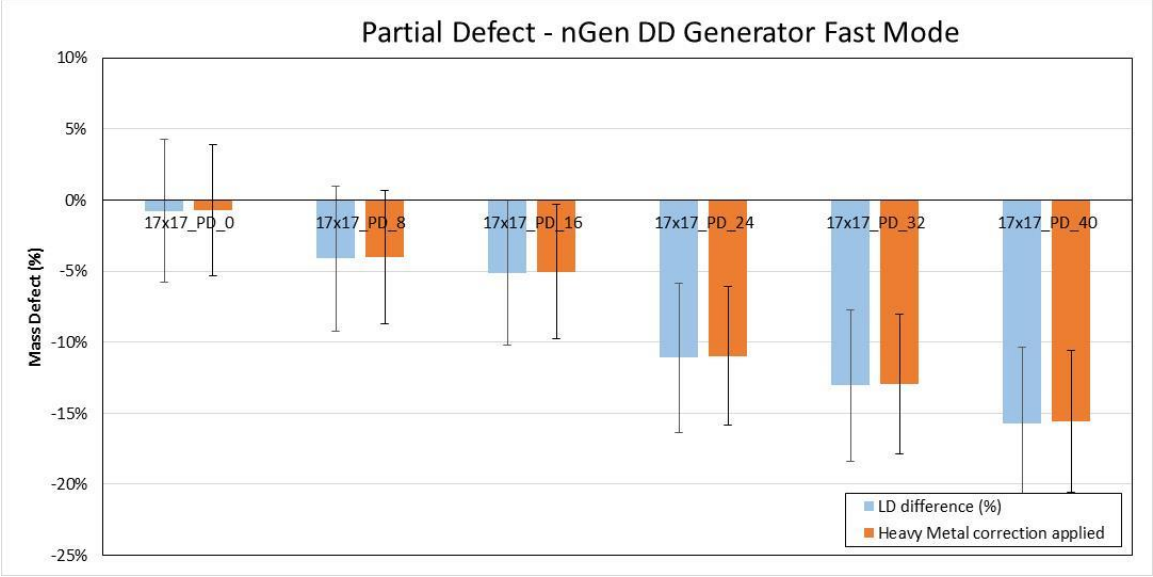

Figure 44. DD/UNCL (nGen-310) fast mode simulated assay results for the partial defect loadings with and without the heavy metal correction.

Table 52. Simulated thermal mode, nGen-310 DD/UNCL measurement results for the partial defect assembly configurations‡

Fuel assembly ID	Declared LD ^{235}U (g/cm)	Singles rate (1/s)	Doubles rate (1/s)	600 sec σ_D (1/s)	1,800 sec σ_D (1/s)	Analyzed LD ^{235}U (g/cm)	600 sec LD uncert (g/cm)	1,800 sec LD uncert (g/cm)	600 sec Total uncert (%)†	1,800 sec Total uncert (%)†
PD_0	54.98	4,304.0	217.1	± 2.08	± 1.20	54.45	± 1.40	± 0.81	3.3	2.5
PD_8	54.98	4,297.9	214.1	± 2.07	± 1.20	52.44	± 1.34	± 0.77	3.2	2.5
PD_16	54.98	4,294.2	212.0	± 2.07	± 1.20	51.10	± 1.29	± 0.75	3.2	2.5
PD_24	54.98	4,284.4	211.4	± 2.07	± 1.19	50.75	± 1.28	± 0.74	3.2	2.5
PD_32	54.98	4,268.6	206.8	± 2.06	± 1.19	48.00	± 1.19	± 0.69	3.2	2.5
PD_40	54.98	4,260.7	205.2	± 2.05	± 1.19	47.08	± 1.16	± 0.67	3.2	2.5

‡ Uncertainties are the expected measurement performance values.
† Includes a 2% systematic contribution to the uncertainty.

Table 53. Simulated DD/UNCL thermal mode, defect analysis results for the partial defect assembly configurations using the nGen-310 generator†

Fuel assembly ID	Defect without correction			HM and poison corrections applied		
	LD mass defect (%)	#σ 600 sec	#σ 1,800 sec	LD mass defect (%)	#σ 600 sec	#σ 1,800 sec
PD_0	−1.0	0.3	0.4	−0.9	0.3	0.4
PD_8	−4.6	1.5	2.0	−4.6	1.5	1.9
PD_16	−7.1	2.4	3.1	−7.0	2.3	3.0
PD_24	−7.7	2.6	3.4	−7.7	2.6	3.4
PD_32	−12.7	4.6	5.9	−12.7	4.6	5.9
PD_40	−14.4	5.3	6.8	−14.3	5.3	6.8

† Cells highlighted in green indicate a reasonable probability of detection of the substitution.

Table 54. Simulated fast mode, nGen-310 DD generator operating at 200,000 n/s measurement results for the partial defect assembly configurations‡

Fuel assembly ID	Declared LD ^{235}U (g/cm)	Singles rate (1/s)	Doubles rate (1/s)	600 sec σ_D (1/s)	1,800 sec σ_D (1/s)	Analyzed LD ^{235}U (g/cm)	600 sec LD uncert (g/cm)	1,800 sec LD uncert (g/cm)	600 sec Total uncert (%)†	1,800 sec Total uncert (%)†
PD_0	54.98	11,429.2	150.2	± 5.30	± 3.06	54.56	± 4.24	± 2.45	8.0	4.9
PD_8	54.98	11,417.9	147.9	± 5.30	± 3.06	52.74	± 4.16	± 2.40	8.1	5.0
PD_16	54.98	11,402.1	147.2	± 5.29	± 3.05	52.19	± 4.13	± 2.38	8.2	5.0
PD_24	54.98	11,396.3	142.9	± 5.29	± 3.05	48.94	± 4.00	± 2.31	8.4	5.1
PD_32	54.98	11,389.6	141.5	± 5.28	± 3.05	47.86	± 3.96	± 2.29	8.5	5.2
PD_40	54.98	11,378.0	139.5	± 5.28	± 3.05	46.38	± 3.90	± 2.25	8.6	5.3

‡ Uncertainties are the expected measurement performance values.
† Includes a 2% systematic contribution to the uncertainty.

Table 55. Simulated DD/UNCL fast mode, defect analysis results for the partial defect assembly configurations using the nGen-310 generator operating at 200,000 n/s†

Fuel assembly ID	Defect without correction			HM and Poison corrections applied		
	LD mass defect (%)	#σ 600 sec	#σ 1,800 sec	LD mass defect (%)	#σ 600 sec	#σ 1,800 sec
PD_0	−0.8	0.1	0.2	−0.7	0.1	0.1
PD_8	−4.1	0.5	0.8	−4.1	0.5	0.8
PD_16	−5.1	0.6	1.0	−5.0	0.6	1.0
PD_24	−11.0	1.4	2.4	−11.0	1.4	2.3
PD_32	−13.0	1.7	2.8	−12.9	1.7	2.8
PD_40	−15.6	2.1	3.4	−15.6	2.1	3.4

† Cells highlighted in green indicate a reasonable probability of detection of the substitution.

7. SIMULATED PERFORMANCE USING A VERY COMPACT DD GENERATOR

The simulated assay responses for the MP320 and the nGen-310 generators are very similar to that obtained from the Am(Li) isotopic sources in terms of systematic bias; however, the measurement precision from the Am(Li)-based analysis is superior to that obtainable from the neutron generators. Unlike the DD/AWCC system [1], the large physical size of the generator tube does not appear to be the limiting factor. To illustrate this point, the above series of simulations were performed for an idealized, compact DD neutron generator of the same total volume as the Am(Li) source tungsten shield (Figure 6). This fictitious neutron generator arrangement is illustrated in Figure 45. Since the COTS MP320 and the nGen-310 both provide functionally equivalent performance to the Am(Li) source–based measurement, only the fast mode performance has been evaluated for the compact generator arrangement.

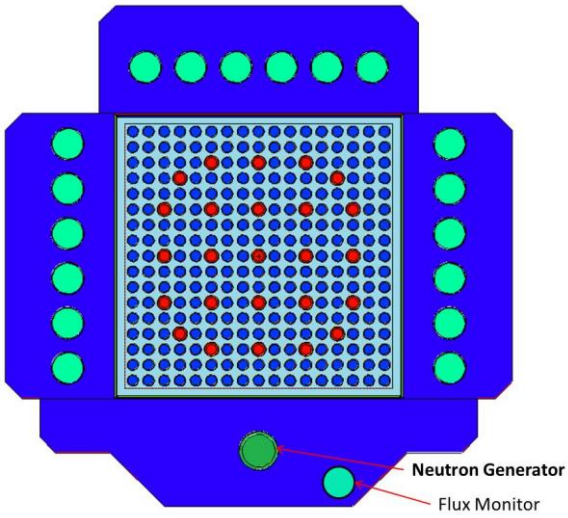

Figure 45. Screenshot of the MCNP VISED displays showing the modified UNCL with the very compact neutron generator.

7.1 COMPACT DD/UNCL SIMULATED CALIBRATION

As was done for the Am(Li) MP320 and nGEN-310 neutron sources the simulated thermal and fast calibration curves for the DD/UNCL were generated using the same assemblies described in Section 3.1. The neutron generator source term was adjusted to best reproduce the match the doubles rates reported by Menlove et al. [6, 3] for the fast mode interrogation mode at the high end of the calibration curve (e.g., 65 g ^{235}U/cm). The simulated rates are provided in Table 56, and a comparison of the resulting calibration curve with the Am(Li)-based curve is shown in Figure 46.

To provide optimal counting precision, the neutron generator would be operated at a much high rate than used to produce the data in Table 56. The generator would normally be operated to produce an interrogating source strength of 200,000 n/s. The rates and precision values at this higher setting are provided in Table 57.

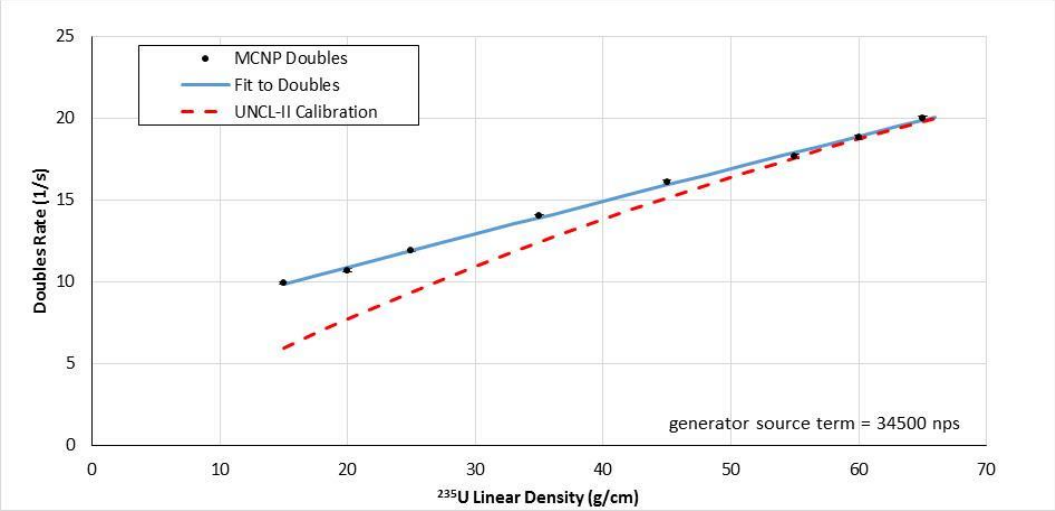

Figure 46. DD/UNCL (compact) fast mode calibration results (34,500 n/s source term) overlain with the measured UNCL-II fast calibration curve [6].

Table 56. Simulated fast mode, compact DD/UNCL measurement results for the calibration assemblies‡ (200,000 n/s source term)

Fuel assembly ID	Declared LD ^{235}U (g/cm)	Singles rate (1/s)	Doubles rate (1/s)	600 sec σ_D (1/s)	1,800 sec σ_D (1/s)	Analyzed LD ^{235}U (g/cm)	600 sec LD uncert (g/cm)	1,800 sec LD uncert (g/cm)	600 sec Total uncert (%)†	1,800 sec Total uncert (%)†
17x17_cal_15	15.0	1,263.2	9.9	± 0.64	± 0.37	15.36	± 3.10	± 1.79	20.3	11.8
17x17_cal_20	20.0	1,266.2	10.7	± 0.65	± 0.37	19.25	± 3.13	± 1.81	16.4	9.6
17x17_cal_25	25.0	1,275.4	11.9	± 0.65	± 0.38	25.08	± 3.18	± 1.84	12.8	7.6
17x17_cal_35	35.0	1,286.8	14.0	± 0.66	± 0.38	35.40	± 3.26	± 1.88	9.4	5.7
17x17_cal_45	45.0	1,297.6	16.1	± 0.67	± 0.39	45.71	± 3.35	± 1.93	7.6	4.7
17x17_cal_55	55.0	1,307.5	17.7	± 0.67	± 0.39	53.85	± 3.42	± 1.97	6.7	4.2
17x17_cal_60	60.0	1,313.2	18.8	± 0.68	± 0.39	59.73	± 3.47	± 2.00	6.1	3.9
17x17_cal_65	65.0	1,317.7	20.0	± 0.68	± 0.39	65.64	± 3.51	± 2.03	5.7	3.7

‡ Uncertainties are the expected measurement performance values.
† Includes a 2% systematic contribution to the uncertainty.

Table 57. Simulated fast mode, compact DD/UNCL measurement results for the calibration assemblies‡ (200,000 n/s source term)

Fuel assembly ID	Declared LD ^{235}U (g/cm)	Singles rate (1/s)	Doubles rate (1/s)	600 sec σ_D (1/s)	1,800 sec σ_D (1/s)	Analyzed LD ^{235}U (g/cm)	600 sec LD uncert (g/cm)	1,800 sec LD uncert (g/cm)	600 sec Total uncert (%)†	1,800 sec Total uncert (%)†
17x17_cal_15	15.0	7,322.9	57.3	± 3.44	± 1.99	15.36	± 2.86	± 1.65	18.7	10.9
17x17_cal_20	20.0	7,340.4	62.0	± 3.45	± 1.99	19.25	± 2.88	± 1.66	15.1	8.9
17x17_cal_25	25.0	7,393.8	68.9	± 3.48	± 2.01	25.08	± 2.93	± 1.69	11.8	7.0
17x17_cal_35	35.0	7,459.7	81.1	± 3.51	± 2.03	35.40	± 3.00	± 1.73	8.7	5.3
17x17_cal_45	45.0	7,522.5	93.1	± 3.54	± 2.05	45.71	± 3.07	± 1.77	7.0	4.4
17x17_cal_55	55.0	7,579.7	102.5	± 3.57	± 2.06	53.85	± 3.13	± 1.80	6.1	3.9
17x17_cal_60	60.0	7,612.8	109.1	± 3.59	± 2.07	59.73	± 3.17	± 1.83	5.7	3.7
17x17_cal_65	65.0	7,639.0	115.8	± 3.60	± 2.08	65.64	± 3.20	± 1.85	5.3	3.5

‡ Uncertainties are the expected measurement performance values.
† Includes a 2% systematic contribution to the uncertainty.

7.2 COMPACT DD/UNCL SIMULATED PERFORMANCE FOR VARIOUS INTACT ASSEMBLIES

A series of simulations were performed using the descriptions for the assorted intact fuel assemblies described in Section 3.2. The simulated assay results are provided in Tables 58 and 59 and are shown in Figure 47 for fast assay mode operation. The results are shown before and after application of the heavy metal correction, illustrating the need to apply the correction factors when considering the relative performance of the measurement for a given assembly. For the DD generator–based measurement, the heavy metal (enrichment) correction becomes more important, relative to the Am(Li) interrogation, because of the increased fission rates in ^{238}U. The functional form is used for the correction

$$k_4 = 1 + \lambda_1 \cdot (\lambda_0 - \lambda) .$$

However, in this case, the parameters λ_0 and $\lambda_1$are determined by a fit to the MCNP simulated rates. For simulations using the calibration assembly description linear density as the reference (taken as a whole, including the poisoned and partial defect assemblies) the data is best represented when

λ_0 = 1297 g/cm
λ_1 = 5.26E-4 cm/g

The results suggest that the heavy metal correction for thermal mode interrogation may require assembly-specific calibrations.

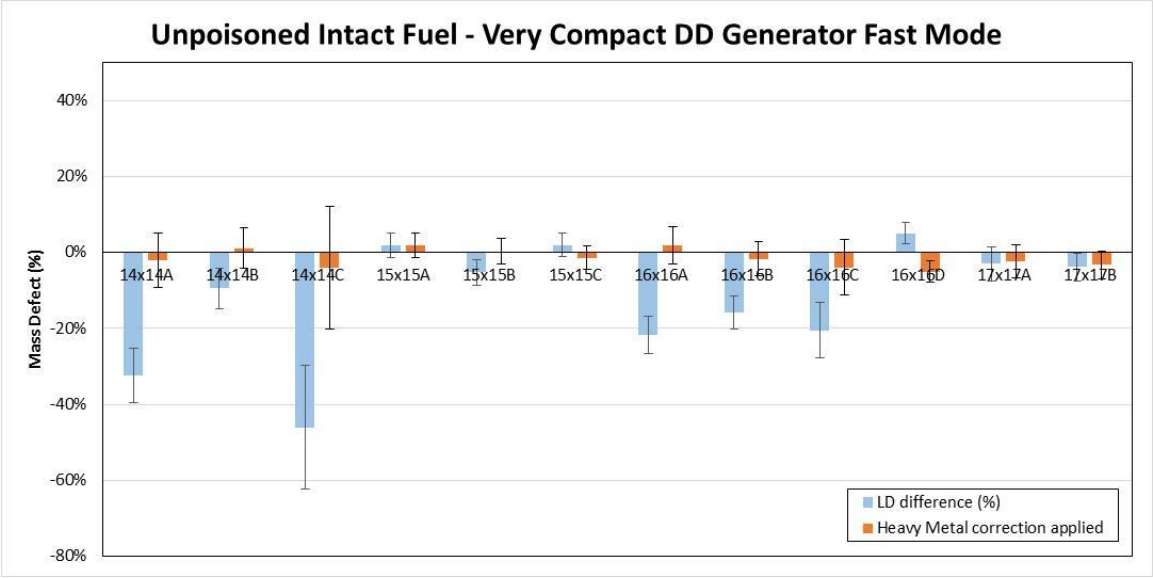

Figure 47. DD/UNCL (compact) fast mode simulated assay results for the assorted intact fuel assemblies. Error bars represent the projected 1 sigma uncertainties for an 1,800 second measurement time.

Table 58. Simulated fast mode, compact DD generator (200,000 n/s) based UNCL measurement results for the unpoisoned, intact fuel assemblies‡

Fuel assembly ID	Declared LD ^{235}U (g/cm)	Singles rate (1/s)	Doubles rate (1/s)	600 sec σ_D (1/s)	1,800 sec σ_D (1/s)	Analyzed LD ^{235}U (g/cm)	600 sec LD uncert (g/cm)	1,800 sec LD uncert (g/cm)	600 sec total uncert (%)†	1,800 sec total uncert (%)†

14x14A	**37.57**	1,340.4	12.0	± 0.64	± 0.37	**25.39**	± 3.11	± 1.79	12.2	7.1
14x14B	**37.31**	1,320.8	13.7	± 0.63	± 0.36	**33.76**	± 3.11	± 1.80	9.4	5.3
14x14C	**19.78**	1,322.3	8.9	± 0.62	± 0.36	**10.67**	± 2.99	± 1.73	28.1	16.2
15x15A	**58.37**	1,354.2	18.8	± 0.65	± 0.38	**59.45**	± 3.33	± 1.92	5.9	3.2
15x15B	**61.54**	1,360.0	18.5	± 0.65	± 0.38	**58.28**	± 3.34	± 1.93	6.1	3.3
15x15C	**60.91**	1,355.7	19.3	± 0.65	± 0.38	**62.12**	± 3.35	± 1.93	5.8	3.1
16x16A	**46.90**	1,341.6	14.3	± 0.64	± 0.37	**36.72**	± 3.17	± 1.83	8.9	5.0
16x16B	**50.16**	1,341.4	15.3	± 0.64	± 0.37	**42.02**	± 3.20	± 1.85	7.9	4.4
16x16C	**30.95**	1,321.9	11.8	± 0.63	± 0.36	**24.61**	± 3.06	± 1.77	12.6	7.2
16x16D	**64.07**	1,331.9	20.3	± 0.64	± 0.37	**67.32**	± 3.33	± 1.92	5.3	2.9
17x17A	**41.29**	1,304.3	15.0	± 0.62	± 0.36	**40.29**	± 3.11	± 1.79	8.0	4.5
17x17B	**54.82**	1,318.5	17.3	± 0.63	± 0.37	**52.09**	± 3.21	± 1.85	6.5	3.6

‡ Uncertainties are the expected measurement performance values.
† Includes a 2% systematic contribution to the uncertainty.

Table 59. Simulated DD generator–based UNCL fast mode using the compact neutron generator operating at 200,000 n/s, defect analysis results for the unpoisoned, intact fuel assemblies using the compact DD neutron generator

Fuel assembly ID	Defect without correction			Defect with HM correction applied		
	LD mass defect (%)	#σ 600 sec	#σ 1,800 sec	LD mass defect (%)	#σ 600 sec	#σ 1,800 sec
14x14A	−32.4	3.9	6.5	−2.1	0.2	0.3
14x14B	−9.5	1.1	1.8	1.1	0.1	0.2
14x14C	−46.0	3.0	5.2	−4.1	0.2	0.4
15x15A	1.9	0.3	0.5	1.9	0.3	0.5
15x15B	−5.3	0.9	1.4	0.3	0.0	0.1
15x15C	2.0	0.3	0.5	−1.5	0.3	0.4
16x16A	−21.7	3.1	5.2	1.8	0.2	0.4
16x16B	−15.8	2.4	3.9	−1.7	0.2	0.4
16x16C	−20.5	2.0	3.5	−3.9	0.4	0.6
16x16D	5.1	0.9	1.4	−5.1	1.0	1.5
17x17A	−3.0	0.4	0.6	−2.4	0.3	0.5
17x17B	−3.9	0.6	1.0	−3.3	0.5	0.8
Average bias	**−12.4%**			**−1.6%**		
Std. deviation	**15.5%**			**2.4%**		

7.3 COMPACT DD/UNCL SIMULATED PERFORMANCE FOR BURNABLE POISONS

The performance of the UNCL for assemblies containing burnable poisons is an important question when considering an alternative neutron interrogation source. The difference in neutron energy distribution from the sources and the change in moderating assembly to accommodate the larger, relative to Am(Li), source will change the relative thermal neutron population in the interrogating neutron distribution. The simulated assemblies containing poison rods allow examination of the potential impact. Figure 48 illustrates the impact of the poison rods on the fast mode mass results for the UNCL using an Am(Li) neutron source. As can be seen the number of poison rods is more important than rod's poison loading. The effectiveness of the poison rod correction can also be seen in the plots as the average bias is reduced

to <1% and the typical deviation from the expected value is reduced to less than 2% in both thermal and fast modes. The simulated rates and defect levels are presented in Table 61 and Table 62.

The parameters in the expression for the poison rod correction factor, k_3, were adjusted by a fit to the MCNP simulations. The expression for k_3 from discussed above in Section 1.3.2 [6] is shown here with the potentially adjustable parameters a, b, and c.

$$k_3 = 1 + \frac{a \cdot n}{N} \cdot \left(1 - e^{-b \cdot Gd}\right) \cdot (1 - c \cdot E_N)$$

where n is the number of poison rods,
N is the number of fuel rods (fuel + poison)
Gd is the weight percent of the Gd in the poison rods and,
E_N is the declared enrichment

The parameters for the compact generator/UNCL system are provided in Table 60.

Table 60. Poison Rod Correction Parameters for the compact generator/UNCL system

Parameter	Thermal mode		Fast mode	
	Am(Li)	Compact generator	Am(Li)	Compact generator
a	9.86	—	0.602	0.461
b	0.647	—	0.647	0.647
c	0.176	—	—	—

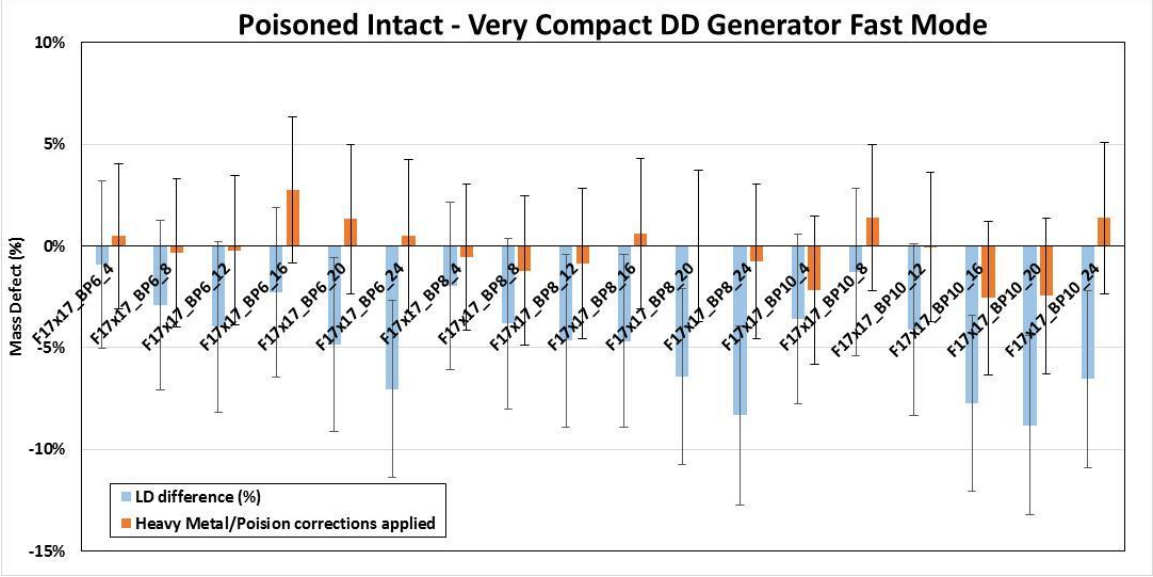

Figure 48. DD/UNCL (very compact generator) fast mode simulated assay results for the various burnable poison loadings with and without the heavy metal and poison rod correction.

Table 61. Simulated fast mode, compact DD generator (200,000 n/s) measurement results for the poisoned, intact fuel assemblies‡

Fuel assembly ID	Declared LD ^{235}U (g/cm)	Singles rate (1/s)	Doubles rate (1/s)	600 sec σ_D (1/s)	1,800 sec σ_D (1/s)	Analyzed LD ^{235}U (g/cm)	600 sec LD uncert (g/cm)	1,800 sec LD uncert (g/cm)	600 sec Total uncert (%)†	1,800 sec Total uncert (%)†
BP6_4	**51.50**	1,302.4	17.1	± 0.63	± 0.36	51.03	± 3.16	± 1.83	6.5	4.1
BP6_8	**51.20**	1,300.0	16.9	± 0.62	± 0.36	49.71	± 3.15	± 1.82	6.6	4.2
BP6_12	**50.90**	1,298.3	16.7	± 0.62	± 0.36	48.88	± 3.14	± 1.81	6.7	4.2
BP6_16	**50.60**	1,296.4	16.8	± 0.62	± 0.36	49.45	± 3.14	± 1.81	6.7	4.2
BP6_20	**50.30**	1,292.0	16.5	± 0.62	± 0.36	47.86	± 3.12	± 1.80	6.8	4.3
BP6_24	**49.90**	1,289.7	16.2	± 0.62	± 0.36	46.39	± 3.11	± 1.80	7.0	4.4
BP8_4	**51.50**	1,300.0	17.0	± 0.62	± 0.36	50.49	± 3.16	± 1.82	6.6	4.1
BP8_8	**51.20**	1,297.7	16.8	± 0.62	± 0.36	49.25	± 3.14	± 1.82	6.7	4.2
BP8_12	**50.90**	1,296.2	16.6	± 0.62	± 0.36	48.53	± 3.14	± 1.81	6.8	4.2
BP8_16	**50.50**	1,294.2	16.5	± 0.62	± 0.36	48.15	± 3.13	± 1.81	6.8	4.3
BP8_20	**50.20**	1,291.0	16.3	± 0.62	± 0.36	46.97	± 3.12	± 1.80	6.9	4.3
BP8_24	**49.90**	1,287.9	16.1	± 0.62	± 0.36	45.75	± 3.10	± 1.79	7.1	4.4
BP10_4	**51.50**	1,302.3	16.8	± 0.63	± 0.36	49.66	± 3.16	± 1.82	6.7	4.2
BP10_8	**51.20**	1,299.1	17.0	± 0.62	± 0.36	50.55	± 3.15	± 1.82	6.6	4.1
BP10_12	**50.80**	1,294.6	16.7	± 0.62	± 0.36	48.71	± 3.13	± 1.81	6.7	4.2
BP10_16	**50.50**	1,290.1	16.2	± 0.62	± 0.36	46.59	± 3.11	± 1.80	7.0	4.3
BP10_20	**50.20**	1,286.9	16.1	± 0.62	± 0.36	45.78	± 3.10	± 1.79	7.1	4.4
BP10_24	**49.80**	1,284.6	16.2	± 0.62	± 0.36	46.54	± 3.10	± 1.79	7.0	4.3

‡ Uncertainties are the expected measurement performance values.
† Includes a 2% systematic contribution to the uncertainty.

Table 62. Simulated fast mode, defect analysis results for the poisoned, intact fuel assemblies using the compact neutron generator operating at 200,000

Fuel assembly ID	Defect without correction			HM and Poison corrections applied		
	LD mass defect (%)	#σ 600 sec	#σ 1,800 sec	LD mass defect (%)	#σ 600 sec	#σ 1,800 sec
BP6_4	−0.9	0.1	0.2	0.5	0.1	0.1
BP6_8	−2.9	0.5	0.7	−0.3	0.1	0.1
BP6_12	−4.0	0.6	1.0	−0.2	0.0	0.0
BP6_16	−2.3	0.3	0.6	2.8	0.4	0.7
BP6_20	−4.8	0.7	1.2	1.3	0.2	0.3
BP6_24	−7.0	1.1	1.7	0.5	0.1	0.1
BP8_4	−2.0	0.3	0.5	−0.6	0.1	0.1
BP8_8	−3.8	0.6	0.9	−1.2	0.2	0.3
BP8_12	−4.7	0.7	1.2	−0.9	0.1	0.2
BP8_16	−4.7	0.7	1.1	0.6	0.1	0.1
BP8_20	−6.4	1.0	1.6	0.0	0.0	0.0
BP8_24	−8.3	1.3	2.1	−0.8	0.1	0.2
BP10_4	−3.6	0.6	0.9	−2.2	0.3	0.5
BP10_8	−1.3	0.2	0.3	1.4	0.2	0.3
BP10_12	−4.1	0.6	1.0	0.0	0.0	0.0
BP10_16	−7.7	1.2	1.9	−2.6	0.4	0.6
BP10_20	−8.8	1.4	2.2	−2.5	0.4	0.6
BP10_24	−6.5	1.0	1.6	1.4	0.2	0.3
Average bias	**−4.7%**			**−0.2%**		
Std. deviation	**2.4%**			**1.4%**		

7.4 COMPACT DD/UNCL SIMULATED PARTIAL DEFECT ANALYSIS

This series of simulations examines the performance of the UNCL using compact DD neutron generator for the substitution configurations. The series examines the expected response with an increasing number of DU rods substituted for LEU fuel rods. The mass defect relative to the declared value is shown in Figure 49 for the fast mode. Rates and performance values are provided in Table 63 through Table 64. Since heavy metal content for the simulated assembly is the same as the simulated calibration assemblies, the heavy metal correction will be equal to 1 so application of the correction will have no impact on the results.

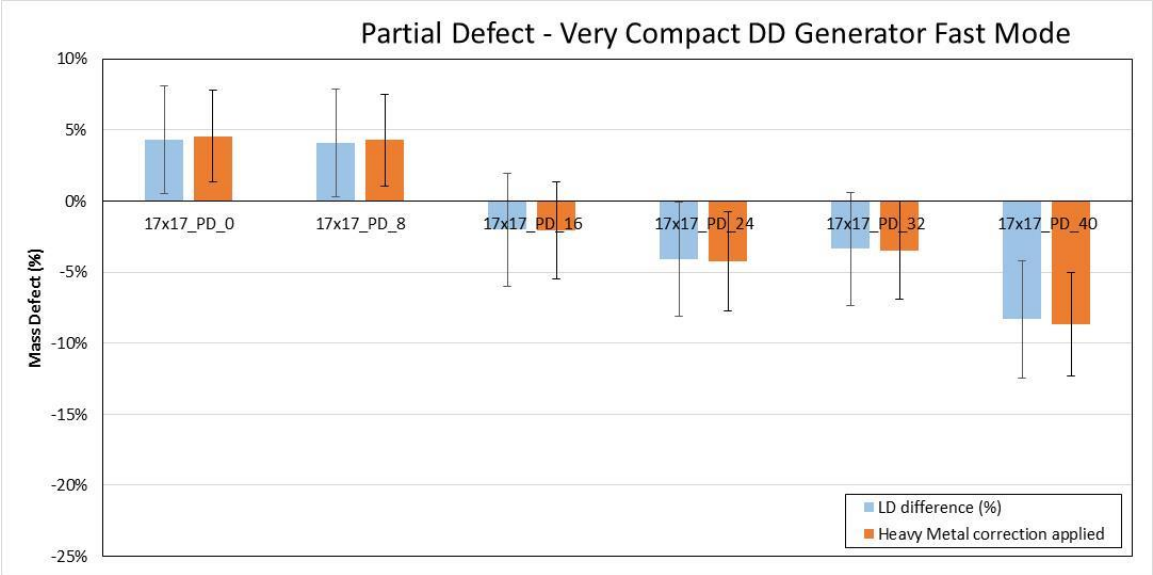

Figure 49. DD/UNCL (very compact generator) fast mode simulated assay results for the partial defect loadings with and without the heavy metal correction.

Table 63. Simulated fast mode, compact DD generator operating at 200,000 n/s measurement results for the partial defect assembly configurations‡

Fuel assembly ID	Declared LD ^{235}U (g/cm)	Singles rate (1/s)	Doubles rate (1/s)	600 sec σ_D (1/s)	1,800 sec σ_D (1/s)	Analyzed LD ^{235}U (g/cm)	600 sec LD uncert (g/cm)	1,800 sec LD uncert (g/cm)	600 sec Total uncert (%)†	1,800 sec Total uncert (%)†
PD_0	54.98	1,311.7	18.4	± 0.63	± 0.36	57.47	± 3.22	± 1.86	5.9	3.8
PD_8	54.98	1,309.9	18.4	± 0.63	± 0.36	57.32	± 3.21	± 1.85	5.9	3.8
PD_16	54.98	1,309.0	17.7	± 0.63	± 0.36	53.82	± 3.19	± 1.84	6.3	4.0
PD_24	54.98	1,307.6	17.4	± 0.63	± 0.36	52.64	± 3.18	± 1.84	6.4	4.0
PD_32	54.98	1,303.9	17.5	± 0.63	± 0.36	53.05	± 3.17	± 1.83	6.3	4.0
PD_40	54.98	1,302.4	17.0	± 0.62	± 0.36	50.20	± 3.15	± 1.82	6.6	4.1

‡ Uncertainties are the expected measurement performance values.
† Includes a 2% systematic contribution to the uncertainty.

Table 64. Simulated DD/UNCL fast mode, defect analysis results for the partial defect assembly configurations using the compact generator operating at 200,000 n/s

Fuel assembly ID	Defect without correction			HM and poison corrections applied		
	LD mass defect (%)	#σ 600 sec	#σ 1,800 sec	LD mass defect (%)	#σ 600 sec	#σ 1,800 sec
PD_0	4.5	0.7	1.1	4.5	0.7	1.1
PD_8	4.3	0.7	1.1	4.3	0.7	1.1
PD_16	−2.1	0.3	0.5	−2.1	0.3	0.5
PD_24	−4.3	0.7	1.1	−4.2	0.7	1.1
PD_32	−3.5	0.6	0.9	−3.5	0.6	0.9
PD_40	−8.7	1.4	2.3	−8.7	1.4	2.3

8. PERFORMANCE COMPARISON OF THE DD/UNCL AND THE AM(LI)/UNCL

8.1 PERFORMANCE COMPARISON FOR THERMAL MODE OPERATION

8.1.1 Thermal Mode Response Function Comparison

To examine the relative mass dependence of the various interrogating neutron sources, the thermal mode calibration curves for the Am(Li), MP320, and nGen-310 interrogation systems were each normalized to their response to the 65 g ^{235}U/cm calibration assembly. The comparison of the simulated calibration curves for each of the neutron sources (Figure 50) reveals that the response function for each of the neutron generator types considered have nearly identical dependence on the ^{235}U content of the assembly.

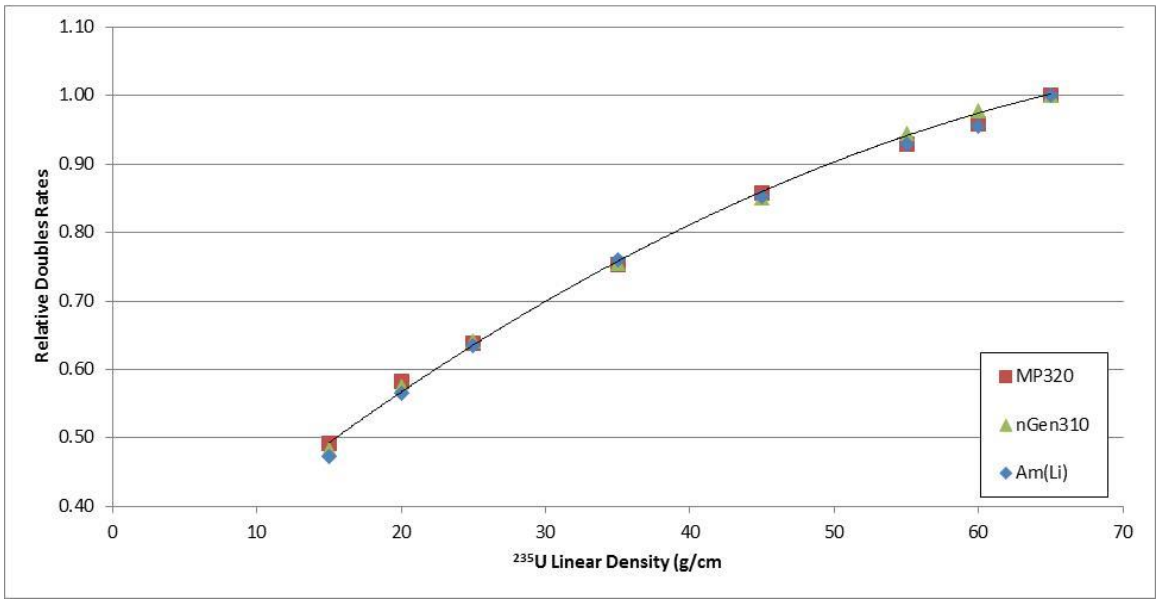

Figure 50. Comparison of the relative thermal mode coincidence rates as a function of ^{235}U linear density for the calibration assemblies (normalized to the 65 g ^{235}U/cm result) for each of the neutron sources considered.

The primary difference in performance between the different neutron source configurations is the measurement precision achievable, which is limited by the singles rate which drives the accidentals coincidence rate. For the neutron generator–based systems, the ratio of the singles rate to the doubles rate is greater than from the Am(Li)-based measurement. Figure 51 provides a comparison of the relative singles rate as a function of the ^{235}U linear mass density for the two generators and the Am(Li) source normalized by the doubles rates at the 65 g ^{235}U/cm Am(Li) loading. From the plots we see that singles rates for the neutron generator–based measurements will be approximately 1.5 times larger than Am(Li)-based measurement to produce equivalent doubles rates.

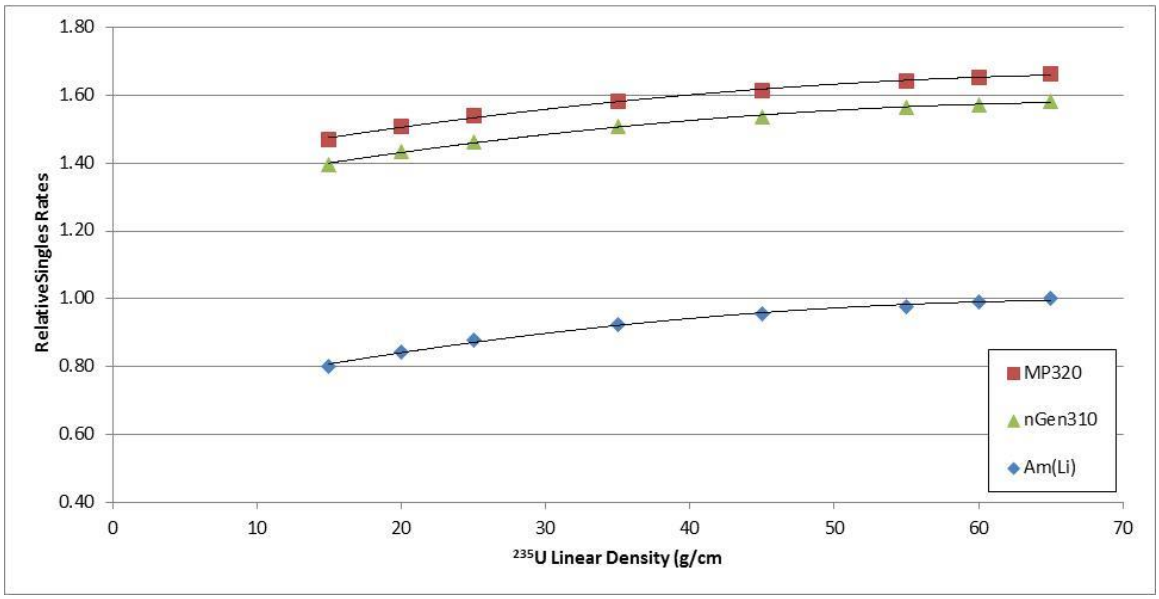

Figure 51. Comparison of the relative thermal mode singles rates as a function of ^{235}U linear density for the calibration assemblies for each of the neutron sources considered.

The relative rates comparisons in Figure 50 and Figure 51 indicate that in thermal interrogation mode, the measurement precision for the Am(Li)-based coincidence measurement will be superior to that from the neutron generators over the entire ^{235}U content range expected for an UNCL measurement. To examine the measurement precision, we must first estimate the uncertainty in the doubles rates under realistic measurement conditions. Appropriate source strengths must be selected, and the room background and the passive signal from the fuel assemblies must be included in the analysis.

The Am(Li) and neutron generator source terms were selected to be representative of an actual measurement. The Am(Li) source term is taken to be 50,000 n/s, which is approximately the same yield as the Am(Li) source used for the validation measurements discussed in a later section of this report. The neutron generator yields are taken as 200,000 n/s operating in a steady-state mode because increasing the neutron generator yield beyond this level does not significantly reduce the measurement precision and would minimize any ALARA considerations for a fieldable instrument (the exposure rate from a 200,000 n/s DD generator is equivalent to a 0.1 µg ^{252}Cf source). The neutron background levels chosen (singles rate = 30 and doubles rate = 0.1) are representative of past UNCL measurements from an operating fuel facility. The passive neutron signals from the fuel assembly were estimated from the MCNP models.

The expected doubles rate precision as a function of ^{235}U linear density is shown in Figure 52 for the Am(Li) and neutron generator–based measurements for measurement times of 1,800 seconds. The corresponding contribution to the linear mass uncertainty is shown in Figure 53. The expected double rate measurement precisions for the two generators are equivalent, but both are roughly 1.5 times larger than the precision obtained from the Am(Li) source measurements. However, compared to the calibration error, the difference in measurement precision in the thermal modes is not significant.

NOTE: Attempts to improve performance by neutron spectrum tailoring (e.g., introduction of stainless steel reflectors near the neutron point of generation were unsuccessful. In general, addition of moderator or replacement of HDPE in proximity to the neutron generator by any reflective material resulted in degradation of the measurement precision.

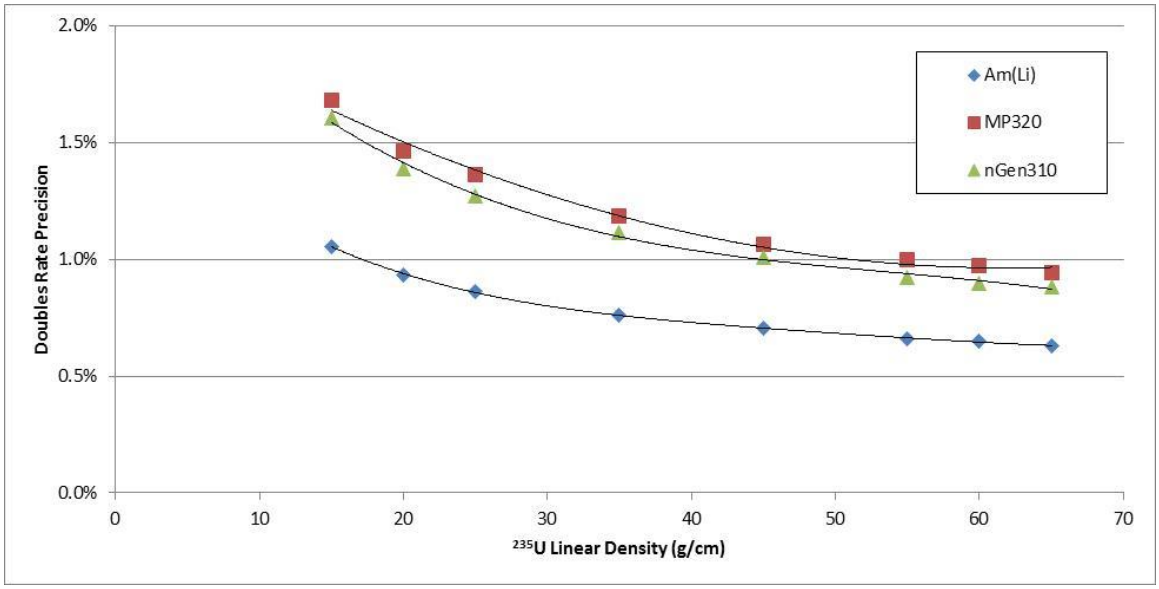

Figure 52. Comparison of the thermal mode doubles rate precision as a function of ^{235}U linear density for the calibration assemblies for each of the neutron sources considered for 1,800 seconds measurement time. Am(Li) = 50,000 n/s, and neutron generators = 200,000 n/s.

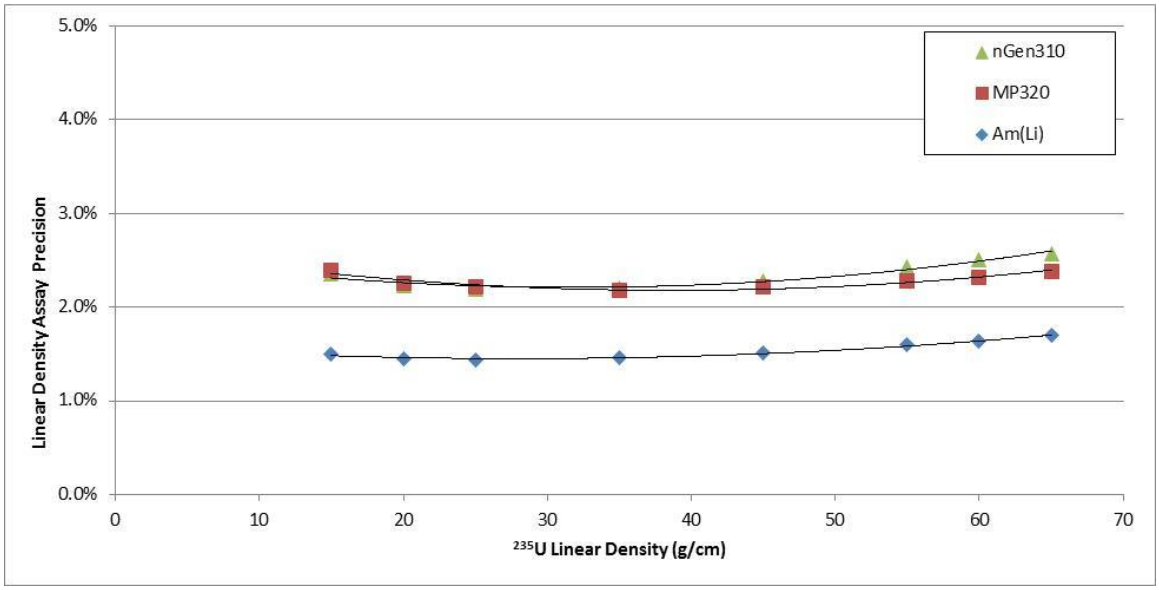

Figure 53. Comparison of the thermal mode assay precision as a function of ^{235}U linear density for the calibration assemblies for each of the neutron sources considered for 1,800 seconds measurement time. Am(Li) = 50,000 n/s, and neutron generators = 200,000 n/s.

8.1.2 Thermal Mode Intact, Unpoisoned Fuel Assembly Comparison

A comparison of the simulated results for the MP320 and nGen-310 neutron generators with the Am(Li) mode based UNCL thermal mode measurements is presented in Figure 54, and the same data with the heavy metal correction applied is shown in Figure 55. Standard deviations for the collection of assemblies and the average biases are presented in Table 65. There is no significant difference qualitatively or quantitatively in the biases predicted by these simulations. Because the measurement precision is small compared to the overall uncertainty in the UNCL result, we conclude that the neutron generators and the

Am(Li) sources provide equivalent performance in thermal mode. We also conclude from these results that the heavy metal correction offers little value for the UNCL operated in the thermal mode.

Table 65. Thermal mode bias comparisons for the intact, unpoisoned fuel assemblies

	Uncorrected assay results				Heavy metal correction applied		
	Am(Li)	**MP320**	**nGen-310**		**Am(Li)**	**MP320**	**nGen-310**
Average bias	−16.0%	−21.3%	−22.2%		−14.7%	−13.9%	−10.1%
Standard deviation	6.8%	9.7%	10.3%		9.5%	10.3%	11.3%
Measurement precision	0.9%	1.5%	1.4%		0.9%	1.5%	1.4%

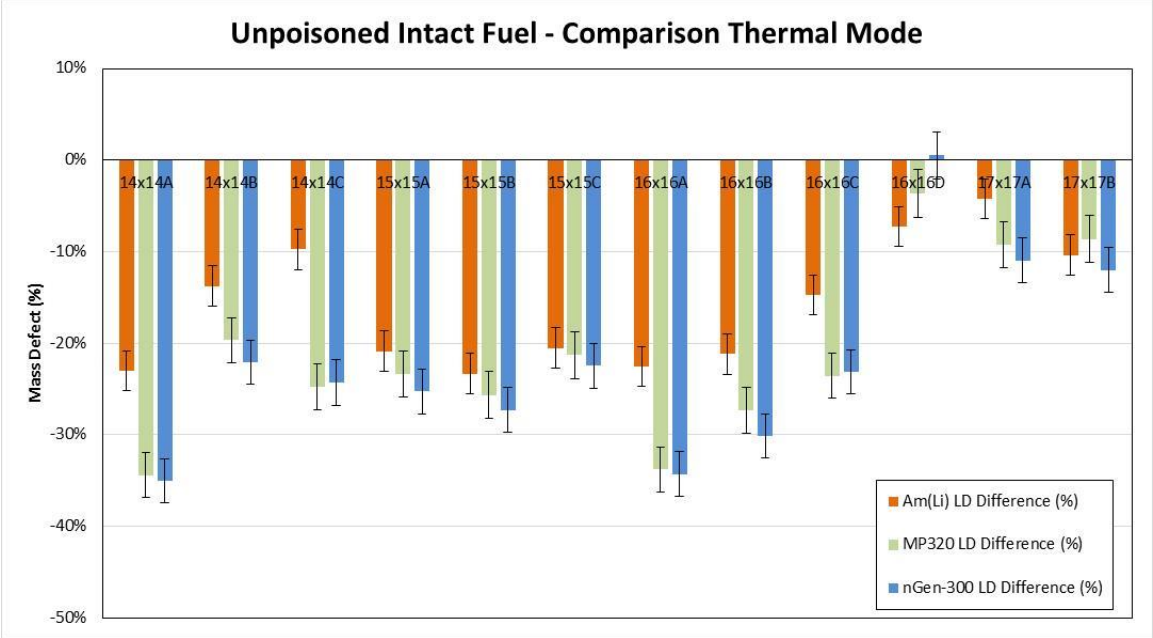

Figure 54. Comparison of the DD/UNCL and Am(Li) thermal mode defect results for the assorted intact fuel assemblies. Error bars represent the projected 1 sigma uncertainties for an 1,800 second measurement time.

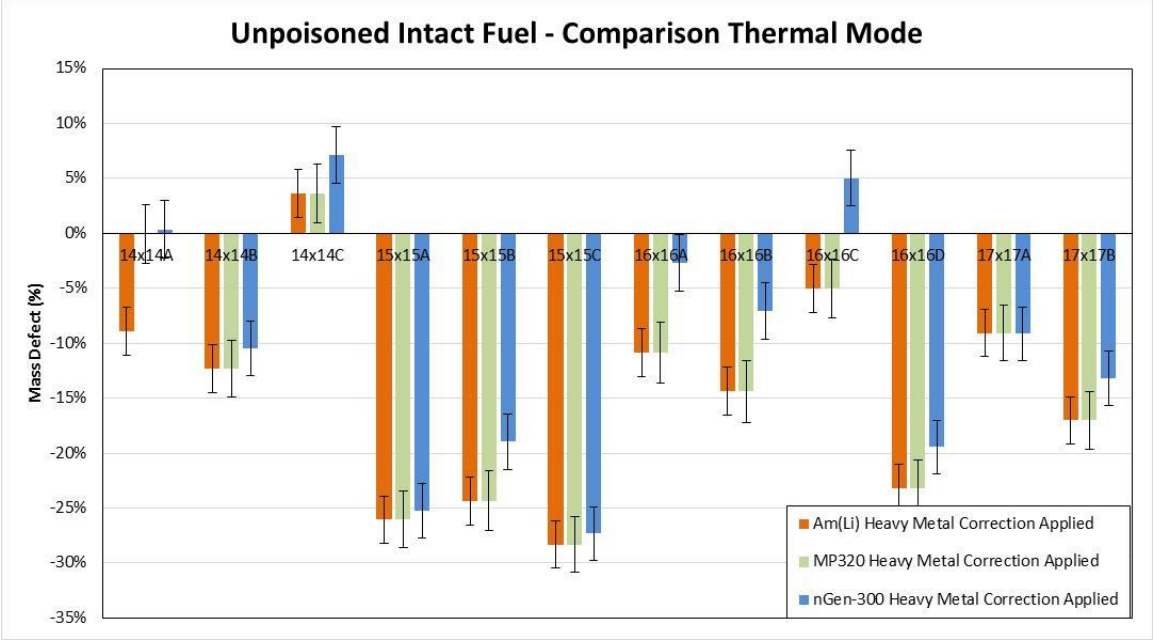

Figure 55. Comparison of the DD/UNCL and Am(Li) thermal mode defect results for the assorted intact fuel assemblies with the heavy metal correction applied. Error bars represent the projected 1 sigma uncertainties for an 1,800 second measurement time.

8.1.3 Thermal Mode Poisoned Fuel Assembly Comparison

A comparison of the simulated results for the MP320 and nGen-310 neutron generators with the Am(Li) mode based UNCL thermal mode measurements for assemblies containing poison rods is presented in Figure 56, and the same data with the heavy metal and poison corrections applied are shown in Figure 57. Standard deviations for the collection of assemblies and the average biases are presented in Table 66.

There is no significant difference qualitatively or quantitatively in the biases predicted by these simulations. Because the measurement precision is small compared to the overall uncertainty in the UNCL result, we conclude that in thermal mode the neutron generators and the Am(Li) sources provide equivalent performance. We also conclude that the poison correction applied in the thermal mode is potentially a very accurate method when the only parameter changing is the number of poison rods present.

Table 66. Thermal mode bias comparisons for the intact, poisoned fuel assemblies

	Uncorrected assay results				Heavy metal correction applied		
	Am(Li)	**MP320**	**nGen-310**		**Am(Li)**	**MP320**	**nGen-310**
Average bias	−34.2%	−30.4%	−31.3%		−0.3%	1.5%	0.1%
Standard deviation	13.6%	13.2%	12.9%		1.6%	3.6%	3.2%
Measurement precision	0.7%	1.4%	1.3%		0.7%	1.4%	1.3%

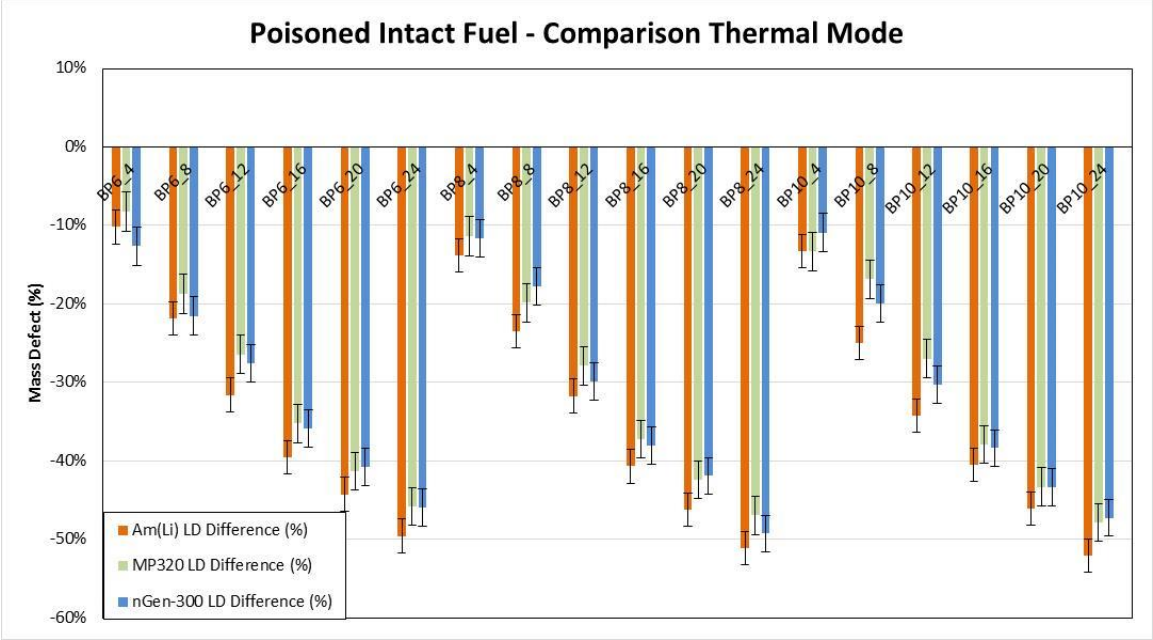

Figure 56. Comparison of the DD/UNCL and Am(Li) thermal mode defect results for the poisoned intact fuel assemblies. Error bars represent the projected 1 sigma uncertainties for an 1,800 second measurement time.

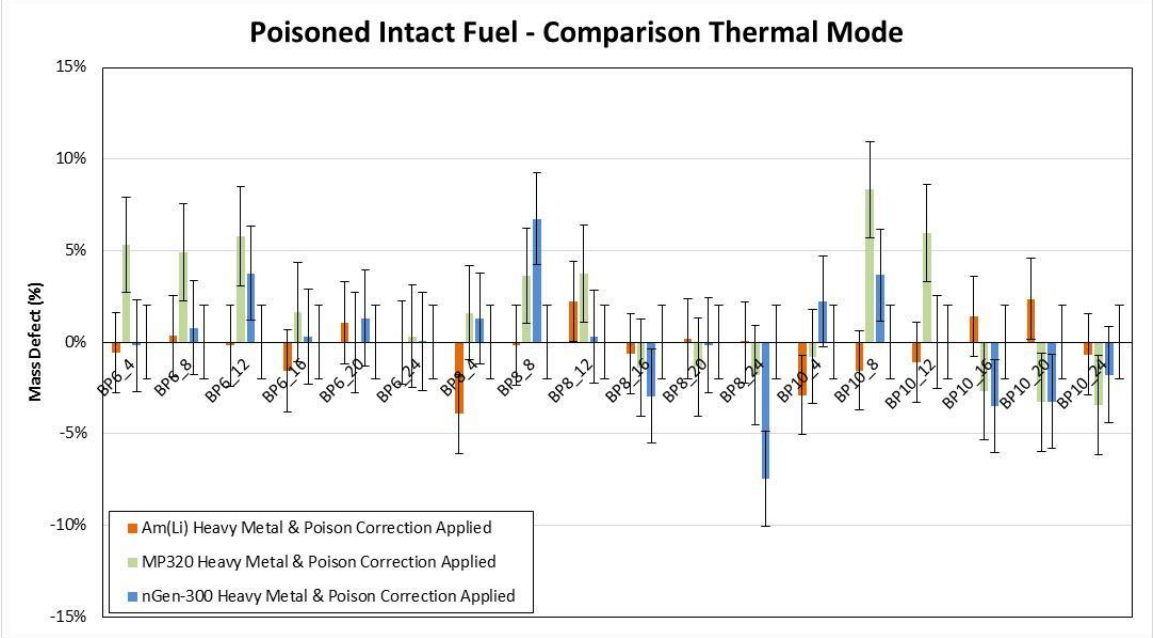

Figure 57. Comparison of the DD/UNCL and Am(Li) thermal mode defect results for the poisoned intact fuel assemblies with the heavy metal correction and poison corrections applied. Error bars represent the projected 1 sigma uncertainties for an 1,800 second measurement time.

8.1.4 Thermal Mode Partial Defect Assembly Comparison

A comparison of the simulated results for the MP320 and nGen-310 neutron generators with the Am(Li) source thermal mode interrogation of the partial defect fuel assemblies is presented in Table 67 and in Figure 58. There is no significant difference in the biases from the three neutron sources. Although the

measurement precision of the Am(Li)-based interrogation is somewhat better than what is obtainable with the neutron generators, the differences in the measurement precision are small relative to the calibration errors and the biases. However, because the Am(Li) source–based measurement provides better measurement precision, it is likely that with assembly-specific calibrations (i.e., direct comparisons to reference assemblies) that the Am(Li) measurement will be able to detect slightly smaller numbers of rod substitutions (e.g., 10 versus 20).

Table 67. Thermal mode bias comparisons for the partial defect fuel assemblies (assay time: 1,800 s).

	Uncorrected assay results				Heavy metal correction applied		
	Am(Li)	**MP320**	**nGen-310**		**Am(Li)**	**MP320**	**nGen-310**
Standard deviation	−7.6%	−6.1%	−7.9%		−14.0%	−6.0%	−7.9%
Average bias	4.3%	7.3%	5.0%		3.8%	7.3%	5.0%
Measurement precision	0.9%	1.6%	1.5%		0.9%	1.6%	1.5%

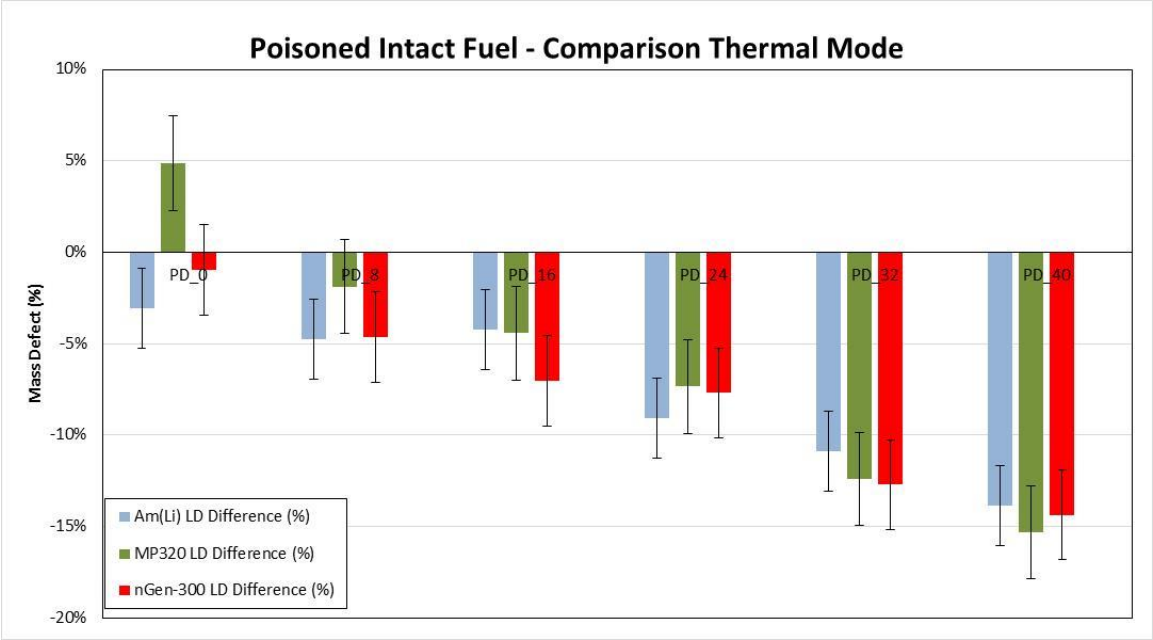

Figure 58. Comparison of the uncorrected DD/UNCL and Am(Li) thermal mode defect results. Error bars represent the projected 1 sigma uncertainties for an 1,800 second measurement time.

8.2 PERFORMANCE COMPARISON OF THE GENERATORS IN FAST MODE

8.2.1 Fast Mode Response Function Comparison

To examine the relative mass dependence of the various interrogating neutron sources, the fast mode calibration curves for the Am(Li), MP320, nGen-310 and the compact generator, interrogation systems were each normalized to their response to the 65 g ^{235}U/cm calibration assembly. The comparison of the simulated calibration curves for each of the neutron sources (Figure 59) reveals that the response function for each of the neutron generator types considered have nearly identical dependence on the ^{235}U content of the assembly, but they have a somewhat lower sensitivity as a function of linear density when compared to the Am(Li)-based measurement. However, the difference in the singles rates for each

neutron source is more pronounced as seen in Figure 60 leading to a degradation in the measurement precision for the neutron generators relative to the Am(Li) source interrogation.

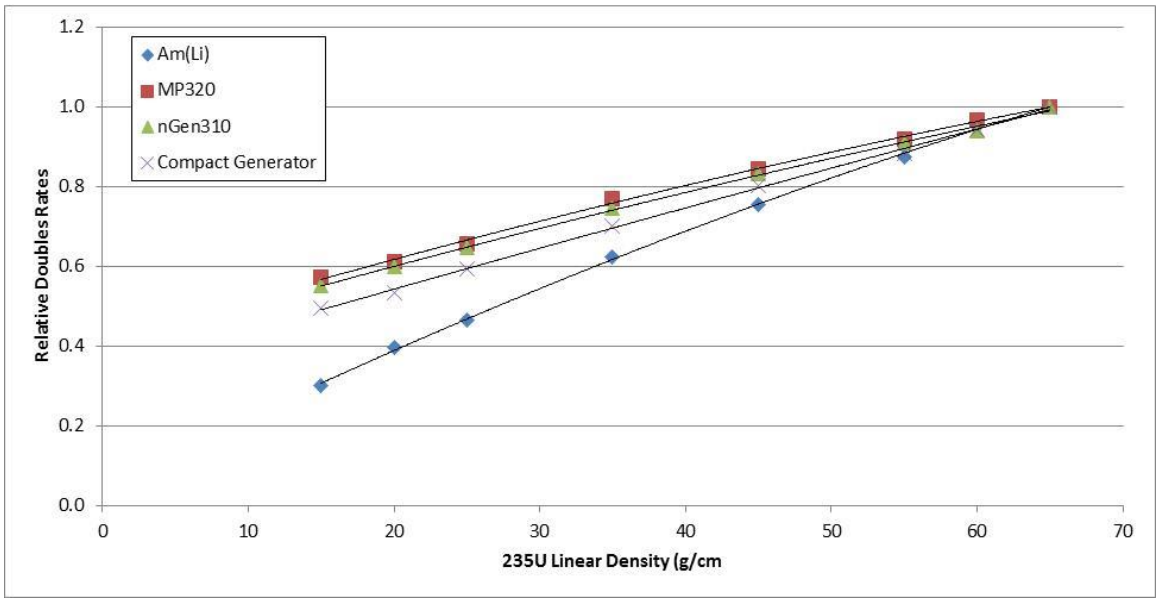

Figure 59. Comparison of the relative fast coincidence rates as a function of ^{235}U linear density for the calibration assemblies for each of the neutron sources considered.

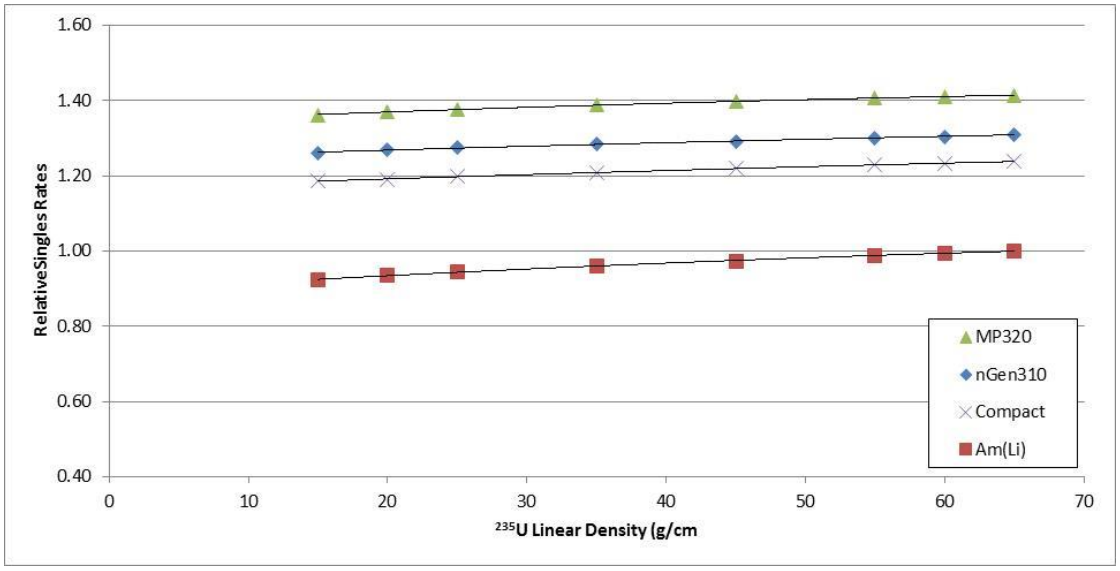

Figure 60. Comparison of the relative fast mode singles rates as a function of ^{235}U linear density for the calibration assemblies for each of the neutron sources considered.

Figure 61 presents a comparison of the expected precision in the UNCL fast mode doubles rates for the Am(Li) and neutron generator–based measurements. The neutron source yield was assumed to be 50,000 n/s and for the Am(Li) source and 200,000 n/s for the neutron generators. There is little difference in the doubles rate precision with the neutron source and as can be seen in the figure, the measurement precision achievable from the neutron generators appears to be somewhat better at the lower ^{235}U linear mass loadings. However, due to the relatively shallow slope of the mass response function for the neutron generator arrangements, the Am(Li)-based system provides about a factor of 2 better assay precision for

the same measurement time. Figure 62 presents a comparison of the expected precision in the UNCL fast mode assay results for the neutron interrogation sources (calibration errors and biases are ignored so that the plot shows only the uncertainty contribution from the expected counting statistics).

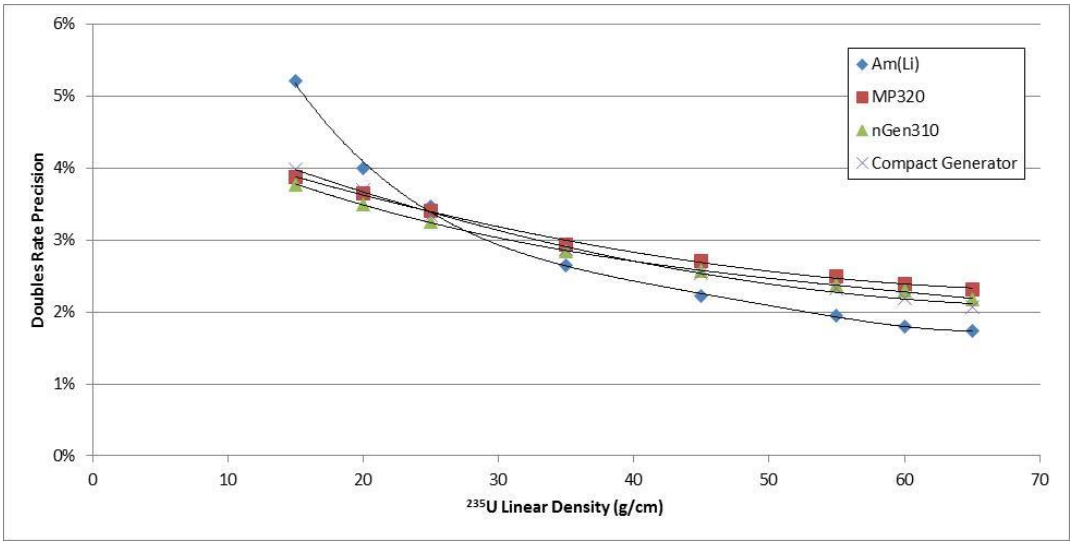

Figure 61. Comparison of the fast mode doubles rate precision as a function of ^{235}U linear density for the calibration assemblies for each of the neutron sources considered for 1,800 seconds measurement time. Am(Li) = 50,000 n/s, and neutron generators = 200,000 n/s.

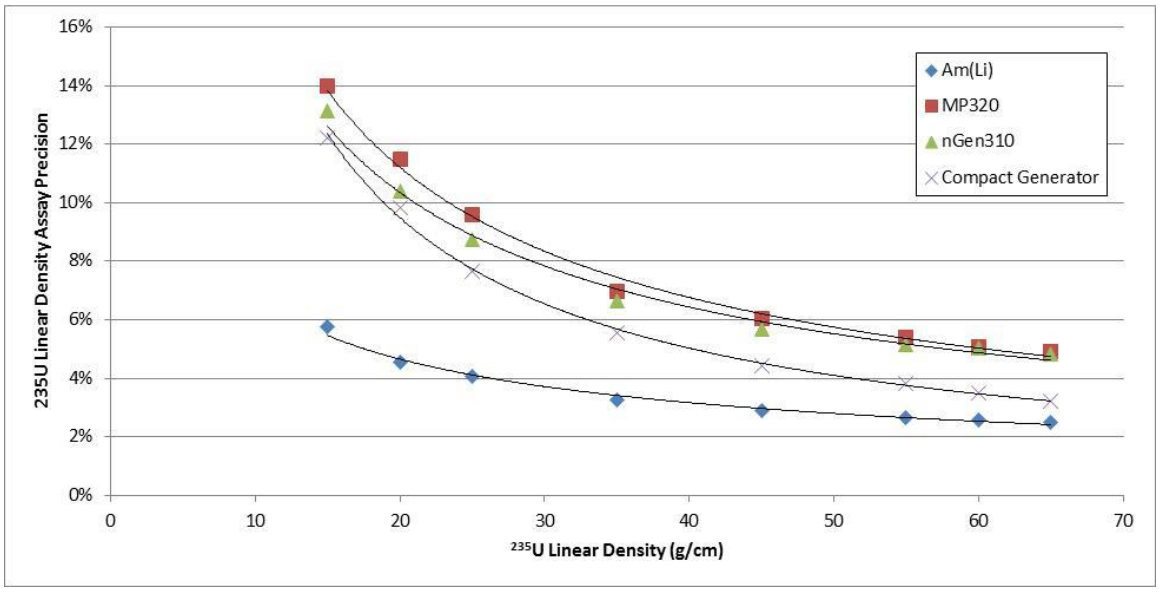

Figure 62. Comparison of the fast mode assay precision as a function of ^{235}U linear density for the calibration assemblies for each of the neutron sources considered for 1,800 seconds measurement time. Am(Li) = 50,000 n/s, and neutron generators = 200,000 n/s.

8.2.2 Fast Mode Intact, Unpoisoned Fuel Assembly Comparison

A comparison of the simulated results for the MP320, nGen-310 and the "very compact" neutron generators with the Am(Li) mode based UNCL fast mode measurements is presented in Figure 63 and the same data with the heavy metal correction applied in Figure 64. Standard deviations for the collection of assemblies and the average biases are present in Table 68. From the data presented in Sections 4 through 7 and as can be seen in the Figure 63 the standard deviation, biases and precision of the uncorrected assay results are larger each generator types considered than achievable from the Am(Li)-based measurement. Following application of a heavy metal correction, there is no significant difference qualitatively or quantitatively in the biases for the corrected linear densities predicted by these simulations. However, the measurement precision achievable using the MP320 or nGEn310 generators is about 2.5 times larger than from the Am(Li). For the fictional very compact generator, the measurement precision is approximately 2 times that from the Am(Li) measurement.

Table 68. Fast mode bias comparisons for the intact, unpoisoned fuel assemblies

	Uncorrected assay results				Heavy metal correction applied			
	Am(Li)	**MP320**	**nGen-310**	**Compact**	**Am(Li)**	**MP320**	**nGen-310**	**Compact**
Average bias	−2.0%	−18.6%	−17.5%	−12.4%	−1.4%	−2.6%	−2.3%	−1.6%
Standard deviation	6.3%	22.0%	21.1%	15.5%	2.9%	2.6%	2.6%	2.4%
Measurement precision	2.9%	8.0%	7.2%	5.5%	2.9%	8.0%	7.2%	5.5%

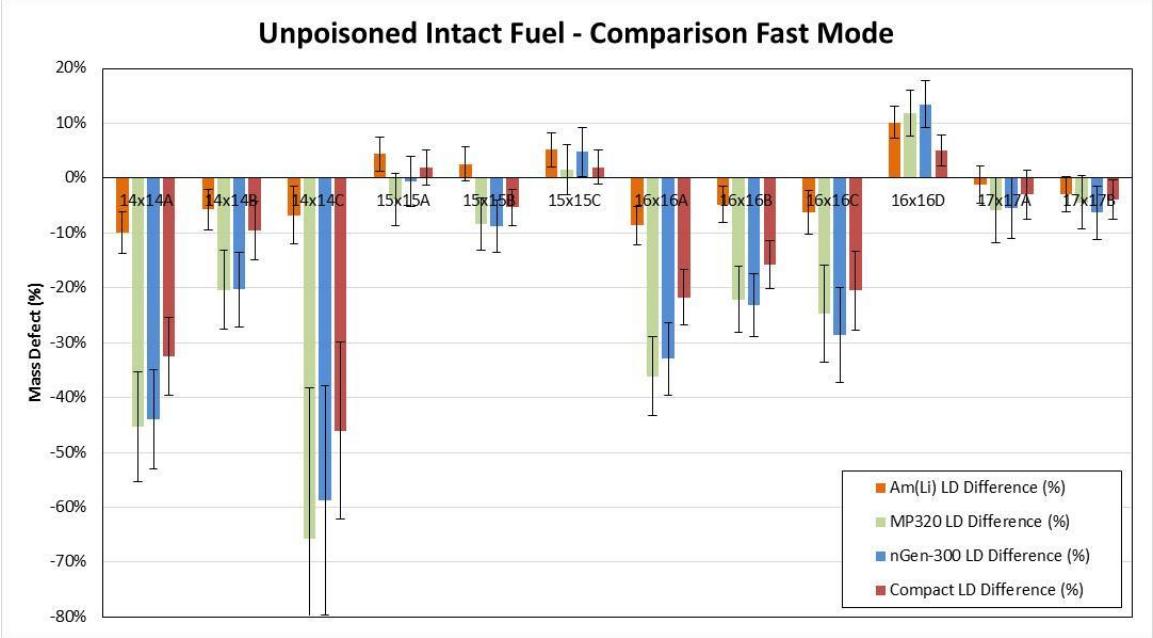

Figure 63. Comparison of the DD/UNCL and Am(Li) fast mode defect results for the assorted intact fuel assemblies. Error bars represent the projected 1 sigma uncertainties for an 1,800 second measurement time.

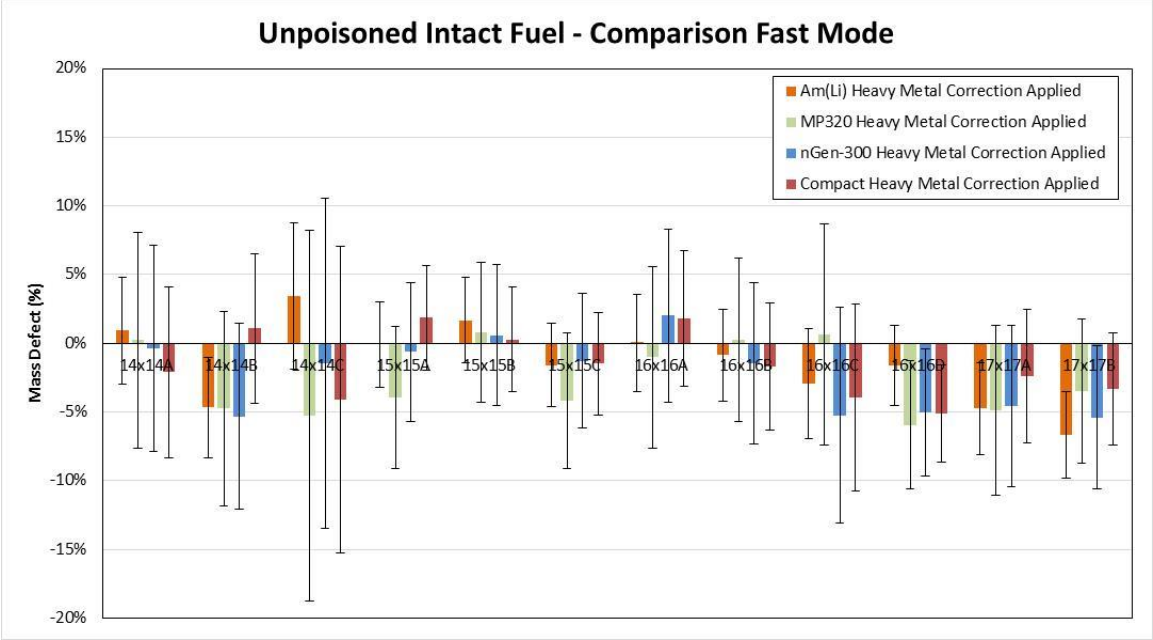

Figure 64. Comparison of the DD/UNCL and Am(Li) fast mode defect results for the assorted intact fuel assemblies with the Heavy Metal correction applied. Error bars represent the projected 1 sigma uncertainties for an 1,800 second measurement time.

8.2.3 Fast Mode Poisoned Fuel Assembly Comparison

A comparison of the simulated results for the MP320, nGen-310 and compact neutron generators with the Am(Li) mode based UNCL fast mode measurements for assemblies containing poison rods is presented in Figure 65 and the same data with the heavy metal and poison corrections applied in Figure 66. Standard deviations for the collection of assemblies and the average biases are present in Table 69.

There is no significant difference qualitatively or quantitatively in the biases predicted by these simulations. However, because the measurement precision is twice as large compared to the overall uncertainty in the UNCL result, we conclude that in fast mode the Am(Li) sources provide superior performance to that achievable from the neutron generators.

We also conclude that the poison correction applied in the fast mode is potentially a very accurate method when the only parameter changing is the number of poison rods present.

Table 69. Fast mode bias comparisons for the intact, poisoned fuel assemblies

	Uncorrected assay results					**Heavy metal and poison rod corrected**			
	Am(Li)	**MP320**	**nGen-310**	**Compact**		**Am(Li)**	**MP320**	**nGen-310**	**Compact**
Average bias	−3.8%	−6.2%	−6.2%	−4.7%		−0.4%	0.8%	0.2%	−0.2%
Standard deviation	3.2%	3.5%	2.9%	2.4%		1.4%	2.2%	1.3%	1.4%
Measurement precision	2.4%	5.1%	4.9%	3.7%		2.4%	5.1%	4.9%	3.7%

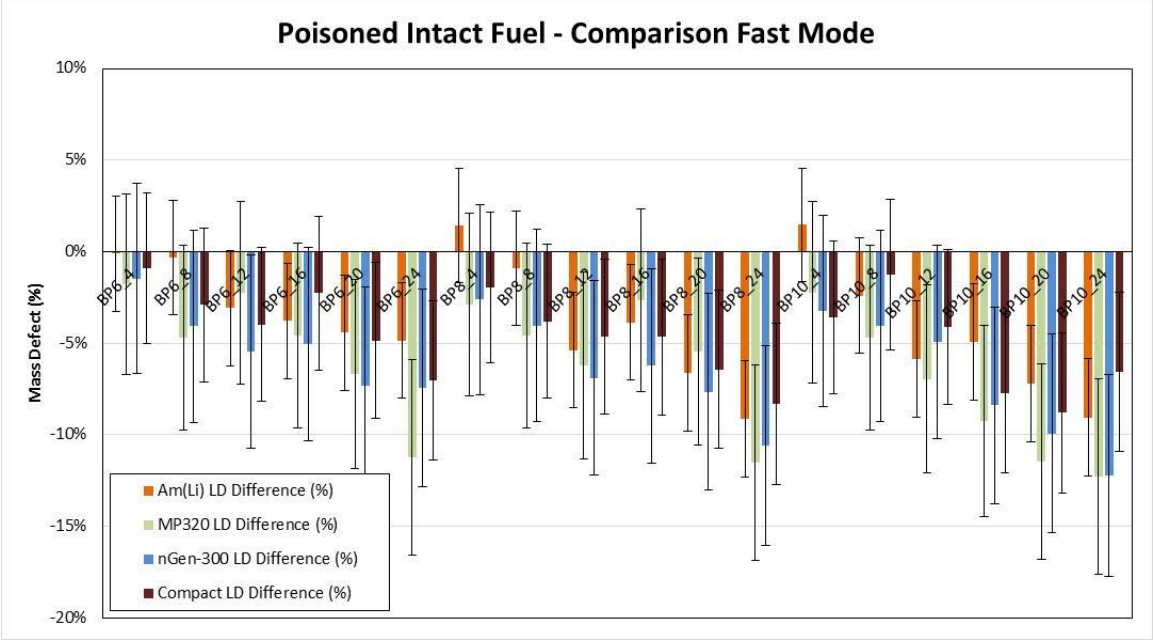

Figure 65. Comparison of the DD/UNCL and Am(Li) fast mode defect results for the poisoned fuel assemblies. Error bars represent the projected 1 sigma uncertainties for an 1,800 second measurement time.

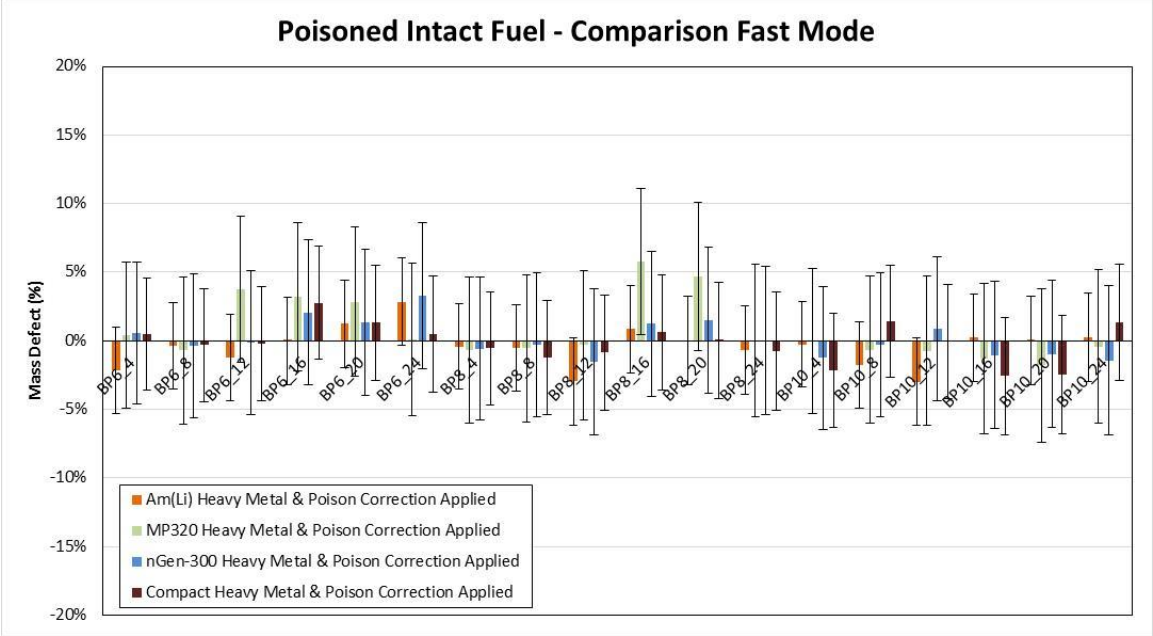

Figure 66. Comparison of the DD/UNCL and Am(Li) fast mode defect results for the poisoned fuel assemblies with the heavy metal correction applied. Error bars represent the projected 1 sigma uncertainties for an 1,800 second measurement time.

8.2.4 Fast Mode Partial Defect Assembly Comparison

A comparison of the simulated results for the MP320 and nGen-310 neutron generators with the Am(Li) source thermal mode interrogation of the partial defect fuel assemblies is presented in Table 70 and in Figure 56 and Figure 57. There is no significant difference in the biases from the three neutron sources.

However, the measurement precision of the Am(Li)-based interrogation is twice as good as that obtainable with the neutron generators.

Because the Am(Li) source based measurement provides better measurement precision, it is likely that with assembly-specific calibrations (i.e., direct comparisons to reference assemblies) that the Am(Li) measurement will be able to detect smaller numbers of rod substitutions (e.g., 26 versus 52).

Table 70. Fast mode bias comparisons for the partial defect fuel assemblies

	Uncorrected assay results					Heavy metal and poison rod corrected			
	Am(Li)	**MP320**	**nGen-310**	**Compact**		**Am(Li)**	**MP320**	**nGen-310**	**Compact**
Average bias	−5.5%	−6.6%	−8.3%	−1.6%		−9.4%	−6.6%	−8.2%	−1.6%
Standard deviation	6.4%	5.9%	5.8%	5.2%		6.1%	5.9%	5.8%	5.2%
Measurement precision	2.4%	4.9%	4.8%	3.4%		2.4%	4.9%	4.8%	3.4%

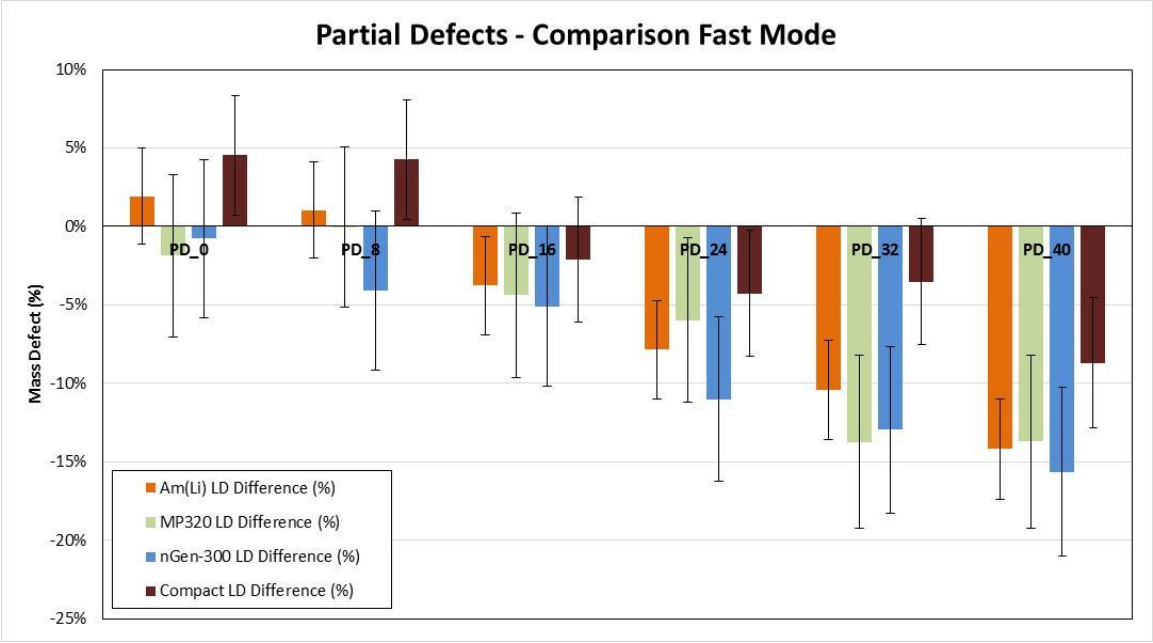

Figure 67. Comparison of the DD/UNCL and Am(Li) fast mode defect results for the partial defect fuel assemblies. Error bars represent the projected 1 sigma uncertainties for an 1,800 second measurement time.

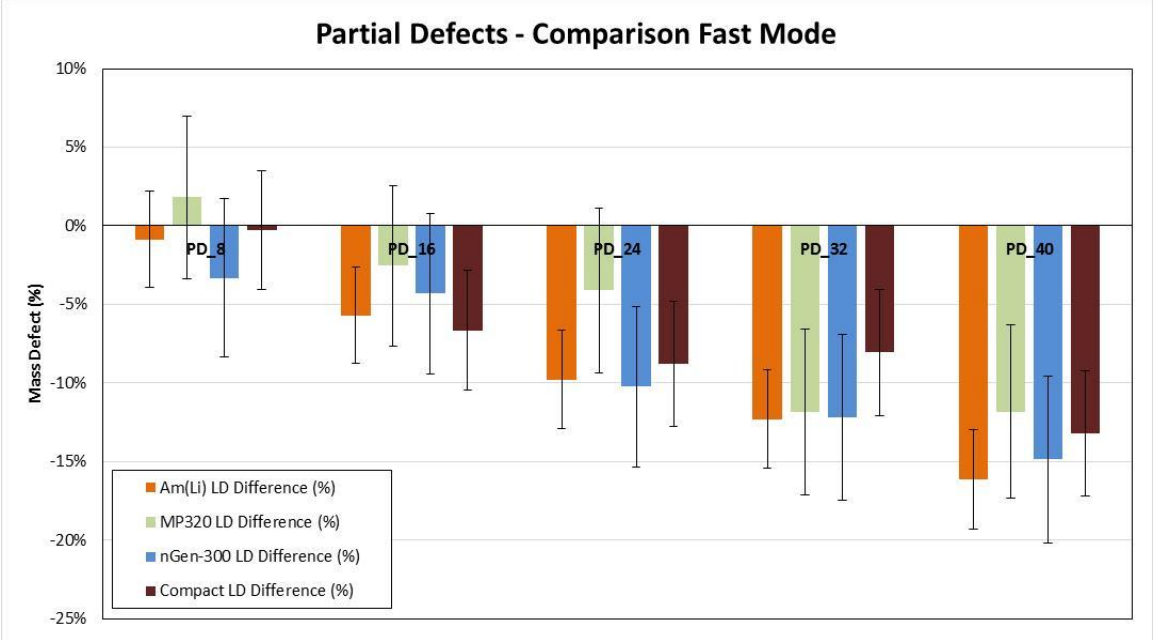

Figure 68. Comparison of the DD/UNCL and Am(Li) fast mode defect results for the partial defect fuel assemblies normalized to the intact assembly. Error bars represent the projected 1 sigma uncertainties for an 1,800 second measurement time.

9. DELAYED NEUTRON COUNTING USING THE MP320 NEUTRON GENERATOR

The primary limitation in the UNCL coincidence measurement is the measurement precision achievable with the current detector configuration and assay methodology. It is not possible to achieve the necessary measurement precision in a reasonable measurement time while at the same time achieving the desired accuracy. The Am(Li) source neutron yield is not large (~50,000 n/s), and although installing a larger neutron source would seem to be a simple means to improve the precision, the measurement precision quickly reaches a minimum beyond which no improvement is possible. This is not the case for delayed neutron counting where the measurement precision achievable is limited by radiation safety considerations associated with the open detector arrangement of the UNCL. In this section the measurement performance of the UNCL combined with an MP320 neutron generator configured for delayed neutron counting will be examined.

The delayed neutron counting methodology using a pulsed neutron generator has been discussed in detail in a previous work on the use of the DD neutron generator as an alternative to Am(Li) in the AWCC [1]. For the UNCL measurements, the neutron generator is operated in pulsed mode, at a low repetition rate, and low duty cycle to provide short, intense bursts of neutrons to induce fission within the fuel assembly. The resulting delayed neutrons are counted during a time window between pulses (following a delay to allow decay of the thermal neutron flux until start of the next pulse) when the background neutron levels are low.

9.1 DELAYED NEUTRON DATA ACQUISITION SYSTEM

To configure the DD/UNCL for delayed neutron counting two multichannel scaling (MCS) acquisition modules (e.g., Canberra LYNX) were added to the system as illustrated in Figure 69. The MCS sweep is synchronized to the neutron generator pulse.

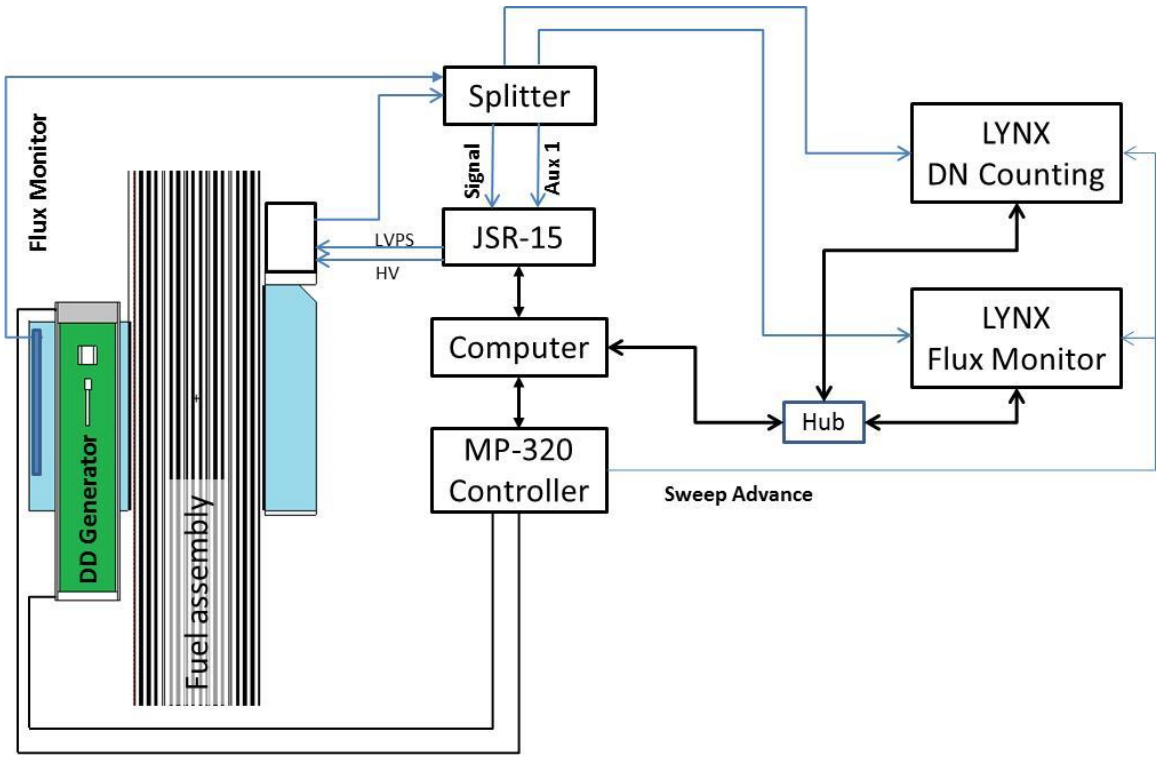

Figure 69. Block diagram illustrating the delayed neutron data acquisition system.

It should be noted that the system complexity can be reduced if desired.

- If coincidence counting is not required, then the JSR-15 can be removed. In this case, the high voltage bias would then be supplied from the LYNX modules and the low-voltage power (+5 V) from the splitter module or other +5 V supply. In this case, data acquisition could be provided from a COTS gamma-ray spectroscopy software platform (e.g., Canberra's Genie-2k or Ortec's Maestro).

- Alternatively, we have found that the flux monitor function can be provided using the JSR-15 Aux input, removing the need for two MCS modules. Although this approach requires both neutron coincidence counting software (e.g., INCC) and a gamma-ray spectroscopy platform (e.g., Canberra's Genie-2k) to be installed on the system.

For the UNCL measurements, the MP320 generator was operated at 80 kV, 60 uA beam current, 250 Hz repetition rate, and 5% duty cycle. These operating parameters produced a nominal 200 μs wide neutron pulse every 4,000 μs with a time average neutron yield of ~2E6 n/s. To avoid counting of the thermalizing neutron flux, room return, or primary induced fission neutrons, the delayed neutron counting window is opened following a delay of at least 2,000 μs. Figure 70 shows the measured time history for the UNCL counter with the MP320 neutron generator. Two traces are shown, the empty chamber (no sample) and with an 8 kg DU metal ingot.

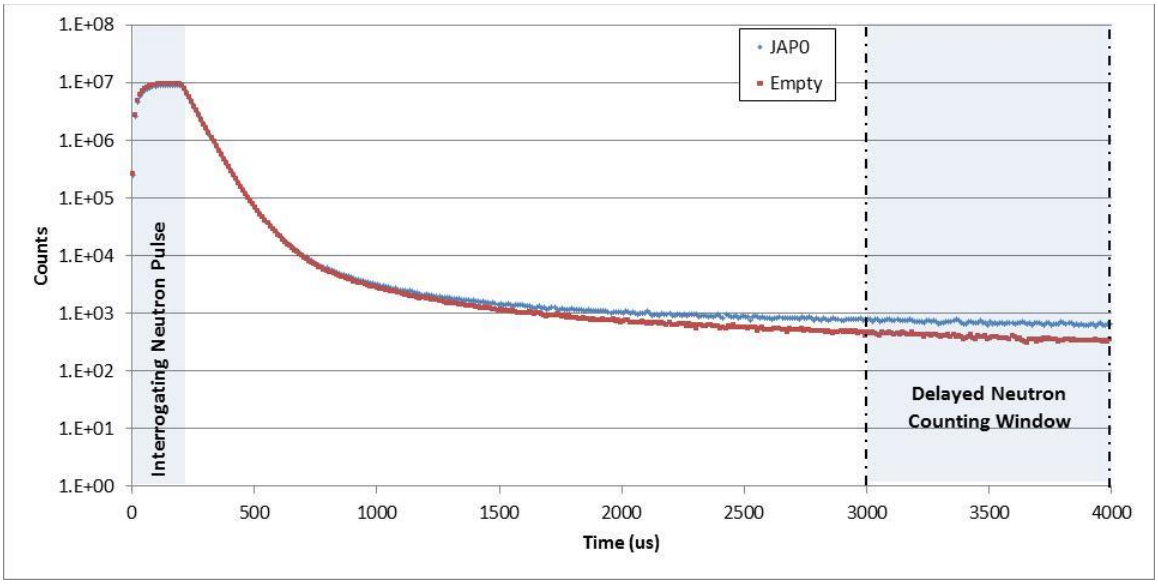

Figure 70. The measured time response of the DD/UNCL in fast pulsed mode for the empty assay cavity and with an 8 kg DU cylinder (JAP0) installed. 10 μs/channel, acquisition time = 5,000 seconds.

Figure 71 shows the difference between the two traces. We can see that the net count rate is constant for times greater than 1,500 μs following the start of the generator pulse. This demonstrates that the net signal is due to the delayed neutrons rather than induced fission neutrons, which would die away with the interrogating neutron flux. In principle it would be possible to count delayed neutrons over the entire time window from 1,500 to 4,000 μs; however, to minimize the impact of the thermalizing neutron flux and to optimize measurement precision, the counting window selected was 3000 to 4000 μs. This short counting window limits the detectable delayed neutron fraction to only 25%. This limitation is a property of the MP320 generator that does not affect the nGen-300c performance as will be discussed in Section 0.

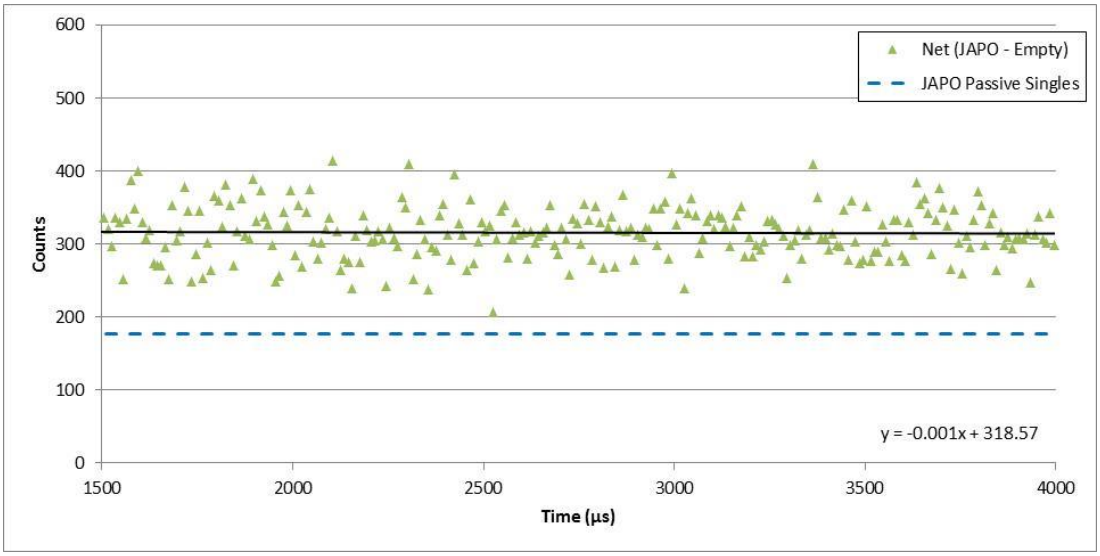

Figure 71. Net count rate as a function of time following the neutron pulse for the available counting window for the MP320 operating at 250 Hz for the assay of the DU cylinder (JAP0). The flat response illustrates that the net count rate is due to delayed neutron emission.

9.2 MP320 DD/UNCL DELAYED NEUTRON ASSAY SIMULATED CALIBRATION

As was done for the Am(Li) source simulations discussed in Section 4, simulated thermal and fast calibration curves for delayed neutron measurements with the DD/UNCL were generated using the assemblies described in Section 3.1. The neutron generator source term was limited for health physics limitations (to restrict the radiation posting limits to no more than 60 cm from the edge of the collar), which in the case of the MP320 was near its upper yield limits of 2E6 n/s. (For comparison, this is equivalent to the neutron yield from a 1 µg ^{252}Cf source.) The simulated thermal mode delayed neutron rates are provided in Table 71, and a comparison of the resulting calibration curve with the Am(Li)-based curve is shown in Figure 72. As can be seen in Figure 72, the response functions are generally similar, but the delayed neutron response has a shallower response due to the increased sensitivity to ^{238}U.

The expected measurement precision in the delayed neutron rates are significantly improved (~2 times) over that obtained from the active coincidence counting measurement; however, because of the increased sensitivity to ^{238}U, the improvement in assay precision is more modest, a factor of 1.5 times better. In both cases, typical calibration errors (~2%) are expected to dominate the total uncertainty so that the measurement performance is expected to be similar in the thermal mode.

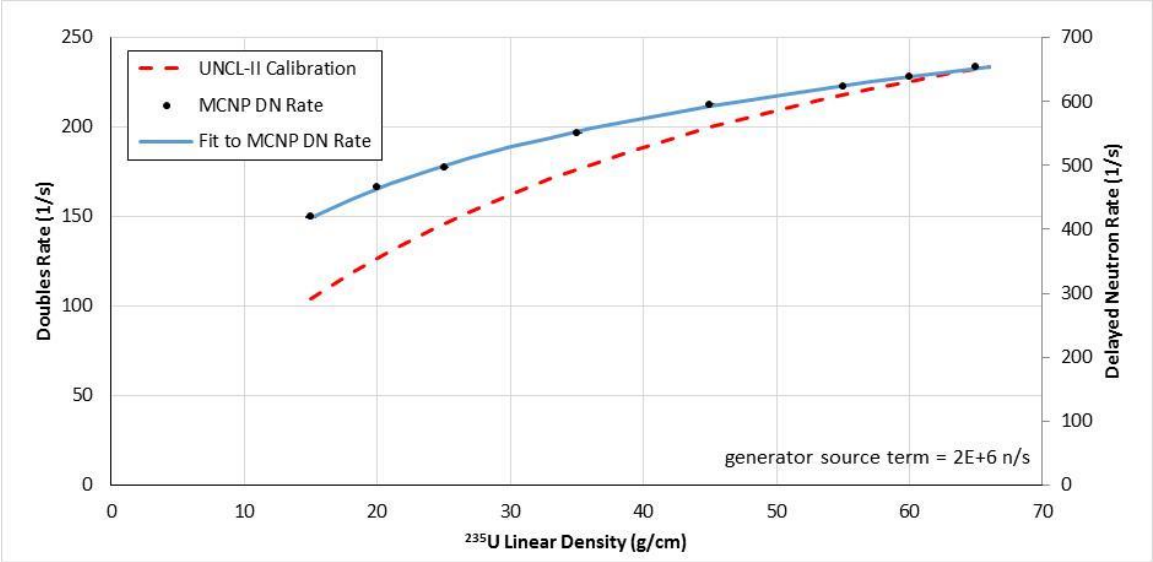

Figure 72. MP320/UNCL operating in pulsed, thermal mode (2E6 n/s, 250 Hz) for delayed neutron counting assay overlain with the measured UNCL-II calibration results [6].

Table 71. Simulated thermal mode, delayed neutron counting UNCL measurement results for the calibration assemblies‡

Fuel assembly ID	Declared LD ^{235}U (g/cm)	Singles background rate (1/s)	Delayed neutron rate (1/s)	600 sec σ_{DN} (1/s)	1,800 sec σ_{DN} (1/s)	Analyzed LD ^{235}U (g/cm)	600 sec LD uncert (g/cm)	1,800 sec LD uncert (g/cm)	600 sec Total uncert (%)	1,800 sec Total uncert (%)
17x17_cal_15	15.0	137.0	419.2	± 2.03	± 1.17	15.05	± 0.19	± 0.11	2.4	2.1
17x17_cal_20	20.0	137.0	466.6	± 2.11	± 1.22	20.30	± 0.27	± 0.16	2.4	2.1
17x17_cal_25	25.0	137.0	496.9	± 2.15	± 1.24	24.59	± 0.33	± 0.19	2.4	2.1
17x17_cal_35	35.0	137.0	549.9	± 2.23	± 1.29	34.34	± 0.48	± 0.28	2.4	2.2
17x17_cal_45	45.0	137.0	595.1	± 2.30	± 1.33	45.68	± 0.66	± 0.38	2.5	2.2
17x17_cal_55	55.0	137.0	622.9	± 2.34	± 1.35	54.44	± 0.80	± 0.46	2.5	2.2
17x17_cal_60	60.0	137.0	638.1	± 2.36	± 1.36	59.94	± 0.89	± 0.52	2.5	2.2
17x17_cal_65	65.0	137.0	653.1	± 2.38	± 1.38	65.89	± 0.99	± 0.57	2.5	2.2

‡ Uncertainties are the expected measurement performance values.
† Includes a 2% systematic contribution to the uncertainty.

The simulated fast mode delayed neutron rates for the MP320 generator operating with 2E6 n/s in pulsed mode are provided in Table 72, and a comparison of the resulting calibration curve with the Am(Li)-based curve is shown in Figure 73. As can be seen in Figure 72, the response function for the delayed neutron measurement is much flatter because of the increased sensitivity to ^{238}U.

The expected measurement precision in the delayed neutron rates are significantly improved (3–9 times) over that obtained from the active coincidence counting measurement; however, because of the increased sensitivity to ^{238}U, the improvement in assay precision is more modest—a factor of 1.3 times better. If we consider an arbitrary 2% calibration uncertainty the total measurement uncertainty improves by a factor of 1.2 relative to the Am(Li)-based coincidence measurement.

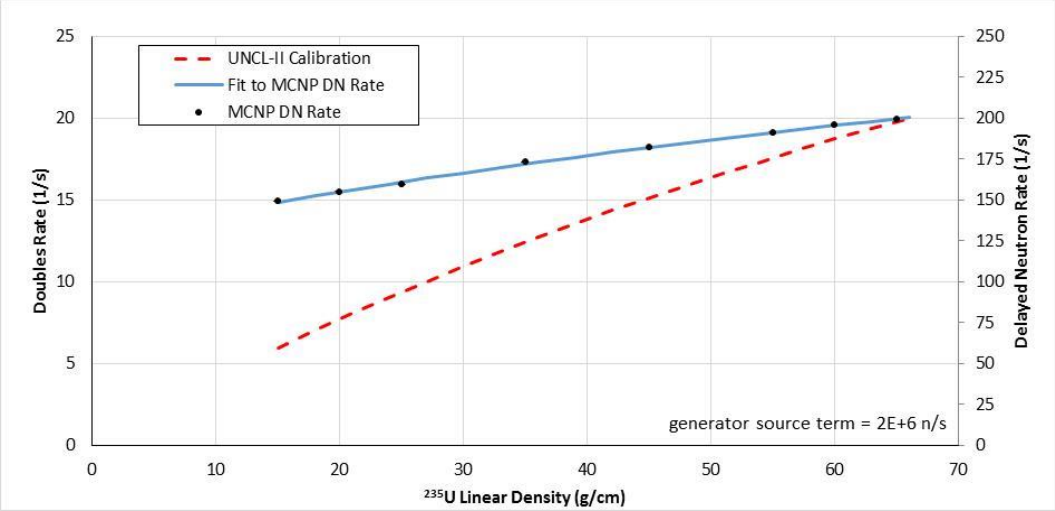

Figure 73. MP320/UNCL operating in pulsed, fast mode (2E6 n/s, 250 Hz) for delayed neutron counting assay overlain with the measured UNCL-II calibration results [6].

Table 72. Simulated fast mode, delayed neutron counting UNCL measurement results for the calibration assemblies‡

Fuel assembly ID	Declared LD ^{235}U (g/cm)	Singles background rate (1/s)	Delayed neutron rate (1/s)	600 sec σ_{DN} (1/s)	1,800 sec σ_{DN} (1/s)	Analyzed LD ^{235}U (g/cm)	600 sec LD uncert (g/cm)	1,800 sec LD uncert (g/cm)	600 sec Total uncert (%)	1,800 sec Total uncert (%)
17x17_cal_15	15.0	137.0	149.2	± 1.44	± 0.83	15.40	± 1.16	± 0.67	7.8	4.8
17x17_cal_20	20.0	137.0	154.9	± 1.46	± 0.84	20.03	± 1.21	± 0.70	6.4	4.0
17x17_cal_25	25.0	137.0	159.4	± 1.47	± 0.85	23.84	± 1.26	± 0.72	5.6	3.6
17x17_cal_35	35.0	137.0	172.8	± 1.50	± 0.86	35.91	± 1.42	± 0.82	4.4	3.0
17x17_cal_45	45.0	137.0	181.9	± 1.52	± 0.88	44.87	± 1.57	± 0.91	4.0	2.8
17x17_cal_55	55.0	137.0	191.2	± 1.54	± 0.89	54.98	± 1.77	± 1.02	3.8	2.7
17x17_cal_60	60.0	137.0	195.7	± 1.55	± 0.89	60.34	± 1.89	± 1.09	3.7	2.7
17x17_cal_65	65.0	137.0	199.2	± 1.56	± 0.90	64.64	± 2.00	± 1.15	3.7	2.7

‡ Uncertainties are the expected measurement performance values.
† Includes a 2% systematic contribution to the uncertainty.

9.3 SIMULATED DELAYED NEUTRON PERFORMANCE FOR VARIOUS INTACT ASSEMBLIES

The series of simulations were performed using the descriptions for the assorted intact fuel assemblies described in Section 3.2. The simulated assay results are provided in Tables 73–76 and shown in Figures 74 and 75 for operation in the delayed neutron counting thermal and fast assay modes. The results are shown before and after application of the heavy metal correction illustrating the need to apply the correction factors when considering the relative performance of the measurement for a given assembly. For the DD generator–based measurement the heavy metal (enrichment) correction becomes more important, relative to the Am(Li) interrogation, because of the increased fission rates in ^{238}U. The functional form is used for the correction

$$k_4 = 1 + \lambda_1 \cdot (\lambda_0 - \lambda)$$

However, in this case the parameters λ_0 and λ_1 are determined by a fit to the MCNP simulated rates. For these simulations using the calibration assembly description linear density as the reference (taken as a whole, including the poisoned and partial defect assemblies) the data is best represented when

Thermal mode	Fast mode
λ_0 = 1,297 g/cm	λ_0 = 1,297 g/cm
λ_1 = 4.63E-4 cm/g	λ_1 = 5.96 E-4 cm/g

The results suggest that the heavy metal correction for thermal mode interrogation may require assembly-specific calibrations.

We see in Table 75 that for simulated fast mode assay rates for assembly 14x14C, the non-heavy metal corrected rate would fall below the calibration range, and results in a negative mass, even though the expected delayed neutron rate is positive. It is necessary to apply the heavy metal correction to the delayed neutron rate to bring this assay into the valid calibration range.

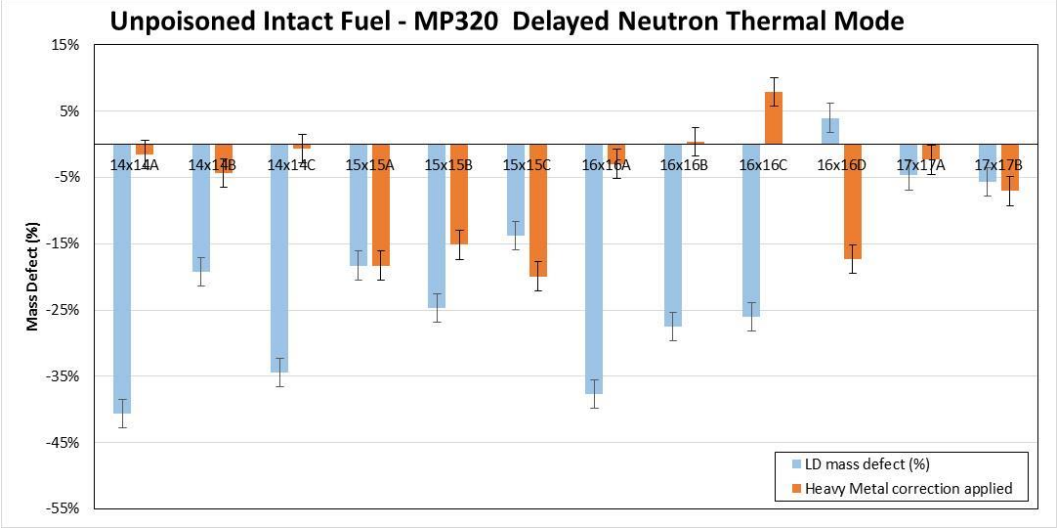

Figure 74. Results of the MCNP simulations for the MP320/UNCL for the assorted intact fuel assemblies in the delayed neutron thermal mode. Error bars represent the project 1 sigma uncertainties for an 1,800 second measurement time.

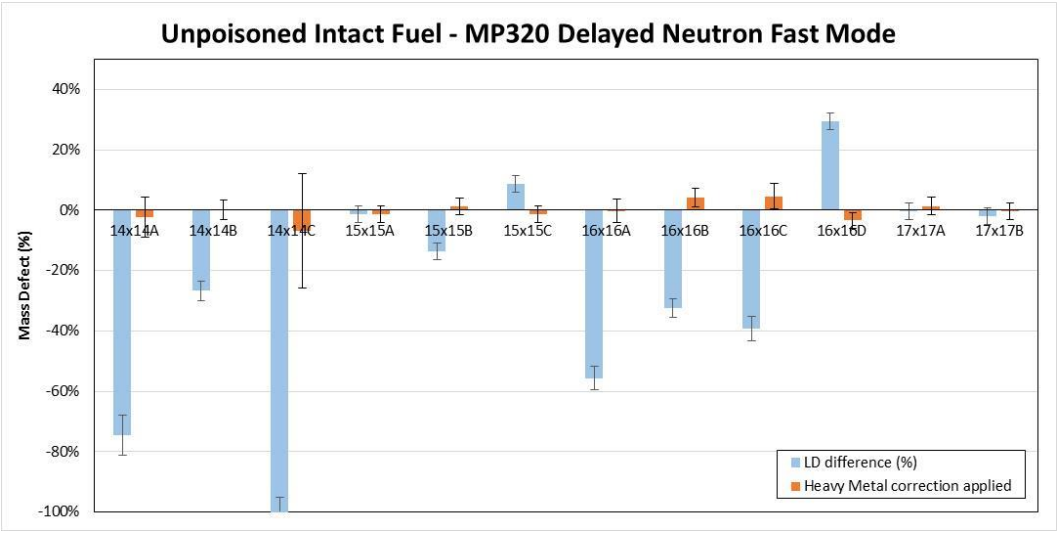

Figure 75. Results of the MCNP simulations for the MP320/UNCL for the assorted intact fuel assemblies in the delayed neutron fast mode. Error bars represent the project 1 sigma uncertainties for an 1,800 second measurement time.

Table 73. Simulated delayed thermal mode, MP320 based UNCL measurement results for the unpoisoned, intact fuel assemblies‡

Fuel assembly ID	Declared LD ^{235}U (g/cm)	Singles background rate (1/s)	Delayed neutron rate (1/s)	600 sec σ_{DN} (1/s)	1,800 sec σ_{DN} (1/s)	Analyzed LD ^{235}U (g/cm)	600 sec LD uncert (g/cm)	1,800 sec LD uncert (g/cm)	600 sec Total uncert (%)†	1,800 sec Total uncert (%)†
14x14A	37.57	105.9	481.4	± 2.08	± 1.20	22.30	± 0.29	± 0.17	2.4	2.1
14x14B	37.31	127.7	529.0	± 2.19	± 1.26	30.11	± 0.42	± 0.24	2.4	2.2
14x14C	19.78	105.9	395.7	± 1.94	± 1.12	12.98	± 0.16	± 0.09	2.3	2.1
15x15A	58.37	138.9	601.9	± 2.31	± 1.33	47.68	± 0.70	± 0.40	2.5	2.2
15x15B	61.54	131.8	597.4	± 2.30	± 1.33	46.36	± 0.67	± 0.39	2.5	2.2
15x15C	60.91	143.4	617.1	± 2.34	± 1.35	52.50	± 0.78	± 0.45	2.5	2.2
16x16A	46.90	111.6	524.4	± 2.16	± 1.24	29.25	± 0.40	± 0.23	2.4	2.1
16x16B	50.16	119.4	558.9	± 2.22	± 1.28	36.37	± 0.51	± 0.29	2.4	2.2
16x16C	30.95	113.5	485.7	± 2.10	± 1.21	22.90	± 0.30	± 0.18	2.4	2.1
16x16D	64.07	152.5	654.8	± 2.41	± 1.39	66.60	± 1.01	± 0.58	2.5	2.2
17x17A	41.29	137.4	571.4	± 2.27	± 1.31	39.35	± 0.56	± 0.32	2.5	2.2
17x17B	54.82	139.8	614.7	± 2.33	± 1.35	51.71	± 0.76	± 0.44	2.5	2.2

‡ Uncertainties are the expected measurement performance values.
† Includes a 2% systematic contribution to the uncertainty.

Table 74. Simulated delayed thermal mode, defect analysis results for the unpoisoned, intact fuel assemblies

Fuel assembly ID	Defect without correction			Defect with HM correction applied		
	LD mass defect (%)	#σ 600 sec	#σ 1,800 sec	LD mass defect (%)	#σ 600 sec	#σ 1,800 sec
14x14A	−40.6	28.6	32.0	−1.6	0.8	1.1
14x14B	−19.3	9.8	11.1	−4.3	2.0	2.4
14x14C	−34.4	22.3	24.7	−0.6	0.3	0.4
15x15A	−18.3	9.1	10.3	−18.3	9.1	10.3
15x15B	−24.7	13.3	15.1	−15.2	7.7	9.0
15x15C	−13.8	6.4	7.4	−19.9	9.6	10.8
16x16A	−37.6	25.0	28.1	−2.9	1.5	1.9
16x16B	−27.5	15.5	17.6	0.4	0.2	0.2
16x16C	−26.0	14.7	16.4	7.9	3.6	4.6
16x16D	3.9	1.5	1.7	−17.3	7.2	7.9
17x17A	−4.7	2.0	2.3	−2.3	1.0	1.1
17x17B	−5.7	2.4	2.8	−7.1	3.0	3.5
Average bias	**−20.7%**			**−6.8%**		
Std. deviation	**13.8%**			**8.8%**		

Table 75. Simulated delayed fast mode, MP320 based UNCL measurement results for the unpoisoned, intact fuel assemblies‡

Fuel assembly ID	Declared LD ^{235}U (g/cm)	Singles background rate (1/s)	Delayed neutron rate (1/s)	600 sec σ_{DN} (1/s)	1,800 sec σ_{DN} (1/s)	Analyzed LD ^{235}U (g/cm)	600 sec LD uncert (g/cm)	1,800 sec LD uncert (g/cm)	600 sec Total uncert (%)†	1,800 sec Total uncert (%)†
14x14A	37.57	105.9	141.8	± 1.35	± 0.78	9.56	± 1.04	± 0.60	11.0	6.6
14x14B	37.31	127.7	163.4	± 1.46	± 0.84	27.33	± 1.28	± 0.74	5.1	3.4
14x14C	19.78	105.9	124.9	± 1.31	± 0.76	-2.81	± 0.92	± 0.53	32.8	19.0
15x15A	58.37	138.9	193.4	± 1.55	± 0.89	57.56	± 1.83	± 1.06	3.8	2.7
15x15B	61.54	131.8	189.6	± 1.52	± 0.88	53.15	± 1.71	± 0.99	3.8	2.7
15x15C	60.91	143.4	200.4	± 1.57	± 0.91	66.19	± 2.06	± 1.19	3.7	2.7
16x16A	46.90	111.6	155.8	± 1.40	± 0.81	20.81	± 1.17	± 0.67	6.0	3.8
16x16B	49.92	121.8	170.6	± 1.46	± 0.84	33.79	± 1.36	± 0.78	4.5	3.1
16x16C	30.95	122.3	153.4	± 1.42	± 0.82	18.82	± 1.17	± 0.67	6.5	4.1
16x16D	64.07	152.5	211.8	± 1.61	± 0.93	82.99	± 2.68	± 1.55	3.8	2.7
17x17A	41.54	138.2	178.5	± 1.51	± 0.87	41.39	± 1.51	± 0.87	4.2	2.9
17x17B	54.19	138.2	189.6	± 1.54	± 0.89	53.13	± 1.73	± 1.00	3.8	2.7

‡ Uncertainties are the expected measurement performance values.
† Includes a 2% systematic contribution to the uncertainty.

Table 76. Simulated fast mode, defect analysis results for the unpoisoned, intact fuel assemblies

Fuel assembly ID	Defect without correction			Defect with HM correction applied		
	LD mass defect (%)	#σ 600 sec	#σ 1,800 sec	LD mass defect (%)	#σ 600 sec	#σ 1,800 sec
14x14A	−74.6	27.0	46.8	−2.3	0.5	0.9
14x14B	−26.8	7.8	13.5	0.1	0.0	0.0
14x14C	−114.2	24.5	42.5	−6.9	1.0	1.8
15x15A	−1.4	0.4	0.8	−1.4	0.4	0.5
15x15B	−13.6	4.9	8.5	1.3	0.4	0.5
15x15C	8.7	2.6	4.4	−1.4	0.4	0.5
16x16A	−55.6	22.3	38.7	−0.2	0.1	0.1
16x16B	−32.3	11.9	20.6	4.2	1.1	1.7
16x16C	−39.2	10.4	18.0	4.6	1.0	1.6
16x16D	29.5	7.1	12.2	−3.4	0.9	1.1
17x17A	−0.4	0.1	0.2	1.3	0.3	0.5
17x17B	−2.0	0.6	1.1	−0.4	0.1	0.1
Average bias	**−26.8%**			**−0.4%**		
Std. deviation	**39.9%**			**3.1%**		

9.4 SIMULATED DELAYED NEUTRON PERFORMANCE FOR BURNABLE POISONS

The performance of the UNCL for assemblies containing burnable poisons is an important question when considering an alternative neutron interrogation source. The difference in neutron energy distribution from the sources and the change in moderating assembly to accommodate the larger, relative to Am(Li), source will change the relative thermal neutron population in the interrogating neutron distribution. The simulated assemblies containing poison rods allow examination of the potential impact. Figure 76 illustrates the impact of the poison rods on the thermal mode mass results for the UNCL using an Am(Li) neutron source and the fast mode results are shown in Figure 77. As can be seen the number of poison rods is more important than rod's poison loading. The effectiveness of the poison rod correction can also be seen in the plots as the average bias is reduced to <1% and the typical deviation from the expected value is reduced to less than 2% in both thermal and fast modes. The simulated rates and defect levels are presented in Tables 78–81.

The parameters in the expression for the poison rod correction factor, k_3, were adjusted by a fit to the MCNP simulations. The expression for k_3 from discussed above in Section 1.3.2 [6] is shown here with the potentially adjustable parameters *a*, *b*, and *c*.

$$k_3 = 1 + \frac{a \cdot n}{N} \cdot \left(1 - e^{-b \cdot Gd}\right) \cdot (1 - c \cdot E_N)$$

where n is the number of poison rods,
N is the number of fuel rods (fuel + poison),
Gd is the weight percent of the Gd in the poison rods,
E_N is the declared enrichment.

It was found that it was only necessary to adjust the parameter, *b*, to obtain results similar to those obtained for the Am(Li)-based UNCL system. The parameters for the MP320/UNCL/DN system are provided in Table 77.

Table 77. Poison rod correction parameters for the MP320/UNCL/DN system

Parameter	Thermal mode		Fast mode	
	Am(Li)	MP320	Am(Li)	MP320
a	9.86	2.313	0.602	0.325
b	0.647	0.420	0.647	0.647
c	0.176	0.177	—	—

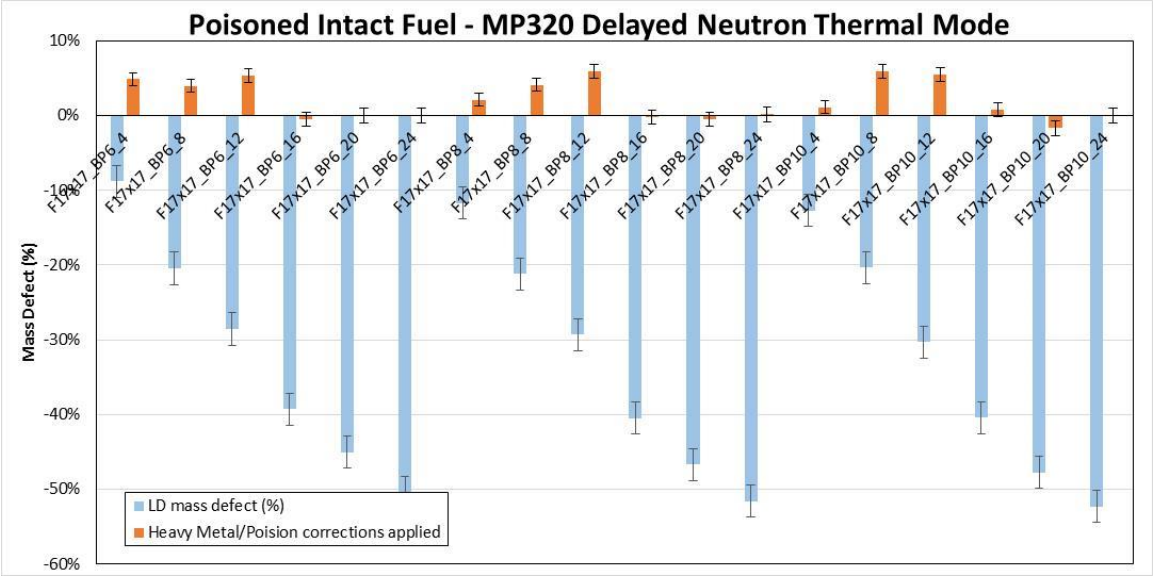

Figure 76. Thermal mode simulated assay results for the various burnable poison loadings with and without the heavy metal and poison rod correction.

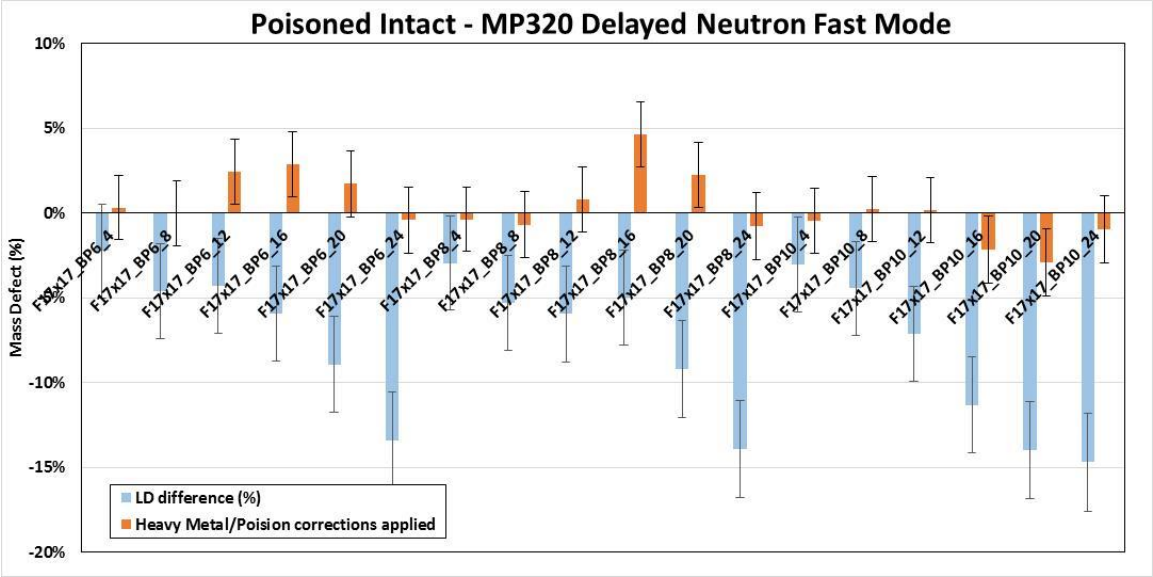

Figure 77. Fast mode assay results for the various burnable poison loadings with and without the heavy metal and poison rod correction.

Table 78. Simulated delayed neutron, thermal mode, MP320-based UNCL measurement results for the poisoned, intact fuel assemblies‡

Fuel assembly ID	Declared LD ^{235}U (g/cm)	Singles rate (1/s)	Doubles rate (1/s)	600 sec σ_D (1/s)	1,800 sec σ_D (1/s)	Analyzed LD ^{235}U (g/cm)	600 sec LD uncert (g/cm)	1,800 sec LD uncert (g/cm)	600 sec Total uncert (%)†	1,800 sec Total uncert (%)†
BP6_4	**51.50**	137.9	599.4	± 2.31	± 1.33	46.95	± 0.68	± 0.39	2.5	2.2
BP6_8	**51.20**	137.1	576.9	± 2.27	± 1.31	40.74	± 0.58	± 0.34	2.5	2.2
BP6_12	**50.90**	136.3	559.0	± 2.25	± 1.30	36.37	± 0.52	± 0.30	2.5	2.2
BP6_16	**50.60**	135.5	532.2	± 2.21	± 1.27	30.71	± 0.43	± 0.25	2.4	2.2
BP6_20	**50.30**	134.7	515.4	± 2.18	± 1.26	27.63	± 0.38	± 0.22	2.4	2.2
BP6_24	**49.90**	133.6	498.0	± 2.15	± 1.24	24.75	± 0.34	± 0.19	2.4	2.1
BP8_4	**51.50**	137.9	594.4	± 2.30	± 1.33	45.47	± 0.66	± 0.38	2.5	2.2
BP8_8	**51.20**	137.1	575.4	± 2.27	± 1.31	40.35	± 0.58	± 0.33	2.5	2.2
BP8_12	**50.90**	136.3	557.2	± 2.24	± 1.30	35.98	± 0.51	± 0.29	2.5	2.2
BP8_16	**50.50**	135.2	528.7	± 2.20	± 1.27	30.05	± 0.42	± 0.24	2.4	2.2
BP8_20	**50.20**	134.4	510.4	± 2.17	± 1.25	26.77	± 0.37	± 0.21	2.4	2.2
BP8_24	**49.90**	133.6	494.2	± 2.15	± 1.24	24.17	± 0.33	± 0.19	2.4	2.1
BP10_4	**51.50**	137.9	592.5	± 2.30	± 1.33	44.95	± 0.65	± 0.38	2.5	2.2
BP10_8	**51.20**	137.1	577.1	± 2.27	± 1.31	40.79	± 0.59	± 0.34	2.5	2.2
BP10_12	**50.80**	136.0	554.7	± 2.24	± 1.29	35.40	± 0.50	± 0.29	2.4	2.2
BP10_16	**50.50**	135.2	528.8	± 2.20	± 1.27	30.07	± 0.42	± 0.24	2.4	2.2
BP10_20	**50.20**	134.4	507.2	± 2.17	± 1.25	26.24	± 0.36	± 0.21	2.4	2.2
BP10_24	**49.80**	133.4	491.4	± 2.14	± 1.24	23.74	± 0.32	± 0.19	2.4	2.1

‡ Uncertainties are the expected measurement performance values.
† Includes a 2% systematic contribution to the uncertainty.

Table 79. Simulated thermal mode, defect analysis results for the poisoned, intact fuel assemblies

Fuel assembly ID	Defect without correction			HM and poison corrections applied		
	LD mass defect (%)	#σ 600 sec	#σ 1,800 sec	LD mass defect (%)	#σ 600 sec	#σ 1,800 sec
BP6_4	−8.8	3.9	4.5	4.9	1.9	2.1
BP6_8	−20.4	10.4	11.9	3.9	1.5	1.7
BP6_12	−28.5	16.3	18.5	5.4	2.0	2.3
BP6_16	−39.3	26.6	30.0	−0.6	0.2	0.3
BP6_20	−45.1	33.8	38.1	0.0	0.0	0.0
BP6_24	−50.4	42.0	47.3	0.0	0.0	0.0
BP8_4	−11.7	5.4	6.1	2.1	0.8	0.9
BP8_8	−21.2	10.9	12.4	4.1	1.6	1.8
BP8_12	−29.3	16.9	19.2	5.9	2.2	2.5
BP8_16	−40.5	28.0	31.6	−0.2	0.1	0.1
BP8_20	−46.7	36.1	40.7	−0.5	0.2	0.2
BP8_24	−51.6	44.1	49.6	0.1	0.1	0.1
BP10_4	−12.7	5.9	6.7	1.1	0.4	0.5
BP10_8	−20.3	10.4	11.8	5.9	2.2	2.5
BP10_12	−30.3	17.8	20.1	5.5	2.0	2.4
BP10_16	−40.4	27.9	31.5	0.8	0.3	0.4
BP10_20	−47.7	37.7	42.5	−1.7	0.7	0.8
BP10_24	−52.3	45.4	51.1	0.0	0.0	0.0
Average bias	**−33.2%**			**2.0%**		
Std. deviation	**14.7%**			**2.7%**		

Table 80. Simulated delayed neutron fast mode, MP320 based UNCL measurement results for the poisoned, intact fuel assemblies‡

Fuel assembly ID	Declared LD ^{235}U (g/cm)	Singles rate (1/s)	Doubles rate (1/s)	600 sec σ_D (1/s)	1,800 sec σ_D (1/s)	Analyzed LD ^{235}U (g/cm)	600 sec LD uncert (g/cm)	1,800 sec LD uncert (g/cm)	600 sec Total uncert (%)†	1,800 sec Total uncert (%)†
BP6_4	**51.50**	138.7	187.0	± 1.53	± 0.89	50.34	± 1.67	± 0.97	3.9	2.8
BP6_8	**51.20**	138.6	185.7	± 1.53	± 0.88	48.84	± 1.65	± 0.95	3.9	2.8
BP6_12	**50.90**	138.5	185.5	± 1.53	± 0.88	48.71	± 1.64	± 0.95	3.9	2.8
BP6_16	**50.60**	138.5	184.5	± 1.53	± 0.88	47.61	± 1.62	± 0.94	3.9	2.8
BP6_20	**50.30**	138.4	182.8	± 1.52	± 0.88	45.81	± 1.59	± 0.92	4.0	2.8
BP6_24	**49.90**	138.1	180.3	± 1.52	± 0.88	43.21	± 1.54	± 0.89	4.1	2.9
BP8_4	**51.50**	138.7	186.7	± 1.53	± 0.88	49.98	± 1.67	± 0.96	3.9	2.8
BP8_8	**51.20**	138.6	185.3	± 1.53	± 0.88	48.48	± 1.64	± 0.95	3.9	2.8
BP8_12	**50.90**	138.5	184.7	± 1.53	± 0.88	47.87	± 1.63	± 0.94	3.9	2.8
BP8_16	**50.50**	138.2	184.9	± 1.53	± 0.88	47.99	± 1.63	± 0.94	3.9	2.8
BP8_20	**50.20**	138.1	182.6	± 1.52	± 0.88	45.58	± 1.58	± 0.91	4.0	2.8
BP8_24	**49.90**	138.1	180.0	± 1.52	± 0.88	42.96	± 1.54	± 0.89	4.1	2.9
BP10_4	**51.50**	138.7	186.7	± 1.53	± 0.88	49.94	± 1.67	± 0.96	3.9	2.8
BP10_8	**51.20**	138.6	185.7	± 1.53	± 0.88	48.93	± 1.65	± 0.95	3.9	2.8
BP10_12	**50.80**	138.3	184.1	± 1.53	± 0.88	47.17	± 1.61	± 0.93	4.0	2.8
BP10_16	**50.50**	138.2	181.8	± 1.52	± 0.88	44.78	± 1.57	± 0.91	4.0	2.8
BP10_20	**50.20**	138.1	180.3	± 1.52	± 0.88	43.19	± 1.54	± 0.89	4.1	2.9
BP10_24	**49.80**	137.8	179.6	± 1.51	± 0.87	42.49	± 1.53	± 0.88	4.1	2.9

‡ Uncertainties are the expected measurement performance values.
† Includes a 2% systematic contribution to the uncertainty.

Table 81. Simulated fast mode, defect analysis results for the poisoned, intact fuel assemblies

Fuel assembly ID	Defect without correction			HM and poison corrections applied		
	LD mass defect (%)	#σ 600 sec	#σ 1,800 sec	LD mass defect (%)	#σ 600 sec	#σ 1,800 sec
BP6_4	−2.2	0.7	1.2	0.3	0.1	0.1
BP6_8	−4.6	1.4	2.5	0.0	0.0	0.0
BP6_12	−4.3	1.3	2.3	2.4	0.6	0.9
BP6_16	−5.9	1.8	3.2	2.9	0.7	1.0
BP6_20	−8.9	2.8	4.9	1.7	0.4	0.6
BP6_24	−13.4	4.3	7.5	−0.4	0.1	0.1
BP8_4	−2.9	0.9	1.6	−0.4	0.1	0.1
BP8_8	−5.3	1.7	2.9	−0.7	0.2	0.2
BP8_12	−6.0	1.9	3.2	0.8	0.2	0.3
BP8_16	−5.0	1.5	2.7	4.7	1.1	1.6
BP8_20	−9.2	2.9	5.0	2.3	0.6	0.8
BP8_24	−13.9	4.5	7.8	−0.8	0.2	0.3
BP10_4	−3.0	0.9	1.6	−0.4	0.1	0.2
BP10_8	−4.4	1.4	2.4	0.2	0.1	0.1
BP10_12	−7.1	2.2	3.9	0.2	0.0	0.1
BP10_16	−11.3	3.6	6.3	−2.1	0.6	0.8
BP10_20	−14.0	4.5	7.9	−2.9	0.8	1.1
BP10_24	−14.7	4.8	8.3	−1.0	0.2	0.3
Average bias	**−7.6%**			**0.4**		
Std. deviation	**4.2%**			**1.8%**		

9.5 SIMULATED DELAYED NEUTRON PERFORMANCE FOR SIMULATED PARTIAL DEFECT ANALYSIS

This series of simulations examines the delayed neutron counting performance of the UNCL using the MP320 DD neutron generator for increasing numbers of rods substituted with DU. The mass defect relative to the declared value is shown in Figure 78 for the thermal mode and in Figure 79 for the fast mode. Rates and performance values are provided in Tables 82–85. Because the heavy metal content for the simulated assembly is the same as the simulated calibration assemblies, the heavy metal correction will be equal to 1, so application of the correction will have no impact on the results.

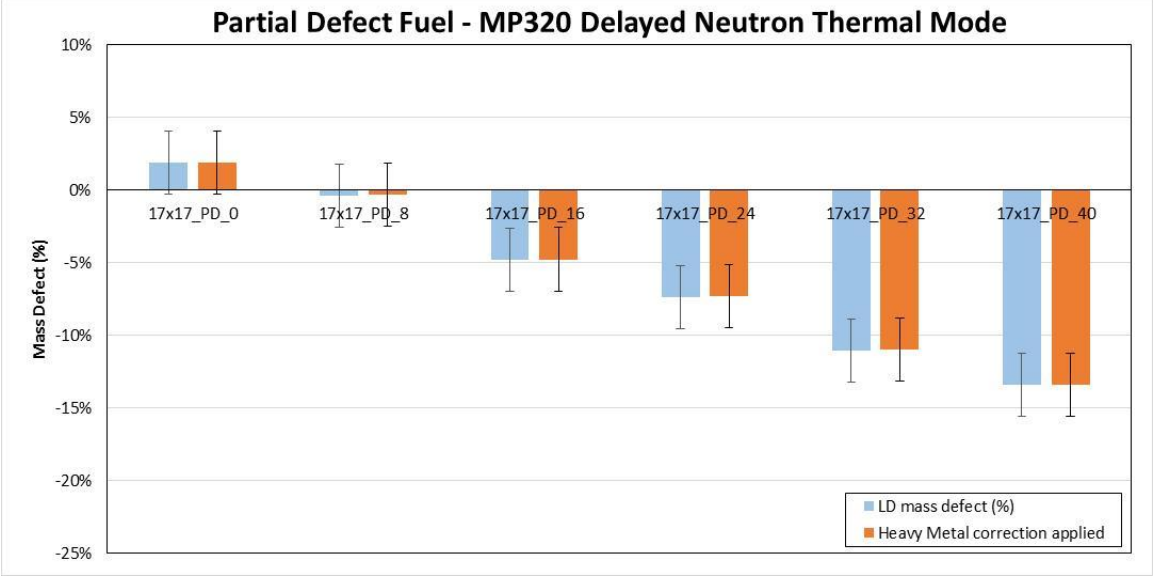

Figure 78. Thermal mode simulated assay results for the partial defect loadings with and without the heavy metal correction.

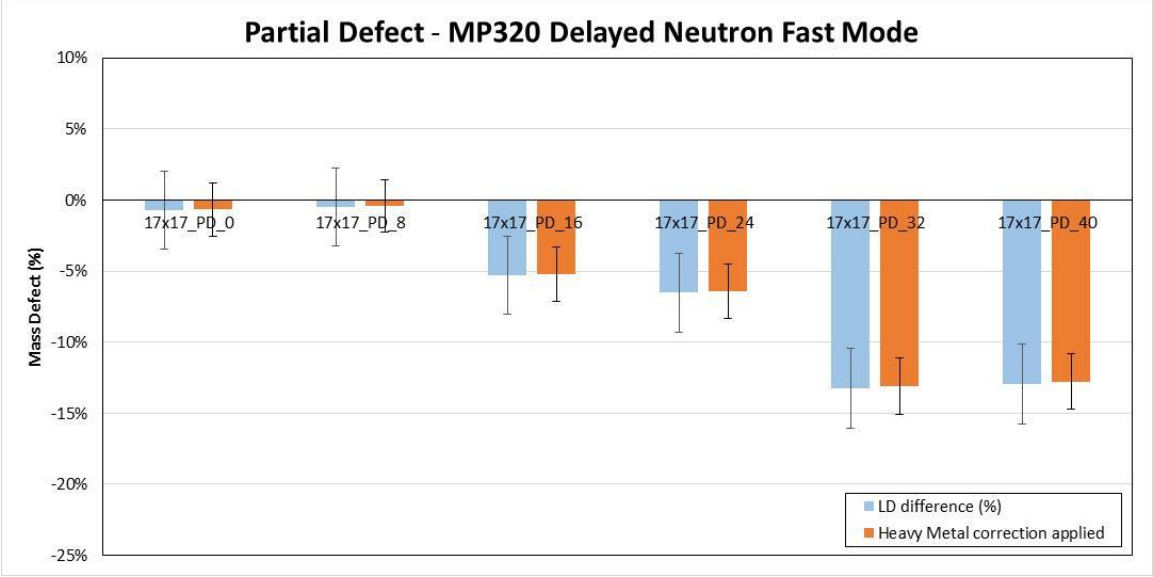

Figure 79. Fast mode simulated assay results for the partial defect loadings with and without the heavy metal correction.

Table 82. Simulated delayed, thermal mode, MP320 based UNCL measurement results for the partial defect assembly configurations‡

Fuel assembly ID	Declared LD ^{235}U (g/cm)	Singles background rate E(1/s)	Delayed neutron rate (1/s)	600 sec σ_{DN} (1/s)	1,800 sec σ_{DN} (1/s)	Analyzed LD ^{235}U (g/cm)	600 sec LD uncert (g/cm)	1,800 sec LD uncert (g/cm)	600 sec Total uncert (%)†	1,800 sec Total uncert (%)†
PD_0	54.98	137.0	627.4	± 2.35	± 1.35	56.02	± 0.83	± 0.48	2.5	2.2
PD_8	54.98	137.0	623.9	± 2.34	± 1.35	54.78	± 0.81	± 0.47	2.5	2.2
PD_16	54.98	137.0	616.7	± 2.33	± 1.35	52.35	± 0.77	± 0.44	2.5	2.2
PD_24	54.98	137.0	612.4	± 2.32	± 1.34	50.94	± 0.75	± 0.43	2.5	2.2
PD_32	54.98	137.0	605.9	± 2.32	± 1.34	48.91	± 0.71	± 0.41	2.5	2.2
PD_40	54.98	137.0	601.6	± 2.31	± 1.33	47.61	± 0.69	± 0.40	2.5	2.2

‡ Uncertainties are the expected measurement performance values.
† Includes a 2% systematic contribution to the uncertainty.

Table 83. Simulated thermal mode, defect analysis results for the partial defect assembly configurations

Fuel assembly ID	Defect without correction			HM and poison corrections applied		
	LD mass defect (%)	#σ 600 sec	#σ 1,800 sec	LD mass defect (%)	#σ 600 sec	#σ 1,800 sec
PD_0	1.9	0.7	0.9	1.9	0.8	0.9
PD_8	−0.4	0.1	0.2	−0.3	0.1	0.1
PD_16	−4.8	2.0	2.3	−4.8	2.0	2.3
PD_24	−7.3	3.2	3.6	−7.3	3.2	3.6
PD_32	−11.0	5.0	5.7	−11.0	5.0	5.7
PD_40	−13.4	6.3	7.1	−13.4	6.2	7.1

Table 84. Simulated delayed neutron, fast mode, MP320 based UNCL measurement results for the partial defect assembly configurations‡

Fuel assembly ID	Declared LD ^{235}U (g/cm)	Singles background rate (1/s)	Delayed neutron rate (1/s)	600 sec σ_{DN} (1/s)	1,800 sec σ_{DN} (1/s)	Analyzed LD ^{235}U (g/cm)	600 sec LD uncert (g/cm)	1,800 sec LD uncert (g/cm)	600 sec Total uncert (%)†	1,800 sec Total uncert (%)†
PD_0	54.98	137.0	190.8	± 1.54	± 0.89	54.58	± 1.76	± 1.01	3.8	2.7
PD_8	54.98	137.0	191.0	± 1.54	± 0.89	54.71	± 1.76	± 1.02	3.8	2.7
PD_16	54.98	137.0	188.6	± 1.53	± 0.88	52.08	± 1.71	± 0.98	3.8	2.8
PD_24	54.98	137.0	188.0	± 1.53	± 0.88	51.41	± 1.69	± 0.98	3.9	2.8
PD_32	54.98	137.0	184.6	± 1.52	± 0.88	47.75	± 1.62	± 0.94	3.9	2.8
PD_40	54.98	137.0	184.8	± 1.52	± 0.88	47.92	± 1.62	± 0.94	3.9	2.8

‡ Uncertainties are the expected measurement performance values.
† Includes a 2% systematic contribution to the uncertainty.

Table 85. Simulated fast mode, defect analysis results for the partial defect assembly configurations

Fuel assembly ID	Defect without correction			HM and Poison corrections applied		
	LD mass defect (%)	#σ 600 sec	#σ 1,800 sec	LD mass defect (%)	#σ 600 sec	#σ 1,800 sec
PD_0	−0.7	0.2	0.3	−0.7	0.2	0.3
PD_8	−0.5	0.1	0.2	−0.4	0.1	0.2
PD_16	−5.3	1.5	2.0	−5.2	1.4	2.0
PD_24	−6.5	1.8	2.5	−6.4	1.8	2.5
PD_32	−13.2	3.8	5.4	−13.1	3.8	5.4
PD_40	−12.8	3.7	5.3	−12.8	3.7	5.2

10. DELAYED NEUTRON COUNTING—NGEN-300C NEUTRON GENERATOR

The results of the simulations for the MP320 and nGen-310 neutron generators indicate that because of the accidentals count rates limitations discussed in Section 2.4 above, there is little performance difference achievable between the neutron generators for active coincidence assays. However, the nGen-300c neutron generator offers two potential advantages over the MP320 for delayed neutron counting. The nGen-300c may be operated at a lower repetition rate and at higher neutron yield (Table 86). These two factors can potentially offer a 15 times increase in the delayed neutron rates.

Table 86. Comparison of the MP320 and the nGen-300c pulse mode properties

	nGen-300c	MP320
Neutron yield:	1×10^7 n/s time avg	$2x10^6$ n/s time avg.
Frequency range:	1 shot to 200 kHz	250 Hz to 20 kHz
Duty cycle:	4%	5%–100% (minimum pulse width 5 μs)

The characteristic die-away of the UNCL is sufficiently slow so that a delayed neutron counting window cannot be opened less than 1,500 μs following the start of the neutron pulse (Figure 70), and to optimize the measurement precision, it is necessary to delay the window to 3,000 μs following the start of the pulse. The 4 ms maximum period of the MP320 neutron pulses limits the available detectable delayed neutron detection fraction to 25%.

Operating the neutron generator at lower repetition rates with a shorter duty cycle allows detection of a larger fraction of the emitted delayed neutrons. For example, a neutron generator operating at 50 Hz would allow a delayed neutron counting window of 16,400 μs for each 20,000 μs period, providing a detectable delayed neutron fraction of 82%. Because the time average yield of the pulsed neutron generator does not change significantly with the repetition rate, there is no penalty in terms of induced fission rates by reducing the frequency. In principle, the nGen-300c generator can provide a factor of 1.8 reduction in the expected measurement precision compared to the MP320 simply by operating at a slower repetition rate and adjusting the delayed neutron counting window accordingly. Further improvements can be achieved by increasing the time average output from 2E6 to 1E7 n/s, however, additional radiation protection considerations might become necessary to accommodate the stronger source term.

In the remainder of this section, we repeat the same MCNP simulation series as in Section 9 for the nGen300-c DD/UNCL combination to ensure that the differences in measurement geometry do not adversely impact the potential biases in the delayed neutron measurement.

10.1 NGEN-300C DD/UNCL DELAYED NEUTRON ASSAY SIMULATED CALIBRATION

The simulated thermal mode delayed neutron rates for the calibration assemblies described in Section 3.1 are provided in Table 87. For these simulations the generator is assumed to operate at a repetition rate of 50 Hz with a 800 μs pulse width, which provides a detectable neutron fraction of 82% with a time average neutron yield of 2E6 n/s. A comparison of the resulting calibration curve with the Am(Li)-based curve is shown in Figure 80. As can be seen in Figure 80, the response functions are generally similar, but the delayed neutron response has a shallower response because of the increased sensitivity to ^{238}U.

The expected measurement precision in the delayed neutron rates are significantly improved (~3 times) over that obtained from the active coincidence counting measurement, but because of the increased sensitivity to ^{238}U, the improvement in assay precision is more modest—a factor of 2 times better. In both cases, typical calibration errors (~2%) are expected to dominate the total uncertainty so that the measurement performance is expected to be similar in the thermal mode.

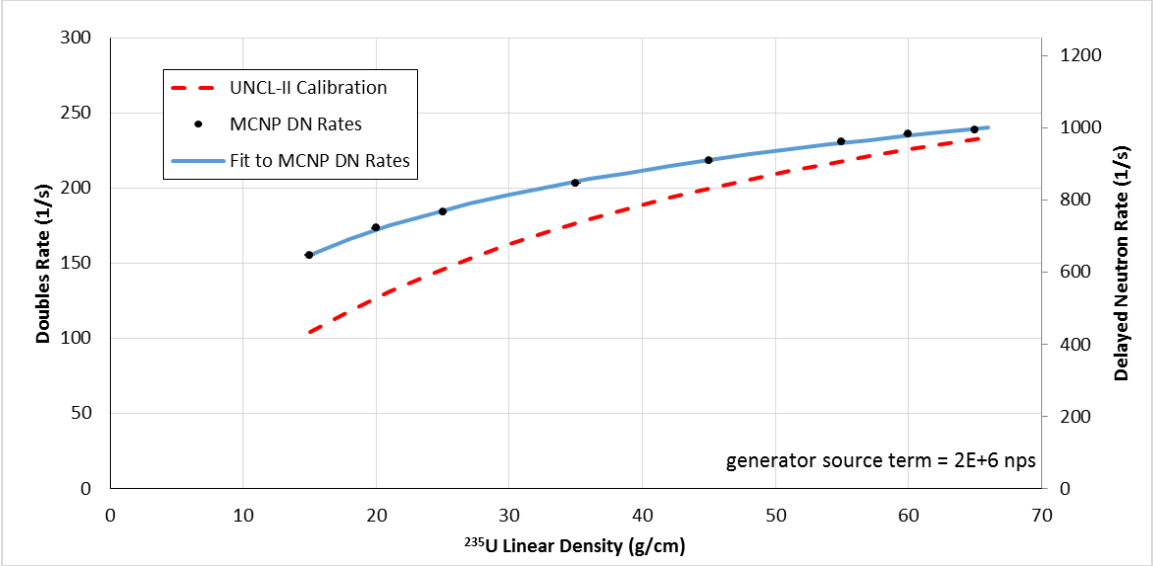

Figure 80. nGen-300c/UNCL operating in pulsed, thermal mode (2E6 n/s, 50 Hz) for delayed neutron counting assay overlain with the measured UNCL-II calibration results [6].

Table 87. Simulated thermal mode, delayed neutron counting UNCL measurement results for the calibration assemblies‡

Fuel assembly ID	Declared LD ^{235}U (g/cm)	Singles background rate (1/s)	Delayed neutron rate (1/s)	600 sec σ_{DN} (1/s)	1,800 sec σ_{DN} (1/s)	Analyzed LD ^{235}U (g/cm)	600 sec LD uncert (g/cm)	1,800 sec LD uncert (g/cm)	600 sec Total uncert (%)	1,800 sec Total uncert (%)
17x17_cal_15	15.0	137.0	647.4	± 1.31	± 0.76	15.71	± 0.07	± 0.04	2.0	2.0
17x17_cal_20	20.0	137.0	722.0	± 1.37	± 0.79	20.35	± 0.10	± 0.06	2.1	2.0
17x17_cal_25	25.0	137.0	767.9	± 1.40	± 0.81	24.02	± 0.12	± 0.07	2.1	2.0
17x17_cal_35	35.0	137.0	846.6	± 1.46	± 0.84	32.64	± 0.20	± 0.11	2.1	2.0
17x17_cal_45	45.0	137.0	907.8	± 1.50	± 0.87	42.73	± 0.30	± 0.17	2.1	2.0
17x17_cal_55	55.0	137.0	962.0	± 1.54	± 0.89	56.26	± 0.48	± 0.28	2.2	2.1
17x17_cal_60	60.0	137.0	983.2	± 1.55	± 0.89	63.53	± 0.59	± 0.34	2.2	2.1
17x17_cal_65	65.0	137.0	994.2	± 1.56	± 0.90	67.97	± 0.66	± 0.38	2.2	2.1

‡ Uncertainties are the expected measurement performance values.
† Includes a 2% systematic contribution to the uncertainty.

The simulated fast mode delayed neutron rates for the MP320 generator operating with 2E6 n/s in pulsed mode are provided in Table 88, and a comparison of the resulting calibration curve with the Am(Li)-based curve is shown in Figure 81. As can be seen in Figure 81, the response function for the delayed neutron measurement is much flatter because of the increased sensitivity to ^{238}U.

The expected measurement precision in the delayed neutron rates are significantly improved (6–12 times better) over that obtained from the active coincidence counting measurement; however, because of the increased sensitivity to ^{238}U, the improvement in assay precision is only a factor of 3 times better. If we consider an arbitrary 2% calibration uncertainty, the total measurement uncertainty improves by a factor of 2 relative to the Am(Li)-based coincidence measurement over most of the linear density range considered.

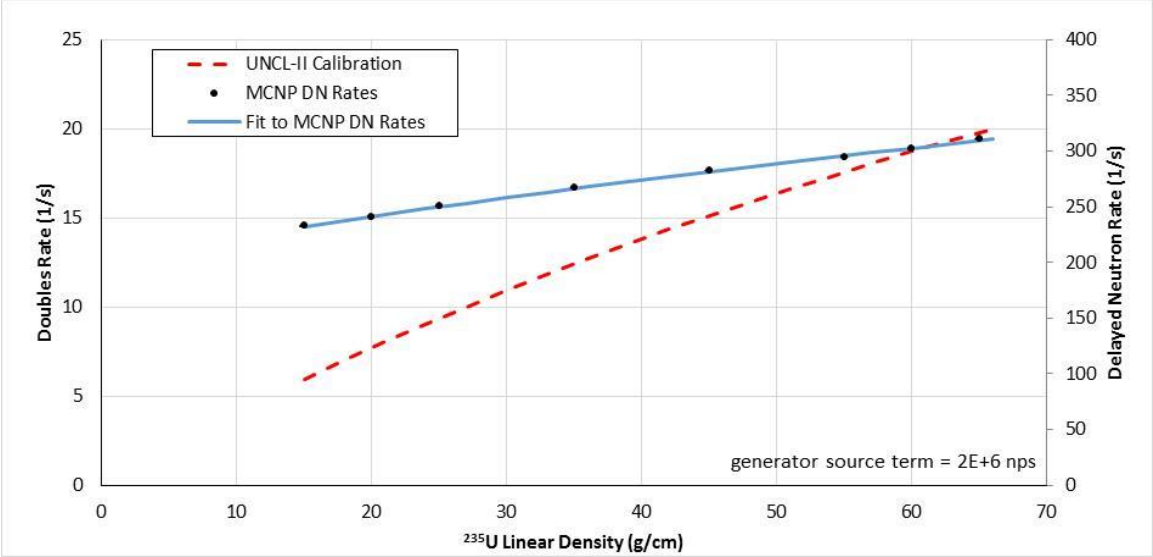

Figure 81. nGen-300c/UNCL operating in pulsed, fast mode (2E6 n/s, 50Hz) for delayed neutron counting assay overlain with the measured UNCL-II calibration results [6].

Table 88. Simulated fast mode, delayed neutron counting UNCL measurement results for the calibration assemblies‡

Fuel assembly ID	Declared LD ^{235}U (g/cm)	Singles background rate (1/s)	Delayed neutron rate (1/s)	600 sec σ_{DN} (1/s)	1,800 sec σ_{DN} (1/s)	Analyzed LD ^{235}U (g/cm)	600 sec LD uncert (g/cm)	1,800 sec LD uncert (g/cm)	600 sec Total uncert (%)	1,800 sec Total uncert (%)
17x17_cal_15	15.0	137.0	232.5	± 0.90	± 0.52	15.03	± 0.50	± 0.29	3.9	2.8
17x17_cal_20	20.0	137.0	240.7	± 0.91	± 0.52	19.65	± 0.52	± 0.30	3.3	2.5
17x17_cal_25	25.0	137.0	250.1	± 0.92	± 0.53	25.11	± 0.54	± 0.31	2.9	2.4
17x17_cal_35	35.0	137.0	267.3	± 0.94	± 0.54	35.63	± 0.59	± 0.34	2.6	2.2
17x17_cal_45	45.0	137.0	282.1	± 0.95	± 0.55	45.34	± 0.65	± 0.37	2.5	2.2
17x17_cal_55	55.0	137.0	294.1	± 0.96	± 0.56	53.74	± 0.70	± 0.40	2.4	2.1
17x17_cal_60	60.0	137.0	301.7	± 0.97	± 0.56	59.39	± 0.73	± 0.42	2.4	2.1
17x17_cal_65	65.0	137.0	310.4	± 0.98	± 0.57	66.15	± 0.78	± 0.45	2.3	2.1

‡ Uncertainties are the expected measurement performance values.
† Includes a 2% systematic contribution to the uncertainty.

10.2 SIMULATED DELAYED NEUTRON PERFORMANCE FOR THE VARIOUS INTACT ASSEMBLIES

The series of simulations were performed using the descriptions for the assorted intact fuel assemblies described in Section 3.2 for the DD/UNCL configured for delayed neutron counting using the nGen-300c neutron generator. The simulated assay results are provided in Tables 89–92 and are shown in Figures 82 and 83for operation in the delayed neutron counting thermal and fast assay modes. The results are shown before and after application of the heavy metal correction, illustrating the need to apply the correction factors when considering the relative performance of the measurement for a given assembly. For the DD generator–based measurement, the heavy metal (enrichment) correction becomes more important, relative to the Am(Li) interrogation, because of the increased fission rates in ^{238}U. The functional form is used for the correction

$$k_4 = 1 + \lambda_1 \cdot (\lambda_0 - \lambda)$$

However, in this case the parameters λ_0 and λ_1 are determined by a fit to the MCNP simulated rates. For these simulations using the calibration assembly description linear density as the reference (taken as a whole, including the poisoned and partial defect assemblies) the data is best represented when

Thermal mode	Fast mode
λ_0 = 1,297 g/cm	λ_0 = 1,297 g/cm
λ_1 = 5.03E-4 cm/g	λ_1 = 5.86 E-4 cm/g

The results suggest that the heavy metal correction for thermal mode interrogation may require assembly-specific calibrations.

We see in Table 75 that for simulated fast mode assay rates for assembly 14x14C, the non-heavy metal corrected rate would fall below the calibration range, and results in a negative mass even though the expected delayed neutron rate is positive. It is necessary to apply the heavy metal correction to the delayed neutron rate to bring this assay into the valid calibration range.

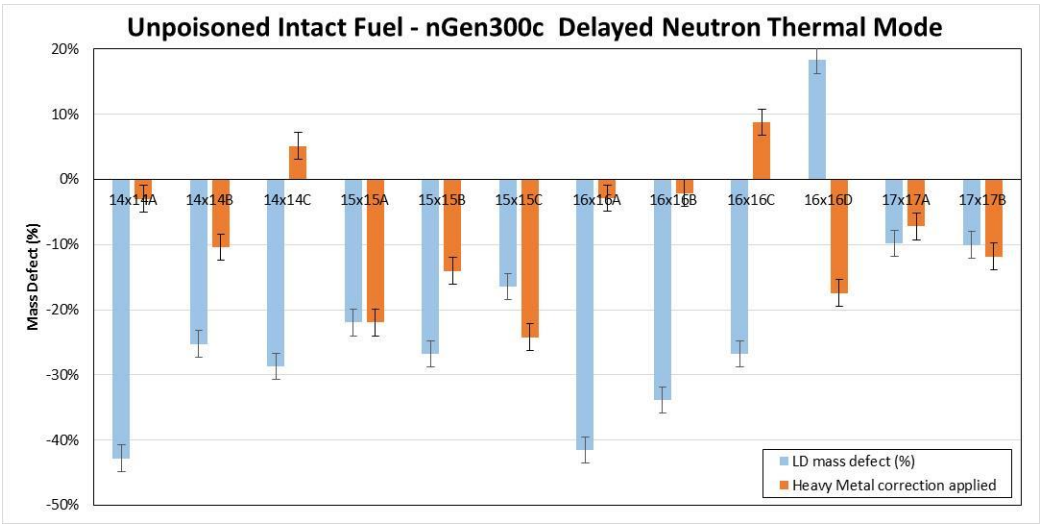

Figure 82. Results of the MCNP simulations for the nGen-300c/UNCL for the assorted intact fuel assemblies in the delayed neutron thermal mode. Error bars represent the project 1 sigma uncertainties for an 1,800 second measurement time.

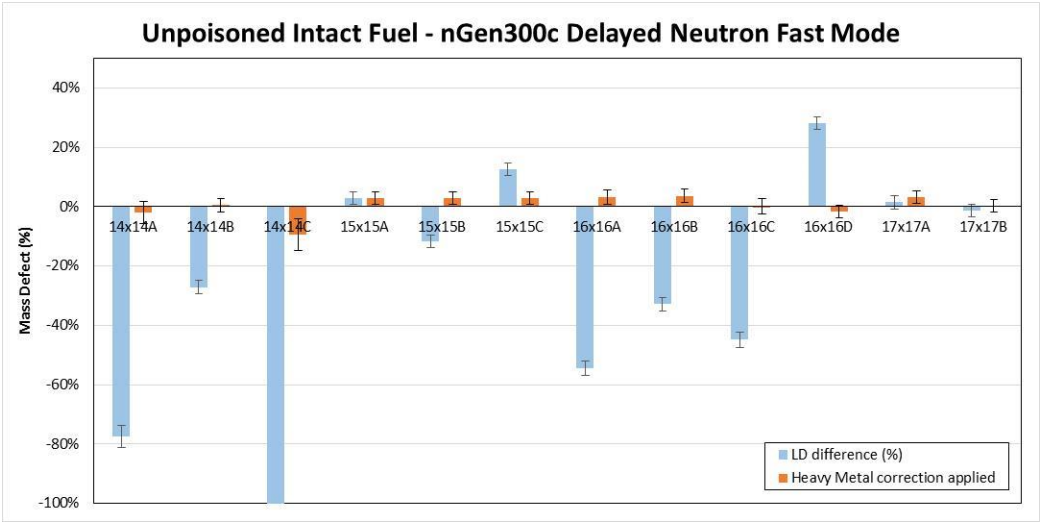

Figure 83. Results of the MCNP simulations for the nGen-300c/UNCL for the assorted intact fuel assemblies in the delayed neutron fast mode. Error bars represent the project 1 sigma uncertainties for an 1,800 second measurement time.

Table 89. Simulated delayed thermal mode, nGen-300c based UNCL measurement results for the unpoisoned, intact fuel assemblies‡

Fuel assembly ID	Declared LD ^{235}U (g/cm)	Singles background rate (1/s)	Delayed neutron rate (1/s)	600 sec σ_{DN} (1/s)	1,800 sec σ_{DN} (1/s)	Analyzed LD ^{235}U (g/cm)	600 sec LD uncert (g/cm)	1,800 sec LD uncert (g/cm)	600 sec Total uncert (%)†	1,800 sec Total uncert (%)†
14x14A	**37.57**	105.9	737.5	± 1.36	± 0.78	21.50	± 0.10	± 0.06	2.1	2.0
14x14B	**37.31**	127.7	807.4	± 1.42	± 0.82	27.89	± 0.15	± 0.09	2.1	2.0
14x14C	**19.78**	105.9	615.5	± 1.26	± 0.73	14.10	± 0.06	± 0.03	2.0	2.0
15x15A	**58.37**	138.9	921.2	± 1.51	± 0.87	45.55	± 0.34	± 0.19	2.1	2.0
15x15B	**61.54**	131.8	919.0	± 1.50	± 0.87	45.06	± 0.33	± 0.19	2.1	2.0
15x15C	**60.91**	143.4	943.3	± 1.53	± 0.88	50.89	± 0.40	± 0.23	2.2	2.1
16x16A	**46.90**	111.6	803.2	± 1.41	± 0.81	27.44	± 0.15	± 0.09	2.1	2.0
16x16B	**50.16**	119.4	850.5	± 1.45	± 0.84	33.17	± 0.20	± 0.12	2.1	2.0
16x16C	**30.95**	113.5	752.2	± 1.37	± 0.79	22.67	± 0.11	± 0.07	2.1	2.0
16x16D	**64.07**	152.5	1011.1	± 1.58	± 0.91	75.84	± 0.81	± 0.47	2.3	2.1
17x17A	**41.29**	137.4	877.6	± 1.48	± 0.85	37.24	± 0.24	± 0.14	2.1	2.0
17x17B	**54.82**	139.8	937.1	± 1.52	± 0.88	49.29	± 0.38	± 0.22	2.1	2.0

‡ Uncertainties are the expected measurement performance values.
† Includes a 2% systematic contribution to the uncertainty.

Table 90. Simulated delayed thermal mode, defect analysis results for the unpoisoned, intact fuel assemblies

Fuel assembly ID	Defect without correction			Defect with HM correction applied		
	LD mass defect (%)	#σ 600 sec	#σ 1,800 sec	LD mass defect (%)	#σ 600 sec	#σ 1,800 sec
14x14A	−42.8	36.3	37.0	−3.0	2.2	2.5
14x14B	−25.3	16.3	16.7	−10.4	6.5	6.8
14x14C	−28.7	19.7	20.0	5.1	3.4	3.5
15x15A	−22.0	13.2	13.8	−22.0	13.2	13.8
15x15B	−26.8	17.2	17.9	−14.1	8.6	9.2
15x15C	−16.4	9.1	9.6	−24.2	13.7	14.2
16x16A	−41.5	34.2	35.0	−2.9	2.1	2.3
16x16B	−33.9	24.5	25.2	−2.1	1.4	1.5
16x16C	−26.7	17.7	18.1	8.7	5.4	5.7
16x16D	18.4	6.9	7.4	−17.4	7.1	7.3
17x17A	−9.8	5.2	5.3	−7.2	3.8	3.9
17x17B	−10.1	5.2	5.5	−11.8	6.2	6.4
Average bias	**−22.1%**			**−8.4%**		
Std. deviation	**16.5%**			**10.2%**		

Table 91. Simulated delayed fast mode, nGen-300c based UNCL measurement results for the unpoisoned, intact fuel assemblies‡

Fuel assembly ID	Declared LD ^{235}U (g/cm)	Singles background rate (1/s)	Delayed neutron rate (1/s)	600 sec σ_{DN} (1/s)	1,800 sec σ_{DN} (1/s)	Analyzed LD ^{235}U (g/cm)	600 sec LD uncert (g/cm)	1,800 sec LD uncert (g/cm)	600 sec Total uncert (%)†	1,800 sec Total uncert (%)†
14x14A	**37.57**	105.9	220.4	± 0.85	± 0.49	8.42	± 0.45	± 0.26	5.8	3.7
14x14B	**37.31**	127.7	253.6	± 0.91	± 0.53	27.18	± 0.55	± 0.32	2.8	2.3
14x14C	**19.78**	105.9	194.7	± 0.82	± 0.47	-4.85	± 0.41	± 0.23	8.6	5.2
15x15A	**58.37**	138.9	302.6	± 0.98	± 0.56	60.04	± 0.74	± 0.43	2.4	2.1
15x15B	**61.54**	131.8	294.9	± 0.96	± 0.55	54.34	± 0.70	± 0.40	2.4	2.1
15x15C	**60.91**	143.4	313.3	± 0.99	± 0.57	68.50	± 0.81	± 0.47	2.3	2.1
16x16A	**46.90**	111.6	243.6	± 0.88	± 0.51	21.33	± 0.51	± 0.29	3.1	2.4
16x16B	**49.92**	121.8	263.9	± 0.92	± 0.53	33.52	± 0.57	± 0.33	2.6	2.2
16x16C	**30.95**	122.3	236.1	± 0.88	± 0.51	17.05	± 0.50	± 0.29	3.5	2.6
16x16D	**64.07**	152.5	329.1	± 1.02	± 0.59	82.13	± 0.94	± 0.54	2.3	2.1
17x17A	**41.54**	138.2	277.3	± 0.95	± 0.55	42.13	± 0.63	± 0.36	2.5	2.2
17x17B	**54.19**	138.2	293.8	± 0.97	± 0.56	53.53	± 0.70	± 0.40	2.4	2.1

‡ Uncertainties are the expected measurement performance values.
† Includes a 2% systematic contribution to the uncertainty.

Table 92. Simulated fast mode, defect analysis results for the unpoisoned, intact fuel assemblies

Fuel assembly ID	Defect without correction			Defect with HM correction applied		
	LD mass defect (%)	#σ 600 sec	#σ 1,800 sec	LD mass defect (%)	#σ 600 sec	#σ 1,800 sec
14x14A	−77.6	64.2	111.2	−2.1	1.1	1.9
14x14B	−27.1	18.5	32.1	0.5	0.2	0.3
14x14C	−124.5	60.6	105.0	−9.5	3.3	5.5
15x15A	2.9	2.3	3.9	2.9	1.2	1.3
15x15B	−11.7	10.3	17.9	2.8	1.3	1.5
15x15C	12.5	9.4	16.3	2.7	1.1	1.2
16x16A	−54.5	50.2	86.9	3.0	1.7	2.4
16x16B	−32.8	28.6	49.6	3.6	1.8	2.3
16x16C	−44.9	27.9	48.2	0.0	0.0	0.0
16x16D	28.2	19.2	33.3	−1.8	0.6	0.7
17x17A	1.4	0.9	1.6	3.1	1.2	1.4
17x17B	−1.2	1.0	1.7	0.3	0.1	0.1
Average bias	**−27.5%**			**0.5%**		
Std. deviation	**43.0%**			**3.7%**		

10.3 SIMULATED DELAYED NEUTRON PERFORMANCE FOR BURNABLE POISONS

The series of simulations were repeated for the descriptions of the intact fuel assemblies containing burnable poisons described in Section 3.2 for the DD/UNCL configured for delayed neutron counting using the nGen-300c neutron generator. Figure 84 illustrates the impact of the poison rods on the thermal mode mass results for the UNCL using an Am(Li) neutron source, and the fast mode results are shown in Figure 85. As can be seen, the number of poison rods is more important than rod's poison loading. The effectiveness of the poison rod correction can also be seen in the plots because the average bias is reduced to <1%, and the typical deviation from the expected value is reduced to less than 2% in both thermal and fast modes. The simulated rates and defect levels are presented in Tables 94–97.

The parameters in the expression for the poison rod correction factor, k_3, were adjusted by a fit to the MCNP simulations. The expression for k_3 from discussed above in Section 1.3.2 [6] is shown here with the potentially adjustable parameters *a*, *b*, and *c*.

$$k_3 = 1 + \frac{a \cdot n}{N} \cdot \left(1 - e^{-b \cdot Gd}\right) \cdot (1 - c \cdot E_N)$$

where n is the number of poison rods,
N is the number of fuel rods (fuel + poison),
Gd is the weight percent of the Gd in the poison rods,
E_N is the declared enrichment.

It was found that it was only necessary to adjust the parameter, *b*, to obtain results similar to those obtained for the Am(Li)-based UNCL system. The parameters for the MP320/UNCL/DN system are provided in Table 93.

Table 93. Poison rod correction parameters for the MP320/UNCL/DN system

Parameter	Thermal mode		Fast mode	
	Am(Li)	MP320	Am(Li)	MP320
a	9.86	2.29	0.602	0.197
b	0.647	0.407	0.647	0.647
c	0.176	0.177	—	—

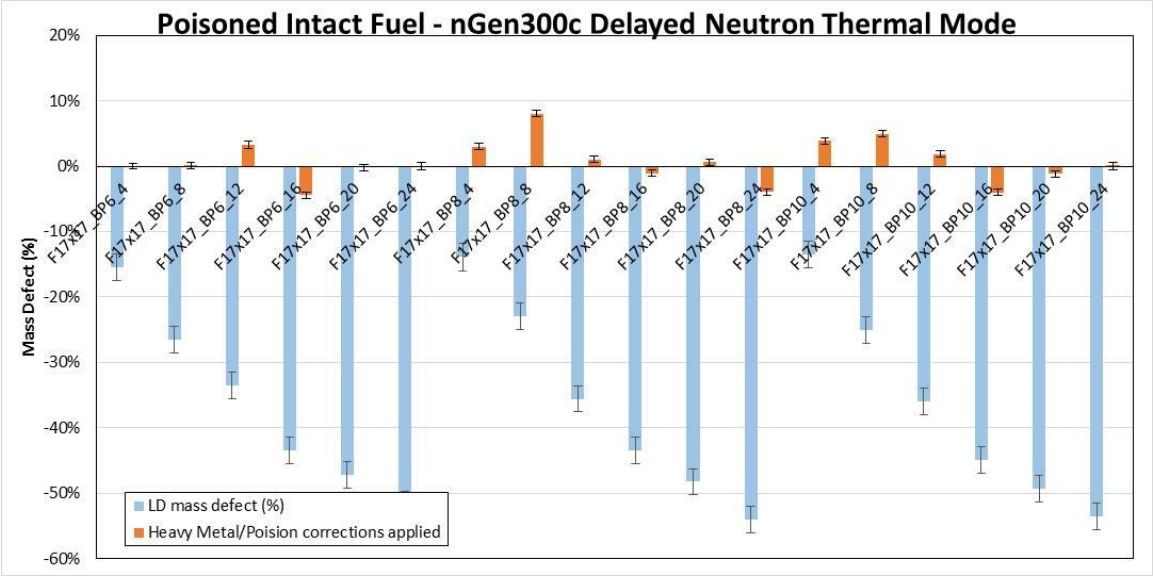

Figure 84. Thermal mode simulated assay results for the various burnable poison loadings with and without the heavy metal and poison rod correction.

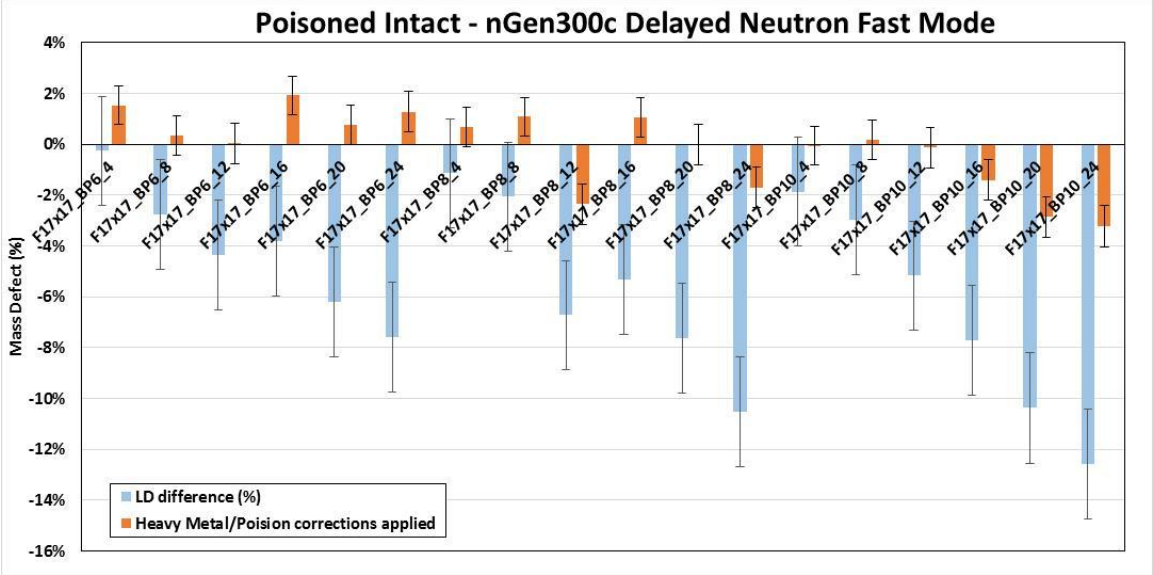

Figure 85. Fast mode assay results for the various burnable poison loadings with and without the heavy metal and poison rod correction.

Table 94. Simulated delayed neutron, thermal mode, nGen-300c based UNCL measurement results for the poisoned, intact fuel assemblies‡

Fuel assembly ID	Declared LD ^{235}U (g/cm)	Singles background rate (1/s)	Delayed neutron rat (1/s)	600 sec σ_{DN} (1/s)	1,800 sec σ_{DN} (1/s)	Analyzed LD ^{235}U (g/cm)	600 sec LD uncert (g/cm)	1,800 sec LD uncert (g/cm)	600 sec total uncert (%)†	1,800 sec total uncert (%)†
BP6_4	51.50	137.9	911.8	± 1.50	± 0.87	43.54	± 0.31	± 0.18	2.1	2.0
BP6_8	51.20	137.1	880.0	± 1.48	± 0.85	37.64	± 0.25	± 0.14	2.1	2.0
BP6_12	50.90	136.3	855.5	± 1.46	± 0.84	33.87	± 0.21	± 0.12	2.1	2.0
BP6_16	50.60	135.5	814.0	± 1.43	± 0.83	28.62	± 0.16	± 0.09	2.1	2.0
BP6_20	50.30	134.7	794.7	± 1.42	± 0.82	26.56	± 0.14	± 0.08	2.1	2.0
BP6_24	49.90	133.6	768.5	± 1.40	± 0.81	24.07	± 0.12	± 0.07	2.1	2.0
BP8_4	51.50	137.9	915.6	± 1.50	± 0.87	44.34	± 0.32	± 0.19	2.1	2.0
BP8_8	51.20	137.1	890.6	± 1.49	± 0.86	39.47	± 0.27	± 0.15	2.1	2.0
BP8_12	50.90	136.3	847.9	± 1.46	± 0.84	32.80	± 0.20	± 0.11	2.1	2.0
BP8_16	50.50	135.2	813.7	± 1.43	± 0.83	28.59	± 0.16	± 0.09	2.1	2.0
BP8_20	50.20	134.4	788.9	± 1.42	± 0.82	25.98	± 0.14	± 0.08	2.1	2.0
BP8_24	49.90	133.6	755.6	± 1.39	± 0.80	22.95	± 0.12	± 0.07	2.1	2.0
BP10_4	51.50	137.9	916.6	± 1.51	± 0.87	44.55	± 0.32	± 0.19	2.1	2.0
BP10_8	51.20	137.1	884.5	± 1.48	± 0.86	38.39	± 0.25	± 0.15	2.1	2.0
BP10_12	50.80	136.0	846.1	± 1.46	± 0.84	32.56	± 0.20	± 0.11	2.1	2.0
BP10_16	50.50	135.2	806.4	± 1.43	± 0.82	27.79	± 0.15	± 0.09	2.1	2.0
BP10_20	50.20	134.4	783.5	± 1.41	± 0.82	25.45	± 0.14	± 0.08	2.1	2.0
BP10_24	49.80	133.4	757.8	± 1.39	± 0.80	23.14	± 0.12	± 0.07	2.1	2.0

‡ Uncertainties are the expected measurement performance values.
† Includes a 2% systematic contribution to the uncertainty.

Table 95. Simulated thermal mode, defect analysis results for the poisoned, intact fuel assemblies

Fuel assembly ID	Defect without correction			HM and poison corrections applied		
	LD mass defect (%)	#σ 600 sec	#σ 1,800 sec	LD mass defect (%)	#σ 600 sec	#σ 1,800 sec
BP6_4	−15.5	8.6	9.0	0.0	0.0	0.0
BP6_8	−26.5	17.1	17.7	0.0	0.0	0.0
BP6_12	−33.4	24.0	24.7	3.3	1.5	1.5
BP6_16	−43.4	37.0	37.9	−4.4	2.1	2.3
BP6_20	−47.2	43.1	44.2	−0.2	0.1	0.1
BP6_24	−51.8	52.0	53.1	0.0	0.0	0.0
BP8_4	−13.9	7.6	7.9	3.0	1.3	1.4
BP8_8	−22.9	14.1	14.6	8.0	3.4	3.6
BP8_12	−35.6	26.4	27.2	1.0	0.5	0.5
BP8_16	−43.4	36.9	37.8	−1.1	0.5	0.5
BP8_20	−48.2	45.0	46.1	0.6	0.3	0.3
BP8_24	−54.0	56.9	58.1	−3.9	1.9	2.0
BP10_4	−13.5	7.3	7.6	3.9	1.7	1.8
BP10_8	−25.0	15.8	16.4	5.0	2.2	2.3
BP10_12	−35.9	26.8	27.6	1.8	0.8	0.9
BP10_16	−45.0	39.4	40.4	−4.0	1.9	2.0
BP10_20	−49.3	47.0	48.1	−1.2	0.6	0.6
BP10_24	−53.5	55.8	57.0	0.0	0.0	0.0
Average bias	**−36.6%**			**0.7%**		
Std. deviation	**14.0%**			**3.2%**		

Table 96. Simulated delayed neutron fast mode, nGen-300c based UNCL measurement results for the poisoned, intact fuel assemblies‡

Fuel assembly ID	Declared LD ^{235}U (g/cm)	Singles background rate (1/s)	Delayed neutron rate (1/s)	600 sec σ_{DN} (1/s)	1,800 sec σ_{DN} (1/s)	Analyzed LD ^{235}U (g/cm)	600 sec LD uncert (g/cm)	1,800 sec LD uncert (g/cm)	600 sec total uncert (%)†	1,800 sec total uncert (%)†
BP6_4	**51.50**	138.7	290.7	± 0.96	± 0.56	51.37	± 0.68	± 0.39	2.4	2.1
BP6_8	**51.20**	138.6	288.5	± 0.96	± 0.55	49.79	± 0.67	± 0.39	2.4	2.1
BP6_12	**50.90**	138.5	286.9	± 0.96	± 0.55	48.69	± 0.67	± 0.39	2.4	2.2
BP6_16	**50.60**	138.5	286.9	± 0.96	± 0.55	48.67	± 0.67	± 0.39	2.4	2.2
BP6_20	**50.30**	138.4	284.8	± 0.96	± 0.55	47.18	± 0.66	± 0.38	2.4	2.2
BP6_24	**49.90**	138.1	283.2	± 0.95	± 0.55	46.11	± 0.65	± 0.38	2.4	2.2
BP8_4	**51.50**	138.7	290.1	± 0.96	± 0.56	50.92	± 0.68	± 0.39	2.4	2.1
BP8_8	**51.20**	138.6	289.0	± 0.96	± 0.55	50.14	± 0.68	± 0.39	2.4	2.1
BP8_12	**50.90**	138.5	285.2	± 0.96	± 0.55	47.48	± 0.66	± 0.38	2.4	2.2
BP8_16	**50.50**	138.2	285.7	± 0.96	± 0.55	47.82	± 0.66	± 0.38	2.4	2.2
BP8_20	**50.20**	138.1	283.6	± 0.95	± 0.55	46.37	± 0.65	± 0.38	2.4	2.2
BP8_24	**49.90**	138.1	281.0	± 0.95	± 0.55	44.65	± 0.64	± 0.37	2.5	2.2
BP10_4	**51.50**	138.7	289.6	± 0.96	± 0.56	50.54	± 0.68	± 0.39	2.4	2.1
BP10_8	**51.20**	138.6	288.4	± 0.96	± 0.55	49.68	± 0.67	± 0.39	2.4	2.1
BP10_12	**50.80**	138.3	286.2	± 0.96	± 0.55	48.18	± 0.66	± 0.38	2.4	2.2
BP10_16	**50.50**	138.2	283.9	± 0.96	± 0.55	46.62	± 0.65	± 0.38	2.4	2.2
BP10_20	**50.20**	138.1	281.6	± 0.95	± 0.55	45.00	± 0.65	± 0.37	2.5	2.2
BP10_24	**49.80**	137.8	279.4	± 0.95	± 0.55	43.54	± 0.64	± 0.37	2.5	2.2

‡ Uncertainties are the expected measurement performance values.
† Includes a 2% systematic contribution to the uncertainty.

Table 97. Simulated fast mode, defect analysis results for the poisoned, intact fuel assemblies

Fuel assembly ID	Defect without correction			HM and Poison corrections applied		
	LD mass defect (%)	#σ 600 sec	#σ 1800 sec	LD mass defect (%)	#σ 600 sec	#σ 1800 sec
BP6_4	−0.3	0.2	0.3	1.5	0.6	0.7
BP6_8	−2.8	2.1	3.6	0.3	0.1	0.2
BP6_12	−4.3	3.3	5.7	0.0	0.0	0.0
BP6_16	−3.8	2.9	5.0	1.9	0.8	0.9
BP6_20	−6.2	4.7	8.2	0.8	0.3	0.4
BP6_24	−7.6	5.8	10.1	1.3	0.5	0.6
BP8_4	−1.1	0.9	1.5	0.7	0.3	0.3
BP8_8	−2.1	1.6	2.7	1.1	0.4	0.5
BP8_12	−6.7	5.2	9.0	−2.4	1.0	1.1
BP8_16	−5.3	4.1	7.0	1.1	0.4	0.5
BP8_20	−7.6	5.9	10.2	0.0	0.0	0.0
BP8_24	−10.5	8.2	14.2	−1.7	0.7	0.8
BP10_4	−1.9	1.4	2.5	−0.1	0.0	0.0
BP10_8	−3.0	2.3	3.9	0.2	0.1	0.1
BP10_12	−5.2	4.0	6.8	−0.1	0.1	0.1
BP10_16	−7.7	5.9	10.3	−1.4	0.6	0.7
BP10_20	−10.4	8.1	14.0	−2.8	1.2	1.4
BP10_24	−12.6	9.8	17.0	−3.2	1.4	1.5
Average bias	**−5.5%**			**−0.2%**		
Std. deviation	**3.5%**			**1.5%**		

10.4 SIMULATED DELAYED NEUTRON PERFORMANCE FOR SIMULATED PARTIAL DEFECT ANALYSIS

This series of simulations examines the delayed neutron counting performance of the UNCL using the nGen-300c neutron generator for increasing numbers of rods substituted with DU. The mass defect relative to the declared value is shown in Figure 86 for the thermal mode and in Figure 87 for the fast mode. Rates and performance values are provided in Tables 98–101. Because the heavy metal content for the simulated assembly is the same as the simulated calibration assemblies, the heavy metal correction will be equal to 1, so application of the correction will have no impact on the results.

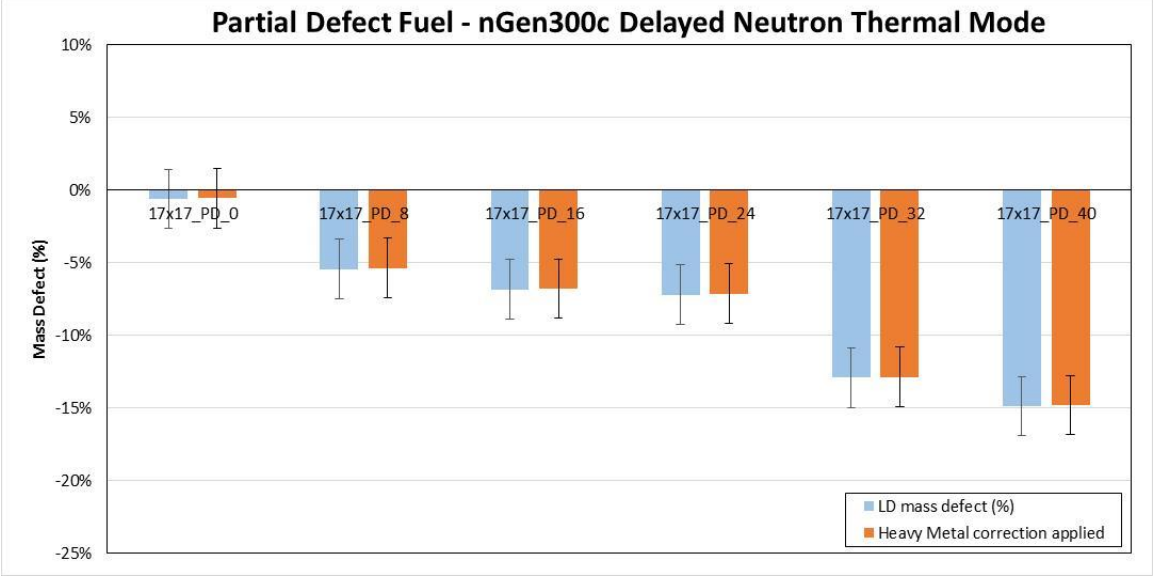

Figure 86. Thermal mode simulated assay results for the partial defect loadings with and without the heavy metal correction.

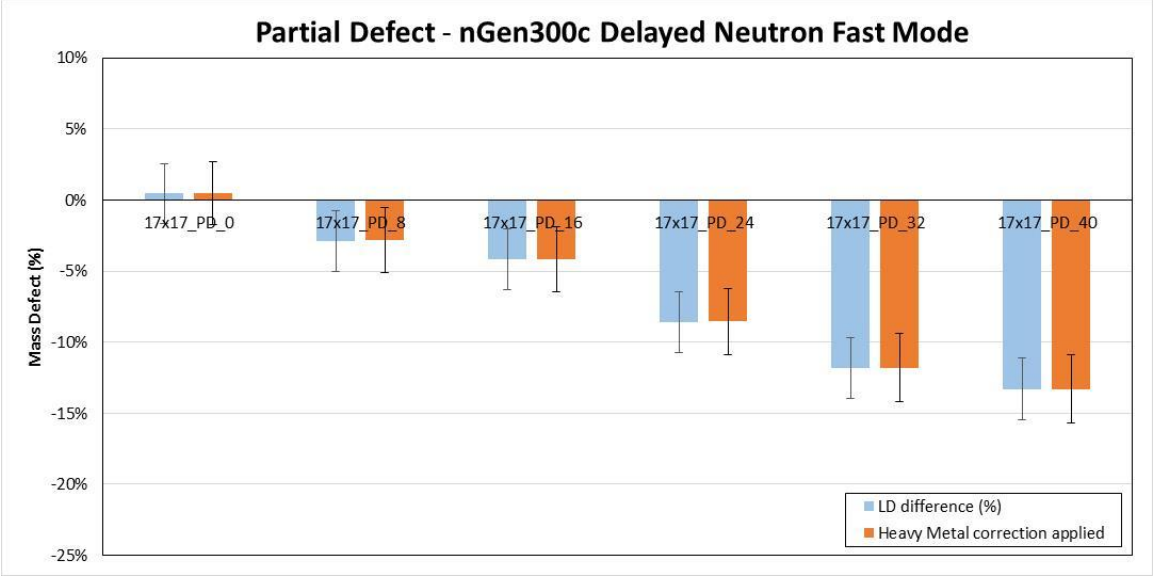

Figure 87. Fast mode simulated assay results for the partial defect loadings with and without the heavy metal correction.

Table 98. Simulated delayed, thermal mode, nGen-300c based UNCL measurement results for the partial defect assembly configurations‡

Fuel assembly ID	Declared LD ^{235}U (g/cm)	Singles background rate (1/s)	Delayed neutron rate (1/s)	600 sec σ_{DN} (1/s)	1,800 sec σ_{DN} (1/s)	Analyzed LD ^{235}U (g/cm)	600 sec LD uncert (g/cm)	1,800 sec LD uncert (g/cm)	600 sec Total uncert (%)†	1,800 sec Total uncert (%)†
PD_0	54.98	137.0	956.7	± 1.53	± 0.88	54.66	± 0.45	± 0.26	2.2	2.1
PD_8	54.98	137.0	947.4	± 1.53	± 0.88	52.00	± 0.42	± 0.24	2.2	2.1
PD_16	54.98	137.0	944.5	± 1.52	± 0.88	51.23	± 0.41	± 0.24	2.2	2.1
PD_24	54.98	137.0	943.8	± 1.52	± 0.88	51.03	± 0.40	± 0.23	2.2	2.1
PD_32	54.98	137.0	931.3	± 1.52	± 0.87	47.89	± 0.36	± 0.21	2.1	2.0
PD_40	54.98	137.0	926.8	± 1.51	± 0.87	46.81	± 0.35	± 0.20	2.1	2.0

‡ Uncertainties are the expected measurement performance values.
† Includes a 2% systematic contribution to the uncertainty.

Table 99. Simulated thermal mode, defect analysis results for the partial defect assembly configurations

Fuel assembly ID	Defect without correction			HM and Poison corrections applied		
	LD mass defect (%)	#σ 600 sec	#σ 1,800 sec	LD mass defect (%)	#σ 600 sec	#σ 1,800 sec
PD_0	−0.6	0.3	0.3	−0.5	0.2	0.3
PD_8	−5.4	2.7	2.8	−5.4	2.6	2.8
PD_16	−6.8	3.4	3.6	−6.8	3.4	3.5
PD_24	−7.2	3.6	3.8	−7.1	3.6	3.7
PD_32	−12.9	6.9	7.2	−12.8	6.9	7.2
PD_40	−14.9	8.2	8.5	−14.8	8.1	8.5

Table 100. Simulated delayed neutron, fast mode, nGen-300c based UNCL measurement results for the partial defect assembly configurations‡

Fuel assembly ID	Declared LD ^{235}U (g/cm)	Singles background rate (1/s)	Delayed neutron rate (1/s)	600 sec σ_{DN} (1/s)	1,800 sec σ_{DN} (1/s)	Analyzed LD ^{235}U (g/cm)	600 sec LD uncert (g/cm)	1,800 sec LD uncert (g/cm)	600 sec total uncert (%)†	1,800 sec total uncert (%)†
PD_0	54.98	137.0	296.1	± 0.97	± 0.56	55.23	± 0.71	± 0.41	2.4	2.1
PD_8	54.98	137.0	293.6	± 0.96	± 0.56	53.39	± 0.69	± 0.40	2.4	2.1
PD_16	54.98	137.0	292.6	± 0.96	± 0.56	52.66	± 0.69	± 0.40	2.4	2.1
PD_24	54.98	137.0	289.2	± 0.96	± 0.55	50.25	± 0.68	± 0.39	2.4	2.1
PD_32	54.98	137.0	286.6	± 0.96	± 0.55	48.46	± 0.66	± 0.38	2.4	2.2
PD_40	54.98	137.0	285.4	± 0.96	± 0.55	47.64	± 0.66	± 0.38	2.4	2.2

‡ Uncertainties are the expected measurement performance values.
† Includes a 2% systematic contribution to the uncertainty.

Table 101. Simulated fast mode, defect analysis results for the partial defect assembly configurations

Fuel assembly ID	Defect without correction			HM and poison corrections applied		
	LD mass defect (%)	#σ 600 sec	#σ 1,800 sec	LD mass defect (%)	#σ 600 sec	#σ 1,800 sec
PD_0	0.4	0.2	0.2	0.5	0.2	0.2
PD_8	−2.9	1.2	1.4	−2.8	1.2	1.4
PD_16	−4.2	1.8	2.1	−4.2	1.8	2.0
PD_24	−8.6	3.9	4.4	−8.6	3.9	4.4
PD_32	−11.9	5.6	6.3	−11.8	5.5	6.2
PD_40	−13.4	6.3	7.2	−13.3	6.3	7.1

11. PERFORMANCE COMPARISON OF THE DELAYED NEUTRON COUNTING DD/UNCL AND THE AM(LI)/UNCL

11.1 PERFORMANCE COMPARISON FOR DELAYED NEUTRON, THERMAL MODE OPERATION OF THE UNCL

11.1.1 Delayed Neutron Thermal Mode Response Function Comparison

To examine the relative mass dependence of the various interrogating neutron sources, the thermal mode calibration curves for the Am(Li), MP320, and nGen-300c interrogation systems were each normalized to their response to the 65 g ^{235}U/cm calibration assembly. The comparison of the simulated calibration curves for each of the neutron sources (Figure 88) reveals that the response functions for each of the neutron generator types considered have nearly identical dependence on the ^{235}U content of the assembly.

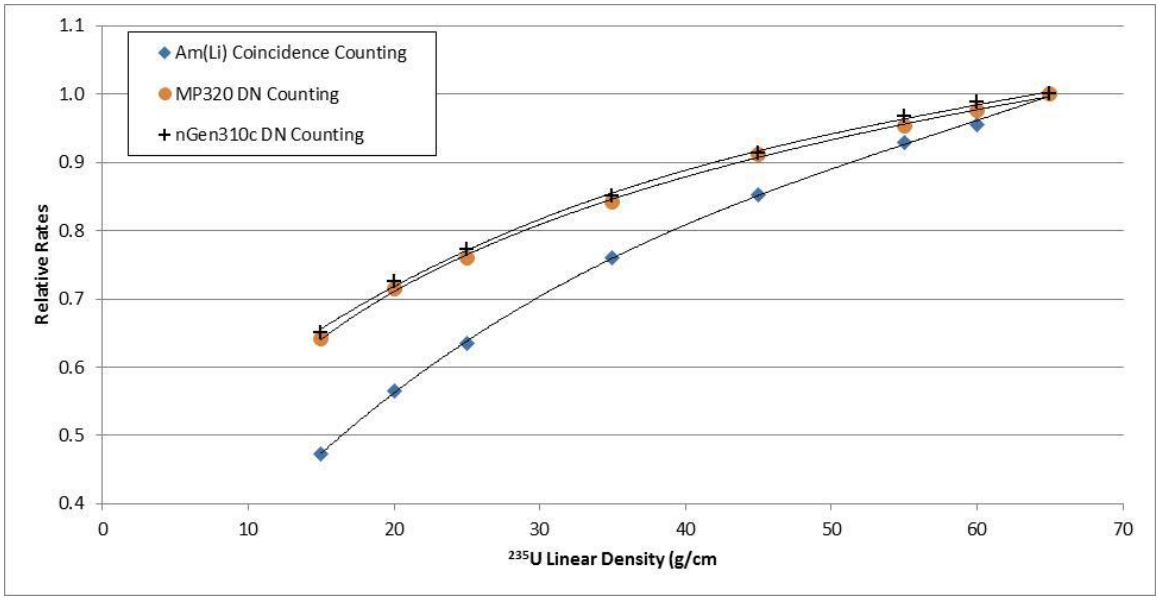

Figure 88. Comparison of the relative thermal mode coincidence rates from the Am(Li) interrogation source and the delayed neutron count rates for the two neutron generators as a function of ^{235}U linear density for the calibration assemblies (normalized to the 65 g ^{235}U/cm result).

The Am(Li) and neutron generator source terms were selected to be representative of an actual measurement. The Am(Li) source term is taken to be 50,000 n/s, which is approximately the same yield as the Am(Li) source used for the validation measurements discussed in a later section of this report. The neutron generator yields are taken as 2,000,000 n/s operating in a pulsed mode (the exposure rate from a 2,000,000 n/s DD generator is equivalent to a 1 µg ^{252}Cf source). The neutron background levels used (singles rate = 30 and doubles rate = 0.1) are representative of past UNCL measurements obtained from an operating fuel facility. The passive neutron signals from the fuel assembly were estimated from the MCNP models.

The expected rates precision as a function of ^{235}U linear density is shown in Figure 89 for the Am(Li) and neutron generator–based measurements for measurement times of 1,800 seconds (doubles rate for the coincidence measurement and delayed neutron counting rates for the neutron generators). The corresponding contribution to the linear mass uncertainty is shown in Figure 90. The expected precision in the delayed neutron rate for the two generators are equivalent but both are roughly 3 times smaller than the precision obtained from the Am(Li) source coincidence measurements. The expected precision in the

reported linear densities are two times lower for the MP320 measurement and three times lower for the nGen-300c relative to the Am(Li)-based coincidence measurement.

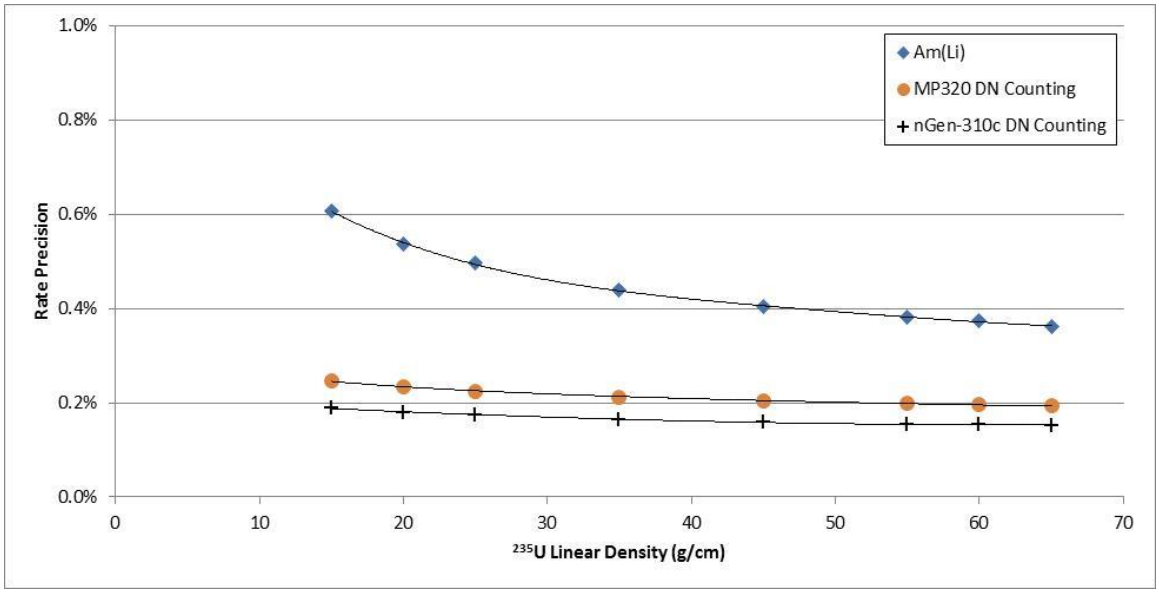

Figure 89. Comparison of the thermal mode rate precision as a function of ^{235}U linear density for the calibration assemblies for each of the neutron sources considered for 1,800 seconds measurement time. Am(Li) = 50,000 n/s, and neutron generators = 200,000 n/s.

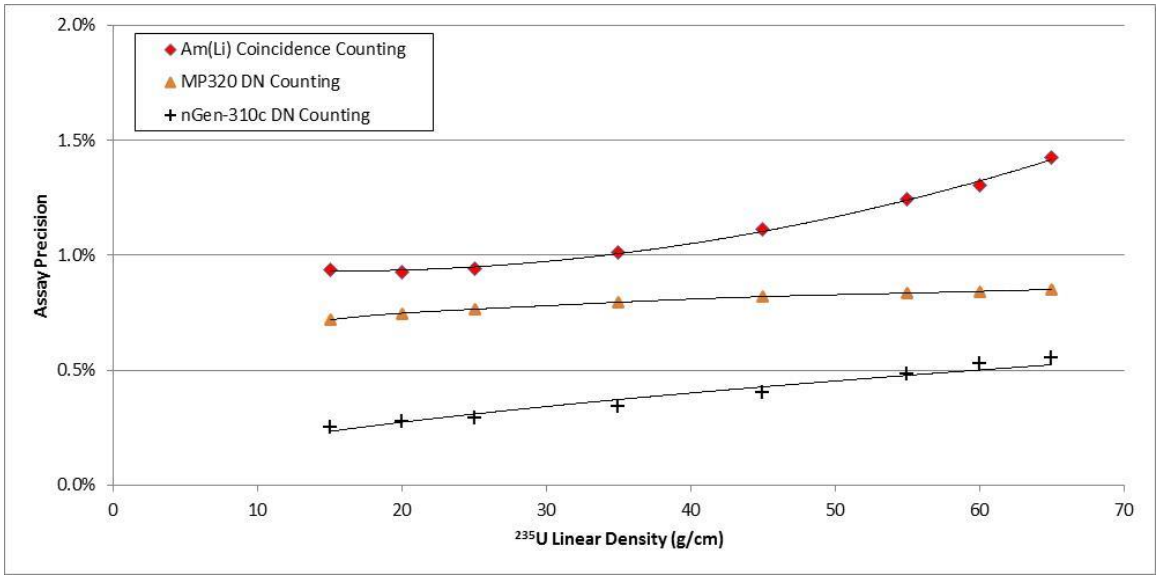

Figure 90. Comparison of the thermal mode assay precision as a function of ^{235}U linear density for the calibration assemblies for each of the neutron sources considered for 1,800 seconds measurement time. Am(Li) = 50,000 n/s, and neutron generators = 200,000 n/s.

11.1.2 Delayed Neutron, Thermal Mode—Intact, Non-Poisoned Fuel Assembly Comparison

A comparison of the simulated results for the MP320 and nGen-300c neutron generator–delayed neutron measurements with the Am(Li) mode based UNCL thermal mode measurements is presented in Figure 91, and the same data with the heavy metal correction applied is presented in Figure 92. Standard deviations for the collection of assemblies and the average biases are presented in Table 102. There is no significant difference qualitatively or quantitatively in the biases predicted by these simulations. Because the measurement precision is small compared to the overall uncertainty in the UNCL result, we conclude that in thermal mode the neutron generators and the Am(Li) sources provide equivalent performance for the 30 minute assay time. However, use of the nGen-300c delayed neutron measurement would allow the current level of precision to be obtained with significantly reduced measurements times. We also conclude from these results that the heavy metal correction offers limited value for the UNCL operated in the thermal mode.

Table 102. Thermal mode bias comparisons for the intact, unpoisoned fuel assemblies.
Am(Li) = coincidence counting, and MP320 and nGen-300c = delayed neutron counting.

	Uncorrected assay results				Heavy metal correction applied		
	Am(Li)	**MP320**	**nGen-300c**		**Am(Li)**	**MP320**	**nGen-300c**
Average bias	−16.0%	−20.7%	−22.1%		−14.7%	−6.8%	−8.4%
Standard deviation	6.8%	13.8%	16.5%		9.5%	8.8%	10.2%
Measurement precision	0.9%	0.8%	0.4%		0.9%	0.8%	0.4%

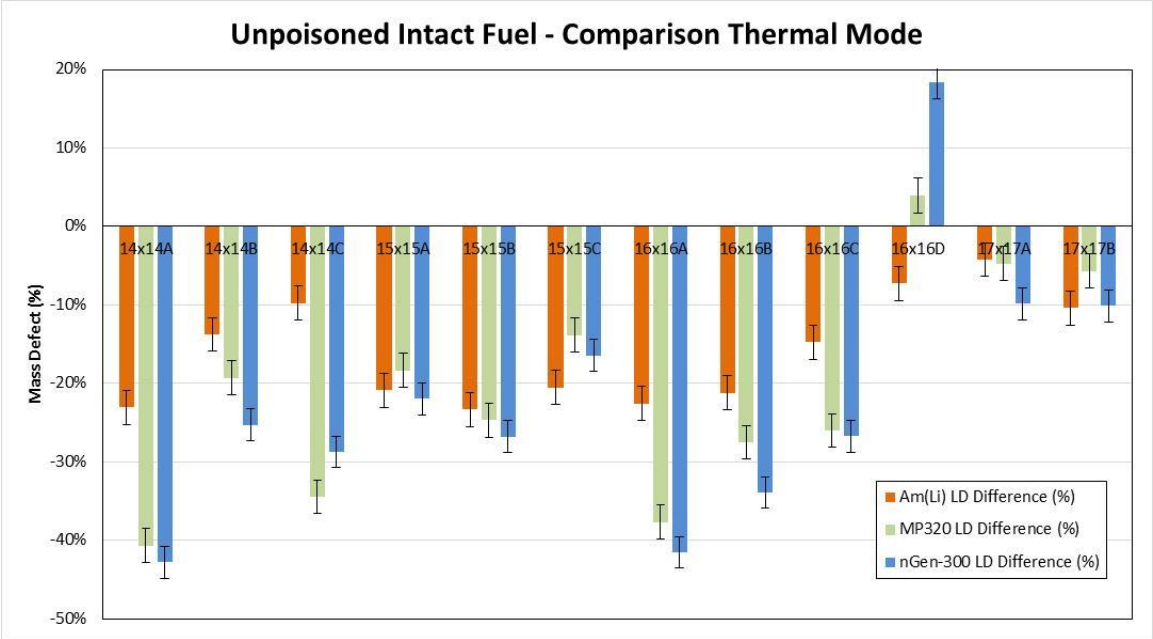

Figure 91. Comparison of the Am(Li) thermal mode and the generator induced delayed neutron thermal mode defect results for the assorted intact fuel assemblies. Error bars represent the projected 1 sigma uncertainties for an 1,800 second measurement time.

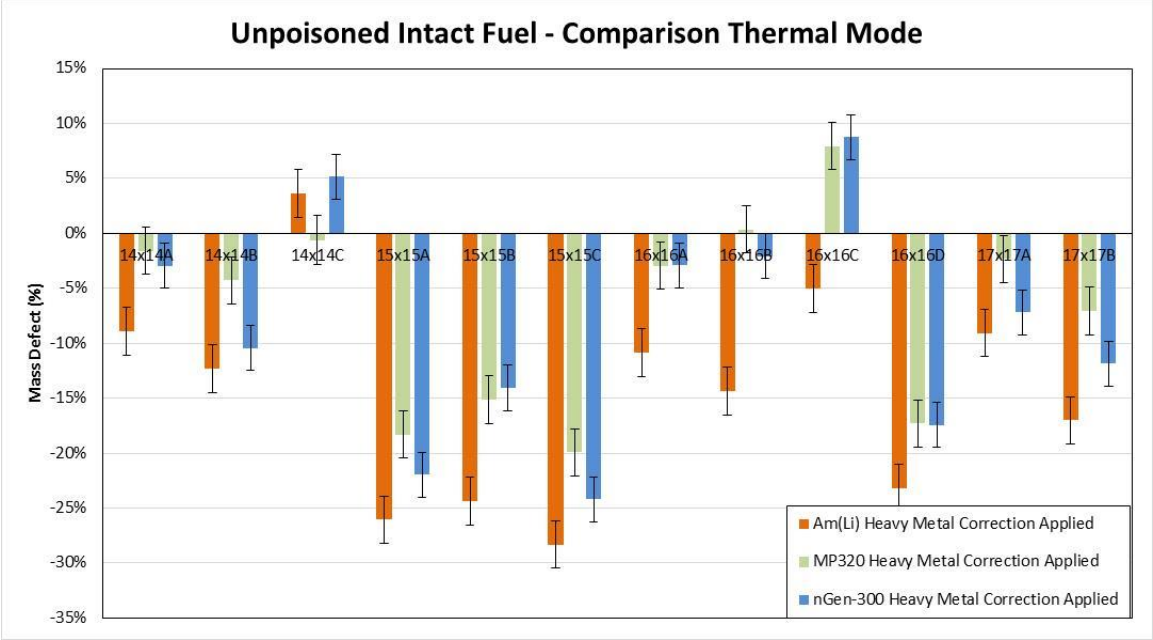

Figure 92. Comparison of the Am(Li) thermal mode and the generator-induced delayed neutron thermal mode defect results for the assorted intact fuel assemblies with the heavy metal correction applied. Error bars represent the projected 1 sigma uncertainties for an 1,800 second measurement time.

11.1.3 Delayed Neutron Thermal Mode Poisoned Fuel Assembly Comparison

A comparison of the simulated results for the MP320 and nGen-300c neutron generators with the Am(Li) mode based UNCL thermal mode measurements for assemblies containing poison rods is presented in Figure 93, and the same data with the heavy metal and poison corrections applied in Figure 94. Standard deviations for the collection of assemblies and the average biases are presented in Table 103.

There is no significant difference qualitatively or quantitatively in the biases predicted by these simulations. Because the measurement precision is small for the 1,800 seconds assay time compared to the overall uncertainty in the UNCL result, we conclude that in thermal mode the neutron generators and Am(Li) sources provide equivalent performance. Again, we note that for shorter measurement times, the performance available from the nGen-300c generator would yield superior measurement precision in the final assay value.

We also conclude that the poison correction applied in the thermal mode is potentially a very accurate method when the only parameter changing is the number of poison rods present.

Table 103. Thermal mode bias comparisons for the intact, poisoned fuel assemblies. Assay time = 1,800 seconds.

	Uncorrected assay results				Heavy metal correction applied		
	Am(Li)	**MP320**	**nGen-300c**		**Am(Li)**	**MP320**	**nGen-300c**
Average bias	−34.2%	−33.2%	−36.6%		−0.3%	2.0%	0.7%
Standard deviation	13.6%	14.7%	14.0%		1.6%	2.7%	3.2%
Measurement precision	0.7%	0.8%	0.3%		0.7%	0.8%	0.3%

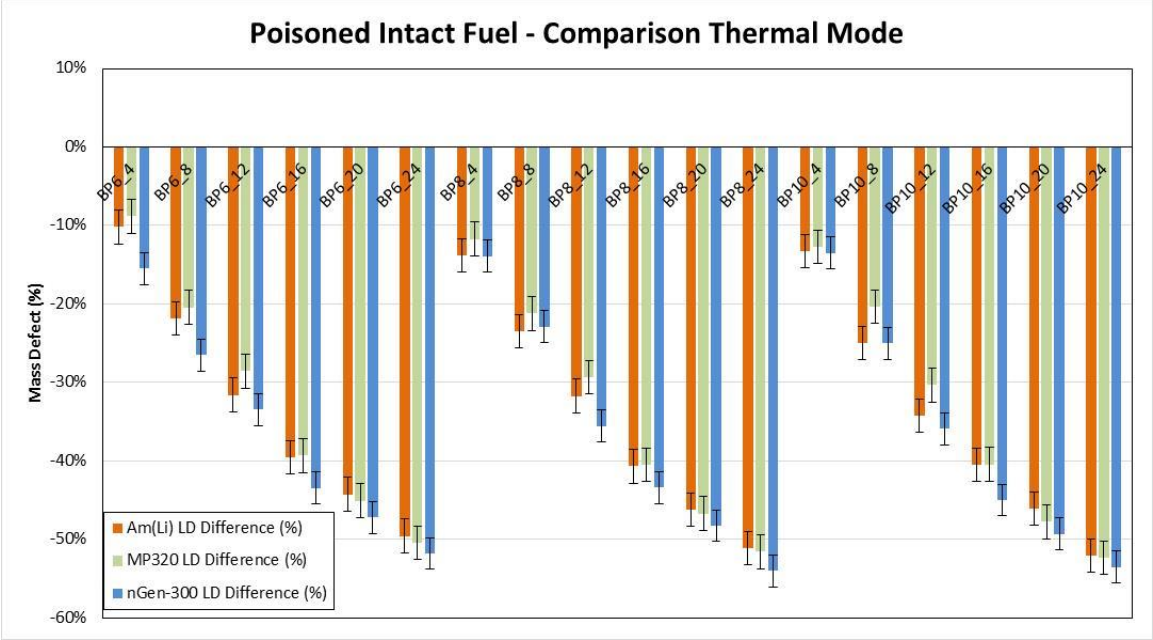

Figure 93. Comparison of the DD/UNCL and Am(Li) thermal mode defect results for the poisoned intact fuel assemblies. Error bars represent the projected 1 sigma uncertainties for an 1,800 second measurement time.

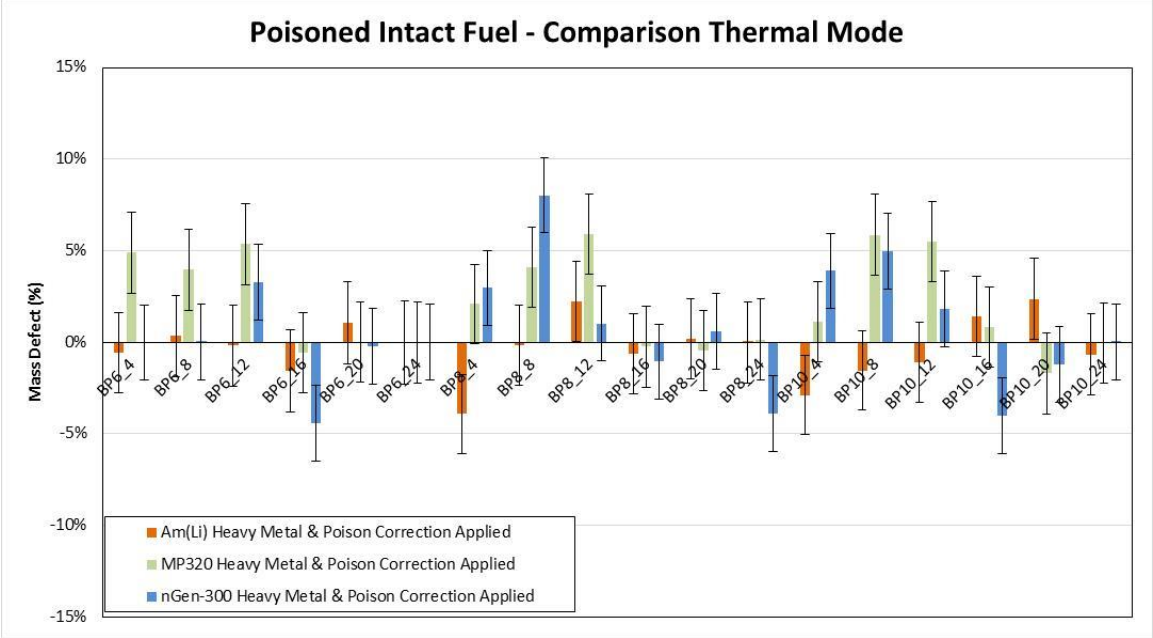

Figure 94. Comparison of the DD/UNCL and Am(Li) thermal mode defect results for the poisoned intact fuel assemblies with the heavy metal correction and poison corrections applied. Error bars represent the projected 1 sigma uncertainties for an 1,800 second measurement time.

11.1.4 Delayed Neutron Thermal Mode Partial Defect Assembly Comparison

A comparison of the simulated results for the MP320 and nGen-300c neutron generators with the Am(Li) source thermal mode interrogation of the partial defect fuel assemblies is presented in Table 104 and in Figure 95. There is no significant difference in the biases from the three neutron sources. Although the

measurement precision of the Am(Li)-based interrogation is somewhat better than what is obtainable with the neutron generators, the differences in the measurement precision are small relative to the calibration errors and the biases. However, because the nGen-300c–based delayed neutron measurement provides better measurement precision, it is possible that with assembly-specific calibrations (i.e., direct comparisons to reference assemblies) that the delayed neutron measurement will be able to detect slightly smaller numbers of rod substitutions (e.g., 5 versus 10).

Table 104. Thermal mode bias comparisons for the partial defect fuel assemblies. Assay time = 1,800 seconds.

	Uncorrected assay results				Heavy metal correction applied		
	Am(Li)	**MP320**	**nGen-300c**		**Am(Li)**	**MP320**	**nGen-300c**
Average bias	−7.6%	−7.8%	−8.0%		−14.0%	−7.7%	−7.9%
Standard deviation	4.3%	5.7%	5.2%		3.8%	5.7%	5.2%
Measurement precision	0.9%	0.8%	0.5%		0.9%	0.8%	0.5%

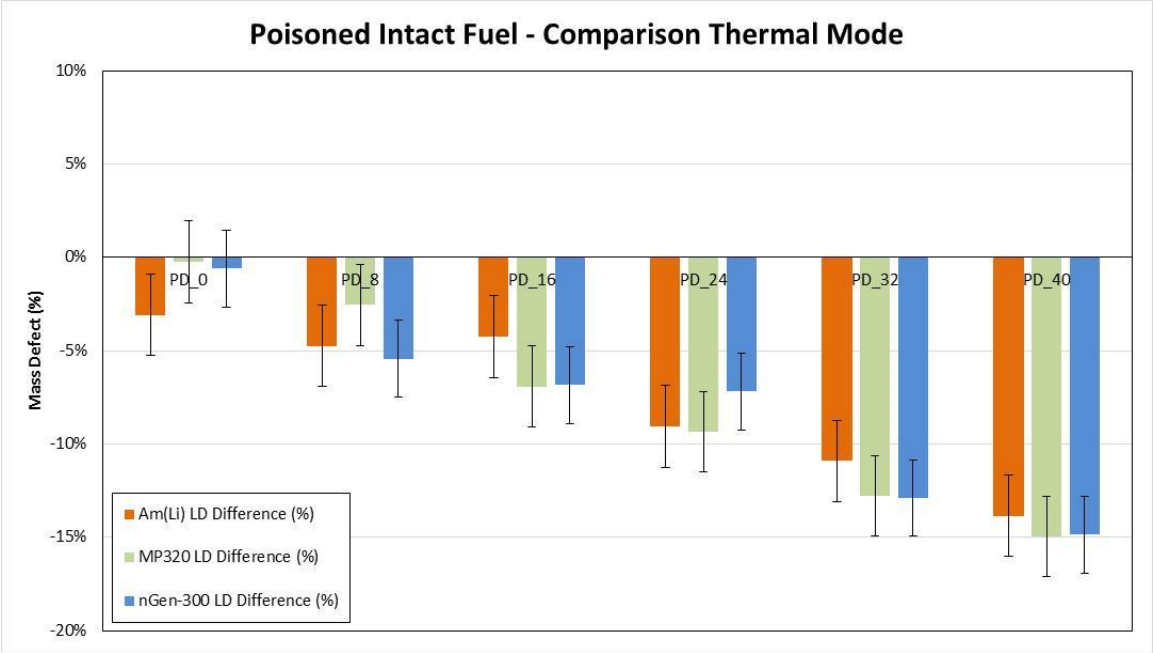

Figure 95. Comparison of the uncorrected DD/UNCL and Am(Li) thermal mode defect results. Error bars represent the projected 1 sigma uncertainties for an 1,800 second measurement time.

11.2 PERFORMANCE COMPARISON FOR DELAYED NEUTRON, FAST MODE OPERATION OF THE UNCL

11.2.1 Delayed Neutron Fast Mode Response Function Comparison

To examine the relative mass dependence of the various interrogating neutron sources, the fast mode calibration curves for the Am(Li), MP320, and nGen-300c interrogation systems were each normalized to their response to the 65 g ^{235}U/cm calibration assembly. The comparison of the simulated calibration curves for each of the neutron sources (Figure 96) reveals that the response function for each of the neutron generator types considered have nearly identical dependence on the ^{235}U content of the assembly

but have a somewhat lower sensitivity as a function of linear density when compared to the Am(Li)-based measurement.

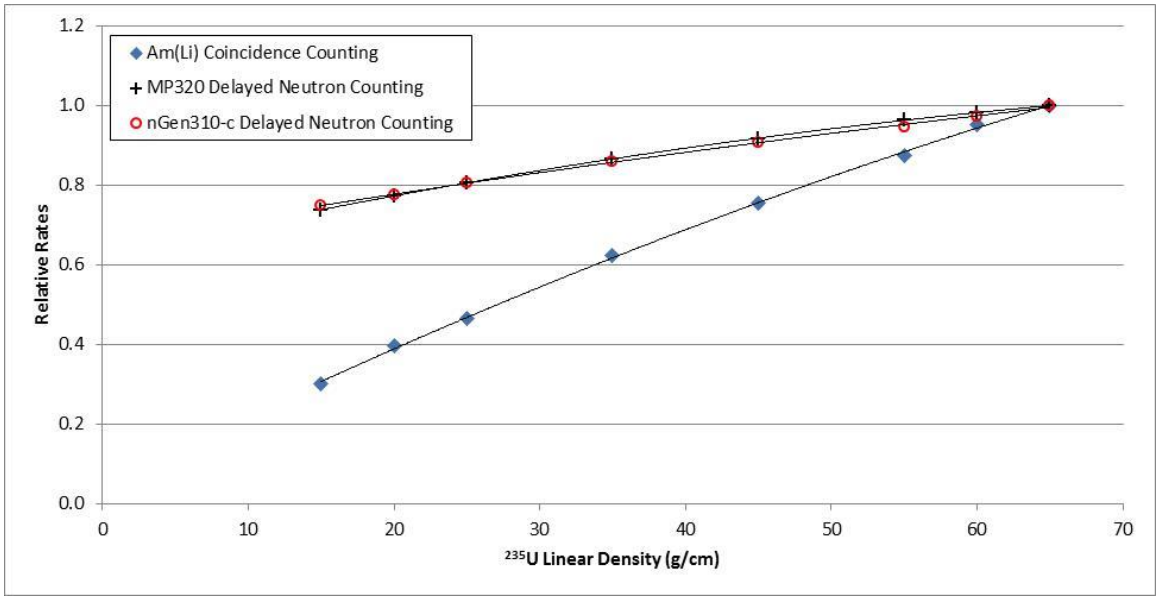

Figure 96. Comparison of the relative fast coincidence rates as a function of ^{235}U linear density for the calibration assemblies for each of the neutron sources considered.

Figure 97 presents a comparison of the expected precision in the UNCL fast mode counting rates for the Am(Li) and neutron generator delayed–neutron based measurements. The neutron source yield was assumed to be 50,000 n/s for the Am(Li) source and 2,000,000 n/s for the neutron generators. The delayed neutron measurements provide dramatically improved precision in the observed counting rates relative to the Am(Li)-based measurements. However, because the delayed neutron measurements are less sensitive to changes in the ^{235}U enrichment, the improvement in assay precision is more modest relative to the traditional Am(Li)-based measurement shown in Figure 98. The expected measurement precision for the nGen300 based measurement is 3 times better than that achievable using the traditional Am(Li)-based measurement. Alternatively, use of the delayed neutron method would allow the same measurement precision to be achieved in 1/9th the current measurement times.

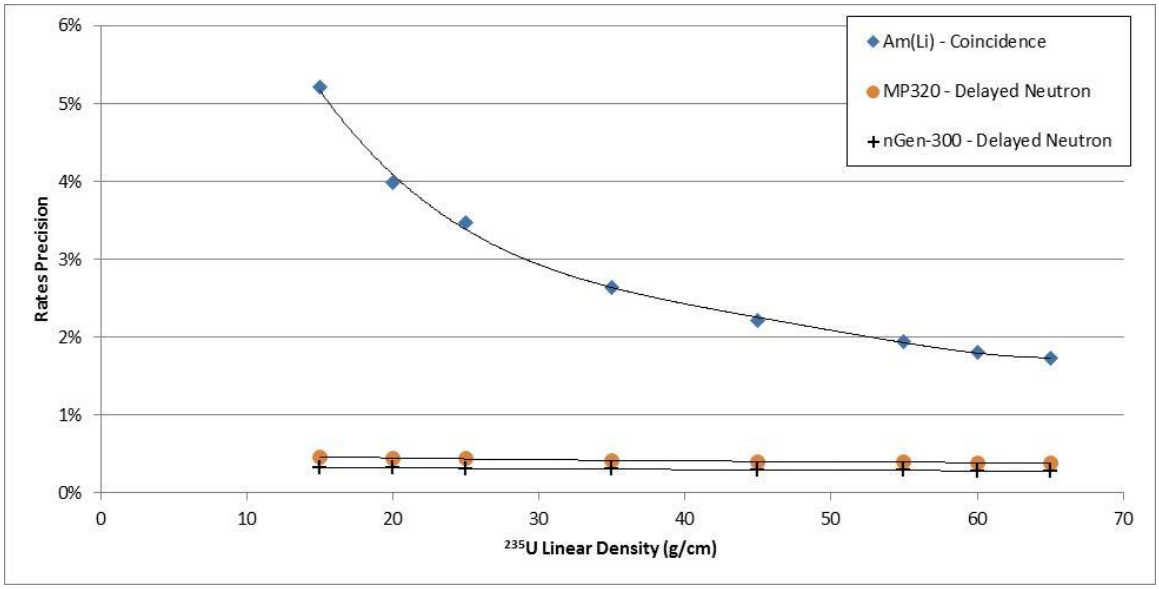

Figure 97. Comparison of the fast mode doubles rate and delayed neutron rate precision as a function of ^{235}U linear density for the calibration assemblies for each of the neutron sources considered for 1,800 seconds measurement time. Am(Li) = 50,000 n/s, and neutron generators = 200,000 n/s.

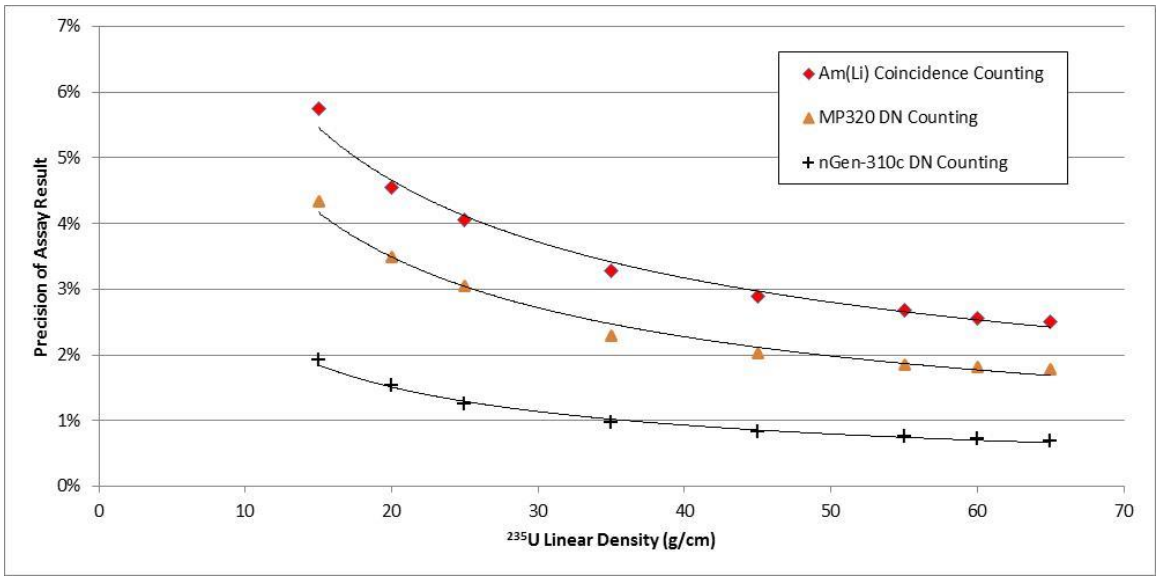

Figure 98. Comparison of the fast mode assay precision as a function of ^{235}U linear density for the calibration assemblies for each of the neutron sources considered for 1,800 seconds measurement time. Am(Li) = 50,000 n/s, and neutron generators = 200,000 n/s.

11.2.2 Delayed Neutron Fast Mode Intact, Unpoisoned Fuel Assembly Comparison

A comparison of the simulated delayed neutron results for the MP320 and nGen-300c neutron generators with the Am(Li) mode–based UNCL fast mode measurements is presented in Figure 99, and the same data with the heavy metal correction applied is presented in Figure 100. Standard deviations for the collection of assemblies and the average biases are presented in Table 105. As can be seen in Figure 63 and Table 105, the standard deviation and biases of the uncorrected assay results are larger for each

generator type considered than is achievable from the Am(Li)-based measurement. Following application of a heavy metal correction, there is no significant difference qualitatively or quantitatively in the biases for the corrected linear densities predicted by these simulations. However, the measurement precision achievable using the nGen-300c generators is about 3 times better than from the Am(Li).

Table 105. Fast mode bias comparisons for the intact, unpoisoned fuel assemblies

	Uncorrected assay results				Heavy metal correction applied		
	Am(Li)	**MP320**	**nGen-300c**		**Am(Li)**	**MP320**	**nGen-300c**
Average bias	−2.0%	−26.8%	−27.5%		−1.4%	−0.4%	0.5%
Standard deviation	6.3%	39.9%	43.0%		2.9%	3.1%	3.7%
Measurement precision	2.9%	0.9%	0.7%		2.9%	0.9%	0.7%

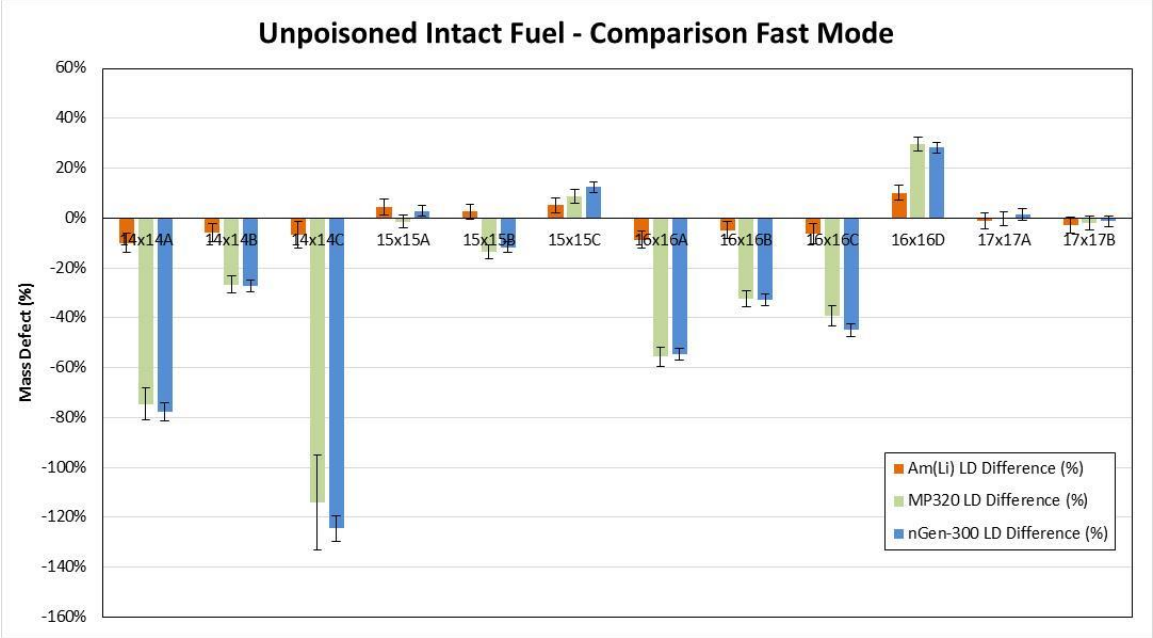

Figure 99. Comparison of the DD/UNCL and Am(Li) fast mode defect results for the assorted intact fuel assemblies. Error bars represent the projected 1 sigma uncertainties for an 1,800 second measurement time.

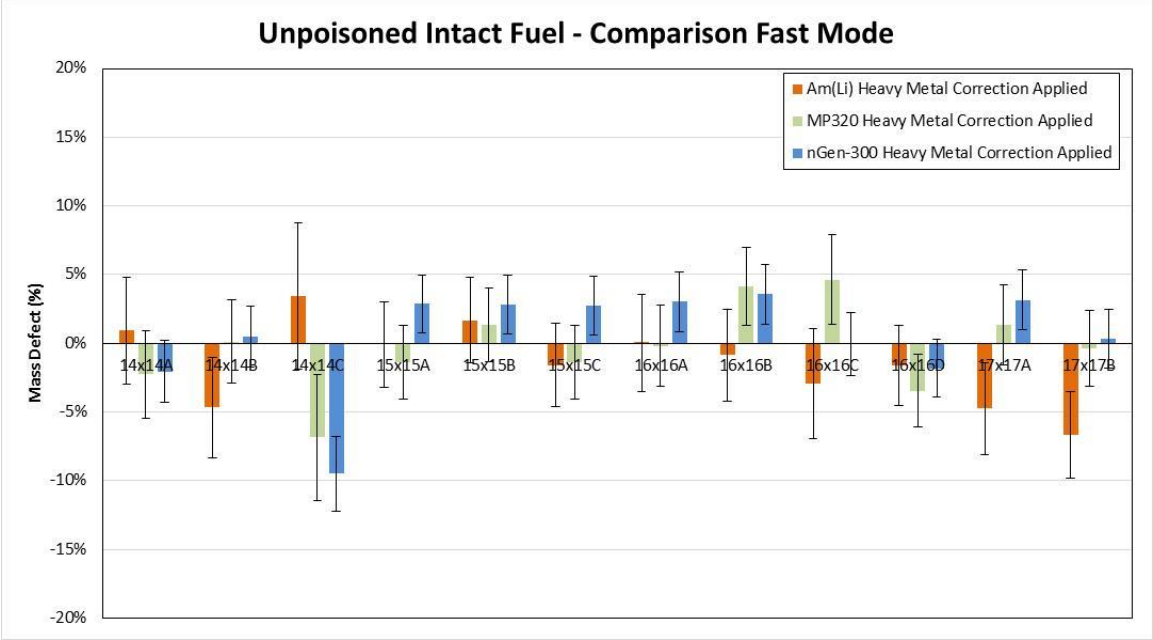

Figure 100. Comparison of the DD/UNCL and Am(Li) fast mode defect results for the assorted intact fuel assemblies with the heavy metal correction applied. Error bars represent the projected 1 sigma uncertainties for an 1,800 second measurement time.

11.2.3 Delayed Neutron Fast Mode Poisoned Fuel Assembly Comparison

A comparison of the simulated results for the MP320 andnGen-300c neutron generators with the Am(Li) mode–based UNCL fast mode measurements for assemblies containing poison rods is presented in Figure 101, and the same data with the heavy metal and poison corrections applied is presented in Figure 102. Standard deviations for the collection of assemblies and the average biases are presented in Table 106.

There is no significant difference qualitatively or quantitatively in the biases predicted by these simulations. However, the delayed neutron measurements are expected to provide improved measurement precision relative to that achievable with the Am(Li)-based coincidence measurements. The improvement in measurement precision achievable with the nGen-300c–based delayed neutron measurements is expected to provide approximately a factor of 2 reduction in measurement error.

Table 106. Fast mode bias comparisons for the intact, poisoned fuel assemblies

	Uncorrected assay results				Heavy metal correction applied		
	Am(Li)	**MP320**	**nGen-300c**		**Am(Li)**	**MP320**	**nGen-300c**
Average bias	−3.8%	−7.6%	−5.5%		−0.4%	0.4%	0.1%
Standard deviation	3.2%	4.2%	3.5%		1.4%	1.8%	1.0%
Measurement precision	2.4%	2.0%	0.8%		2.4%	2.0%	0.8%

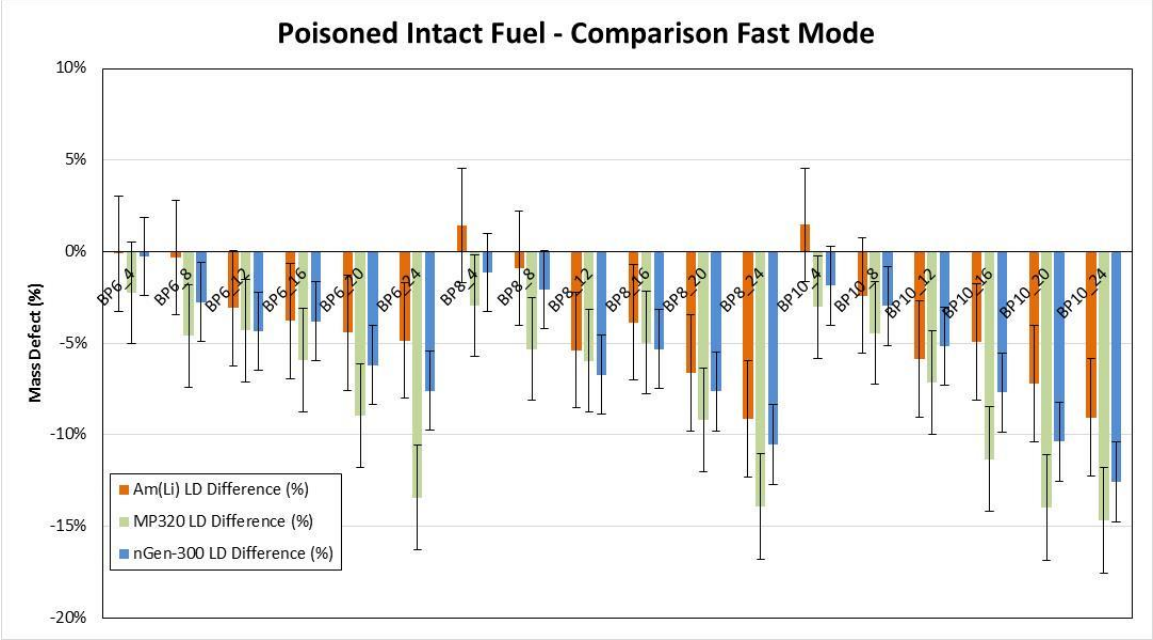

Figure 101. Comparison of the DD/UNCL delayed neutron and Am(Li) fast mode defect results for the poisoned fuel assemblies. Error bars represent the projected 1 sigma uncertainties for an 1,800 second measurement time.

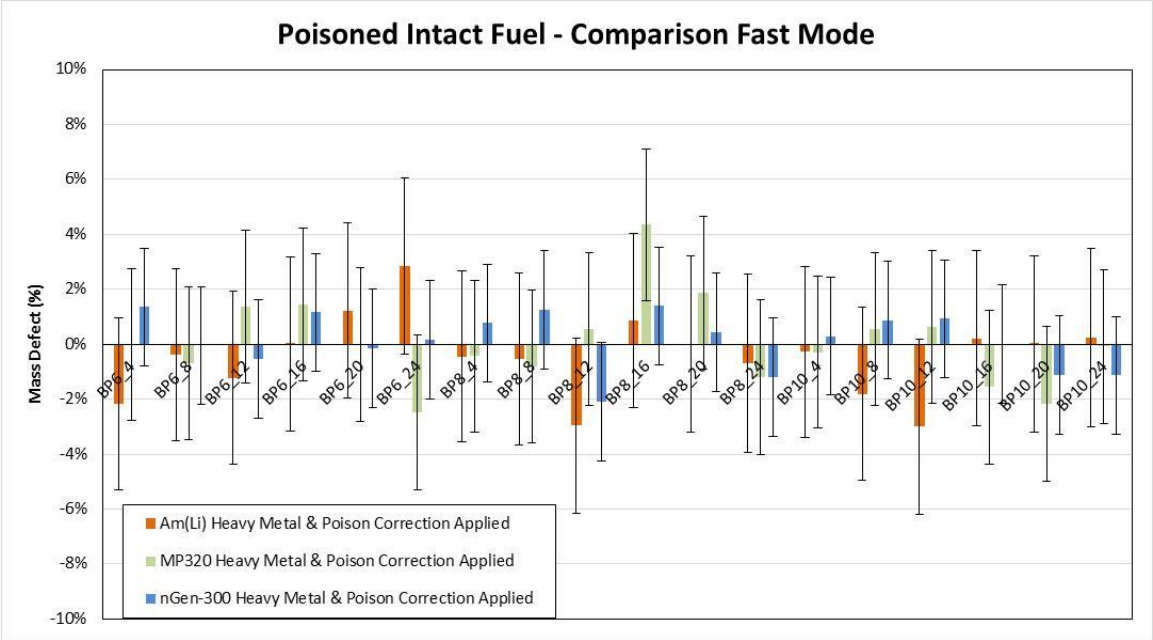

Figure 102. Comparison of the DD/UNCL delayed neutron and Am(Li) fast mode defect results for the poisoned fuel assemblies with the heavy metal correction applied. Error bars represent the projected 1 sigma uncertainties for an 1,800 second measurement time.

11.2.4 Delayed Neutron Fast Mode Partial Defect Assembly Comparison

A comparison of the simulated results for the MP320 and nGen-300c neutron generators with the Am(Li) source thermal mode interrogation of the partial defect fuel assemblies is presented in Table 70 and in Figure 103. There is no significant difference in the biases from the interrogation method. However, the

delayed neutron measurements are expected to provided improvement in measurement relative to the coincidence measurements.

Because the delayed neutron based measurements provide better measurement precision, it is likely that with assembly-specific calibrations (i.e., direct comparisons to reference assemblies) that the delayed neutron generator measurements will be able to detect smaller numbers of rod substitutions (e.g., 10 versus 26).

Table 107. Fast mode bias comparisons for the partial defect fuel assemblies

	Uncorrected assay results				Heavy metal correction applied		
	Am(Li)	**MP320**	**nGen-300c**		**Am(Li)**	**MP320**	**nGen-300c**
Average bias	−5.5%	−6.5%	−6.8%		−9.4%	−6.4%	−6.7%
Standard deviation	6.4%	5.6%	5.4%		6.1%	5.6%	5.4%
Measurement precision	2.4%	1.9%	0.8%		2.4%	1.9%	0.8%

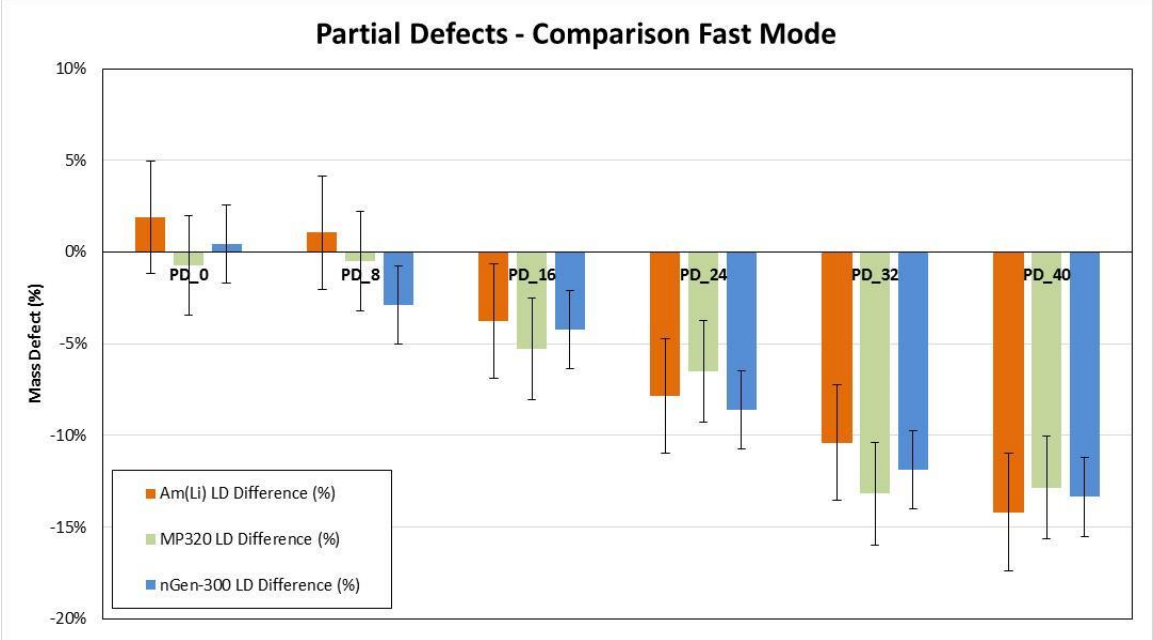

Figure 103. Comparison of the DD/UNCL and Am(Li) fast mode defect results for the partial defect fuel assemblies. Error bars represent the projected 1 sigma uncertainties for an 1,800 second measurement time.

12. CONCLUSION

From the performance comparisons in Sections 8 and 11 we have seen that the biases in the uncorrected simulated assay results for the UNCL operating in either fast or thermal modes follow the same trends independent of the neutron interrogation or data collection methodology. In general, the magnitude of the biases are similar for these different methodologies, however, the impact of the fuel assembly type (e.g., 14 × 14 versus 17 × 17 array) is more pronounced for the neutron generator simulations when the UNCL is configured in fast mode (Figures 63 and 99). The increased sensitivity to fuel assembly configuration in the fast mode is an artifact of the historical analysis approach used with the UNCL where a single calibration function is applied to all fuel assemblies. (Assembly type specific calibrations would eliminate the need for the heavy metal correction factor and the biases, and the differences observed in Figures 63 and 99 would be reduced significantly). Following application of the traditional correction factors, the biases in the simulated assay results for the UNCL operating in either fast or thermal modes are independent of the neutron interrogation or data collection methodology. We can conclude that accuracy of the UNCL fuel collar measurements using the neutron generator interrogation source is equivalent to that currently achievable using the Am(Li) neutron source.

It was not possible to match the measurement precision of the Am(Li)-based UNCL measurement using the neutron generators with a coincidence counting analysis. The use of the neutron generator, regardless of configuration, resulted in an increase in the ratio of source neutrons detected to induced fission rate in comparison to the Am(Li) source interrogation. Attempts to tailor the neutron spectrum by adding/subtracting moderators or reflector materials offered little improvement in the measurement precision. Simulations of a fictitious very compact DD neutron generator offered some improvement over the COTS neutron generators but did not match the performance of the Am(Li) source measurements (Figure 62). The assay precision using the COTS generators is expected to be approximately twice as large as the current Am(Li)-based measurements.

The use of delayed neutron counting was considered because of the lack of success in matching the Am(Li) source measurement precision with the DD neutron generators in a coincidence counting analysis. The delayed neutron measurement precision is not limited by the accidentals coincidence rate, and although the delayed neutron emission rate is only a fraction of the induced fission rate, the greater efficiency for singles neutron counting compared to the doubles counting and the much stronger interrogating source term lead to significant improvement in measurement precision.

Figure 104 provides a comparison of the expected assay precision for the thermal mode interrogation with the Am(Li) coincidence measurement and the neutron generators' coincidence, and delayed neutron counting techniques. The delayed neutron counting measurement using the MP320 pulsed neutron generator is expected to be equivalent or slightly better measurement precision than achievable using the Am(Li)-based coincidence measurement. The delayed neutron counting measurement using the nGen-300c pulsed neutron generator is expected to improve the precision in the assay result by a factor of 2. Alternatively, the measurement time could be reduced by a factor of 4 and provide the current level of performance achieved with Am(Li).

Figure 105 provides a comparison of the expected assay precision for the fast mode interrogation with the Am(Li) coincidence measurement and the neutron generators coincidence and delayed neutron counting techniques. The delayed neutron counting measurement using the MP320 pulsed neutron generator is expected to provide equivalent or slightly better measurement precision than what is achievable using the Am(Li)-based coincidence measurement. The delayed neutron counting measurement using the nGen-300c pulsed neutron generator is expected to improve the precision in the assay result by a factor of 3. Alternatively, the measurement time could be reduced by a factor of 9 and provide the current level of performance achieved with Am(Li). We note that the delayed neutron counting measurement precision

achievable with the nGen-300c configured for fast mode is equivalent to that achievable for the Am(Li) source thermal mode interrogation.

The neutron generators can serve as a viable alternative to the current Am(Li)-based UNCL measurement. However, as a "drop in" replacement for coincidence counting, the generators will require a factor of 2 or more increase in measurement time to achieve comparable measurement precision to what is currently achieved with Am(Li). Adopting a delayed neutron counting methodology, the neutron generators can significantly improve measurement precision in equivalent assay time without loss of accuracy.

The delayed neutron method would require development of a new software analysis package (or integration of the rather simple methodology into an existing software package). The required acquisition electronics (i.e., almost any current multichannel analyzer used by the International Atomic Energy Agency) are readily available and relatively inexpensive.

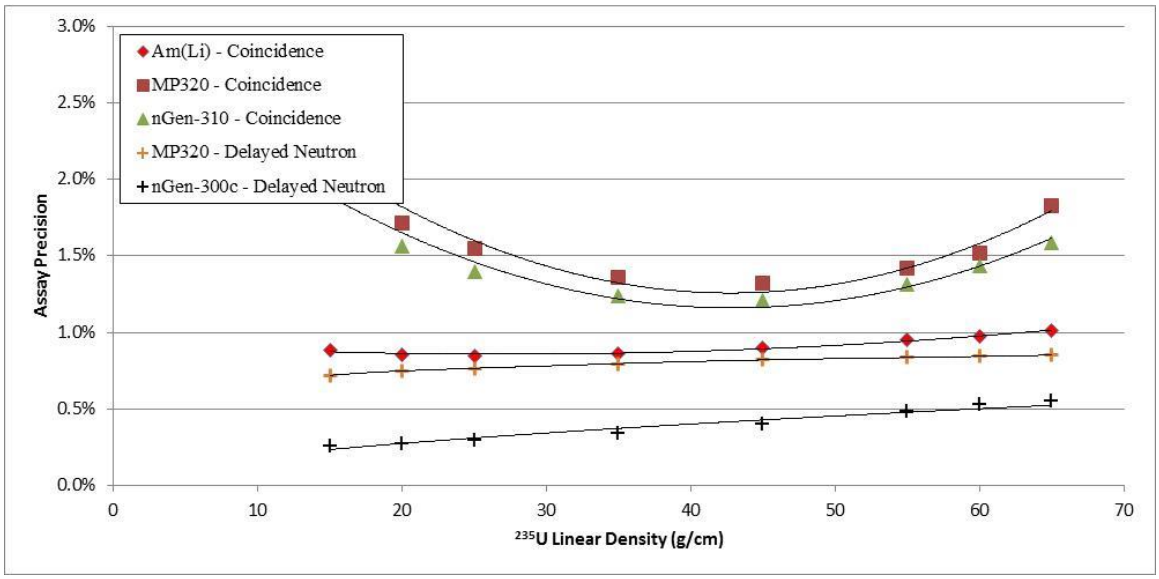

Figure 104. Comparison of the thermal mode assay precision as a function of ^{235}U linear density for the calibration assemblies for each of the neutron sources considered for 1,800 seconds measurement time. Am(Li) = 5E4 n/s, neutron generators coincidence counting = 2E5 n/s, and neutron generators delayed neutron counting = 2E6 n/s.

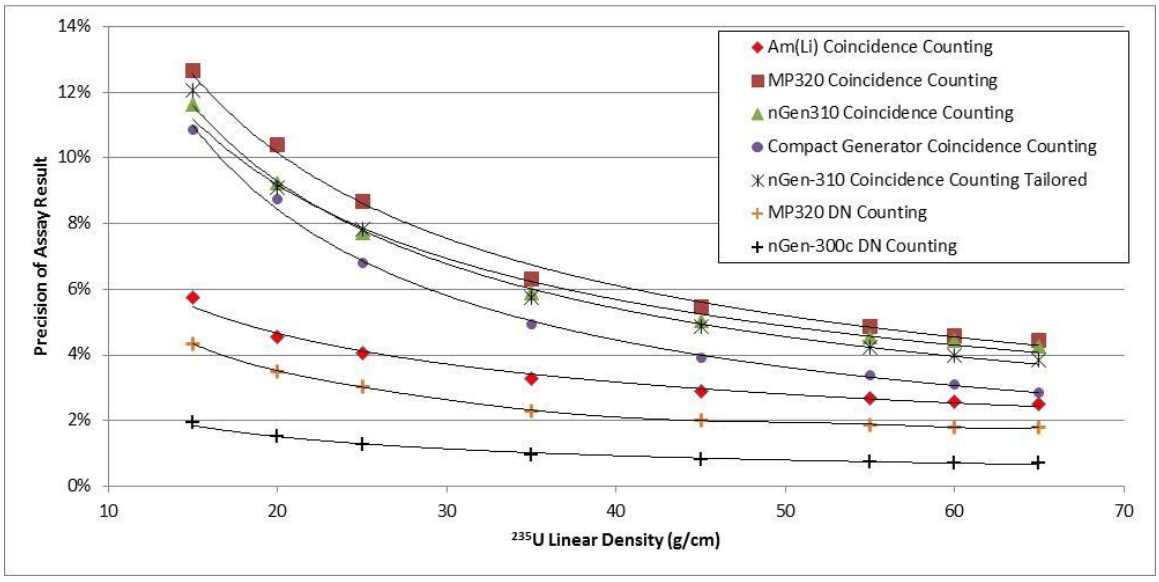

Figure 105. Comparison of the fast mode assay precision as a function of ^{235}U linear density for the calibration assemblies for each of the neutron sources considered for 1,800 seconds measurement time. Am(Li) = 5E4 n/s, neutron generators coincidence counting = 2E5 n/s, and neutron generators delayed neutron counting = 2E6 n/s.

REFERENCES

[1] R. D. McElroy, Jr. and S. L. Cleveland, "The D-D Neutron Generator as an Alternative to Am(Li) Isotopic Neutron Source in the Active Well Coincidence Counter", ORNL Technical Report ORNL/TM-2017/57," Oak Ridge National Laboratory, Oak Ridge, TN, 2017.

[2] A. Belian, A. Dougan, A. Iyengar, D. Chichester, S. Clark, S. Croft, D. Decman, W. Geist, P. Hauladen, H. Jianwei, R. McElroy, H. Menlove, J. Newby, S. Pozzi, M. Prasad, J. Sanders, T. Shin, S. Thompson and J. Verbeke, "Advanced Neutron Detection Technology Rodeo," in *ESARDA 39th Annual Meeting*, Dusseldorf, Germany, 2017.

[3] H. O. Menlove and J. E. Pieper, "Neutron Collar Calibration for LWR Fuel Assemblies, LA-10827-MS," Los Alamos National Laboratory, Los Alamos, NM, 1987.

[4] H. O. Menlove, "Description and Performance Characteristics for the Neutron Coincidence Collar for Verification of Reactor Fuel Assemblies," Los Alamos National Laboratory Report LA-9839-MS (ISPO-142), Los Alamos, NM, 1981.

[5] Canberra Industries, "Model JCC-71, 72, & 73 Specification Sheet," [Online]. Available: http://www.canberra.com/products/waste_safeguard_systems/pdf/JCC-71-72-73-SS-C38898.pdf. [Accessed 7 9 2017].

[6] H. O. Menlove, J. E. Stewart, S. Z. Qiao, T. R. Wenz and G. P. D. Verrecchia, "Neutron Collar Calibration Evaluation for Assay of LWR Fuel Assemblies Container Burnable Neutron Absorbers, LA-11965-MS (ISPO 323)," Los Alamos National Laboratory, Los Alamos, NM, 1990.

[7] P. Hausladen, J. Newby and R. D. McElroy, "Simulations of a PSD Plastic Neutron Collar For Assaying Fresh Fuel; ORNL/TM-2016/680," Oak Ridge National Laboratory, Oal Ridge. TN, 2016.

[8] M. Prasad, D. Shumaker, N. Snyderman, J. Verbeke and J. wong, "Prototype Stilbene Neutron Collar; LLNL-TR-707598;," Lawrence Livermore National Laboratory, Livermore, CA, 2016.

[9] S. Croft, A. Favalli, M. T. Swinhoe and C. D. Rael, "“State of the Art Monte Carlo Modeling of Active Collar Measurements and Comparison with Experiment,” LA-UR-11-03760," *Proceedings of the 52nd Annual INMM Meeting,* 2011.

[10] Starfire Industries, "nGen-300c for Sharp Pulsed Neutrons," [Online]. Available: http://www.starfireindustries.com/uploads/2/2/1/1/22111816/datasheet_ngen-300c_pulsed_rev00-18.pdf. [Accessed 16 November 2107].

[11] Starfire Industries, "nGen for Portable CW Neutrons," [Online]. Available: http://www.starfireindustries.com/uploads/2/2/1/1/22111816/datasheet_ngen-310_rev00-17.pdf. [Accessed 16 November 2017].

[12] J. T. Goorley and et.al., "Initial MCNP6 Release Overview - MCNP6 version 1.0, LA-UR-13-22934," Los Alamos National Laboratory, Los Alamos, NM, 2013.